HARMONIC ANALYSIS AND MITIGATION IN SELECTED NIGERIAN 33KV DISTRIBUTION NETWORKS

BY

ADESINA, LAMBE MUTALUB

B.Eng. (Ilorin), M.Eng. (Kano)

A Thesis in the Department of Electrical and Electronic Engineering,
Submitted to the Faculty of Technology in partial fulfillment of
the requirements for the Degree of

DOCTOR OF PHILOSOPHY

of the

UNIVERSITY OF IBADAN

JUNE 2016.

ABSTRACT

The non-linear characteristics of power electronic loads introduce harmonics, which may result in power distribution losses and reduction of the operational efficiency of equipment. Therefore, minimization of power harmonics is highly desirable in electrical power networks. Various techniques to mitigate against harmonics have been developed but do not meet the ultimate quality power supply and voltage level of 5% for total harmonic distortion (THD) and 3% for any individual harmonics, as specified by IEEE standard 519-1992. This study aimed at the development of an improved technique for minimisation of harmonic contents in distribution networks.

Power flow analysis of a selected Nigerian 33 kV distribution network in Southwestern Nigeria was carried out to obtain its bus voltage and power characteristics (active and reactive power) using Newton-Raphson numerical technique. An algorithm was developed to induce power harmonics on the bus voltages resulting from the power flow analysis in order to obtain harmonic contents in each distribution line of network considered. Single and n-stage cascaded harmonic reduction networks were developed using standard procedure. The distribution network, with induced harmonics, was inserted into the developed harmonic reduction network. Effects of harmonics on distribution lines less than 1 km (short) and long lines of 7 km were observed. Data were analysed using Anova at p=0.05

Bus voltages at the 1^{st} harmonic range from 32.553 to 32.997 kV, with percentage deviations varying from 0.01 to 1.35% of the nominal voltage of 33 kV. Reactive power (MVar) in the network was 61.97% of the active power supplied to the system at a given load. Unwanted harmonics generated in the network is in the frequency range of 100-1450Hz. Harmonic impedances for 2^{nd} and 29^{th} harmonics ranges from $10^{1.962}\Omega$ to $10^{2.118}\Omega$ and $10^{1.556}\Omega$ to $10^{2.007}\Omega$ respectively at different switching times. Mitigation, using single and 2^{nd} stage cascaded harmonic reduction networks revealed that the peak harmonic impedance amplitude was reduced by 46.0% and 98.0% respectively. The number of harmonic components in the induced harmonics were reduced by single and 2^{nd} stage reduction techniques, with 2^{nd} stage reduction technique having much reduced harmonic amplitudes. The 2^{nd} harmonic was completely removed in the single stage reduction technique, while the 2^{nd} stage

reduction technique eliminated the 2^{nd} and 6^{th} harmonics. The average impedance amplitudes of the remaining harmonics for single and 2^{nd} stage reduction techniques were $10^{2.1}\Omega$ and $10^{2.0}\Omega$, respectively. Harmonic impedance at the 2^{nd} harmonic remained constant for short distribution line distance of less than 1 km. The 3^{rd} harmonic and above were associated with distribution feeders of long distances of up to 7 km. Analysed data showed that the 2^{nd} stage is significantly better than the single stage technique of harmonic reduction.

The developed algorithm for harmonic analysis and its mitigation in power system resulted in improved supply voltage in short distribution feeders. Further mitigation in the 2^{nd} stage technique enhanced power quality in the selected distribution network.

Keyword: Distribution network, Power flow, Harmonic reduction network, Harmonic mitigation, Total harmonic distortion

Word count: 477

ACKNOWLEDGEMENT

This dissertation covers the work carried out since October 2007 at Electrical &Electronic Engineering Department, Faculty of Technology, University of Ibadan, Nigeria, and constitutes my Doctoral thesis.

I seize this opportunity to express my gratefulness to Almighty Allah, the beneficent and most merciful, who gave me the initiative and ability to pursue the programme, and for his protection and guidance throughout the period of the research programme.

First of all, I would like to express my deepest gratitude and appreciation to my supervisor, Dr. O. A. Fakolujo of the Department of Electrical and Electronic Engineering, University of Ibadan, for his advice, support and encouragement during this research project.

I am indebted to Professor A Olatunbosun, Head of Department, Electrical &Electronic Engineering, Faculty of Technology, University of Ibadan, whose efforts cannot be quantified both morally and academically. Also, my sincere appreciation goes to Dr. Melodi Adegoke, of the Federal University of Technology, Akure, for putting me through at the beginning of the research work. May the Lord continue to bless them. My profound gratitude goes to the staff and colleagues of Eko Electricity Distribution PLC, Marina-Lagos, Nigeria, for their valuable and immeasurable contributions to the success of this research work. These include Engr. G. K. Ikperite, Engr. Olatokun Seyi and Engr. Adjekpiyede Ovie of Network Planning Department, Engr. Olorundare Michael Kayode and Engr. Ebere Iheanyichukwu of Inspection and Quality Assurance Department, and Engr. Moruf Oloruntele of Key Customer Group Department. I appreciate you all.

Also, my parents deserve special mention for their inseparable support and prayers. I am indebted to my mother and father for their love, encouragement and understanding throughout my entire life. I am also very grateful to my wife, Alhaja Ameenat Bola Adesina Lambe for her contributions, patience and endurance.

Lastly, I appreciate the contributions of my friends, Dr. A.R. Zubair of Electrical &Electronic Engineering Department, University of Ibadan, Engr. L.O. Abdulkareem, Deputy General Manager (Civil Engineering), Nigerian Metrological Agency, Headquarters office, Abuja, and Alhaji Tunde Sheu Atagisoro, Psychology Department, 2nd Division Army Hospital, Ibadan. Thanks to everybody; I am grateful.

CERTIFICATION

I certify that this work was carried out by Mr. L.M. Adesina in the Department of Electrical and Electronic Engineering, University of Ibadan

……

Supervisor

Dr. O.A. Fakolujo

B.Sc. (Ife), Ph.D. (London), D.I.C.

Reader, Department of Electrical and Electronic Engineering,

University of Ibadan, Nigeria.

TABLE OF CONTENTS

NOMENCLATURE

SYMBOL	REPRESENTATION
SB	Line Start Bus
RB	Line End Bus
LD	Line Distance
SV	Send end Voltage
RV	Receiving end Voltage
SF	Supply Frequency
HRM	Harmonic
ALG	Alagbon
ADM	Ademola
ALG–L	Alagbon Local
ANI	Anifowoshe
FOW	Fowler
MAR	Maroko
BAN–I	Banana Island
HZ	Hertz
Ω	Ohm
THD	Total Harmonic Distortion
U_{rms}	Root Mean Square value of harmonic voltage
ω	Angular
t	Time
PCC	Point of Common Connection
LRT	Likelihood Ratio Test
X(t)	Non Sinusoidal periodic function
A_o	Average Value of function X (t) in Fourier series or Magnitude of DC component
a_n	The Even h^{th} order harmonic magnitude
b_n	The Odd h^{th} order harmonic magnitude

Ψ	**Gamma function**
T	**Period**
F	**Frequency**
AC	**Alternating Current**
HVDC	**High Voltage Direct Current**
TCR	**Thyristor Controlled Reactor**
ASD	**Adjustable Speed Drives**
VSD	**Variable Speed Drives**
FACTS	**Flexible AC Transmission Systems**
IEEE	**Institute of Electrical and Electronics Engineers**
P	**Active (or real power) in megawatts**
Q	**Reactive (or imaginary power) in megavolt ampere**
I	**Current**
∈	**Power mismatch current**
*	**Conjugate**
k	**Iteration count**
‖	**Modulus**
e	**Real voltage**
f	**Imaginary voltage**
R	**Resistance**
X	**Reactance**
Ƶ	**Impedance**
G	**Conductance**
B	**Susceptance**
Y	**Admittance**
c	**Real current**

L	**Inductor**
C	**Capacitance**
X_L	**Inductive reactance**
X_C	**Capacitive reactance**
PF	**Power Factor**
S	**Apparent Power**
d	**Imaginary current**
J	**Jacobian matrix**
NB	**Number of buses**
NL	**Number of Lines**
SL	**Slack bus**
V	**Bus voltage in complex form**
YSHT	**Shunt admittance**
NRPF	**Newton-Raphson Power Flow solution**
MW	**Megawatt**
MVar	**Megavolt ampere reactive**
kV	**Kilovolt**
kVA	**Kilovolt ampere**
MVA	**Megavolt ampere**
Δ	**Incremental value**
α	**Acceleration factor**
Σ	**Summation**
M_h	**RMS value of harmonic component, h, of the quantity M, which is either voltage or current**
APF	**Active Power Filter**
PWM	**Pulse Width Modulation**
D/L	**Distribution Line**
Deg.	**Degree**
PFC	**Power Factor Correction**
h	**Harmonic Count**
I_{SC}	**Maximum Short Circuit Current at PCC**
I_L	**Maximum Demand Load Current at PCC**

TDD	**Total Distribution Distortion**
L_S	**Source Inductance**
VOL	**Voltage**
V/ANG	**Voltage Angle**
IP	**Input**
OP	**Output**
IPP	**Input Active Power**
IPQ	**Input Reactive Power**
LD	**Line Distance**
C/ANG	**Current Angle**
LAG	**LOADING**

LIST OF TABLES

LIST OF FIGURES

CHAPTER ONE

INTRODUCTION

1.1 Background

Power system harmonics is not a new phenomenon. In fact, a text published by Steinmetz in 1916, devoted considerable attention to the study of harmonics in 3-phase power systems. In Steinmetz's days, the main concern was third harmonic currents, caused by saturated iron in transformers and machines (Owen, 1998). He was the first to propose Delta connections for mitigating third harmonic currents. After Steinmetz's important discovery, improvements were made in transformer and machine design. However, the problem of harmonics was not largely solved until the 1930's and 40's.

With the advent of rural electrification and telephones, power and telephone circuits were placed on a common right-of-way. Transformers and rectifiers in power systems produced harmonic currents that inductively coupled into adjacent open wire telephone circuits and produced audible telephone interference. This problem was gradually alleviated by filtering and by minimizing transformer core magnetizing currents. Isolated telephone interference problems still occur, but these problems are infrequent because open-wire telephone circuits have been replaced with twisted pair cables, buried cables and fibre optics.

The late 80's and early 90's saw the emergence of power electronic loads. They however, draw non-sinusoidal currents from AC power systems, and these currents react with system impedances to create voltage harmonics and in some cases, resonance. Studies have shown that harmonic distortion levels in distribution systems are rising as power electronic loads continue to proliferate (Mansoor, et al., 1995). Generally, harmonic analysis can benefit from effective monitoring(Mc Granaghan, 2002). The collected waveforms of voltage and current are also useful in testing current and voltage algorithms (George and Agarwal, 2003).

1.2 Statement of the Problem

Distribution line and the general network harmonic shave become an important issue in electric power systems since the increased use of power electronic devices and equipment sensitive to harmonics has increased the number of adverse harmonic-related events. The use of nonlinear power electronic equipment in the control of power apparatus and the presence of sensitive electronic equipment are discovered to be part of the source of these harmonic currents, which result in additional losses in distribution system equipment, interference with communication systems, and misoperation of control (Raneru, 2013). Generally, harmonic is a component of a periodic wave having a frequency that is an integral multiple of the fundamental power line frequency. Traditional harmonic producing loads are the rotating machines and transformers in electric power systems. Because of uneven distribution of flux in the air gap of the rotating machine, non-sinusoidal voltages and currents are generated by rotating machines such as synchronous machines. Overloaded transformers generate harmonic currents. Transformer excitation currents will be non-sinusoidal because of core-saturation, magnetic imbalance or DC magnetization resulting in harmonic currents (Grady, et al., 2002).Small power equipment such as televisions, computers, Adjustable Speed Drives (ASD), Uninterrupted Power Supply (UPS) systems, electronic ballasts and office equipment such as printers and fax machines draw non-sinusoidal voltages and currents. The current harmonics consumed by these loads flowing through the line impedances causes distorted voltages and, the significant harmonics are extended to the rest of the network (Benoudjafer, et al., 2014). Individual effects of this type of equipment to harmonic distortion may be negligible, but the combined effects of a larger number of these to harmonic distortion in power systems can be substantial. Thus, the power problem, and the means of keeping it under control is a growing concern (Raneru, 2013).

There are a number of studies done to investigate the implication of some home appliances and office equipment in producing harmonic distortions in power systems. For reliable and efficient power generation and delivery, modern power systems are equipped with devices which control and adjust the active and reactive power flow and regulate voltage. These devices are called Flexible AC Transmission Systems (FACTS) (Gursey,

2007). These are high power components with solid state switching that provides a fast control action to voltage and power flow regulation (Ekrem, 2007). Because of the power electronic devices used in these devices, these transmission devices produce distorted voltage and current wave forms (Ekrem, 2007). Other high powered sources of harmonics include the High Voltage Direct Current (HVDC) technologies producing non-sinusoidal voltage and currents because of the converters used in the front end of the transmission lines, arc furnaces, which produce non-characteristic harmonics, thyristor-controlled reactors (TCR), ASDs and many others(Ekrem, 2007).

The industrial application of power electronics became significantly effective, since the invention of the Silicon-Controlled Rectifier (SCR) in 1957. The improved efficiency and productivity provided by the power electronic devices however, is offset by the disturbance of the utility grid due to the injection of harmonic currents by these devices. Hence, came the concept of active filtering, first introduced by Sasaki and Machida in 1971 (Sasaki and Machida, 1971). In 1976, Gyugyi et al. (Gyugyiet al., 1976) and in 1977, Mohan et al (Mohan et al., 1977) did some pioneering work and proposed a family of active filter systems based on Pulse Width Modulated (PWM), Current Source Inverters (CSI) and Voltage Source Inverters (VSI) to reduce the flow of harmonic current from the nonlinear load to the utility system. In the 1980's, with the availability of suitable power semiconductor devices, the application of active filter systems at the industrial level became feasible. Consequently, Power Quality as a defined subject was introduced in the early 1980's. However, till date, there is still a disagreement on the usage of the term. Bollen (Bollen, 2000) and Sankowa (Sankowa, 2001) published textbooks which define power quality and other associated terms.

Furthermore, Diwan, et al. carried out harmonic distortion minimization on 6.6kV bus with six pulse rectifier load using shunt passive filters (Diwan, et al., 2010 and Diwan et al, 2011) and have basis for comparison of the effectiveness of single tuned and high pass filters. Srivastava, et al. discussed the consequences of harmonics on distribution and transmission systems, including the design process for two types of passive shunt filters, namely: single-tuned filter and high pass filter, for the mitigation of harmonics in the power system (Srivastava, et al., 2013). Khan, et al. studied a method that detects the harmonics present in the current drawn by the induction motor by analysing current

waveform through an oscilloscope and then designed harmonic filter using MATLAB programming (Khan, et al., 2011). This was implemented on a single phase induction motor for removing the harmonics. Sandesh, et al. improved power factor of consumer loads or equipment by using power factor correction switches banks to generate locally the reactive energy necessary for the transfer of electrical useful power, allows a better and more rational technical – economical management of the plants. When the power factor is reduced to unity, the harmonic distribution would have been reduced (Sandesh, et al., 2012). Ghallab M.R. studied various techniques for damping harmonic resonances in power systems. It involves the connection of a Reactor in series with the shunt power factor correction capacitor, damping resistance across inductor terminals of LC passive filter, derating the harmonic generating equipment, and by using hybrid active filters (Ghallab, 2011). Significant improvement of in damping of harmonic resonances was recorded, compared with the passive filter when used alone.

Majority of the aforementioned works done so far on harmonics were mainly on low voltage networks, i.e. 3-phase-4-wire networks or on specific customer equipment. Also, not all parts of the network are often involved in the analysis. Thus, it would be difficult to generalize the results of harmonic mitigation carried out for the whole network. This work, therefore, proposes harmonic analysis and mitigation of a network of seven (7) Busbars, 33kV interconnected distribution system of Island Business District, Eko Electricity Distribution Plc, Nigeria. The work to be carried out on the network would include power flow analysis, harmonic analysis, as well as harmonic mitigation using passive filters.

1.3 Research Aim and Objectives

The aim of this research work is to investigate harmonics and its effective control on a 33kVpowerdistribution networks to enhance quality power supply to the esteemed customers. In pursuing this goal, the objectives to be achieved in the course of this research are as follows:

i. Comparative study of existing methodologies of computing power flow and harmonics.
ii. Modelling and simulation of a typical 33kV distribution network for power flow.

iii. Formulation of harmonic simulation algorithms for selected network topology to suit the evaluation of the harmonics.

iv. Implementation of algorithm in (iii) above using MATLAB and with the application of the results obtained in (ii) above.

v. Development of a solution/method for mitigating harmonics in the studied network.

vi. Analysis of the results obtained in power flow, harmonic evaluation and its mitigation effects.

1.4 Contribution of the Thesis to Knowledge

1. Research on previous work done on harmonic mitigation reveals that passive filter approach to harmonic mitigation was very common to low voltage distribution networks, i.e. 3-phase-4-wire networks, but this research has successfully presented passive filter approach to harmonic mitigation on a 33kV distribution network.
2. The following four academic papers have all been published in both local and international journals:
    i. "Harmonic Analysis in a 33kV Distribution Network: A Case Study of Island Business District" - Published in Vol 8., No. 2, June 2015 issue of the African Journal of Computing and ICTs (AJOCICT).
    ii. "Harmonic Mitigation on a 33kV Distribution Line using Passive Filters", also Published in Vol 8, No. 2, June 2015 issue of the IEEEs African Journal of Computing and ICTs (AJOCICT).
    iii. "Power Flow Analysis of Island Business District 33kV Distribution Grid System with Real Network Simulations", Published in Vol. 5, Issue 7 (Part - 1), July 2015 of the International Journal of Engineering Research and Applications (IJERA).
    iv. "Determination of Total Harmonic Distortion (THD) on a 33kV Distribution Network: A Case Study of Island Business District", Published in Vol. 34, No. 4, October 2015 issue of the Nigerian Journal of Technology (NIJOTECH).

1.5 Thesis Organisation

A brief introduction to power quality and background information on harmonics in power systems has been provided. This has been followed by a description of the problem statement and objectives of this research. The remainder of this research is organized as follows:

Chapter two presents a literature review of iterative power flow solution methods and convergence of the Newton-Raphson method. A brief discussion on harmonic sources, their impact or effects on power system and power system components are provided. A discussion on IEEE 519-1992 standard is also provided. Harmonic representation and measurement as well as existing methods for determining sources of harmonic distortion were extensively discussed. Methods of minimizing harmonics on the distribution line are also discussed.

Chapter three presents NEPLAN software for power flow Analysis and its application to Island Business District's 33kV Distribution Network, Eko Electricity Distribution Plc. It also presents Network modelling and Newton-Raphson Power flow algorithm. Modelling of a distribution line and the development of a flowchart for harmonic analysis are also presented. Harmonic simulation algorithm, modelling of a distribution line for harmonic control and the mitigation of harmonics are all presented.

The power flow analysis, harmonics generation on the line, as well as harmonic mitigation results are presented in chapter four. A detailed discussion on power flow results and the comparison of harmonic results for the two days considered in this research are also presented in this chapter. Total Harmonic Distortion (THD) of the network for the two days considered was evaluated through summation of THD of the distribution lines. Harmonic mitigation results are also analysed and discussed.

Chapter five presents the conclusions of this thesis and discusses the specific observations on this research along with recommendations for future work.

CHAPTER TWO

LITERATURE REVIEW

2.1 Power System Frequency and Voltage Regulation

A power system is required to maintain a continuous balance between electrical generation and varying load demand so that system frequency and voltage are maintained at their statutory levels. This calls for the control of the generated power in response to the demanded power. If the generated power is higher than the demand, the generator's speed tends to increase with the increase in generated voltage, and the grid frequency. On the other hand, should the total generated power be insufficient to meet the demand, both frequency and voltage will tend to fall.

Generating sets have frequency control loops for regulating the supply frequency. Also, grid frequency control is achieved through load and generation scheduling. This frequency is continuously monitored so that when any tendency to rise or fall is noticed, the control engineers take appropriate action by regulating the generators' power outputs.

However, several approaches are available to control the grid network voltage. The voltage can be controlled by injecting into the power system network, appropriate reactive power. The three methods of injection currently available are:

1. Static shunt capacitors and reactors
2. Static series capacitors
3. Synchronous compensators.

Shunt capacitors are used for lagging power factor circuits; whereas reactors are used on those with leading power factors such as created by lightly loaded cables. In both cases, the effect is to supply the requisite reactive power to maintain the values of the voltage. These capacitors are connected either directly to a Busbar or to the tertiary winding of a main transformer to minimize the losses and voltage drops. The series capacitors are connected in series with the line conductors and are used to reduce the inductive reactance between the supply point and the load. It produces high overvoltage

such that when a short-circuit current flows through the capacitor, special protective devices such as spark gap, etc. are incorporated. A synchronous compensator is a synchronous motor running without a mechanical load, and have varying values of excitation that can be absorbed. When used with a voltage regulator, the compensator can automatically run over-excited at times of high load and under-excited at light load.

Furthermore, the voltage can be controlled using tap-changing transformers. This is achieved by changing the transformation ratio, thus, the voltage in the secondary circuit is varied and voltage control obtained. This method constitutes the most popular and widespread form of voltage control at all voltage levels.

2.2 Iterative Power Flow Solution Methods

In Power System Engineering, the load (or power) flow study is an important tool involving numerical studies applied to a power system. A power flow study uses simplified notation such as a one line diagram and per unit system, and focuses on various forms of AC power (i.e. reactive, real and apparent) rather than voltage and current. It analyses the power system in normal steady state operation (Shukla and Bhaoria, 2013).In the process of power flow study, investigation is required in regards to bus voltages and amount of power flow through transmission lines. Power flow study aims at reaching to the steady state solution of complete power networks. Power flow equations represent a set of non-linear simultaneous algebraic equations (Kim, et al., 2007).

The iterative techniques for solving the non-linear network equations for the power flow problem are reviewed in the following subsections.

2.2.1 Gauss Method

Gauss method finds the solution of the function f (x) = 0 by first rearranging the equation in the form,

$$x = f(x) \tag{2.1}$$

The algorithm for the iterative process is then:

$$x^{(k+1)} = f\left(x^{(k)}\right) \tag{2.2}$$

where k is the iteration counter.

Gauss method first assumes a value for x. $x^{(0)}$, and then uses equation (2.2) to solve for new values of x. The new value is compared to its most recent value and the process continues until the change in voltage is very small, i.e.,

$$x^{(k+1)} - x^{(k)} < \in \quad \textbf{(2.3)}$$

The net power injected at a bus is expressed as:

$$\frac{(P_p - jQ_p)}{E_p^*} = \sum_{\substack{q=1 \\ q \neq p}}^{NB} \left[Y_{qp} E_p\right] + Y_{pp} E_p \quad \textbf{(2.4)}$$

In order to apply Gauss' iterative method to the solution of equation (2.4), the equation is re-written with E_p as the subject. Thus, the voltage at iteration number k is given by,

$$E_p^{(k)} = \frac{1}{Y_{pp}} \frac{P_p - jQ_p}{E_p^{(k-1)*}} - \frac{1}{Y_{pp}} \sum_{\substack{q=1 \\ q \neq p}}^{NB} Y_{qp} E_p{}^{(k-1)} \quad \textbf{(2.5)}$$

The iteration process starts at iteration 1 with an initial guess of all voltages $E^{(0)}$ and continues until the convergence criterion (Arrillaga, et al., 2000)is satisfied:

$$\left| E_p^{(k)} - E_p^{(k-1)} < \in \right| \quad \textbf{(2.6)}$$

where, $\in$ is a certain small number.

Note that the voltage for the slack bus need not be computed in the above iterative process. Since for the slack bus, voltage is already specified. Having calculated all the voltages at the buses, the current can then be determined (Arrillaga, et al., 2000) using Equation (2.7) and line flows and losses evaluated. The process is illustrated in the flowchart of Figure 2.1. The method is simple; however, it has the disadvantage of slow convergence and sometimes, the process may not converge at all depending on the starting value selected (Jonas, 1996):

$$I_{p=\frac{(P_p - J\dot{Q}_p)}{E_p^*}} \quad \textbf{(2.7)}$$

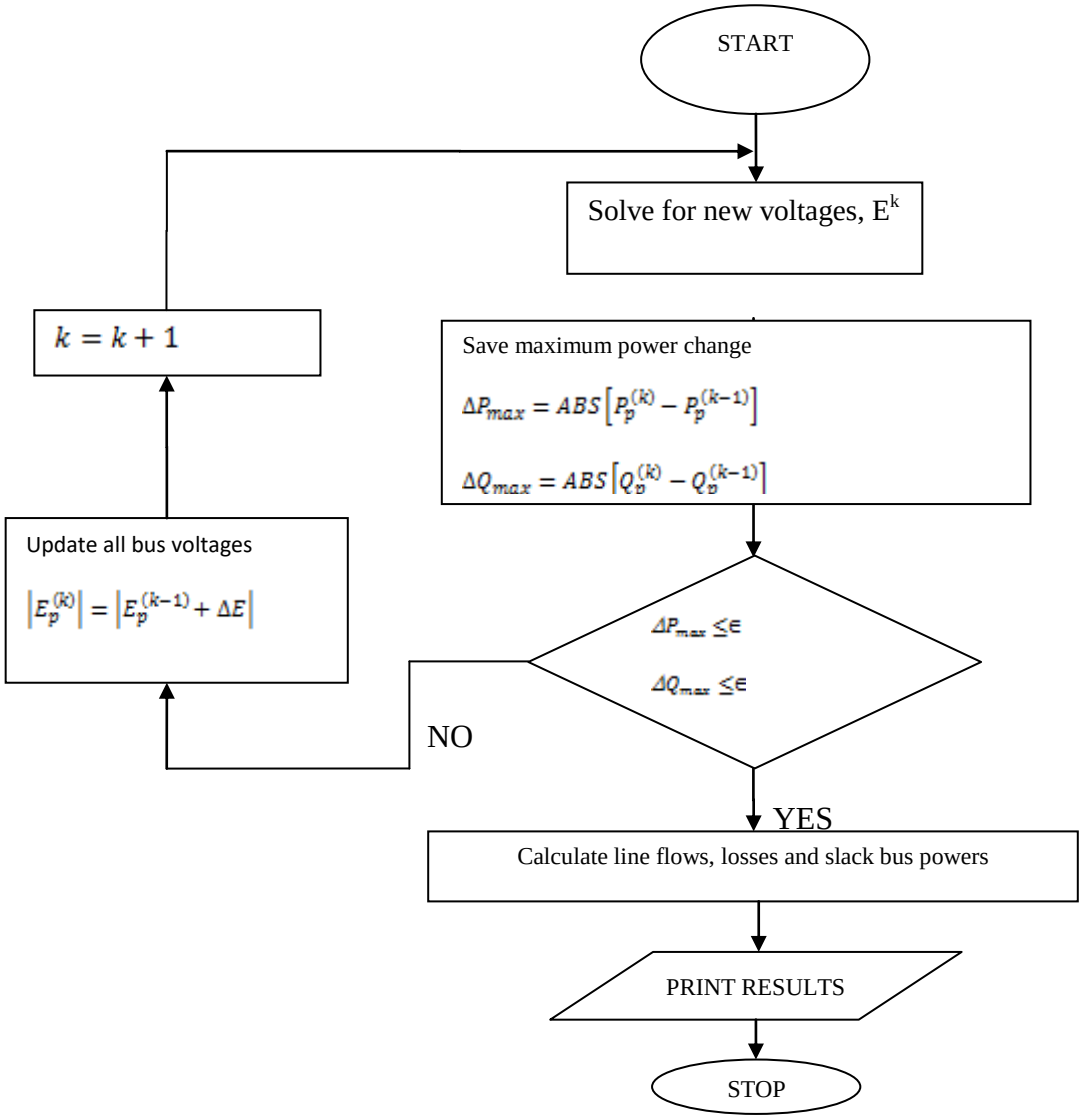

Figure 2.1: Flowchart of the Gauss Power Flow Solution

2.2.2 Gauss-Seidel Method

The Gauss-Seidel (G-S) method is a modification of the Gauss method, whereby, new iterates are utilized as soon as they are available. G-S method was the first AC power flow method to be developed for solution on digital computers (Allen,et al., 2012 and Alqadi, et al. 2007). Gauss-Seidel method is also known as the method of successive displacements (Isa, 2007). Thus, the process converges much faster than the Gauss method. In this solution procedure, calculation for a new voltage at each bus is made based on the most recently calculated voltage at all neighboring buses. At any node p, the already scanned nodes up to q will have new values appropriate to iteration count k and the nodes yet to be scanned (q > p) are appropriate to the iteration (K – 1). Thus, the voltage at node p, at the kth iteration is given by (Allen and Bruce, 2012):

$$E_p^{(k)} = \frac{1}{Y_{pp}} \frac{P_p - jQ_p}{E_p^{(k-1)*}} - \frac{1}{Y_{pp}} \sum_{\substack{q>p \\ q \neq p}}^{NB} Y_{qp} E_p{}^{(k-1)} + \frac{1}{Y_{pp}} \sum_{\substack{q<p \\ q \neq p}}^{NB} Y_{qp} E_p{}^{(k)} \qquad \textbf{(2.8)}$$

Where p = 1,2,3 , ….,...,NB; $p \neq s$

The Gauss-Seidel method is characteristically long in solving due to its slow convergence compared with other methods in systems with one or more of the features as under (j - VTU e-Learning Centre):

- Systems having large number of radial lines
- Systems with short and long lines terminating on the same bus
- Systems having negative values of transfer admittances
- Systems with heavily loaded lines, etc.

Often, difficulty is experienced with unusual network conditions such as negative reactance branches (Allen and Bruce, 2012). However, it is easily adoptable and efficient for systems with fewer numbers of buses. The flowchart is the same as that for Gauss method except that new voltages are computed using Equation (2.8).

2.2.3 Relaxation Method

This method is used for solving power flow problems, such that Equation (2.6) becomes:

$$Y_p - I_p = R_p \quad \textbf{(2.9)}$$

Where, R_p = Residual and represents the error in current at the bus p, resulting from the assumed voltage solution.

The equation is written for all buses except the slack bus whose voltage is specified. With the set of assumed voltages, bus currents can be calculated; and then bus residuals are calculated from Equation (2.9).

A voltage correction is obtained for that bus at which the residual R_p is a maximum. If the current at bus p remains constant, the residual R_p would be reduced to zero by the voltage correction ΔE given as:

$$E_p^{(k)} = -\frac{R_p^{(k)}}{Y_{pp}} \quad \textbf{(2.10)}$$

Where, Y_{pp} = the diagonal admittance and k = iteration count. An improved estimate of voltage for bus p is then:

$$E_p^{(k)} = E_p^{(k-1)} + \Delta E_p^{(k-1)} \quad \textbf{(2.11)}$$

And the new current is:

$$I_p^{(k)} = \frac{P_p - jQ_p}{E_p^{(k)*}} \quad \textbf{(2.12)}$$

Consequently, the actual residual at bus p is:

$$R_p^{(k)} = I_p^{(k-1)} - I_p^{(k)} \quad \textbf{(2.13)}$$

Using the voltage$E_p^{(k)}$, the new residuals for buses other than p and the slack bus are calculated from (Arrillaga, Bollen and Watson, 2000):

$$R_p^{(k)} = R_p^{(k-1)} + Y_{qp}\Delta E_p^{(k-1)} \quad \textbf{(2.14)}$$

$$q = 1,2,3,\dots,N; q \neq p$$

The process is repeated, each time correcting the value of the voltage corresponding to the largest residual, until all residuals are less than or equal to a specified tolerance. The process is illustrated in the flowchart of Figure 2.2.

2.2.4 Newton-Raphson Method

The Gauss Seidel method offers some advantages in the power flow problem solution. Principally, it offers ease of programming and low memory requirements; most especially when Y_{bus} formulation is sparsely programmed. Its principal disadvantage, which is its relatively slow convergence, motivated the development of Newton-Raphson method of solving power flow problems.

The method involves the idea of finding a vector $x \in IR^{N}$ such that,

$$F(x) = 0 \tag{2.15}$$

where F is a vector valued function of dimension N. let X_s be the vector solution. Expand Equation (2.15) in a Taylor series about: $x = x_s$,

$$F(x) = F(x_s) + J(x - x_s) + higherorderterms \tag{2.16}$$

Note that F vanishes at x_s and Equation (2.16) may be solved for x_s if higher order terms are ignored.

$$x_s = x - J^{-1}F(x) \tag{2.17}$$

Due to the error in neglecting the higher order terms in the Taylor series, Equation (2.17) is only approximate, but is used to iteratively determine $x_{s;}$ i.e., for iteration k,

$$x^{(k+1)} = x^{(k)} - \frac{F(x^{(k)})}{F'(x^{(k)})} \tag{2.18}$$

Extending this to the multivariable case yields:

$$x^{(k+1)} = x^{(k)} - J^{-1}x^{(k)}F\left(x^{(k)}\right) \tag{2.19}$$

Where x and F are column vectors and $J^{-1}x^{(k)}$ is the Jacobian matrix evaluated at the k^{th} - iteration.

Consider now, the application of an n-bus power system, for a line connecting buses p and q of admittance:

$$Y_{pq} = G_{pq} - jB_{pq} \quad \textbf{(2.20)}$$

And,

$$G_{pq} = \frac{R_{pq}}{(R_{pq})^2 + (X_{pq})^2} \quad \textbf{(2.21)}$$

$$B_{pq} = \frac{X_{pq}}{(R_{pq})^2 + (X_{pq})^2} \quad \textbf{(2.22)}$$

Where,

G_{pq}= Conductance of the line pq
B_{pq}= Capacitive susceptance of the line pq
R_{pq}= Resistance of the line pq
X_{pq}= Reactance of the line pq

The power at bus p is:

$$P_p - jQ_{pq} = V_p^* I_p = V_p^* \sum_{q=1}^{NB} Y_{pq} V_q \quad \textbf{(2.23)}$$

Where, the voltage V_p at bus p is,

$$V_p = e_p + \mathrm{j} f_p \quad \textbf{(2.24)}$$

And the current is:

$$I_p = C_p + \mathrm{j} d_p \quad \textbf{(2.25)}$$

Then the power at bus p may be expressed as (Pradhan and Thatoi, 2012):

$$P_p - jQ_p = (e_p + \mathrm{j} f_p) \sum_{q=1}^{NB} [(G_{pq} - B_{pq})(e_p + \mathrm{j} f_p)] \quad \textbf{(2.26)}$$

From the Equation (2.26)

$$P_p = \sum_{q=2}^{NB} [e_p (e_q G_{pq} + f_p B_{pq}) + f_p (f_p G_{pq} - e_q B_{pq})] \quad \textbf{(2.27)}$$

$$Q_p = \sum_{q=2}^{NB} [f_p (e_q G_{pq} + f_p B_{pq}) - e_q (f_q G_{pq} - e_q B_{pq})] \quad \textbf{(2.28)}$$

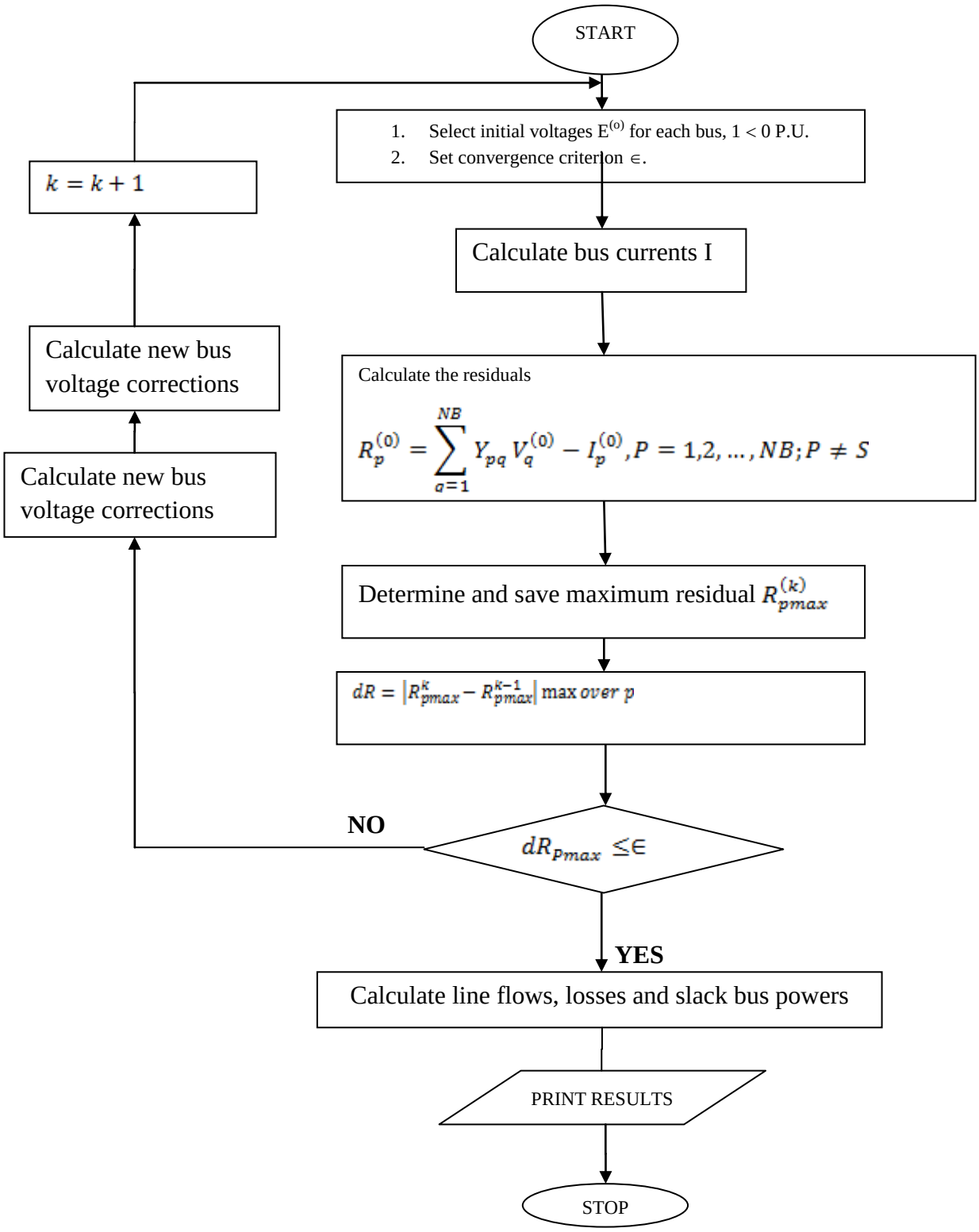

Figure 2.2: Flowchart of the Relaxation of Power Flow Solution

It has been assumed that the slack bus is the bus number 1 of the network. Changes in p and q are related to changes in e and f by taking partial derivatives in Equations (2.27) and (2.28) e.g.:

$$\Delta P_1 = \frac{\partial P_2 \Delta e_2}{\partial e_2} + \frac{\partial P_2 \Delta e_3}{\partial e_3} + \cdots \quad \textbf{(2.29)}$$

Similar equations hold in terms of ΔP and Δf, and ΔQ in terms of Δe and Δf. The equations may be generally expressed as follows(Adejumobi, et al., 2013):

$$\begin{bmatrix} \Delta P \\ \cdots\cdots\cdots\cdots \\ \Delta Q \end{bmatrix} = \begin{bmatrix} \frac{\partial P}{\partial e} & \frac{\partial P}{\partial f} \\ \cdots\cdots & \cdots\cdots \\ \frac{\partial Q}{\partial e} & \frac{\partial Q}{\partial f} \end{bmatrix} \begin{bmatrix} \Delta e \\ \cdots\cdots\cdots\cdots \\ \Delta f \end{bmatrix} = [J] \begin{bmatrix} \Delta e \\ \Delta f \end{bmatrix} \quad \textbf{(2.30)}$$

where J is the Jacobian matrix which for convenience may be partitioned as:

$$J = \begin{bmatrix} J^1 & J^2 \\ \cdots\cdots & \cdots\cdots \\ J^3 & J^4 \end{bmatrix}$$

The entries of the Jacobian matrix are computed as follows:

Submatrix J^1

$$J^1{}_{pq} = \frac{\partial P_p}{\partial e_q} = e_q G_{pq} - f_p B_{pq}, \ p \neq q \quad \textbf{(2.31a)}$$

$$J^1{}_{pp} = \frac{\partial P_p}{\partial e_p} = e_p G_{pp} - f_p B_{pp} + C_p \quad \textbf{(2.31b)}$$

Submatrix J^2

$$J^2{}_{pq} = \frac{\partial P_p}{\partial f_q} = e_q B_{pq} + f_p G_{pq}, \ p \neq q \quad \textbf{(2.31c)}$$

$$J^2{}_{pp} = \frac{\partial P_p}{\partial f_p} = e_p B_{pp} + f_p G_{pp} + d_p \quad \textbf{(2.31d)}$$

Submatrix J^3

$$J^3{}_{pq} = \frac{\partial Q_p}{\partial e_q} = e_q B_{pq} + f_p G_{pq},\ p \neq q \quad \textbf{(2.31e)}$$

$$J^3{}_{pp} = \frac{\partial Q_p}{\partial e_p} = e_p B_{pp} + f_p G_{pp} - d_p \quad \textbf{(2.31f)}$$

Submatrix J^4

$$J^4{}_{pq} = \frac{\partial Q_p}{\partial f_p} = -e_p G_{pq} + f_p B_{pq},\ p \neq q \quad \textbf{(2.31g)}$$

$$J^4{}_{pp} = \frac{\partial Q_p}{\partial f_q} = -e_p G_{pp} + f_p B_{pp} + C_p,\ p \neq q \quad \textbf{(2.31h)}$$

The solution starts with the iteration counter k set to zero and all the buses except the slack bus being assigned voltages,

$$V_p = 1 + j0 \text{ per unit.}$$

Also, J^1, J^2, J^3, and J^4 actually are related to kind of buses. For PV-buses the variable need to optimize are x and ΔQ, and for PQ-buses, x and ΔP, so J^1, J^2, J^3, and J^4 can be written as shown in Equations (2.31a-h) (Syai'in & Soeprijanto, 2012).

The main program then calls SUB powers, which computes P and Q using Equations (2.27) and (2.28). It also calculates the power mismatches:

$$\Delta P_p^{(k)} = P_{sp} - P_p^{(k)} \quad \textbf{(2.32)}$$

$$\Delta Q_p^{(k)} = Q_{sp} - Q_p^{(k)} \quad \textbf{(2.33)}$$

For p = 2,3,…,NB, $p \neq$ Generator buses

Furthermore, the maximum mismatches ΔP_{max} and ΔQ_{max} are stored in memory. If $\Delta P_{max} \leq \in$ per unit and $\Delta Q_{max} \leq \in$ per unit, then the iterative process has converged and

control transfers to SUB Power flows; otherwise, controlled transferred to SUB currents to compute the bus currents using:

$$I_p^{(k)} = \frac{P_p^{(k)} - jQ_p^{(k)}}{V_p^{(k)*}} = c_p^{(k)} + jd_p^{(k)} \quad \textbf{(2.34a)}$$

but,

$$v_p^{(k)*} = e_p^k - jf_p^k$$

$$I_p^{(k)} = \frac{P_p^{(k)} e_p^k + Q_p^{(k)} f_p^k - j\left(Q_p^{(k)} e_p^k\right) P_p^{(k)} + f_p^k}{\left(e_p^k\right)^2 + \left(f_p^k\right)^2} \quad \textbf{(2.34b)}$$

thus,

$$c_p^{(k)} = \frac{P_p^{(k)} e_p^k + Q_p^{(k)} f_p^k}{\left(e_p^k\right)^2 + \left(f_p^k\right)^2} \quad \textbf{(2.35)}$$

$$d_p^{(k)} = \frac{P_p^{(k)} f_p^k - Q_p^{(k)} e_p^k}{\left(e_p^k\right)^2 + \left(f_p^k\right)^2} \quad \textbf{(2.36)}$$

After the currents have been calculated, control transfers to SUB Jacobian which computes the elements of the Jacobian matrix using Equation (2.31) SUB voltages is then called to solve the linear system of Equations (2.30) for the voltages Δe and Δf. This subroutine makes use of triangular factorisation and forward and back substitution to solve for the voltages.

The Jacobian J is factorised into two matrices.

$$J = LU \quad \textbf{(2.37)}$$

where L is the lower left triangular (i.e. $L_{rc} = 0$ for c <r) and U is upper right triangular (i.e. $U_{rc} = 0$ for r > c).

Specifically,

$$L = \begin{bmatrix} L_{11} & 0 & 0 & - & - \\ L_{21} & L_{22} & 0 & - & - \\ L_{31} & L_{32} & L_{33} & - & - \\ - & - & - & - & - \end{bmatrix}$$

$$U = \begin{bmatrix} u_{11} & u_{12} & u_{13} & - & - \\ 0 & u_{22} & u_{23} & - & - \\ 0 & 0 & u_{33} & - & - \\ - & - & - & - & - \end{bmatrix}$$

In general, the factors are computed using,

$$L_{rc} = \frac{J_{rc} - \sum_{q-1}^{c-1} L_{rq} u_{qc}}{u_{cc}} \quad \textbf{(2.38)}$$

$$c = 1,2, \dots, r-1$$

$$u_{rc} = \frac{\sum_{q-1}^{r-1} L_{rq} u_{qc}}{u_{cc}} \quad \textbf{(2.39)}$$

$$c = 1,2, \dots, r+1 \dots, N$$

In general, the rules for the formation of L and U are as follows:

1. Row I of J is not modified. (the elements correspond to those of the first row of u)
2. Row 2 of J is modified to yield one L and (n-1) U's. These entries are found using equations (2.38) and (2.39). For these equations, when summation upper index is zero, there are no terms in the sum (i.e. ignore the summation term). When the upper and lower indices of the summation are the same, there is a single term in the sum.
3. Rule (2) is repeated for each row and J is replaced by the factors. In row r, there will be (r-1) L – terms calculated and (n - r+1) U – terms.

Having found the factors of the solution,

$$Lw = \begin{bmatrix} \Delta P \\ \Delta Q \end{bmatrix} = b \quad \textbf{(2.40)}$$

$$\mathrm{U}\begin{bmatrix}\Delta e\\ \Delta f\end{bmatrix} = w \text{ or } Ux = w \qquad \textbf{(2.41)}$$

The vector b is converted into w, since L_{11} is unity w_1, b_2 with w_2, etc. having found w, a similar process is used to find:

$$x = \begin{bmatrix}\Delta e\\ \Delta f\end{bmatrix}$$

The last row of (2.38) is:

$$u_{nn}x_n = w_n$$

and x_n is readily found. Again, x_n replaces w_n. in row n-1,

$$U_{n-1,\ n-1}\, x_{n-1} + U_{n-1,\ n}\, x_n = w_{n-1}$$

and

$$x_{n-1} = \frac{w_{n-1} - U_{n-1,\ n}\, x_n}{U_{n-1,\ n-1}}$$

Element x_{n-1}replaces w_{n-1}. The process continues for rows n-2,n-3,…,1. In row r,

$$x_r = \frac{w_r - \sum_{q=r+1}^{n} U_{rq}x_q}{U_{rr}}$$

This completes the solution for the voltage corrections, $\Delta e^{(p)}$ and $\Delta f^{(p)}$.

The subroutine then updates the voltages for the next iteration as,

$$e_p^{(k+1)} = e_p^{(k)} + \Delta e_p^{(k)}$$

$$f_p^{(k+1)} = f_p^{(k)} + \Delta f_p^{(k)}$$

The iteration count is increased by 1, i.e. k = k + 1, and control is transferred to Sub Powers.

When the power mismatch becomes negligible, then control is transferred to SUB a power flow which evaluates the power flows as well as the power losses in the lines. In SUB power flows, the power flowing from Bus p to Bus q and measured at Bus p is given as:

$$S_{pp} = P_{pq} - jQ_{pq} \qquad \textbf{(2.42)}$$

$$= E_p^*\left(E_p - E_q\right)Y_{pq} + E_p^* E_p \frac{Y_{pq\,sht}^*}{2}$$

Separating the real and imaginary parts yields:

$$P_{pq} = G_{pq}\left(e_p^2 + f_p^2\right) + B_{pq}\left(e_p f_q - f_p e_q\right) - G_{pq}(e_p e_q + f_p f_q) \qquad \textbf{(2.43)}$$

$$Q_{pq} = B_{pq}\left(e_p^2 + f_p^2\right) + G_{pq}\left(f_p e_q - e_p f_q\right) - B_{pq}\left(e_p e_q + f_p f_q\right) + \frac{Y_{sht}(e_p^2 + f_p^2)}{2} \qquad \textbf{(2.44)}$$

Similarly, the power q to p and metered at q is given by:

$$P_{qp} = G_{pq}\left(e_p^2 + f_p^2\right) + B_{pq}\left(e_q f_p - f_q e_p\right) - G_{pq}(e_q e_p + f_q f_p) \qquad \textbf{(2.45)}$$

$$Q_{qp} = B_{pq}\left(e_p^2 + f_p^2\right) + G_{pq}\left(f_q e_p - e_q f_p\right) - B_{pq}\left(e_q e_p + f_q f_p\right) + \frac{Y_{sht}(e_q^2 + f_q^2)}{2} \qquad \textbf{(2.46)}$$

Power losses in each branch of the network are obtained as the algebraic sum of the power calculated using Equations (2.45) and (2.46) and that calculated using Equations (2.43) and (2.44) respectively. While the total power losses in the system is the sum of the absolute values of the calculated power losses in each branch of the network.

The above method of obtaining a converging solution for a set of nonlinear equations can be used for solving the load flow problem. Since the final voltage solution is not much different from the nominal values, Newton-Raphson method is particularly suited to the load flow problem(Murthy, 2007).

The slack bus power is determined by summing the power flows on the lines terminating at the slack bus.

The solution to the Newton-Raphson power flow runs according to the flowchart of Figure 2.2

2.2.5 Fast-Decoupled Method

It was demonstrated in the late 1970s that the storage and computing requirements of the Newton-Raphson method could be reduced very significantly by introducing a series of well-sustained simplifying assumptions (Adejumobi, et al., 2013). These assumptions are based on physical properties exhibited by power systems, particularly those of high-voltage transmission systems. The resulting formulation is no longer a Newton-Raphson method but a derived formulation described as Fast-decouple Newton-Raphson method (Adejumobi, et al., 2013). The power mismatch equations of both methods are identical but their Jacobians are quite dissimilar; the Jacobian elements of the Newton–Raphson method are voltage–dependent, while those of the Fast-decoupled Newton-Raphson method are voltage-independent (i.e. constant parameters). Moreover, the number of Jacobian entries used in the Fast-decoupled Newton-Raphson method is only half of those used in the Newton-Raphson method but has strong convergence characteristics. However, an asset of the Fast decouple Newton- Raphson method is the fact that one of its iterations takes only a fraction of the time required by Newton-Raphson's method of iterations. The decoupled equation requires considerable less time to solve compared to the time required for the solution by the Newton-Raphson Method (Prechanon, 2010 and Adejumobi, et al., 2013).

The fast-decoupled power flow provides rapid solution for power systems with low resistance and susceptance ratio (Kumkratug, 2010).

2.3 The Convergence of the Newton-Raphson Method

Newton-Raphson method is an extremely powerful technique. In general, the convergence is quadratic; as the method converges on the root, the difference between the root and the approximation is squared at each step. However, there are some difficulties with the method.

The equation, $0 \approx f(x_0) + hf'(x_0)$, comprises of informal and imprecise symbols. However, no numerical procedure works for all equations. We quite conclude that $h \approx \frac{f(x_0)}{f'(x_0)}$. This can be wrong if $f'(x_0)$ is close to 0. Thus, it could be seen that first derivatives close to 0 would be bad for the Newton-Raphson method. These informal

considerations can be turned into positive theorem about the behavior of the error in the Newton-Raphson method. For example, if $\frac{f''(x)}{f'(x)}$ is not too large near r, and we start with x_o close enough to r, the Newton-Raphson method converges very fast to r.

Furthermore, Newton-Raphson method requires that the derivative be calculated directly. An analytical expression for the derivative may not be easily obtainable and could be expansive to evaluate. In this situation, it may be appreciable to approximate the derivative using the slope of a line through two nearby points on a function. This approximation would result in Secant method whose convergence is slower than that of the Newton-Raphson method.

2.4 Comparison of Iterative Power Flow Solution Methods

1. The time taken to perform an iteration of the computation is relatively smaller in case of Gauss-Seidel method as compared to Newton-Raphson method.
2. The number of iterations required by Gauss-Seidel method for a particular system is greater compared to Newton-Raphson method and they increase with an increase in the size of the system. In case of Newton-Rapson method, the numbers of iterations is more or less independent of the size of the system and vary between 3-5 iterations.
3. The convergence characteristics of Newton-Raphson method are not affected by the selection of a slack bus, whereas, that of Gauss-Seidel method is sometimes adversely affected and the selection of a particular bus may result in poor convergence (Hota and Mallick, 2011)

2.5 NEPLAN Planning and Optimization Software

The Electrical Engineering Department of Petru Maior University has made efforts to provide students and researchers with simulation tools that cover different aspects of power system analysis. Two of the advanced and professional simulation packages are currently being used by their power system group: NEPLAN (since 2002) and EDSA (since 2006). The basic aim of computer-based simulation for power system is to reproduce real phenomena through computer-based simulation as an efficient solution for didactic and research purposes (Bica, et al., 2008).NEPLAN planning and

optimization software for electrical, heat, gas and water networks has been developed by the BCP group in Switzerland. It is used to analyze, plan, optimize and manage power transmission and distribution networks which includes optimal power flow, transient stability and reliability analysis. It can provide reliability indices for individual load points and the overall power system. It can also provide information based on the cost of unreliability along with investment analysis and the Net Present Value (NPV) of different investment alternatives. NEPLAN uses the homogenous Markov process for its calculations and handles up to second order contingencies. The NEPLAN tool is very flexible and user friendly planning tool where network designers can compile different topologies (Winter, 2011).NEPLAN as a reliability analysis tool is based on the Markov method. The output of this evaluation approach is reliability indices for both load point and the overall system along with load flow constraints (Winter, 2011).

Today, NEPLAN is a power system software applied worldwide for network planning, modelling and analysis. NEPLAN is used in more than 80 countries and by more than 600 companies, such as small and large electrical utilities, industries and universities. Petru Maior University of Tg.Mureş, through the Power System Group and Energy Systems Research Centre, became the first research and education institute in Romania which used NEPLAN software in 2002. Recently, due to a fruitful partnership with BCP team, the latest 5.3.5 version of NEPLAN and the university student version for student's education are implemented for the Power System Laboratory. Tracking the course content in a logic way, the Power Systems laboratories and project works focuses on modelling, simulation and analysis on computers, which represent a very efficient method for obtaining experience and enhance skills with power system. The recent availability of NEPLAN5.3isknown to be the university version for students, with advanced features and friendly interface, which permit an excellent practice–oriented work for each power system engineering phase and has plenty possibilities to enter graphically all the power systems elements, various analysis tools and flexibility (Bica, et al., 2008 and Pacis, et al. 2010).

Some features and modules of NEPLAN software are performed also at the appropriate courses for electric networks, reliability of power systems, protection systems and power quality.

NEPLAN permits to define, develop and manage the power systems elements, data, library and graphics. The main elements used currently in educational process for network design and applications are (Bica, et al., 2008, Dwane, 2003):

i. Transmission network elements: AC and DC transmission lines, two-, three- or four-winding transformers and buses;
ii. Classic compensating and Voltage Control devices: shunt capacitors, series capacitors, shunt reactors, synchronous condensers, regulating transformers such as tap-changing transformers;
iii. FACTS devices: Controlled static VAR compensators SVC, Static Compensators STATCOM, Thyristor Controlled Series Capacitors TCSC, United Power Flow Controller UPFC, Phase Shift Transformer PST; Excitation system, Automatic Voltage Regulator AVR, Power System Stabilizer PSS;
iv. Power System Loads: static loads, induction motors and load.

The Power System Group developed a set of theoretical descriptions, modules, practical exercises and case studies, which allow students to become familiar with NEPLAN. The main applications, features and contents which has currently available for Bachelor Degree and Master Degree programs are:

1. Graphic User Interface: The main toolbars and work menus; network input and representation; elements and symbol libraries.
2. Elements parameters and modeling: Power system static elements; Power system dynamic elements.
3. Load Flow analysis. The load flow analysis calculate the steady state buses voltage (magnitude and angle), branch currents, real and reactive power flows and losses: calculation parameters; setting of reference values; result representation in single line diagram and tables; limits control and change of buses type; automatic tap-changer of transformers; area interchange schedule; calculation of sensitivities of active power losses; contingency analysis.
4. Short circuit calculation: calculation parameters; short circuit between different voltage levels; calculation of extreme short circuit currents; results representation on single-line diagram and tables.

5. Optimal Power Flow: control variables; limits and constraints; objective functions.
6. Small-signal stability analysis: euigen values analysis of power systems; computation and plotting of euigen values, euigen vectors, mode shapes, and participation factors for euigen values and state variables (Bica, 2008 and Mc Granaghan, 2002).

2.6 Sources of Harmonics

This section reviews the harmonic-producing loads, as well as the negative effect of the equipment on a power system network. It also analyse the detrimental effect of certain harmonics (such as even and odd harmonics) on the loads in which they occur.

2.6.1 Harmonic Producing Loads

In order to understand the injection of harmonic currents in power distribution networks, it is necessary to discuss the general characteristics of nonlinear loads. Nonlinear loads inject harmonic currents or voltages into the distribution network even when fed by a sinusoidal voltage or current waveform. Nonlinear loads can be broadly divided into two categories (Mazumdar, 2006):

- Harmonic current source type loads;
- Harmonic voltage source type loads.

Thyristor controlled loads such as those used for dc drives; current source inverters (CSI), etc. constitute harmonic current source type loads. These loads produce harmonic currents on the AC supply side of the rectifier for their operation, analogous to induction motors which require reactive currents (Mazumdar, 2006). In contrast, diode rectifiers with dc side capacitors constitute harmonic voltage source type loads. These loads produce voltages on the ac side of the rectifier to operate, and are becoming prevalent due to their use in domestic electronic equipment, variable speed drives (VSDs), etc. Harmonic currents in the supply result due to harmonic voltages and are determined by the ac side impedance (Mazumdar, 2006).

The associated harmonic current passing through the system impedance causes voltage drops for each harmonic frequency based on Ohm’s Law. The vector sum of all

the individual voltage drops results in total voltage distortion, the magnitude of which depends on the system impedance, available system impedance and available system fault current levels of harmonic currents at each harmonic frequency(Siemens, 2013). The effects of harmonics can be summarized as follows:

- High fault current (stiff system)
  - Distribution system impedance and distortion is low
  - Harmonic current draw is high
- Low fault current (soft system)
  - Distribution system impedance and distortion is high
  - Harmonic current draw is low

For general purposes, the harmonic sources can be divided into three categories (Arrillaga, et al. 2000,Singla, et al. 2011, Sriranjai, et al. 2012 and Sriranjani, et al. 2013):

1. A large number of distributed nonlinear components of small rating (i.e. mass products), consists mainly of: single phase diode bridge rectifiers, power supplies of low voltage appliances (SMPS in TV sets, PCs and other IT equipment), and gas discharge lamps.
2. Large static power converters (SPC) are used more extensively for controlling loads. There are many forms of SPC: rectifiers, inverters, cyclo-converters, single-phase, three-phase, twelve-pulse, six-pulse, but all have the same character. They are all nonlinear and they inject non-sinusoidal current into the power system.
3. Large and continuously varying nonlinear loads. This refers mainly to electric metal-melting arc furnaces with power ratings in the tens of megawatts and connected directly to the transmission network. The furnace arc impedance varies randomly and extremely asymmetrical, since the carbon electrodes in contact with iron have dissimilar impedances between the positive and negative flows of current. Resistance welding has the same characteristics, where the copper electrodes and the steel being welded have dissimilar impedances between the positive and negative flows of current.

Figure 2.3 shows in detail the effect individual harmonic currents have on the impedances within the power system and the associated voltages drops for each. Note that the “total

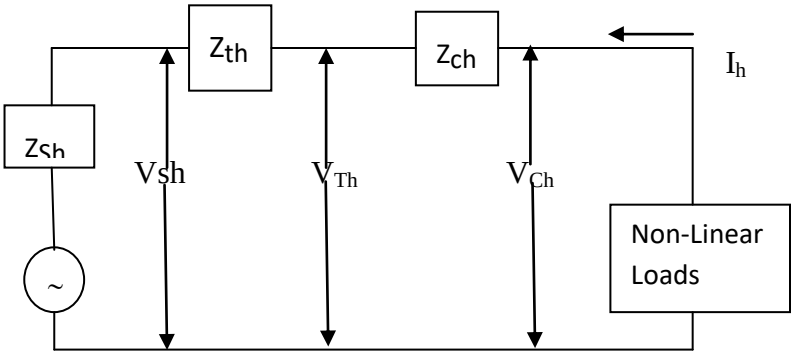

Figure 2.3: Individual harmonic voltage drops across system impedances

(Siemens, 2013)

harmonic voltage distortion", $\%THD_v$ (based on the vector sum of all individual harmonics), is reduced at source as more impedance is introduced between the nonlinear load and source (Siemens, 2013).

$$V_h = I_h \times Z_h \quad \textbf{(2.47)}$$

At load:

$$V_h = I_h \times (Z_{ch} + Z_{Th} + Z_{Sh}) \quad \textbf{(2.48)}$$

At transformer:

$$V_{Th} = I_h \times (Z_{Th} + Z_{Sh}) \quad \textbf{(2.49)}$$

At source:

$$V_h = I_h \times Z_{sh} \quad \textbf{(2.50)}$$

Where:

Z_h = Impedance at frequency of harmonic (e.g., 5^{th} harmonic, $5 \times 60 = 300$)

V_h = Harmonic voltage at h^{th} harmonic (e.g., 5^{th})

I_h = Harmonic current at h^{th} harmonic (e.g., 5^{th})

2.6.2 Impact of Harmonics

As far as the impact of harmonics on power system equipment is concerned, it can be generally stated that harmonics causes equipment (both in networks and in user's installations) to be subjected to voltages and currents at frequencies for which it was not designed (Mazumdar, 2006). The effects of such exposure are usually not instantly visible, but can have serious consequences in the medium and long term. Proliferation of three phase diode and thyristor bridge rectifiers for dc power supplies and as front-end rectifiers for inverter based applications such as VSDs and uninterrupted power supplies (UPS), has resulted in serious harmonic, reactive power, flicker and resonance problems in industrial applications and in transmission/distribution systems. Practically speaking, utilities frequently encounter harmonic related problems (Mazumdar, 2006, Jong-Gyeun, et al. 2011 and Key, et al' 1996).

In comparison with utility power supplies, the effects of harmonic voltages and harmonic currents are significantly more pronounced on generators (esp. stand-alone generators used a back-up or those on the ships or used in marine applications) due to their source impedance being typically three to four times that of utility transformers(Siemens, 2013).

The major impact of voltage and current harmonics is to increase the machine heating due to increased iron losses, and copper losses, since both are frequency dependent and increase with increased harmonics. To reduce this effect of harmonic heating, the generators supplying nonlinear loads are required
to be derated. In addition, the presence of harmonic sequence components with nonlinear loading causes localized heating and torque pulsations with torsional vibrations (Siemens, 2013, Babu, et al. 2010, Balci, et al. 2014, Bandgar, et al. 2013, Bangia, et al. 2013 and Uzunoglu, 2005).

2.6.2.1 Effect on Transformers

The effect of harmonic currents at harmonic frequencies causes increase in core losses due to increased iron losses (i.e., eddy currents and hysteresis) in transformers. In addition, increased copper losses and stray flux losses result in additional heating, and winding insulation stresses, especially if high levels of dv/dt (i.e., rate of rise of voltage) are present. Temperature cycling and possible resonance between transformer winding inductance and supply capacitance can also cause additional losses. The small laminated core vibrations are increased due to the presence of harmonic frequencies, which can appear as an additional audible noise. The increased rms current due to harmonics will increase the I^2R (copper) losses. The distribution transformers used in four-wire (i.e., three-phase and neutral) distribution systems have typically a delta-wye configuration. Due to delta connected primary, the odd (i.e. 3rd, 9th, 15th…) harmonic currents cannot propagate downstream but circulate in the primary delta winding of the transformer causing localized overheating. With linear loading, the three-phase currents will cancel out in the neutral conductor.

However, when nonlinear loads are being supplied, the triplen harmonics in the phase currents do not cancel out, but instead add cumulatively in the neutral conductor at a frequency of predominately 180 Hz (3rd HRM.), overheating the transformers and occasionally causing overheating and burning of neutral conductors. Typically, the uses of appropriate “K factor” rated units are recommended for non-linear loads (Siemens, 2013).

2.6.2.2 Effect on Induction Motors

Harmonics distortion raises the losses in AC induction motors in a similar way as in transformers and cause increased heating, due to additional copper losses and iron losses(eddy current and hysteresis losses) in the stator winding, rotor circuit and rotor laminations. These losses are further compounded by skin effect, especially at frequencies above 300 Hz. Leakage magnetic fields caused by harmonic currents in the stator and rotor end windings produce additional stray frequency eddy current dependent losses. Substantial iron losses can also be produced in induction motors with skewed rotors due to high-frequency-induced currents and rapid flux changes (i.e., due to hysteresis) in the stator and rotor. Excessive heating can degrade the bearing lubrication and result in bearing collapse. Harmonic currents also can result in bearing currents, which can be however prevented by the use of an insulated bearing, a very common practice used in AC variable frequency drive-fed AC motors. Overheating imposes significant limits on the effective life of an induction motor. For every 10°C rise in temperature above rated temperature, the life of motor insulation may be reduced by as much as 50%. Squirrel cage rotors can normally withstand higher temperature levels compared to wound rotors. The motor windings, especially if insulation is class B or below, are also susceptible to damage due high levels of dv/dt (i.e., rate of rise of voltage) such as those attributed to line notching and associated ringing due to the flow of harmonic currents (Siemens, 2013).

Harmonic sequence components also adversely affect induction motors. Positive sequence components (i.e., 7th, 13th, 19th…) will assist torque production, whereas the negative sequence components (5th, 11th, 17th…) will act against the direction of rotation resulting in torque pulsations. Zero sequence components (i.e, triple n harmonics) are capable of stationary motor (i.e not rotating), therefore, any harmonic energy associated with them is dissipated as heat. The magnitude of torque pulsations generated due to these harmonic sequence components can be significant and cause shaft torsional vibration problems (Siemens, 2013).

2.6.2.3 Effect on Cables

Cable losses, dissipated as heat, are substantially increased when carrying harmonic currents due to elevated I^2R losses, the cable resistance, R, determined by its DC value plus skin and proximity effect. The resistance of a conductor is dependent on the frequency of the current being carried. Skin effect is a phenomenon whereby current tends to flow near the surface of a conductor where the impedance is least. An analogous phenomenon, proximity effect, is due to the mutual inductance of conductors arranged closely parallel to one another. Both of these effects are dependent upon conductor size, frequency, resistivity and the permeability of the conductor material. At fundamental frequencies, the skin effect and proximity effects are usually negligible, at least for smaller conductors. The associated losses due to changes in resistance, however, can increase significantly with frequency, adding to the overall I^2R losses (Siemens, 2013).

2.6.2.4 Effect on Breakers and Fuses

The vast majority of low voltage thermal-magnetic type circuit breakers utilize bi-metallic trip mechanisms which respond to the heating effect of the rms current. In the presence of nonlinear loads, the rms value of current will be higher than for linear loads of same power. Therefore, unless the current trip level is adjusted accordingly, the breaker may trip prematurely while carrying nonlinear current. Circuit breakers are designed to interrupt the current at a zero crossover. On highly distorted supplies which may contain line notching and/or ringing, spurious “zero crossovers” may cause premature interruption of circuit breakers before they can operate correctly in the event of an overload or fault. However, in the case of a short circuit current, the magnitude of the harmonic current will be very minor in comparison to the fault current. Fuse ruptures under over current or short-circuit conditions is based on the heating effect of the rms current according to the respective I^2tcharacteristic. The higher the rms current, the faster the fuse will operate. On nonlinear loads, the rms current will be higher than for similarly-rated linear loads, therefore fuse derating may be necessary to prevent premature opening. In addition, fuses at harmonic frequencies, suffer from skin effect and more importantly, proximity effect, resulting in non-uniform current distribution across the fuse elements, placing additional thermal stress on the device (Siemens, 2013).

2.6.2.5 Effect on Lighting Systems

One noticeable effect on lighting is the phenomenon of "flicker" (i.e., repeated fluctuations in light intensity). Lighting is highly sensitive to rms voltage changes; even a slight deviation (of the order of 0.25%) is perceptible to the human eye in some types of lamps. Superimposed inter-harmonic voltages in the supply voltage are a significant cause of light flicker in both incandescent and fluorescent lamps (Siemens, 2013).

2.6.2.6 Other Negative Effects of Harmonics

Practically speaking, utility companies frequently encounter the following harmonic related problems (Mazumdar, 2006):

- Voltage distortion in distribution feeders;
- Increased RMS currents, heating and line losses;
- Overheating of power transformers, which requires higher K-factor transformers;
- Derating of distribution equipment;
- Overloading of phase and neutral conductors - neutral currents in a typical commercial office building may carry more than phase RMS currents;
- Amplification of harmonic currents in the utility system due to series and parallel resonances between the utility system and nonlinear loads;
- Overloading and fuse blowing of power factor correction capacitors;
- Tripping of voltage harmonic sensitive equipment;
- Failure of control electronics, micro-processors;
- Reduced accuracy of measuring instruments (such as watt-hour meters);
- Malfunction of solid-state fuses, breakers and relays;
- Reactive power and resonance problems;
- Reduced system stability and safe operating margins. Power factor correction capacitors are generally installed in industrial plants and commercial buildings. Fluorescent lighting used in these facilities also normally has capacitors fitted internally to improve the individual light fittings' own power factor. The harmonic currents can interact with these capacitances and system

inductances, and occasionally excite parallel resonance which can over heat, disrupt and/or damage the plant and equipment (Siemens, 2013).

- Power cables carrying harmonic loads act to introduce EMI (electromagnetic interference) in adjacent signal or control cables via conducted and radiated emissions. This "EMI noise" has a detrimental effect on telephones, televisions, radios, computers, control systems and other types of equipment. Correct procedures with regard to grounding and segregation within enclosures and in external wiring systems must be adopted to minimize EMI.
- Any telemetry, protection or other equipment which relies on conventional measurement techniques or the heating effect of current will not operate correctly in the presence of nonlinear loads. The consequences of under measure can be significant; overloaded cables may go undetected with the risk of catching fire. Fuses and circuit breakers will not offer the expected level of protection. It is therefore important that only instruments based on true RMS techniques be used on power systems supplying nonlinear loads.
- At the installations where power conductors carrying nonlinear loads and internal telephone signal cable are run in parallel, it is likely that voltages will be induced in the telephone cables. The frequency range, 450Hz to 1000Hz (9th harmonic to 20th harmonic at 50 Hz fundamental) can be troublesome.
- There is also the possibility of both conducted and radiated interference above normal harmonic frequencies with telephone systems and other equipment due to variable speed drives and other nonlinear loads, especially at high carrier frequencies. EMI filters at the inputs may have to be installed on drives and other equipment to minimize the possibility of inference.
- Conventional meters are normally designed to read sinusoidal-based quantities. Nonlinear voltages and currents impressed on these types of meters introduce errors into the measurement circuits which result in false readings.

Power quality issues also include unbalanced and sub-synchronous frequency currents (caused by cyclo-converters) which contribute to voltage sags and surges, and are the most common cause of VSD nuisance tripping. A rapid increase in the installed capacity of power electronic loads, which is a prerequisite for achieving energy

efficiency and productivity benefits, has brought utilities to crossroads. The user achieves energy efficiency at the expense of increased system losses and reduced system stability and safe operating margin for the utilities. The problems and issues, both technical and nontechnical, arising from the proliferation of harmonic producing loads, is a major concern for the utilities as transmission and distribution lines and equipment are operating near their design limits and severe harmonic interactions have caused load and line outages adversely affecting industrial productivity (Mazumdar, 2006).The important power quality issues are as follows (Siriadi, 2006, Subhash, et al. 2012 and Thakker, et al. 2014):

- Displacement power factor;
- Supply/load current harmonics and IEEE 519 harmonic current distortion limits;
- Supply voltage distortion and IEEE 519 harmonic voltage distortion limits;
- Source/sink resonances;
- Line voltage regulation under voltage sags or swells and interruptions;
- Line voltage problems resulting from load switching, network reconfiguration following fault, capacitor switching;
- Transients which include capacitor switching, line voltage notching;
- Repeated tripping of ASD loads;
- Sensitivity of harmonic filtering solutions to system parameters and operating range;
- Electro-magnetic interference (EMI) issues;

Harmonic currents are injected from harmonic producing loads into the utility network in radial distribution feeders. These harmonic currents affect the operation of other electrical and electronic equipment connected on the same distribution feeder, including the harmonic producing loads. Deeper into the utility distribution and transmission system, it becomes difficult to discern the direction of harmonic power flow, partly due to the highly interconnected and meshed nature of such systems, and partly due to the impact on voltage support capacitors used by the utility and its customers. Resonances between line and transformer reactances, and capacitors in the system can result in amplification of voltage and / or current harmonics. As a result, even small

harmonic sources can cause high levels of harmonic current flow between the utility and a customer. Further, as utilities and customers change their connected loads, system impedance also changes, resulting into resonances and harmonic problems, which were initially none existent (Heydt and Risal, 1996). Such problems are not easily identified without a detailed system analysis (Fauri and Ribeiro, 1996).

In particular the detrimental effect of certain harmonics like even harmonics, triple -n etc are listed as follows:

The second harmonic has an impact on peak voltage asymmetry. One half-cycle has a higher peak voltage than the next half cycle and this effect can be accentuated in the presence of other harmonics. There are many loads sensitive to peak voltage asymmetries. For single-phase and three phase rectifiers with large dc filter capacitors, these devices start injecting dc in response to the 2nd harmonic(Rice, 1994). This injected dc biases transformers and causes saturation (Mansoor, et al., 1995) and also causes the voltage zero-crossings to be unequal. Common Sources of the 2^{nd} harmonic include three-phase half-controlled rectifiers or blasted arc furnaces. However, there are not many field cases reported on annoyances caused by the 2nd harmonic. It is looked upon as a very aggressive harmonic; however its presence in the supply voltage is not high, slightly more than 0.5 %. Other even harmonics are very rare, and are therefore not investigated in this thesis (Mazumdar, 2006).

The 3rd harmonic (or the other triples, i.e. 9th, 15th, etc.) is mainly zero-sequence. It raises the potential of the neutral. It has a much stronger effect on communication lines than the 5^{th} and the 7^{th} harmonics, because it loads the neutral conductor causing additional losses in the neutral current path, even when the load is balanced but nonlinear. The worldwide measurements campaigns have confirmed its significant appearance at every power system voltage level, documenting its steady increasing level even at the high voltage level (about 2 % on many transmission networks). Harmonic surveys show a steady increase of the 5th harmonic level over the last three decades. This increase can be estimated as a constant growth of 1 % point over each 10-year period (Sanjeev, et al., 2014, Sandoval, et al. 2005 and Sanjay, et al. 2011).

The harmonics of order seven, eleven, and thirteen are also present in supply voltages. However their levels are lower than the fifth and vary between 1% to 2% (Mazumdar,

2006). Their stronger presence compared to the fifth harmonic is mainly caused by resonance phenomena within a power system. The same goes for harmonics of higher orders (Bachry, 2004). To alleviate harmonic related problems, utilities are beginning to enforce IEEE 519 recommended harmonic standards. IEEE 519 recommends utilities to meet voltage distortion limits, and specifies limits on harmonic currents based on the short circuit ratio at the point of common connection (PCC). As harmonic compensation by itself provides no direct benefit to the user, the widespread use of any form of active filter will only be realized if utilities enforce the IEEE 519 standard for large industrial power electronics loads. This will increase the need for cost-effective and practical approach to the harmonic filter design problem (Mazumdar, 2006).

2.7 Harmonic Standards

In 1981, the IEEE 519 harmonic standard was issued for harmonic-related issues and its control. IEEE 519 Standard attempts to establish reasonable harmonic goals for electrical systems that contain nonlinear loads. The objective is to propose steady state harmonic limits that are considered reasonable by both electrical utilities and their customers. For voltage and current harmonics, the obtained information (magnitude and phase) are usually compared with standards like IEEE 519 to evaluate the influence in the power system. IEEE 519 applies to all voltage levels, including 220V single-phase residential services. While it does not specifically state the highest-order harmonic to limit, the widely accepted range of application is through the 50^{th} harmonic. A brief outline of the IEEE 519 standard is given in appendix A.

2.7.1 IEEE 519-1992 Guidelines

IEEE 519 was initially introduced in 1981 as an “IEEE Guide for Harmonic Control and Reactive Compensation of Static Power Converters”. It originally established levels of voltage distortion acceptable to the distribution system for individual non-linear loads. With the rising increase usage of industrial non-linear loads, such as variable frequency drives, it became necessary to revise the standard.

In USA, IEEE applies whereas in Europe, a different standard (IEC) applies. Measured harmonics significantly higher than the recommended levels are considered unacceptable. All the standards make use of the total harmonic distortion (THD) voltage or current, defined as (Belgin and Kaypmaz, 1999):

$$THD = \frac{100\sqrt{\sum_{n=2}^{k} U_n^2}}{U_1} \quad \textbf{(2.51)}$$

Where U_1 is the fundamental component and U_n are the harmonic components respectively.

The main standards are the followings (Belgin and Kaypmaz, 1999):

i. IEEE 519: this standard sets limits for percentage "individual harmonic component distortion" and "THD". It limits both utility voltage and end user current distortion at the point of common coupling.
ii. a) IEC 1000-2-4 (1994): it prescribes the compatibility levels for industrial and non-public networks. It applies to low and medium voltage supplies.
    b) IEC 1000-1-1 (1992): Definitions used in IEC 1000
    c) IEC 1000-2-2 (1990): It defines the compatibility levels for individual harmonic voltages in public low voltage systems.

The IEEE working groups of the Power Engineering Society and the Industrial Applications Society prepared recommended guidelines for power quality that the utility must supply and the industrial user can inject back onto the power distribution system. The revised standard was issued on April 12, 1993 and titled.

This revised 1992 version of IEEE 519 established recommended guidelines for harmonic voltages on the utility distribution system as well as harmonic currents within the industrial distribution system(Siemens, 2013). According to the standard, the industrial system is responsible for controlling the harmonic currents created in the industrial workplace. Since harmonic currents reflected through distribution system impedances generate harmonic voltages on the utility distribution systems, the standard proposes guidelines based on industrial distribution system design. IEEE 519-1992defines levels of harmonic currents and voltages that an industrial user can inject onto the utility distribution system as shown in Appendix A for reference (Hoevenarrs

and LeDoux, 2003, Halpin, 2003, Rafiei and Ghazi, 2002, Ludbrook, 2001, Rivas, et al. 2003, Roger, et al. 1996).

2.7.2 Future Revisions to IEEE 519-1992

In 2004, an IEEE working group named "519 Revision Task Force (PES/T&D Harmonics WG)" was created to revise the 1992 version of IEEE 519 (Recommended Practices and Requirements for Harmonic Control in Electric Power Systems) and develop an application guide IEEE 519.1 (Guide for Applying Harmonic Limits on Power Systems). A revision to IEEE 519 includes the changes based on the significant experience gained in the last 20 years with regard to power system harmonics, their effects on power equipment, and how they should be limited. In addition, this document contains certain material dedicated to the harmonization of IEEE and other international standards where possible. Whereas, the application guide IEEE 519.1 contains significant rationale for and numerous example scenarios of the limits recommended in IEEE 519 and provides procedures for controlling harmonics on the power system along with recommended limits for customer harmonic injection and overall power system harmonic levels (Shah, 2014).

2.8 Representation of Harmonics and Measurements

This section outlines some of the fundamental concepts and mathematical relationships for representation and analysis of harmonic distortion in power systems.

2.8.1 Harmonic Components

A method to represent any non-sinusoidal periodic function $u(t)$using an infinite series of cosine and sine functions and coefficients as shown in Equation (2.52) was first proposed by Baron Jean Fourier in 1822:

$$u(t) = A_o + \sum_{h=1}^{\infty}[A_o cos(h\omega_o t) + B_o sin(h\omega_o t)]$$
$$= A_o + \sum_{h=1}^{\infty} C_h cos(h\omega_o t + \Psi_h) \quad \textbf{(2.52)}$$

Where $u(t)$ is a periodic function of frequency f_o, angular frequency$\omega_o = 2\pi f_o$, and period $T = \frac{1}{f_o} = 2\pi/\omega_o$. $C_1 cos(h\omega_o t + \Psi_1)$ represents the fundamental component, and

$C_h cos(h\omega_o t + \Psi_h)$ represents the h^{th} harmonic component of amplitude C_h, frequency $h\omega_o$ and phase Ψ_h relative to the fundamental.

Generally, for power systems, the fundamental frequency is either50Hz or 60Hz. Power systems in Nigeria are typically operated at 50Hz and thus, harmonic frequencies will appear as multiples of 50Hz (i.e100Hz, 150Hz, 200Hz, etc.). The Fourier series coefficients C_1, C_2,…C_h and relative phases $\Psi_{1,}\Psi_{2,\ldots\ldots}\Psi_h$make up the harmonic spectrum of the waveform are found using Equations (2.53) through (2.57):

$$A_o = \frac{1}{T}\int_0^T u(t)dt = \frac{1}{2\pi}\int_0^{2\pi} u(t)dx\,, where\ x = \omega_o t \quad \textbf{(2.53)}$$

$$A_h = \frac{2}{T}\int_0^T u(t)cos(h\omega_o t)dt = \frac{1}{\pi}\int_0^{2\pi} u(t)cos(hx)dx \quad \textbf{(2.54)}$$

$$B_h = \frac{2}{T}\int_0^T u(t)sin(h\omega_o t)dt = \frac{1}{\pi}\int_0^{2\pi} u(t)sin(hx)dx \quad \textbf{(2.55)}$$

$$C_h = \sqrt{A_h^2 + B_h^2} \quad \textbf{(2.56)}$$

$$\Psi_h = \tan^{-1}\frac{A_h}{B_h} \quad \textbf{(2.57)}$$

Conversely, if the harmonic spectrum of a given current or voltage waveform *u(t)* is known the original waveform can be constructed using the Fourier series summation:

$$u_t = \sum_{h=1}^{\infty} U_h \cos\,(h\omega_0 t + \Psi_h) \quad \textbf{(2.58)}$$

Where U_h is the h^{th} harmonic peak current or voltage, $\Psi_h$is the hth harmonic phase, $\omega_0$is the fundamental angular frequency, $\omega = 2\pi f_o$ and f_o is the fundamental frequency, typically 50Hz.

2.8.2 Total Harmonic Distortion (THD)

Although the harmonic content of a power system may be quite small relative to the fundamental in most circumstances, for exactness the rms value of a current or voltage waveform requires the harmonic content to be considered such that:

$$U_{rms} = \sqrt{\sum_{h=1}^{\infty}\left(\frac{1}{\sqrt{2}}U_h\right)^2} \quad \textbf{(2.59)}$$

Where, Urms is the rms value of voltage or current.

The rms voltage or current can also be used to quantify the level of distortion of the waveform. The total harmonic distortion of voltage or current waveform (THD_U) is calculated using equation (2.60):

$$TDH_U = \sqrt{\sum_{h=2}^{\infty}(U_h)^2} = \sqrt{\left(\frac{U_{rms}}{U_{1rms}}\right)^2 - 1} \quad \textbf{(2.60)}$$

Where, THD_U represents voltage or current total harmonic distortion (alternatively represented as THD_V and THD_I respectively) and $U_{1rms}$is the rms fundamental voltage or current. Alternatively, rms voltage or current can be represented in terms of total harmonic distortion:

$$U_{rms} = \sqrt{\sum_{h=1}^{\infty} {U_{hrms}}^2} = U_{1rms}\sqrt{1 + TDH_U^2} \quad \textbf{(2.61)}$$

As distribution system fundamental voltage and current rarely remain static in magnitude at different times throughout the day, the definition for total harmonic distortion may at times provide a misleading value for the harmonic distortion level. This is especially true for distribution system fundamental currents that fall close to zero at certain periods of the day, resulting in large values of THD_I. For this reason a modified index for harmonic distortion may be used with the harmonic content of the waveform expressed as a percentage of a fixed nominal value rather than the fundamental value, giving total demand distortion (TDD_U) (Belgin and Kaypmaz, 1999):

$$TDD_u = \frac{1}{U_{nom}}\sqrt{\sum_{h=2}^{\infty}\left(\frac{1}{\sqrt{2}}U_h\right)^2} \quad \textbf{(2.62)}$$

The fixed value U_{nom} is required to be specified and may be a maximum rms value, maximum demand, average or selected nominal system value.

2.8.3 Harmonic Measurements

One of the most important tools for understanding and analyzing of harmonics as well as for the standardization work is harmonic measurements. The estimation of harmonics is of high importance for efficiency of the power system network (Kumar B. , 2011). Harmonic measurements are also important for grid companies and end users to characterize the performance of their networks and develop solutions to harmonic problems. Basically, harmonic measurements can be used to (Kumar, et al. 2012, Kumar, et al. 2013, Mahmoud, et al. 2011, Muhammad and Samimi 2014):

i. Characterize system performance and determine if the harmonic levels are acceptable according to standards. This is perhaps the most common use of harmonic measurements. To characterize system performance usually requires

that measurements are performed over a long period of time. By knowing the normal or baseline harmonic performance of a system, problems that arise can more quickly be identified. Overtime, substantiated harmonic baseline information can be provided to customers to help them match the system compatibility performance of their equipment with realistic harmonic characteristics of the system.

ii. Characterize and track harmonic sources and (possible) problems. This can often be accomplished with short term monitoring at specific locations where problems are being experienced. When the problems have been identified, solutions can be developed. If customers are to be billed based on their responsibility to harmonic distortion, continuous monitoring is required. When continuous measurements are performed, the measurements may be used to develop billing schemes to bill customers according to their contribution to harmonic distortion.

iii. Develop and verify enhanced power delivery services that can be offered to customers. An example of such can be the offering of differentiated levels of power quality to match the needs of specific customers. This can be achieved with modifications in the power delivery system or by installation of appropriate equipment at the customer premises. In either case, monitoring is required to verify that the promised levels of power quality are achieved.

iv. Determine the impact of the harmonic voltage and/or current distortion on, for example, the voltage and current waveforms. Some of the effects of harmonics do not depend solely on the magnitude of the harmonic content of a waveform, but on the shape of the waveform depends on the phase relationship between the harmonics and the fundamental.

v. Estimate and calibrate computer models. The computer models may be used to determine the voltage and/or current harmonic levels in the system. To be able to calculate harmonic voltages and currents at other buses in the system, it is important that the harmonic currents injected into the system at different buses are known. It is also important that impedances of the power system at harmonic frequencies are known. Thus, estimating harmonic sources and impedances is an important, but complex, use of harmonic measurements.

vi. Estimate the sensitive harmonic measurements. Many harmonic studies involve the estimation of harmonic levels after changes in the system operating condition, for example after the installation of a filter or a new load. Changing the operating condition of a power system might change the harmonic currents injected by the loads in the network. Thus, to study the impact on harmonic levels by different actions made in the system, it is important that the models used are valid for different operating conditions.

There are a number of different measurement instruments available for harmonic measurement. The simplest instruments are single-phase and can determine individual harmonic components up to the 50^{th} harmonic, as well as rms and Total Harmonic Distortion (THD). Some of this single phase instruments can also measure both magnitude and phase angle. More advanced harmonic measurement instruments (harmonic or spectrum analyzers) normally have the capability to simultaneously monitor, at least, three-phase voltages and currents plus neutrals. The instruments normally save the raw data in internal storage. From the raw data, a number of different outputs and harmonic indexes can be calculated and displayed. Important examples are voltage and current waveforms, harmonic power flows, power factor, Total Harmonic Distortion (THD), crest factor and K-factor.

Digital oscilloscopes can be used for harmonic measurements. Some digital oscilloscopes have waveform analysis capability (energy calculation, spectrum analysis) Digital oscilloscopes can also be obtained with communications so that waveform data can be uploaded to a PC for additional analysis.

The success of a power system harmonic study depends critically on the data used to model power system components. While much work has been done in modeling typical power system components, the data to represent aggregated network models are still very difficult o obtain. This is mainly due to the fact that the composition of a distribution feeder, and the loads connected, to a large extent is unknown in many cases. Thus, harmonic measurements are often needed to obtain aggregated models of loads and networks. To model large distribution networks in detail is normally not possible since the cost associated with such studies is very high. The number of components in real distribution networks may be thousands. Perhaps, the most important model possible to

estimate from measurements is the harmonic impedance. Knowing the impedance of both the supply and load side networks, the understanding of many harmonic issues will increase. The accuracy of the harmonic studies will increase, which in the end will lead to more economical measures taken to solve problems.

It is also worthy of note that in order to prevent or correct harmonic problems that could occur within an industrial facility, an evaluation of system harmonics should be performed if:

- A plant is expanded and significant non-linear loads are added
- A power factor correction capacitor banks or a line harmonic filters are added at the service entrance or in the vicinity.
- A generator is added in the plant as an alternate stand-by power source.
- The utility company imposes more restrictive harmonic injection limits to the plant. Often, the vendor or supplier of non-linear load equipment, such as variable frequency drives, evaluates the effects that the equipment may have on the distribution system. This usually involves details related to the distribution system design and impedances, similar to performing a short circuit study evaluation.

2.9 Existing Methods for Determining Sources of Harmonic Distortion

Harmonic distortions have become an important concern for power utility distribution companies. Two basic approaches have been proposed in industry for controlling the amount of harmonic pollution present in a distribution system (Mazumdar, 2006). The first scheme involves the establishment of limits (IEEE Standard 519-1992, 1993) on the amount of harmonic currents and voltages generated by customers and utilities (Sharma and Thomson, 1993). A second scheme, inspired by the power factor management practice, is an incentive based scheme, proposes to charge harmonic generators an amount commensurate with their harmonic pollution level when the limits are exceeded (Mazumdar, 2006). A pioneering work was described by Grady et al. (Grady, et al., 2002, Thunberg, et al. 1998, Sadeghi, et al. 2000 and Sakshi, et al. 2013).

The biggest challenge towards the implementation of the above schemes is the need to separate the harmonic contribution of a customer from that of the supply system. Srinivasan specifically addressed this issue (Srinivasan, 1996). This is not a new issue and researchers have proposed various approaches, mainly analytical, to provide a solution to this problem. Some of the methods adopted by researchers are highlighted in the following sub-sections.

2.9.1 Harmonic Power Flow Direction Method

A common method for harmonic source detection is the power direction method which checks the direction of harmonic power flow. The side that generates harmonic power is considered to contain the dominant harmonic source or to have a larger contribution to the harmonic distortions observed at the measurement point. Detailed work has been reported in Xu and Li, 2000, Li and Xu, 2002 and Xu, 2004.

2.9.2 Load Impedance Variation Method

This method is based on finding the interrelationship between the distorted voltage waveform, the distorted current waveform, and the link that relates these waveforms, i.e. the load parameters (*R* and *L*). Monitoring the load parameter (*R*&*L* values) variations under the influence of harmonics plays an important role for determining the origin of harmonic distortion and evaluating the load nonlinearity. The load with higher *R*&*L* value variations contains more nonlinear elements and produces larger harmonic magnitudes. A sinusoidal voltage applied to a linear load yields a sinusoidal current. On the other hand, a distorted current waveform will result if a sinusoidal voltage is applied to a non linear load. Likewise, if a sinusoidal current is injected through nonlinear impedance, the voltage across that element will be distorted. Thus, nonlinear loads indicate distorted voltage and/or distorted current waveforms but the opposite is not true. A load with a distorted current or voltage waveform is not necessarily nonlinear. So, considering only the distorted current and voltage waveforms, it is not possible to pronounce the source of the harmonics. It is mainly dependent on the behaviour of the load impedance. Thus, the first step is to find a simple way to monitor the load pattern under the influence of harmonics.

Generally for a *RL* load,

$$v(t) = R.i(t) + L\frac{di(t)}{dt} \quad \textbf{(2.63)}$$

If v(t) indicates an instantaneous voltage value for a distorted voltage waveform for certain load, and i(t) indicates an instantaneous current value for the corresponding distorted current waveform, then R &L indicate the load pattern under the influence of harmonics. For two successive time intervals $t_1$and t_2, the equations can be written as:

$$\begin{bmatrix} v(t_1) \\ v(t_2) \end{bmatrix} = \begin{bmatrix} i(t_1) & \frac{di(t_1)}{dt_1} \\ i(t_2) & \frac{di(t_2)}{dt_2} \end{bmatrix} * \begin{bmatrix} R \\ L \end{bmatrix} \quad \textbf{(2.64)}$$

Solving the above equation numerically yields the solution as:

$$z = [i]^{-1}.v \quad \textbf{(2.65)}$$

The above calculation should be repeated for n successive intervals for the current and voltage waveforms with period T-. So for times t_1 to t_n, there are $\frac{n}{2}$sets of values for R & L.

This mathematical approach can be applied to any set of measured values of v and *i*, for any load category. From the plots of load parameter variation versus time, it can be predicted whether the load that possesses sharp variations in its *R*&*L* parameters would be the higher harmonic producing load.

2.9.3 Online Impedance Measurement

Knowledge of the network impedance values is important for performing power system modeling and simulation. Without this knowledge, it is not possible to simulate or predict harmonic propagation within a power system. Olivio, Oliveira, et al. proposed procedures based on current injection for online impedance measurement and extended the method for extra high voltage (EHV) transmission networks.

Two distinct current injection methods have been used by researchers. The first method proposed by Rhode et al. involves systematically injecting a small sinusoidal current signal at each harmonic frequency of interest. By measuring the phase and amplitude of the voltage and current at the point of injection, the impedance may be calculated at each frequency. The second method proposed by Thomas et al. involves injecting a narrow current spike to the network. The injected current and voltage transient

are recorded and the impedance at the point of injection is calculated. The calculation is carried out in the frequency domain and is given by;

$$Z(f) = \frac{F(V(t))}{F(I(t))} \quad \textbf{(2.66)}$$

Where, F is the Fourier transform.

The biggest disadvantage of the above methods is the need for power electronic converters to inject the current pulse. During online measurements, the converters too becomes a part of the power system and introduces its own nonlinearity models which take into account the time varying and probabilistic nature of harmonic loads and their interaction.

2.9.4 Probabilistic Methods

Baghzouz and Tan introduced the idea of probabilistic modelling of power system harmonic current injection and propagation. Their research focused on models which take into account the time varying and probabilistic nature of harmonic loads and their interaction. Correlations exist among currents, voltages and impedances in a power system. Using this information, Testa et al. developed a probabilistic model of impedance. Ribeiro et al. summarized the probabilistic aspects of harmonics and new developments.

2.9.5 Neural Network Based Methods

Computational intelligence (AI) techniques, particularly the neural networks, have recently had an impact on power systems and the area of power electronics. Neural networks have created a new and advancing frontier in power systems, which is already a complex and multi-disciplinary technology that has been going through a dynamic evolution in the recent years. Pioneers like Harley, Venayagamoorthy, Bose, El-Sharkawi, and Habetler among many others are in the forefront of this effort to promote the application of neural networks in power systems, machines and power electronics.

Specifically, in the area of power system applications, Sone et al., Vasquez et al. applied neural networks for harmonic detection in power system waveforms and used it for active power filtering. To detect each harmonic component using the Fourier technique, it needs 2*n* sampling points from more than one cycle length of current waveform and the analysis

is conducted after all the samples have been input to the system. This method was specifically used to demonstrate the function identification property of neural networks as an alternative approach to first Fourier transform (FFT) based methods. A number of researchers have also applied neural network techniques for estimation of harmonic components in power systems. Hoffman et al. used neural networks for identification of types of distortion sources in power systems. Neural networks based methods have also been proposed to predict the voltage at the PCC and also to identify harmonic sources. These methods have been typically useful for predicting the harmonic components of a known waveform and have been shown to be faster since only the harmonics of interest are computed and not the whole spectrum. All these methods assume that the voltage at the PCC is sinusoidal and that the load current contains the true harmonics injected by the load.

2.10 Harmonic Minimization Methods

Majority of large power (typically three-phase) electrical nonlinear equipment often requires mitigation equipment in order to attenuate the harmonic currents and associated voltage distortion to within necessary limits. Depending on the type of solution desired, the mitigation may be supplied as an integral part of nonlinear equipment (e.g., an AC line reactor or a line harmonic filter for AC PWM drive) or as a discrete item of mitigation equipment (e.g., an active or passive filter connected to a switchboard) (Siemens, 2013). There are many ways to reduce harmonics, ranging from variable frequency drive designs to the addition of auxiliary equipment. Few of the most prevailing methods used today to reduce harmonics are explained in the following sub-sections.

2.10.1 Isolation Transformers

An isolation transformer provides a good solution in many cases to mitigate harmonics generated by nonlinear loads. The advantage is the potential to "voltage match" by stepping up or stepping down the system voltage, and by providing a neutral ground reference for nuisance ground faults. This is the best solution when utilizing AC or DC drives that use SCRs as bridge rectifiers.

2.10.2 Use of Reactors

Use of reactor is a simple and cost effective method to reduce the harmonics produced by nonlinear loads and is a better solution for harmonic reduction than an isolation transformer. Reactors or inductors are usually applied to individual loads such as variable speed drives and available in standard impedance ranges such as 2%, 3%, 5% and 7.5%. When the current through a reactor changes,a voltage is induced across its terminals in the opposite direction of the applied voltage, which consequently opposes the rate of change of current. This induced voltage across the reactor terminals is represented by equation below.

$$e = L\frac{di}{dt} \quad \textbf{(2.67)}$$

Where:

e = Induced voltage across the reactor terminals

L = Inductance of the reactor, in Henrys

di/dt = Rate of change of current through reactor in Ampere/Second

This characteristic of a reactor is useful in limiting the harmonic currents produced by electrical variable speed drives and other nonlinear loads.

The introduction of strict legislation such as IEEE519 limits the maximum amount of harmonics THD that a supply system can tolerate for a particular type of load (Reena, 2014).

In addition, the AC line reactor reduces the total harmonic voltage distortion (THDv) on its line side as compared to that at the terminals of the drive or other nonlinear load. In electrical variable speed drives, the reactors are frequently used in

addition to the other harmonic mitigation methods. On AC drives, reactor can be used either on the AC line side (called AC line reactors) or in the DC link circuit (called DC link or DC bus reactor) or both, depending on the type of the drive design and/or necessary performance of the supply. AC line reactor is used more commonly in the drive than the DC bus reactor, and in addition to reducing harmonic currents; it also provides surge suppression for the drive input rectifier. The disadvantage of use of reactor is a voltage drop at the terminals of the drive, approximately in proportion to the percentage reactance at the terminals of the drive. In large drives, both AC line and DC bus reactors may be used especially when the short circuit capacity of a dedicated supply is relatively low compared to the drive kVA or if the supply is susceptible to disturbances.

2.10.3 Passive (or Line) Harmonic Filters

Passive filters are in combination of inductance, capacitance and resistance elements configured and tuned to reduce the impact of harmonics in the power systems (Parthasarathy and Jeyasri, 2014).

Passive harmonic filters techniques are among the oldest and perhaps the most widely used techniques for filtering the power line harmonics. Besides the harmonics reduction passive filters can be used for the optimization of apparent power in a power network (Sher, et al., 2013).The classical solution for reducing current harmonic distortion is to connect a shunt LC-series filter nearby the harmonic source in order to drain the current harmonics generated by the load, trying to keep the main source current sinusoidal (Deckmann, et al., 2005). This approach considered that the non-linear load is a harmonic current source. In such situation the voltage at the PCC (point of common coupling) is determined almost only by the supply voltage source (Deckmann, et al., 2005).

Passive harmonic filters are also known as harmonic trap filters and are used to eliminate or control more dominant lower order harmonics specifically 3^{rd} 5^{th}, 7^{th}, 9^{th}, 11^{th}, $13^{th}$and 15^{th} and are the more severe examples of triplet harmonics that produce bigger problems to engineers because they possess more distortion in voltage (Dugan, et al., 2002, Hasan, et al. 2007, Hernandez, et al. 2009, Kamen, et al. 2008, Jansen, 2011 and Jayakrishna, et al. 2013). It can be either used as a stand-alone part integral to a large

nonlinear load (such as a 6-pulse drive) or can be used for a multiple small single phase nonlinear loads by connecting it to a switch board. Passive Harmonic Filter comprised of a passive L-C circuit (and also frequently resistor R for damping) which is tuned to a specific harmonic frequency which needs to be mitigated (for example, 5th, 7th, etc). Their operation relies on the "resonance phenomenon" which occurs due to variations in frequency in inductors and capacitors. The series tuned filters are used to compensate the dominant harmonics of the supply current. The cost of the passive filter is very low and it is easy to tune to the particular frequency (Sriranjani and Jayalalitha, 2012). This filter acts as zero impedance at the tuning frequency that absorbs the harmonics.

The resonant frequency for a series resonant circuit and (in theory) for a parallel resonant circuit, can be given as:

$$f_r = \frac{1}{2\pi\sqrt{LC}} \quad \textbf{(2.68)}$$

Where:

f_r= Resonant frequency, Hz

L = Filter inductance, Henrys,

C = Filter capacitance, Farads

The passive filters are usually connected in parallel with nonlinear load(s) and are "tuned" to offer very low impedance to the harmonic frequency to be mitigated. In practical application, above the 13th harmonic, their performance is poor, and therefore, they are rarely applied on higher-order harmonics.

Passive filters are affected by changes in source and load impedances. They attract harmonics from other sources (i.e. from downstream of the PCC), and therefore, this must be taken into account in their design. Harmonic and power system studies are usually undertaken to calculate their effectiveness and to explore possibility of resonance in a power system due to their proposed use.

Passive filters are made of passive elements like resistors, capacitors and inductors. Passive filters have a value-added function of achieving power-factor correction of inductive loads. This function brings an advantage to passive filters in many cases, but not in all cases (Akagi, 2006). However, the disadvantages of passive filter implementations to filter out the current harmonics include, possibility of resonances with the source impedance, supply impedance dependent system performance and fixed

compensation (Bukka, et al., 2014).These filters are fixed and once installed they become part of the network and they need to be redesigned to get different filtering frequencies. They are considered best for three phase four wire network (Sher, et al., 2013). They are mostly the low pass filter that is tuned to desired frequencies. Giacoletto and Park presented an analysis on reducing the line current harmonics due to personal computer power supplies (Sher, et al., 2013). Their work suggested that the use of such filters is good for harmonics reduction but this will increase the reactive component of line current. Various kinds of passive filter techniques are given in Sher, et al., 2013:

i. Series passive filters
ii. Shunt passive filters
iii. Low pass filters or line LC trap filters
iv. Phase Shifting Transformers

2.10.3.1 Series Passive Filters

Series passive filters are parallel LC filters in series with the supply and the load. Series passive filter shown in Figure 2.4 are considered good for single phase applications and specially to mitigate the third harmonics (Sher, et al., 2013). However, they can be tuned to other frequencies also. They do not produce resonance and offer high impedance to the frequencies they are tuned to. These filters must be designed such that they can carry full load current. These filters are maintenance free and can be designed to significantly raise power values up to those of MVARs (Sher, et al., 2013). Compared to the solutions that employ rotating parts like synchronous condensers they need lesser maintenance.

2.10.3.2 Shunt Passive Filters

These type of filters are also based on passive elements and offer good results for filtering out odd harmonics especially the 3rd, 5th and 7th. Some researchers have named them as single tuned filters, second order damped filters and C type damped filters (Sher, et al., 2013). As all these filters come in shunt with the line they fall under the cover of shunt passive filters, as shown in Figure 2.5. Increasing the order of harmonics makes the filter more efficient in working but it reduces the ease in design. They offer low

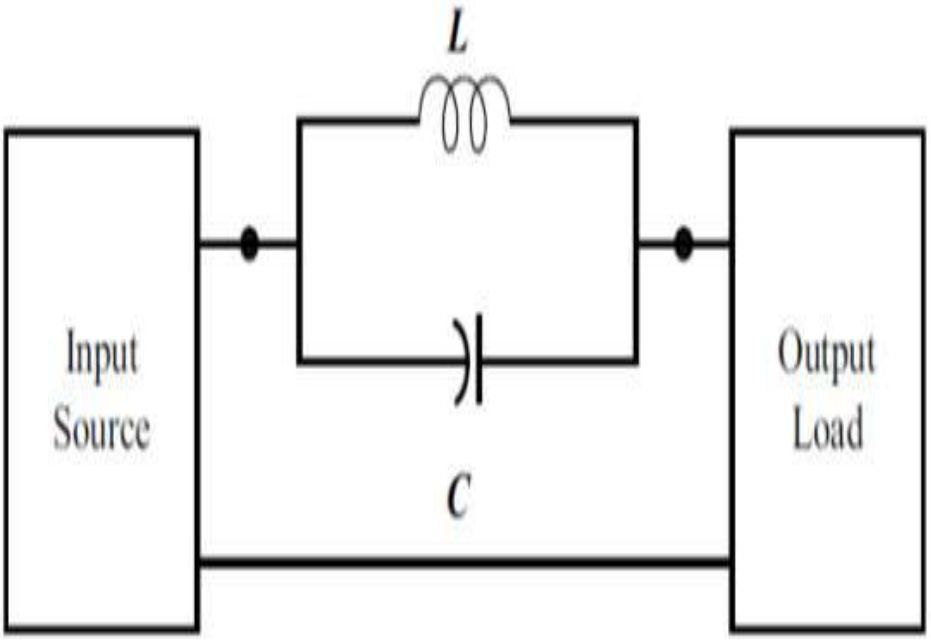

Figure 2.4: Series Passive Filter (Sher, et al., 2013)

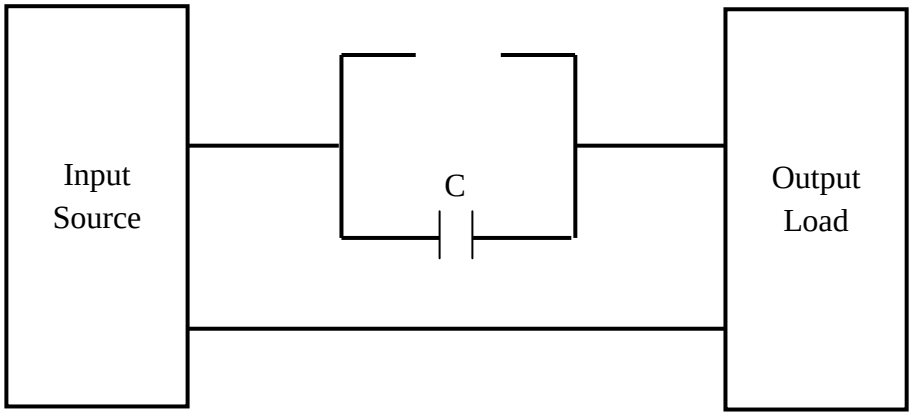

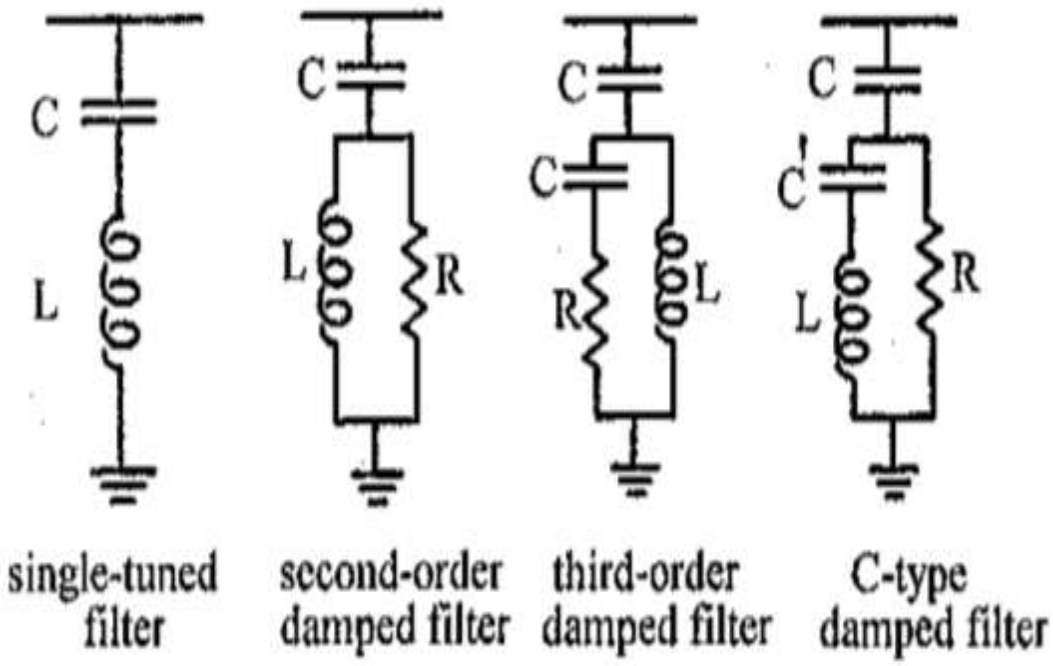

Figure 2.5: Different order type Shunt Filters (Sher, et al., 2013)

Single-tuned filter

Second-order damped filter

impedance to the frequencies they are tuned for. Since they are connected in shunt, they are thus, designed to carry only harmonic current.

Their nature of being in shunt makes them a load itself to the supply side and can carry 30-50% load current if they are feeding a set of electric drives (Sher, et al., 2013). Economic aspects reveal that shunt filters are always economical than the series filters due to the fact that they need to be designed only on the harmonic currents. Therefore, they need comparatively smaller size of L and C, thereby reducing the cost. Furthermore, they are not designed with respect to the rated voltage, thus making the components less costly than it is for series filters. However, these types of filters can create resonant conditions in the circuit.

2.10.3.3 Low Pass Filter

Low pass filters are widely used for mitigation of all type of harmonic frequencies above the threshold frequency. They can be used only on nonlinear loads. They do not pose any threats to the system by creating resonant conditions (Sher, et al., 2013). They improve power factor but they must be designed such that they are capable of carrying full load current. Some researchers have referred them as line LC trap filters (Sher, et al., 2013). These filters block the unwanted harmonics and allow a certain range of frequencies to pass. However, very fine designing is required as far as the cut off frequency is concerned (Sher, et al., 2013).

2.10.3.4 Phase Shifting Transformers

The unwanted harmonics in power system are mostly odd harmonics. One way to restrict their interference in the power system is by the use of phase shifting transformers. It takes harmonics of the same kind from several sources in a network and shifts them alternately to 180° and then combines them, thus, resulting in cancelation (Sher, et al., 2013). The use of phase shifting transformers has produced considerable success in suppressing harmonics in multilevel hybrid converters (Sher, et al., 2013, Ganguli, et al 2014 and Eid, et al 2009).

2.10.4 Active Power Filters

Active Power Filters (APF) use power electronics to introduce current components to remove harmonic distortions produced by the non-linear load. Figure2.6 shows the basic concept of an active filter (Sher, et al., 2013). They detect the harmonic components in the line and then produce and inject an inverting signal of the detected wave in the system (Sher, et al., 2013). The two driving forces in research of APF are the control algorithm for current and load current analysis method (Sher, et al., 2013).

Active filters can also be classified as follows:

i. Series Active Filters

ii. Shunt Active Filters

Since, it uses power electronic based components therefore in literature a lot of work has been done on the control of active filters.

2.10.4.1 Series Active Filter

The series filter which is connected in series with the ac distribution network, serves to offset harmonic distortions caused by the load as well as that present in the AC system. These types of active filters are connected in series with load using a matching transformer. They inject voltage as a component and can be regarded as a controlled voltage source (Sher, et al., 2013). The downside of this is that they only take care of voltage harmonics and in case of short circuit at the load; the matching transformer has to 'tolerate' it.

In construction, the series active filter is placed between an ac source and the harmonics producing load. It forces the source current to become sinusoidal. In other words, the series active filter presents high impedance to the harmonic current of the load to flow from the ac source and vice versa (Mishra and Gupta, 2011).

2.10.4.2 Shunt Active Filter

The Shunt (parallel) filter is connected in parallel with the AC distribution network. Parallel filters are also known as shunt filters and offset the harmonic distortions caused by the non-linear load. They work on the same principle as the series active filters

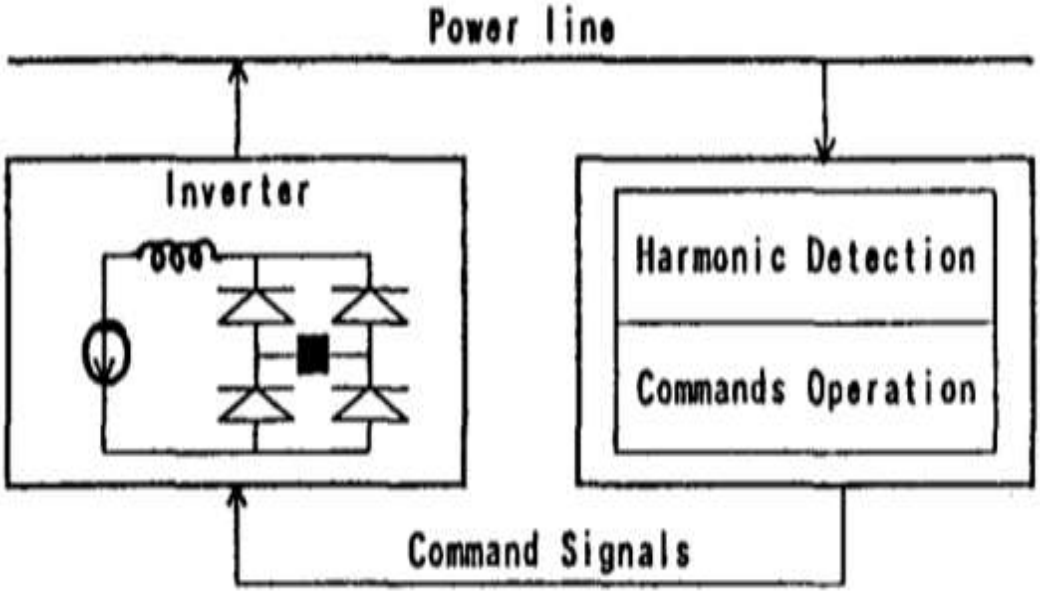

Figure 2.6: Conceptual Demonstration of Active filter (Sher, et al., 2013)

but they are connected in parallel; that is they act as a current source in parallel with load (Sher, et al., 2013). They use high computational capabilities to detect the harmonics in line.

The shunt active filter is connected to the supply mains through the transformer. The instantaneous reactive power theory is used to control the Shunt active filter. The supply current is sinusoidal and power factor reaches to unity. In this Shunt active filter, Passive filters are connected to the supply mains to compensate the voltage fluctuation and voltage distortion due to the DC drives (Sriranjani and Jayalitha, 2012).

2.10.5 Power Factor Corrections

The power factor of an AC electrical power system is defined as the ratio of the real power flowing to the load to the apparent power in the circuit (Sandesh, et al., 2012). It is a measure of electrical efficiency and is given by the ratio of active power consumed by the load to apparent power delivered to the load (Allah, 2014).In an ac circuit, there is generally a phase difference between voltage and current. The term cosϕ is known as power factor of the circuit (Khanchi and Garg, 2013). It varies with load and it has a value from 0 to 1. Apparent power is the product of the current and voltage of the circuit. Due to energy stored in the load and returned to the source, or due to a non-linear load that distorts the wave shape of the current drawn from the source, the apparent power will be greater than the real power. In an electric power system, a load with a low power factor draws more current than a load with a high power factor for the same amount of useful power transferred. The higher currents increase the energy lost in the distribution system, and require larger wires and other equipment. Because of the costs of larger equipment and wasted energy, electrical utilities will usually charge a higher cost to industrial or commercial customers where there is a low power factor (Rashid, 2001).

Power factor improvement leads to a big reduction of apparent power drawn from the ac source which in turn saves energy and minimizes the transmission losses. It generally employs means that control reactive power in power system network (Sandesh, et al., 2012). Different systems are available to produce reactive energy and improve the power factor (Al-Naseem and Adi, 2003). The process is usually denoted by reactive power compensation which is a productive technology employed for improving power

systems performance. In recent years, the demand for controllable reactive power source has gone up mainly for efficient and reliable operation of ac electric power system. VAR compensators should be controlled to provide rapid and continuous reactive power supports during static and dynamic power system operating conditions (Sandesh, et al., 2012). Power quality problem can occur as a non-standard voltage, current and frequency. The power quality has serious economic implications for customers, utilities and electrical equipment manufacturers.

The harmonic filters can also provide a large percentage of reactive power for the power factor correction (Hsiao, 2001). Power factor correction in non-linear loads (Passive PFC) is the simplest way to control the harmonic current. It is possible to design a filter that passes current only at line frequency (50 or 60 Hz). This filter reduces the harmonic current, which means that the non-linear device now looks like a linear load. At this point the power factor can be brought to near unity, using capacitors or inductors as required. This filter requires large-value high-current inductors, however, which are bulky and expensive. A passive PFC requires an inductor larger than the inductor in an active PFC, but costs less. This is a simple way of correcting the nonlinearity of a load by using capacitor banks. It is not as effective as active PFC (Sandesh, et al., 2012).

Passive PFCs are typically more power efficient than active PFCs. Efficiency is not to be confused with the PFC, though many computer hardware reviews conflate them. A passive PFC on a switching computer PSU has a typical power efficiency of around 96%, while an active PFC has a typical efficiency of about 94% (Sandesh, et al., 2012).

An "active power factor corrector" (active PFC) is a power electronic system that changes the wave shape of current drawn by a load to improve the power factor. The purpose is to make the load circuitry that is power factor corrected appear purely resistive (apparent power equal to real power). In this case, the voltage and current are in phase and the reactive power consumption is zero. This enables the most efficient delivery of electrical power from the power company to the consumer. Some types of active PFC include Boost PFC, Buck PFC and Buck-boost PFC (Sandesh, et al., 2012).

2.11 Design of Filters

Filters are normally used to modify the frequency spectrum of a signal and are therefore specified in the frequency domain (Sergio, 2003). This section briefly analysis the design procedure for the passive filter used in the harmonic mitigation process. The filter circuits can be constructed entirely from passive components such as resistors, inductors and capacitors.

2.11.1 Design of Passive Filters

The most common type of shunt filters used in harmonic mitigation is the Single Tuned Filter (STF) which is either a low pass or band pass filter (Diwan, et al., 2011). This type of filter is simplest to design and least expensive to implement (Diwan, et al., 2010). The basic principle of operating a passive filter is that at the tuned frequency, the filter will have low impedance to current through which harmonic currents tend to divert in the system. Secondly, passive filters come with the property of reactive power compensation. A very simple arrangement of single tuned filter (Artega, et al., 2000) is shown is shown in Figure 2.7, which also gives the connection arrangement used in the single tuned filter designing (Singh, et al., 1999).

It can easily be seen in Figure 2.7, that single tuned filters are the simple series connection R-L-C component and LC components. The equation of resonant frequency for a single tuned frequency is given by the following equation (Srivastava, et al., 2013):

$$f_o = \frac{1}{2\pi\sqrt{LC}} \quad \textbf{(2.69)}$$

Where,

f_o = Frequency at resonance in Hertz

L = Inductance of filter in Henry

C = Capacitance of filter in Farads

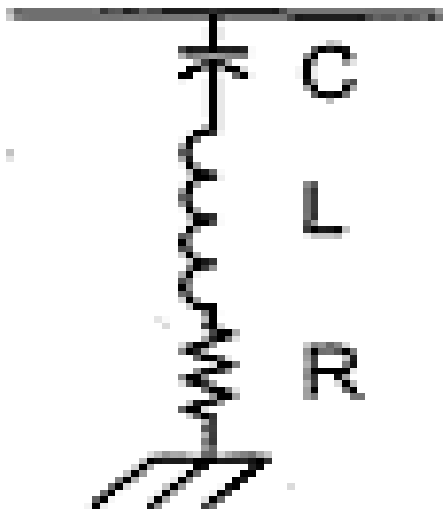

Figure 2.7: Single Tuned Filter (Artega, et al., 2000)

Another important term, which is necessary to keep in mind, is the design of the filter quality factor. The term "Quality factor" is the ratio of the reactance at resonant condition to the resistance of the circuit as follows (Srivastava, et al. 2013):

$$Q_f = \frac{(X_L or X_c)}{R} \quad \textbf{(2.70)}$$

Where,

Q_f = Quality factor (for a normal distribution system, typical value of Q_f varies between 15 and 80).

R = Resistance of the filter in Ohms.

In a Single Tuned Filter, the inductive and capacitive reactance at the tuned frequency is given by (Das J. , 2004):

$$Z = R + j\omega L + \frac{1}{j\omega C} \quad \textbf{(2.71)}$$

Where,

ω = Angular frequency (2πf) of power system

R = Resistance of filter branch

C = Capacitance of filter branch

L = Inductance of filter branch.

If h is the ratio between the fundamental and harmonic frequencies, then the value of capacitance and inductance can be obtained using the following equations that relate the harmonic and electronic component of filters (Srivastava, et al., 2013):

$$X_{Lh} = h \times 2\pi f \quad \textbf{(2.72a)}$$

$$X_{Ch} = \frac{1}{h \times 2\pi f} \quad \textbf{(2.72b)}$$

Again, at the tuning of the filter, the impedance value of the filter must be low; for this, if we inspect the simple circuit of filter and find that the only way to minimize the impedance of the filter is to make both of the reactance cancel out, this can be made possible through the resonant condition viz:

$$X_{Lh} = X_{Ch} \quad \textbf{(2.73)}$$

Now, when we put the value of X_{Ch} and X_{Lh}in Equation (2.73), another relationship between harmonic and passive components which is important for filter design, will be achieved:

$$h = \sqrt{\frac{X_C}{X_L}} \quad \textbf{(2.74)}$$

Again, if X_o is the reactance of the capacitor, or filter reactor at its tuning frequency,

$$X_o = \omega_n L = \frac{1}{C\omega_n} = \sqrt{\frac{L}{C}} \quad \textbf{(2.75)}$$

but,

$$Q = \frac{X_o}{R} = \frac{\sqrt{\frac{L}{C}}}{R} \quad \textbf{(2.76)}$$

The pass band is bounded by frequencies at which(Das J. , 2004):

$$|Z_f| = \sqrt{2}R \quad \textbf{(2.77)}$$

$$f = \frac{\omega - \omega_n}{\omega_n} \quad \textbf{(2.78)}$$

The sharpness of tuning is dependent on R as well as X_o and reducing these can reduce the impedance of the filter at resonant frequency. Note that, at parallel resonance, the equation of a resonant frequency for a single tuned frequency is given as:

$$f_{o(parallel\ load)} = \frac{1}{2\pi\sqrt{(L_s + L)/C}} \quad \textbf{(2.79)}$$

Where,

$f_{o(\text{parallel load})}$= Frequency at resonance for networks involving nonlinear loads in Hertz

L_s = Inductance present in the network (source inductance) before connection of filter in Henry

L = Inductance of filter in Henry

C = Capacitance of filter in Farads

In this condition, the total source impedance will be so high that the resonant condition of the system will occur just before the tuning frequency; usually, about 3 – 6% of its desired value (Maswood and Haque, 2002).

Also, when there are multiple harmonic filters connected in the system, the resonance of the filter circuit will be affected for all the harmonic filters.

CHAPTER THREE
METHODOLOGY

3.1 INTRODUCTION

In chapter two, attention was partially focused on the power flow problem of electric power systems with emphasis on the solution methods. The Newton-Raphson method was found to possess several advantages over other methods.

A crucial aspect of the power flow problem for large power systems is the availability of computer software, which permits ready and easy implementation of the solution methods. Therefore, in order to enable the solution of power flow problem using the Newton-Raphson method, a suitable software package called NEPLAN was sourced and used for this purpose. NEPLAN software was chosen among other available software, because of its application on network expansion planning, i.e. determination of load centre using a Geographical Information System (GIS), load forecasting (adding future plans in the network for modeling and simulation) and N-1 contingency planning.

3.2 Power Flow Modelling and Analysis

This section provides the approach for power flow studies using NEPLAN software application for the modelling. Data for the power flow analysis were sourced from Eko Electricity Distribution Plc, Marina – Lagos, the Headquarter office of Island Business District, which was used as case study. The details of power flow analysis are as follows.

3.2.1 Power Flow Study of the Eko Electricity Distribution Plc (EKEDP) 33kV Grid

This section presents a case study of the power flow on Island Business Unit's 33kV grid network of EKEDP. NEPLAN software package was used for this purpose. The Island Business Unit's 33kV grid network is shown in Figure 3.1; while the developed flowchart which provides the algorithms for power flow analysis is shown in Figure 3.2.

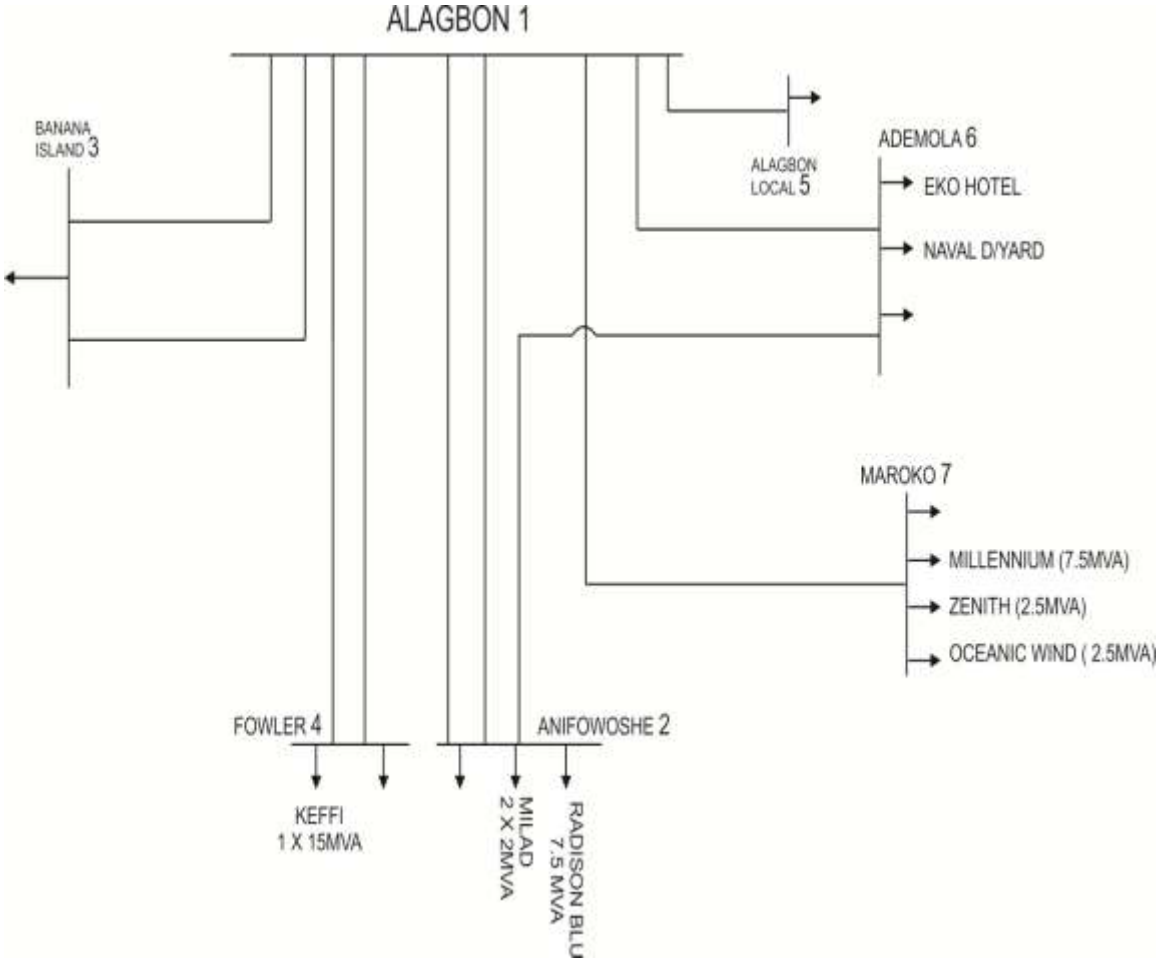

Figure 3.1: 33kV Network of Island Business Unit, EKEDP

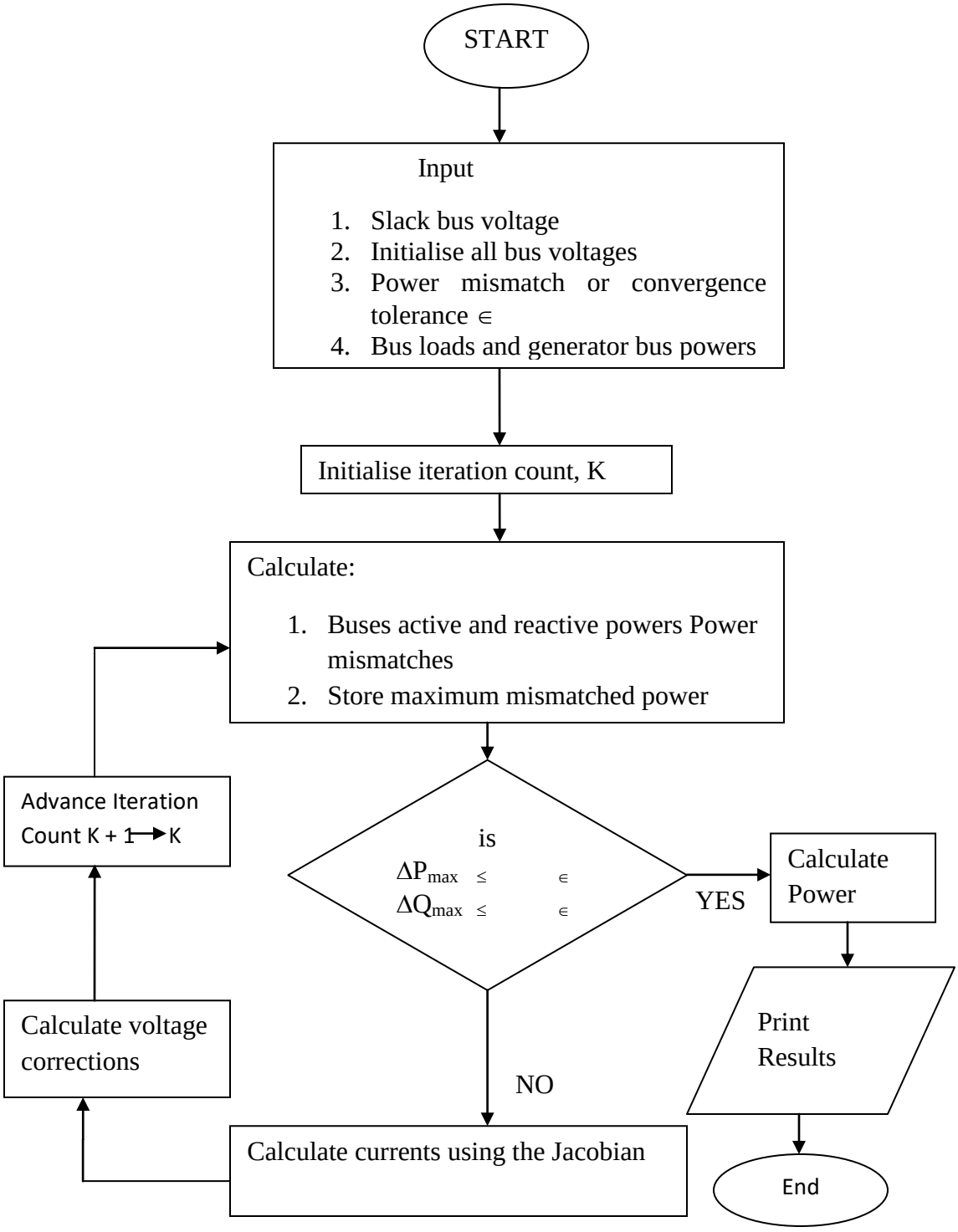

Figure 3.2: Flow Chart of Newton-Raphson Power Flow Solution

The network of Figure 3.1 has seven (7) nodes (buses) without any generator bus. There are six (6) distribution lines (branches) of which one is mainly transformers connected in parallel. Although, Alagbon busbar was considered as the slack bus, it is not a generator bus bar; however, it is the only source of supply to other busbars. Table 3.1 shows the line parameters and the route length of the 33 kV distribution network considered.

A compiled EKEDP hourly load readings of the various injection station busbars obtained by the distribution substation operators (DSO) were used as a source data and are shown in Table 3.2. Two days, 17th and 20th January, 2014 were chosen, while some hours of scenario of supply availability for the two (2) days are also presented in the same table.

3.2.2 Network Modelling for Power Flow Studies

To carry out power flow analysis, Figure 3.1 is modeled to suit the application of the NEPLAN software as shown in Figure 3.3. It involves opening of dialog box and inputting all the necessary parameters in the box as shown in Figure 3.3.

3.2.3 Newton-Raphson Power Flow Algorithms

1. Input Network Parameters
    - Line Resistance (R)
    - Line Reactance (X)
    - Line Susceptance (B)
    - Busbar scheduled active power (P_s)
    - Busbar scheduled reactive power (Q_s)
2. With bus 1 chosen as a slack bus and the only source of supply to the network; The following assumptions were made:
    - Initial Bus voltage (E) = 33kV
    - Power mismatch Tolerance, $\in$ = 0.001
    - Initialize iteration count, k
3. Compute Shunt Admittance (Y_{sh})
4. Calculate Power P_k and Q_k
5. Calculate all ΔP, ΔQ and save ΔP_{max} and ΔQ_{max}

6. Obtain Jacobian matrix

7. Solve for $\Delta|E_p|$ and $\Delta\theta_p$ by triangular factorisation

   If yes, go to step 13

8. Compare: is $\Delta P_{max} \leq \in$ and $\Delta Q_{max} \leq \in$

9. Update all bus voltages

   $|E^k| = |E^{k-1}| + \Delta E$

   $\theta^k = \theta^{k-1} + \Delta\theta$

10. Increase iteration k = k+1

11 Go to step 4

12. Calculate line flow losses and slack bus power

13. Print Results

14. End

Table 3.1: Line Parameters and Route Length of the 33kV Distribution Network Considered.

S/N	BUSBAR LINKS	MODEL	TOTAL ROUTE LENGTH (km)
1.	Alagbon-Ademola	Underground Cable	6.13
2.	Alagbon-Alagbon Local	Underground Cable	0.15
3.	Alagbon-Anifowoshe	Underground Cable	6.84
4.	Alagbon-Fowler	Underground Cable	3.00
5.	Ademola-Maroko	33kV Interconnector cable	1.80
6.	Ademola-Anifowoshe	33kV Interconnector cable	2.40
7.	Alagbon-Banana Island	33kV Interconnector cable	5.00

Table 3.2: Hourly Loads (in MW) on the 33kV Bus bars for Selected Days Showing the Condition of the Network

		17-01-2014						20-01-2014					
Specified Hours		**02**	**06**	**09**	**12**	**21**	**23**	**02**	**06**	**09**	**12**	**21**	**23**
S/N	**Hourly Load Feeders**												
1	Fowler 1	8.7	-	-	-	9.7	-	-	4.4	5.8	12	-	-
2	Fowler 2	-	-	9.6	-	-	-	-	6.3	8	8	-	-
3	Ademola 1	-	-	10.6	-	6.7	-	9.7	-	-	-	-	-
4	Ademola 2	-	-	-	-	-	-	-	-	-	-	-	-
5	Anifowoshe	-	-	11.7	-	9.3	3.0	-	6	-	-	-	-
6	Banana 1	-	-	3	-	-	-	-	-	3	3	-	-
7	Banana 2	-	-	-	-	-	-	-	-	-	-	-	-
8	Alagbon T1 1 X 15 MVA	-	-	3.6	-	-	-	6.5	4.1	7.5	7.5	-	-
9	Alagbon T2 1 X 15 MVA	4.5	-	-	-	-	-	-	-	2.7	2.7	-	-
10	Maroko	-	-	-	-	-	-	16.5	18.5	7	7	-	12

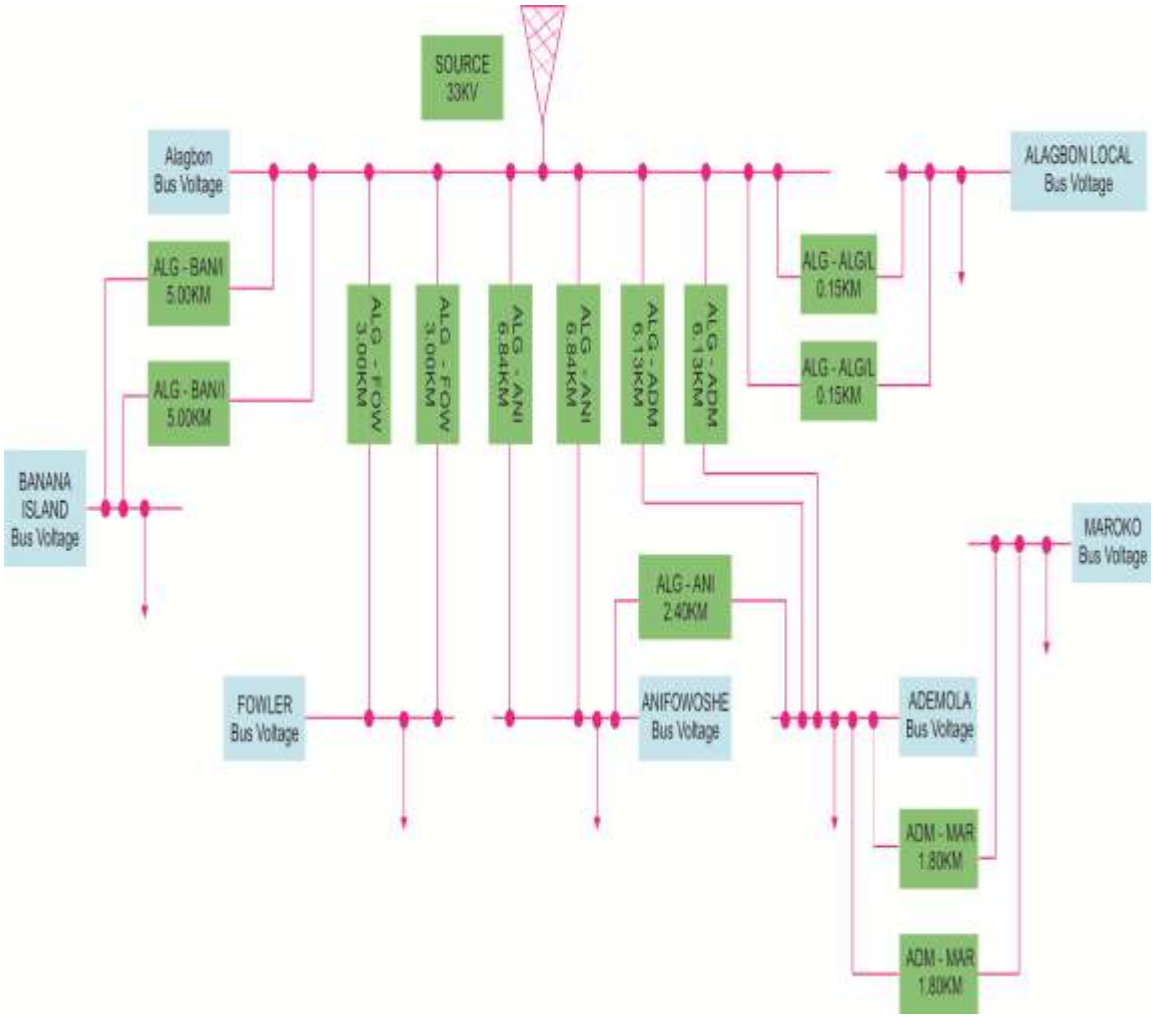

Figure 3.3: Model of the Setup of Islands Business Unit for Power Flow analysis using the NEPLAN software

3.3 Harmonic Voltage Analysis

This section involves modelling of a Distribution line between two buses for harmonic generation. An algorithm required to achieve this was developed. A flowchart was also developed to summarize this algorithm process. Details of harmonic voltage analysis procedure are as follows.

3.3.1 Modelling of Distribution Line between Two Buses

Generally, transmission or distribution lines are modelled using any of these networks:π-network, T – network orπ and T networks, depending on the distance of the line. Since the longest distribution route length in this research work is 6.84km, a π distribution line modelling approach was adopted using the MATLAB/Simulink environment. The π-modelled diagram or circuit suitable for the display of harmonics flowing between two buses is shown in Figure 3.4. It comprises the source, which is the input and the electrical line parameters such as resistance, reactance, and susceptance. It also has two oscilloscopes placed at Fowler and Alagbon busbars to measure the output and input voltage variation due to harmonic flow on the line. A reactor is connected for power control, while a current source is included to act as non-linear loads, which generate harmonics.

3.3.2 Harmonic Simulation Algorithm and Development of Flowchart for Harmonic Evaluation on the Line between Two Buses

The harmonic simulation algorithm involved in obtaining harmonic flow on the line between two buses using MATLAB simulation approach (Cascaded pi Distribution Model) are listed as follows:

1. Obtain a suitable Model Network as shown in Figure 3.4
2. Obtain Power flow results of hours of scenario for a chosen day.
3. For the line in consideration, insert system frequency and the sending end voltage obtained from power flow analysis results into the MATLAB block parameters of AC voltage source.
4. Display the sending end signal on scope b (Input).

5. On MATLAB Shunt reactor (110Mvar) block parameters, input-
    - Nominal Voltage V_n (rms)
    - Nominal Frequency (50Hz)
    - Active Power P(w)
    - Inductive reactive power Q_L (positive var)
6. Vary the parameter in 5 above (i.e. Nominal Voltage V_n) until an exact corresponding receiving end Voltage is achieved via scope o
7. When step 6 is achieved, display the bus bar receiving end voltage signal (output) on scope o.
8. In the state-space model block, compute distribution line steady state parameters in magnitude and phase values. The parameters to be displayed will include values of:
    a) States:
        i. Current I_i through Z_i
        ii. Voltage V_c across Z_i (RLC)
        iii. Current I_i through Z_o
        iv. Voltage V_c across Z_o
        v. Current I_i through shunt Reactor 110MVar
        vi. Input Voltage V_c at the beginning of Distribution line (Bus bar 1)
        vii. Current I through the pi section (Distribution line)
        viii. Output voltage V_c at the end of Distribution line (Bus bar 2)
    b) Measurements:
    Magnitude and phase values of:
        i. Measured voltage V_o at scope o (output)
        ii. Measured voltage V_b at scope b (Input)
    c) Sources:
    Magnitude and phase values of:
        i. Bus bar voltage in volts
        ii. Load on Bus bar in Amperes
9. Plot the power system impedance against frequency to display the harmonics on the distribution line.

10. From the plot, record harmonic frequencies and the corresponding harmonic impedance.
11. Repeat step 2-10 for other lines within the same time scenario. In these cases, the parameters (SE Voltage and RE Voltage) may be different in values.
12. Prepare a table of Distribution line Harmonics and their impedance.
13. Go to “Next hour scenario”
14. Repeat steps 2-12.
15. Go to “Next day scenario” and repeat step 1-14
16. End

Figure 3.5 summarises the procedures involved in the above algorithm.

3.4 Modelling of Distribution Lines for Harmonic Mitigation

In this aspect of the research work, the 33kV distribution line between Alagbon and Fowler Bus bars was selected and used as a case study. The existing distribution line model shown in Figure 3.4 was modified as shown in Figure 3.6 by connecting any of the desired filter circuit such as Band pass (RLC) or LC filter.

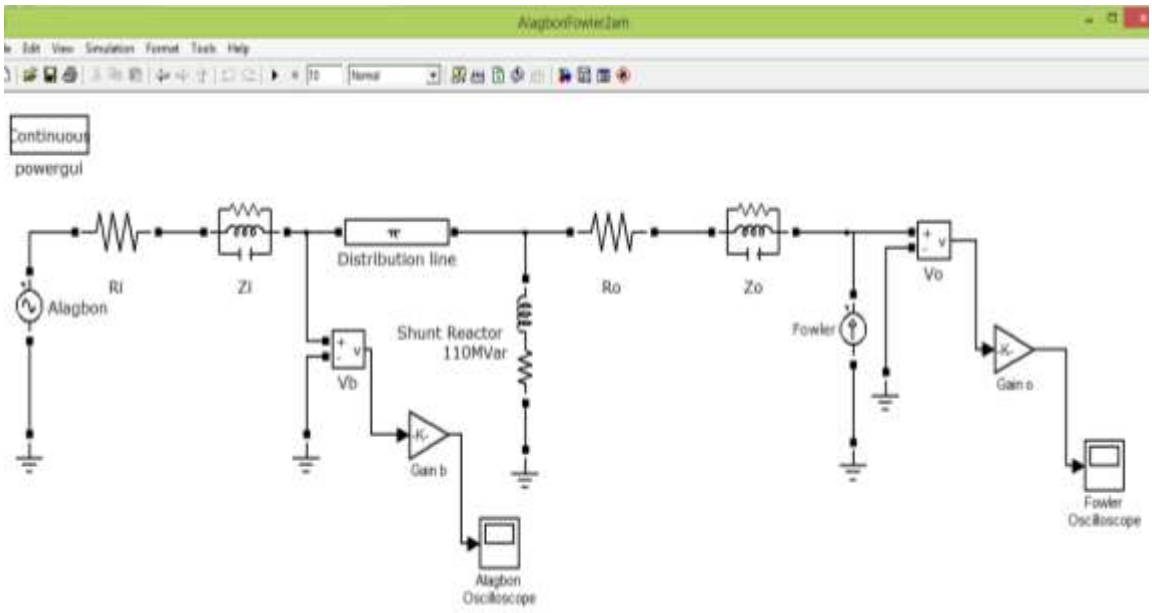

Figure 3.4: Model of the Initial setup of the Alagbon – Fowler Distribution Line

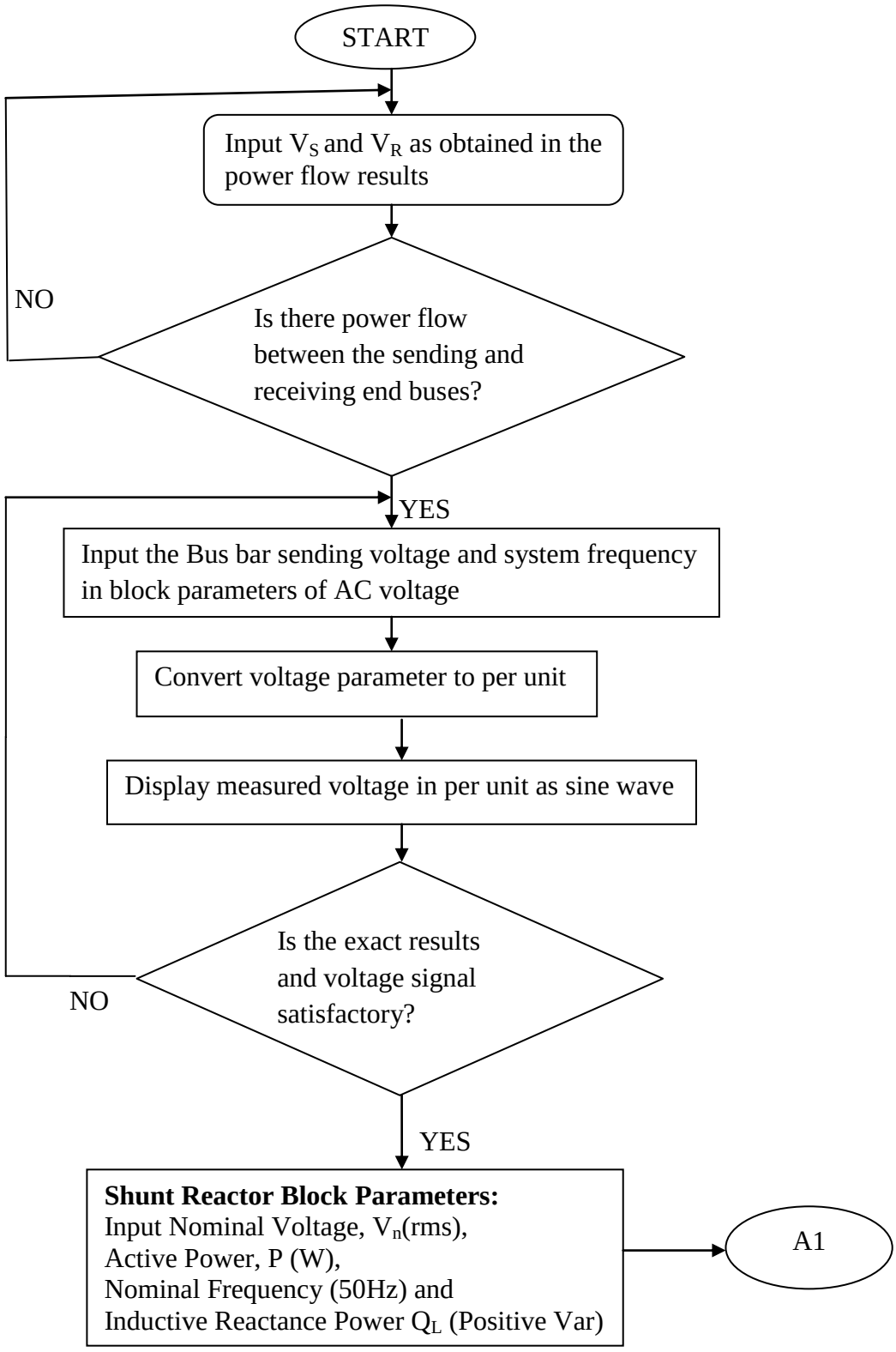
START
Input V_S and V_R as obtained in the power flow results
NO
Is there power flow between the sending and receiving end buses?
YES
Input the Bus bar sending voltage and system frequency in block parameters of AC voltage
Convert voltage parameter to per unit
Display measured voltage in per unit as sine wave
Is the exact results and voltage signal satisfactory?
NO
YES
Shunt Reactor Block Parameters:
Input Nominal Voltage, V_n(rms),
Active Power, P (W),
Nominal Frequency (50Hz) and
Inductive Reactance Power Q_L (Positive Var)
A1

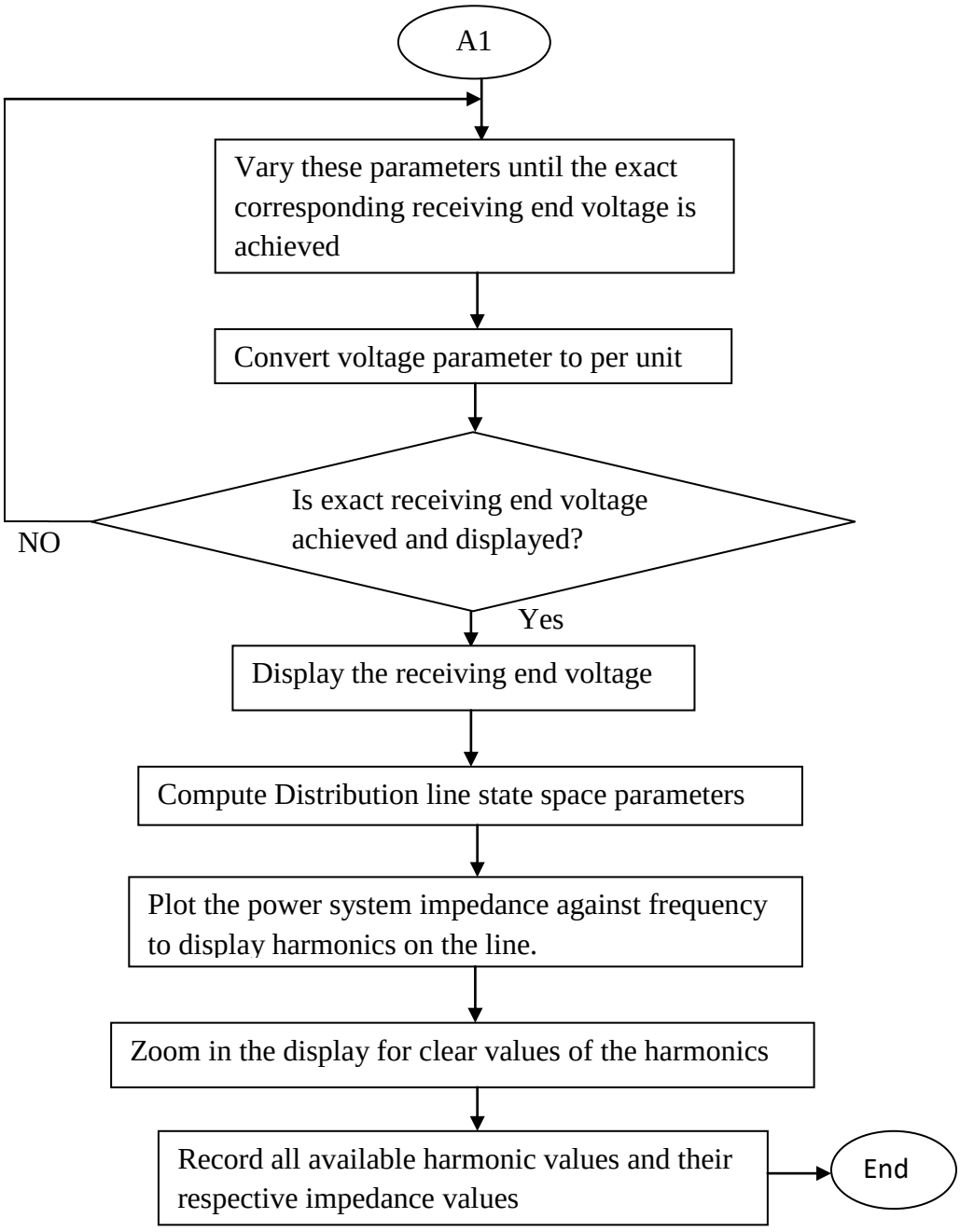

Figure 3.5: Development of flowchart for Harmonic Evaluation on Modelled π Distribution Lines between two Busbars

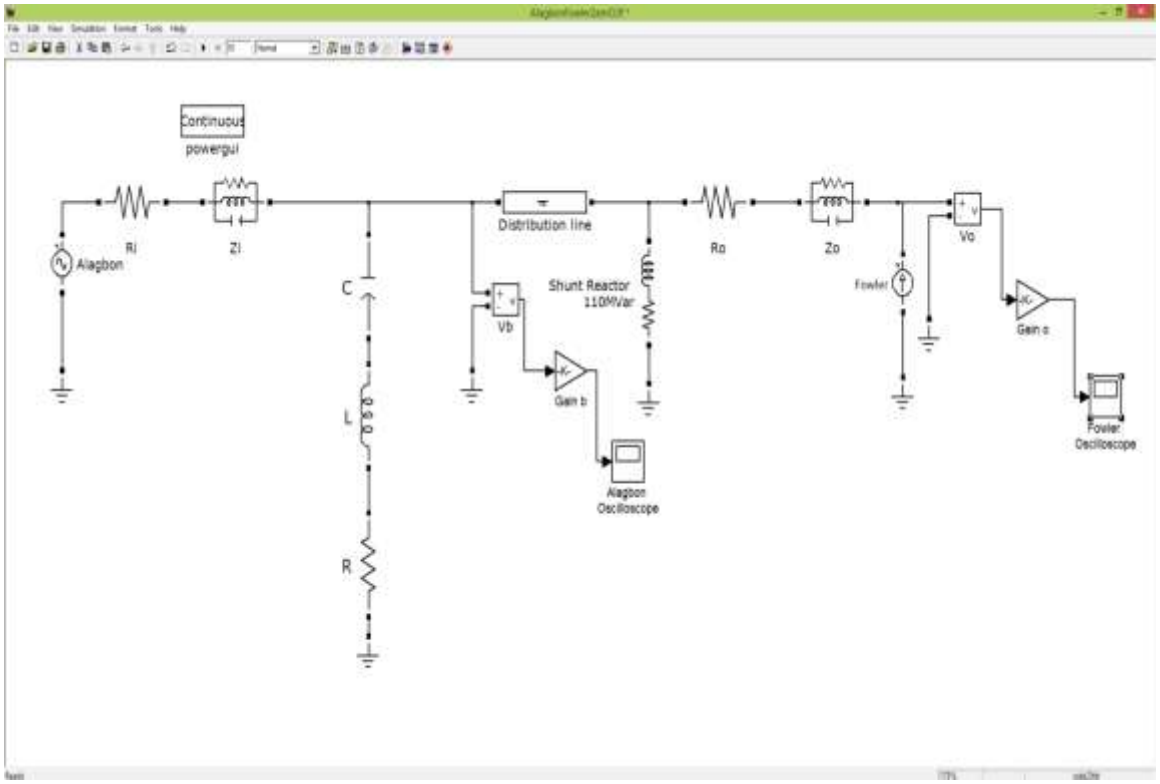

Figure 3.6: Model showing the Introduction of an RLC Band Pass Filter into the Existing Alagbon - Fowler D/L

CHAPTER FOUR

RESULTS AND DISCUSSION

4.1 INTRODUCTION

The results of the power flow analysis, Harmonic analysis and mitigation carried out in chapter three were recorded and discussed in this chapter. The result of the power flow and a comparison of harmonic results of scenario hours on 17th and 20th January, 2014 are presented in sections 4.2.1 and 4.2.2 respectively and necessary discussions are provided in sections 4.3.1 and 4.3.2 respectively. Total Harmonic Distortion (THD) analysis of the distribution lines for the selected scenario hours on both 17th and 20th January, 2014 are also discussed in section 4.3.4. The passive filter harmonic mitigation results are presented in section 4.2.3, while the discussion on this mitigation is provided in section 4.3.5.

4.2 Power Flow, Harmonic Simulation and Harmonic Mitigation Results

4.2.1 Power Flow Results

The results of the power flow studies carried out for the two chosen days i.e. 17/01/2014 and 20/01/2014, which converges at iterations, $k = 3\ to\ 5$, are presented in Tables 4.1 to 4.6:

Table 4.1: Bus bar Power Flow Results at Different Times of 17th January 2014

Table 4.1a: Bus Bar Power Flow Results at 02:00Hrs

S/N	NAME OF BUS	VOL (kV)	% VOL	V/ANG (Deg.)	P (MW)	Q (MVar)	IPP (MW)	IPQ (MVar)
1	Ademola	0	0	0	0	0	0	0
2	Alagbon	33	100	0	0	0	13.19	8.161
	Alagbon							
3	Local	32.997	99.99	-0.1	4.5	2.789	0	0
4	Anifowoshe	0	0	0	0	0	0	0
	Banana							
5	Island	0	0	0	0	0	0	0
6	Fowler	32.881	99.64	-0.1	8.7	5.342	0	0
7	Maroko	0	0	0	0	0	0	0

Table 4.1b: Bus Bar Power Flow Results at 06:00Hrs

S/N	NAME OF BUS	VOL (kV)	% VOL	V/ANG (Deg.)	P (MW)	Q (MVar)	IPP (MW)	IPQ (MVar)
1	Ademola	0	0	0	0	0	0	0
2	Alagbon	33	100	0	0	0	0	0
3	AlagbonLocal	0	0	0	0	0	0	0
4	Anifowoshe	0	0	0	0	0	0	0
5	Banana Island	0	0	0	0	0	0	0
6	Fowler	0	0	0	0	0	0	0
7	Maroko	0	0	0	0	0	0	0

Table 4.1c: Bus Bar Power Flow Results at 09:00Hrs

S/N	NAME OF BUS	VOL (kV)	% VOL	V/ANG (Deg.)	P (MW)	Q (MVar)	IPP (MW)	IPQ (MVar)
1	Ademola	32.711	99.12	-0.1	10.6	6.569	0	0
2	Alagbon	33	100	0	0	0	38.725	18.658
3	Alagbon-Local	32.997	99.99	0	3.6	2.231	0	0
4	Anifowoshe	32.645	98.93	-0.2	11.7	7.251	0	0
5	Banana-Island	32.942	99.83	0	3	1.859	0	0
6	Fowler	32.868	99.6	-0.1	9.6	5.95	0	0
7	Maroko	0	0	0	0	0	0	0

Table 4.1d: Bus Bar Power Flow Results at 12:00Hrs

S/N	NAME OF BUS	VOL (kV)	% VOL	V/ANG (Deg.)	P (MW)	Q (MVar)	IPP (MW)	IPQ (MVar)
1	Ademola	0	0	0	0	0	0	0
2	Alagbon	33	100	0	0	0	0	0
3	Alagbon Local	0	0	0	0	0	0	0
4	Anifowoshe	0	0	0	0	0	0	0
5	Banana Island	0	0	0	0	0	0	0
6	Fowler	0	0	0	0	0	0	0
7	Maroko	0	0	0	0	0	0	0

Table 4.1e: Bus Bar Power Flow Results at 21:00Hrs

S/N	NAME OF BUS	VOL (kV)	% VOL	V/ANG (Deg.)	P (MW)	Q (MVar)	IPP (MW)	IPQ (MVar)
1	Ademola	32.825	99.47	-0.1	6.7	4.152	0	0
2	Alagbon	33	100	0	0	0	25.83	11.922
3	Alagbon-Local	0	0	0	0	0	0	0
4	Anifowoshe	32.725	99.17	-0.2	9.3	5.764	0	0
5	Banana-Island	0	0	0	0	0	0	0
6	Fowler	32.867	99.6	-0.1	9.7	6.012	0	0
7	Maroko	0	0	0	0	0	0	0

Table 4.1f: Bus Bar Power Flow Results at 23:00Hrs

S/N	NAME OF BUS	VOL (kV)	% VOL	V/ANG (Deg.)	P (MW)	Q (Mvar)	IPP (MW)	IPQ (Mvar)
1	Ademola	0	0	0	0	0	0	0
2	Alagbon	33	100	0	0	0	10.281	4.565
3	Alagbon-Local	0	0	0	0	0	0	0
4	Anifowose	32.695	99.08	-0.2	10.2	6.321	0	0
5	Banana-Island	0	0	0	0	0	0	0
6	Fowler	0	0	0	0	0	0	0
7	Maroko	0	0	0	0	0	0	0

Table 4.2: Power Flow Results Showing Network Loading at Different Times of 17th January 2014

Table 4.2a: Power Flow Results Showing Network Loading at 02:00Hrs

S/N	SUBSTATION/BUSBAR	ACTIVE POWER (MW)	REACTIVE POWER (MVar)	CURRENT (kA)	CURRENT ANGLE (Degree)
1	Ademola	0	0	0	0
2	Alagbon Local	4.5	2.789	0.093	-31.8
3	Anifowoshe	0	0	0	0
4	Banana Island	0	0	0	0
5	Fowler	8.7	5.392	0.18	-31.8
6	Maroko	0	0	0	0
		13.2	**8.181**		

Table 4.2b: Power Flow Results Showing Network Loading at06:00Hrs

S/N	SUBSTATION/BUSBAR	ACTIVE POWER (MW)	REACTIVE POWER (Mvar)	CURRENT (kA)	CURRENT ANGLE (Degree)
1	Ademola	0	0	0	0
2	Alagbon-Local	0	0	0	0
3	Anifowoshe	0	0	0	0
4	Banana Island	0	0	0	0
5	Fowler	0	0	0	0
6	Maroko	0	0	0	0
		0	**0**		

Table 4.2c: Power Flow Results Showing Network Loading at09:00Hrs

S/N	SUBSTATION/BUSBAR	ACTIVE POWER (MW)	REACTIVE POWER (MVar)	CURRENT (kA)	CURRENT ANGLE (Degree)
1	Ademola	10.6	6.569	0.225	-32.2
2	Alagbon-Local	3.6	2.231	0.074	-31.8
3	Anifowoshe	11.7	7.251	0.246	-32.1
4	Banana Island	3	1.859	0.062	-31.8
5	Fowler	9.6	5.95	0.198	-31.8
6	Maroko	0	0	0	0
		38.5	**23.86**		

Table 4.2d: Power Flow Results Showing Network Loading at 12:00Hrs

S/N	SUBSTATION/BUSBAR	ACTIVE POWER (MW)	REACTIVE POWER (Mvar)	CURRENT (kA)	CURRENT ANGLE (Deg.)
1	Ademola	0	0	0	0
2	Alagbon Local	0	0	0	0
3	Anifowoshe	0	0	0	0
4	Banana Island	0	0	0	0
5	Fowler	0	0	0	0
6	Maroko	0	0	0	0
		0	**0**		

Table 4.2e: Power Flow Results Showing Network Loading at21:00Hrs

S/N	SUBSTATION/BUSBAR	ACTIVE POWER (MW)	REACTIVE POWER (Mvar)	CURRENT (kA)	CURRENT ANGLE (Degree)
1	Ademola	6.7	4.152	0.142	-32.2
2	Alagbon Local	0	0	0	0
3	Anifowoshe	9.3	5.764	0.195	-32.1
4	Banana Island	0	0	0	0
5	Fowler	9.7	6.012	0.2	-31.8
6	Maroko	0	0	0	0
		25.7	**15.928**		

Table 4.2f: Power Flow Results Showing Network Loading at23:00Hrs

S/N	SUBSTATION/BUSBAR	ACTIVE POWER (MW)	REACTIVE POWER (MVar)	CURRENT (kA)	CURRENT ANGLE (Deg.)
1	Ademola	0	0	0	0
2	Alagbon Local	0	0	0	0
3	Anifowoshe	10.2	6.321	0	0
4	Banana Island	0	0	0	0
5	Fowler	0	0	0	0
6	Maroko	0	0	0	0
		10.2	**6.321**		

Table 4.3: Lines Power Flow Results at Different Times of 17th January 2014

Table 4.3a: Lines Power Flow Results at 02:00Hrs

S/N	SB	RB	LD (KM)	P (MW)	Q (MVar)	I (kA)	C/ANG (Deg.)	% LAG	P LOSS (MW)	Q LOSS (Mvar)
1	ALG	BAN-I	5.00	0	0	0	0	0	0	0
2	ALG	BAN-I	5.00	0	0	0	0	0	0	0
3	ALG	FOW	3.00	0	0	0	0	0	0	0
4	ALG	FOW	3.00	0	-0.377	0.007	89.9	1.54	0	-0.377
5	ALG	ANI	6.84	0	0	0	0	0	0	0
6	ALG	ANI	6.84	0	0	0	0	0	0	0
7	ALG	ADM	6.13	0	0	0	0	0	0	0
8	ALG	ADM	6.13	0	0	0	0	0	0	0
9	ALG	ALG-L	0.15	0	0	0	0	0	0	0
10	ALG	ALG-L	0.15	0	0	0	0	0	0	0
11	ADM	MAR	1.80	0	0	0	0	0	0	0
12	ADM	MAR	1.80	-4.5	-2.77	0.092	148.4	21.45	0.0004	-0.0186
13	ADM	ANI	2.40	0	0	0	90	0	0	-0.019
				-4.5	**-3.147**				**0.0004**	**-0.4146**

Table 4.3b: Lines Power Flow Results at 06:00Hrs

S/N	SB	RB	LD (KM)	P (MW)	Q (MVar)	I (kA)	C/ANG (Deg.)	% LAG	P LOSS (MW)	Q LOSS (Mvar)
1	ALG	BAN-I	5.00	0	0	0	0	0	0	0
2	ALG	BAN-I	5.00	0	0	0	0	0	0	0
3	ALG	FOW	3.00	0	0	0	0	0	0	0
4	ALG	FOW	3.00	0	0	0	0	0	0	0
5	ALG	ANI	6.84	0	0	0	0	0	0	0
6	ALG	ANI	6.84	0	0	0	0	0	0	0
7	ALG	ADM	6.13	0	0	0	0	0	0	0
8	ALG	ADM	6.13	0	0	0	0	0	0	0
9	ALG	ALG-L	0.15	0	0	0	0	0	0	0
10	ALG	ALG-L	0.15	0	0	0	0	0	0	0
11	ADM	MAR	1.80	0	0	0	0	0	0	0
12	ADM	MAR	1.80	0	0	0	0	0	0	0
13	ADM	ANI	2.40	0	0	0	0	0	0	0
				0	**0**				**0**	**0**

Table 4.3c: Lines Power Flow Results at 09:00Hrs

S/N	SB	RB	LD (KM)	P (MW)	Q (MVar)	I (kA)	C/ANG (Deg.)	% LAG	P LOSS (MW)	Q LOSS (Mvar)
1	ALG	BAN-I	5.00	-3	-1.228	0.057	157.7	13.18	0.0044	-0.6276
2	ALG	BAN-I	5.00	0	-0.631	0.011	89.9	2.56	0	-0.6307
3	ALG	FOW	3.00	0	-0.377	0.007	89.9	1.54	0	-0.3767
4	ALG	FOW	3.00	-9.6	-5.573	0.195	149.8	45.24	0.033	-0.3469
5	ALG	ANI	6.84	-11.7	-6.28	0.235	151.6	54.49	0.1077	-0.7544
6	ALG	ANI	6.84	0	-0.847	0.015	89.8	3.48	0.0001	-0.8474
7	ALG	ADM	6.13	10.68	5.113	0.207	-25.6	48.06	0.0796	-0.6936
8	ALG	ADM	6.13	0	0	0	90	0	0.0001	-0.7625
9	ALG	ALG-L	0.15	-3.6	-2.212	0.074	148.4	17.15	0.0002	-0.0187
10	ALG	ALG-L	0.15	0	-0.019	0	90	0.08	0	-0.019
11	ADM	MAR	1.80	0	0	0	0	0	0	0
12	ADM	MAR	1.80	0	0	0	0	0	0	0
13	ADM	ANI	2.40	0	-0.124	0.002	89.8	0.51	0	-0.1239
				-17.22	**-12.178**				**0.2251**	**-5.2014**

Table 4.3d: Lines Power Flow Results at 12:00Hrs

S/N	SB	RB	LD (KM)	P (MW)	Q (Mvar)	I (kA)	C/ANG (Deg.)	% LAG	P LOSS (MW)	Q LOSS (MVar)
1	ALG	BAN-I	5.00	0	0	0	0	0	0	0
2	ALG	BAN-I	5.00	0	0	0	0	0	0	0
3	ALG	FOW	3.00	0	0	0	0	0	0	0
4	ALG	FOW	3.00	0	0	0	0	0	0	0
5	ALG	ANI	6.84	0	0	0	0	0	0	0
6	ALG	ANI	6.84	0	0	0	0	0	0	0
7	ALG	ADM	6.13	0	0	0	0	0	0	0
8	ALG	ADM	6.13	0	0	0	0	0	0	0
9	ALG	ALG-L	0.15	0	0	0	0	0	0	0
10	ALG	ALG-L	0.15	0	0	0	0	0	0	0
11	ADM	MAR	1.80	0	0	0	0	0	0	0
12	ADM	MAR	1.80	0	0	0	0	0	0	0
13	ADM	ANI	2.40	0	0	0	0	0	0	0
				0	**0**				**0**	**0**

Table 4.3e: Lines Power Flow Results at 21:00Hrs

S/N	SB	RB	LD (KM)	P (MW)	Q (Mvar)	I (kA)	C/ANG (Deg.)	% LAG	P LOSS (MW)	Q LOSS (Mvar)
1	ALG	BAN-I	5.00	0	0	0	0	0	0	0
2	ALG	BAN-I	5.00	0	0	0	0	0	0	0
3	ALG	FOW	3.00	0	-0.377	0.007	89.9	1.54	0	-0.3767
4	ALG	FOW	3.00	-9.7	-5.635	0.197	149.8	45.72	0.0337	-0.3463
5	ALG	ANI	6.84	-9.3	-4.788	0.185	152.6	42.82	0.066	-0.796
6	ALG	ANI	6.84	0	-0.852	0.015	89.8	3.49	0.0001	-0.8515
7	ALG	ADM	6.13	6.73	2.641	0.126	-21.4	29.35	0.03	-0.7433
8	ALG	ADM	6.13	0	0	0	90	0	0.0001	-0.7678
9	ALG	ALG-L	0.15	0	0	0	0	0	0	0
10	ALG	ALG-L	0.15	0	0	0	0	0	0	0
11	ADM	MAR	1.80	0	0	0	0	0	0	0
12	ADM	MAR	1.80	0	0	0	0	0	0	0
13	ADM	ANI	2.40	0	-0.124	0.002	89.8	0.51	0	-0.1245
				-12.27	**-9.135**				**0.1299**	**-4.0061**

Table 4.3f: Lines Power Flow Results at 23:00Hrs

S/N	SB	RB	LD (KM)	P (MW)	Q (MVar)	I (kA)	C/ANG (Deg.)	% LAG	P Loss (MW)	Q Loss (MVar)
1	ALG	BAN-I	5.00	0	0	0	0	0	0	0
2	ALG	BAN-I	5.00	0	0	0	0	0	0	0
3	ALG	FOW	3.00	0	0	0	90	0	0.0001	-0.8623
4	ALG	FOW	3.00	0	0	0	0	0	0	0
5	ALG	ANI	6.84	0	0	0	0	0	0	0
6	ALG	ANI	6.84	0	0	0	90	0	0	-0.126
7	ALG	ADM	6.13	0	0	0	0	0	0	0
8	ALG	ADM	6.13	0	0	0	0	0	0	0
9	ALG	ALG-L	0.15	0	-0.126	0.002	89.9	0.51	0	-0.126
10	ALG	ALG-L	0.15	-3	-0.871	0.055	163.7	12.71	0.0057	-0.8586
11	ADM	MAR	1.80	0	0	0	0	0	0	0
12	ADM	MAR	1.80	0	0	0	0	0	0	0
13	ADM	ANI	2.40	0	0	0	0	0	0	0
				-3	**-0.997**				**0.0058**	**-1.9729**

Table 4.4: Bus bar Power Flow Results at Different Times of 20th January 2014

Table 4.4a: Bus bar Power Flow Results at 02:00Hrs

S/N	Name of Bus	VOL (kV)	% VOL	V/ANG (deg.)	P (MW)	Q (MVar)	IPP (MW)	IPQ (Mvar)
1	Ademola	32.737	99.2	-0.1	9.7	6.012	0	0
2	Alagbon	33	100	0	0	0	16.267	8.532
3	Alagbon Local	32.995	99.99	0	6.5	4.028	0	0
4	Anifowoshe	0	0	0	0	0	0	0
5	Banana Island	0	0	0	0	0	0	0
6	Fowler	0	0	0	0	0	0	0
7	Maroko	0	0	0	0	0	0	0

Table 4.4b: Bus Bar Power Flow Results at 06:00Hrs

S/N	Name of Bus	VOL (kV)	% VOL	V/ANG (deg.)	P (MW)	Q (Mvar)	IPP (MW)	IPQ (Mvar)
1	Ademola	0	0	0	0	0	0	0
2	Alagbon	33	100	0	0	0	20.847	10.295
3	Alagbon Local	32.997	99.99	0	4.1	2.541	0	0
4	Anifowoshe	32.833	99.49	-0.1	6	3.718	0	0
5	Banana Island	0	0	0	0	0	0	0
6	Fowler	32.926	99.77	0	10.7	6.631	0	0
7	Maroko	0	0	0	0	0	0	0

Table 4.4c: Bus Bar Power Flow Results at 09:00Hrs

S/N	Name of Busbar	VOL (kV)	% VOL	V/ANG (deg.)	P (MW)	Q (Mvar)	IPP (MW)	IPQ (Mvar)
1	Ademola	0	0	0	0	0	0	0
2	Alagbon	33	100	0	0	0	27.04	14.712
3	Alagbon Local	32.996	99.99	0	10.2	6.321	0	0
4	Anifowoshe	0	0	0	0	0	0	0
5	Banana Island	32.942	99.83	0	3	1.859	0	0
6	Fowler	32.904	99.71	0	13.8	8.552	0	0
7	Maroko	0	0	0	0	0	0	0

Table 4.4d: Bus Bar Power Flow Results at12:00Hrs

S/N	Name of Bus	VOL (kV)	% VOL	V/ANG (deg.)	P (MW)	Q (Mvar)	IPP (MW)	IPQ (Mvar)
1	Ademola	0	0	0	0	0	0	0
2	Alagbon	33	100	0	0	0	138.839	83.544
3	Alagbon Local	32.96	99.88	0	11.2	6.941	0	0
4	Anifowoshe	32.553	98.64	-0.2	14.5	8.986	0	0
5	Banana Island	0	0	0	0	0	0	0
6	Fowler	32.834	99.5	-0.1	12	7.437	0	0
7	Maroko	0	0	0	0	0	0	0

Table 4.4e: Bus Bar Power Flow Results at21:00Hrs

S/N	Name of Bus	VOL (kV)	% VOL	V/ANG (deg.)	P (MW)	Q (Mvar)	IPP (MW)	IPQ (Mvar)
1	Ademola	0	0	0	0	0	0	0
2	Alagbon	33	100	0	0	0	0	0
3	Alagbon Local	0	0	0	0	0	0	0
4	Anifowoshe	0	0	0	0	0	0	0
5	Banana Island	0	0	0	0	0	0	0
6	Fowler	0	0	0	0	0	0	0
7	Maroko	0	0	0	0	0	0	0

Table 4.4f: Bus Bar Power Flow Results at 23:00Hrs

S/N	Name of Bus	VOL (kV)	% VOL	V/ANG (deg.)	P (MW)	Q (Mvar)	IPP (MW)	IPQ (Mvar)
1	Ademola	0	0	0	0	0	0	0
2	Alagbon	33	100	0	0	0	0	0
3	Alagbon Local	0	0	0	0	0	0	0
4	Anifowoshe	0	0	0	0	0	0	0
5	Banana Island	0	0	0	0	0	0	0
6	Fowler	0	0	0	0	0	0	0
7	Maroko	0	0	0	0	0	0	0

Table 4.5: Power Flow Results Showing Network Loading at Different Times of 20th January 2014

Table 4.5a: Power Flow Results Showing Network Loading at 02:00Hrs

S/N	Substation/Busbar	Active power (MW)	Reactive power (Mvar)	Current (kA)	Current Angle (Deg.)
1	Ademola	9.7	6.012	0.212	-32.5
2	Alagbon Local	6.5	4.028	0.134	-31.8
3	Anifowoshe	0	0	0	0
4	Banana Island	0	0	0	0
5	Fowler	0	0	0	0
6	Maroko	0	0	0	0
		16.2	**10.042**		

Table 4.5b: Power Flow Results Showing Network Loading at06:00Hrs

S/N	Substation/Busbar	Active power (MW)	Reactive power (Mvar)	Current (kA)	Current Angle (Deg.)
1	Ademola	0	0	0	0
2	Alagbon Local	4.1	2.541	0.084	-31.8
3	Anifowoshe	6	3.718	0.125	-32
4	Banana Island	0	0	0	0
5	Fowler	10.7	6.631	0.221	-31.8
6	Maroko	0	0	0	0
		20.8	**12.89**		

Table 4.5c: Power Flow Results Showing Network Loading at 09:00Hrs

S/N	Substation/Busbar	Active power (MW)	Reactive power (Mvar)	Current (kA)	Current Angle (Deg.)
1	Ademola	0	0	0	0
2	Alagbon Local	10.2	6.321	0.21	-31.8
3	Anifowoshe	0	0	0	0
4	Banana Island	3	1.859	0.062	-31.8
5	Fowler	13.8	8.552	0.285	-31.8
6	Maroko	0	0	0	0
		27	**16.732**		

Table 4.5d: Power Flow Results Showing Network Loading at 12:00Hrs

S/N	Substation/Busbar	Active power (MW)	Reactive power (Mvar)	Current (kA)	Current Angle (Deg.)
1	Ademola	0	0	0	0
2	Alagbon Local	112	69.411	0.231	-31.8
3	Anifowoshe	14.5	8.986	0.094	-32
4	Banana Island	0	0	0	0
5	Fowler	12	7.437	0.248	-31.9
6	Maroko	0	0	0	0
		138.5	**85.834**		

Table 4.5e: Power Flow Results Showing Network Loading at 21:00Hrs

S/N	Substation/Busbar	Active power (MW)	Reactive power (Mvar)	Current (kA)	Current Angle (Deg.)
1	Ademola	0	0	0	0
2	Alagbon Local	0	0	0	0
3	Anifowoshe	0	0	0	0
4	Banana Island	0	0	0	0
5	Fowler	0	0	0	0
6	Maroko	0	0	0	0
		0	**0**		

Table 4.5f: Power Flow Results Showing Network Loading at 23:00Hrs

S/N	Substation/Busbar	Active power (MW)	Reactive power (Mvar)	Current (kA)	Current Angle (Deg.)
1	Ademola	0	0	0	0
2	Alagbon Local	0	0	0	0
3	Anifowoshe	0	0	0	0
4	Banana Island	0	0	0	0
5	Fowler	0	0	0	0
6	Maroko	0	0	0	0
		0	**0**		

Table 4.6: Lines Power Flow Results at Different Times of 20th January 2014

Table 4.6a: Lines Power Flow Results at 02:00Hrs

S/N	SB	RB	LD (km)	P (MW)	Q (Mvar)	I (kA)	C/ANG (Deg.)	% LAG	P Loss (MW)	Q Loss (Mvar)
1	ALG	BAN-I	5.00	0	0	0	0	0	0	0
2	ALG	BAN-I	5.00	0	0	0	0	0	0	0
3	ALG	FOW	3.00	0	0	0	0	0	0	0
4	ALG	FOW	3.00	0	0	0	0	0	0	0
5	ALG	ANI	6.84	0	0	0	0	0	0	0
6	ALG	ANI	6.84	0	0	0	0	0	0	0
7	ALG	ADM	6.13	-9.7	-5.248	0.195	151.4	45.13	0.066	-0.7072
8	ALG	ADM	6.13	0	-0.764	0.013	89.9	3.13	0.0001	-0.7637
9	ALG	ALG-L	0.15	6.501	3.991	0.133	-31.5	30.96	0.0008	-0.0182
10	ALG	ALG-L	0.15	0	0	0	90	0	0	-0.019
11	ADM	MAR	1.80	0	0	0	0	0	0	0
12	ADM	MAR	1.80	-13.562	-8.405	0.297	147.4	49.55	0.0465	-0.1576
13	ADM	ANI	2.40	0	0	0	0	0	0	0
				-16.761	**-10.426**				**0.1134**	**-1.6657**

Table 4.6b: Lines Power Flow Results at 06:00Hrs

S/N	SB	RB	LD (km)	P (MW)	Q (Mvar)	I (kA)	C/ANG (Deg.)	% LAG	P Loss (MW)	Q Loss (Mvar)
1	ALG	BAN-I	5.00	0	0	0	0	0	0	0
2	ALG	BAN-I	5.00	0	0	0	0	0	0	0
3	ALG	FOW	3.00	-5.35	-3.315	0.11	148.2	25.61	0.0104	-0.369
4	ALG	FOW	3.00	5.36	2.946	0.107	-28.8	24.83	0.0104	-0.369
5	ALG	ANI	6.84	-5.35	-3.315	0.11	148.2	25.61	0.0104	-0.369
6	ALG	ANI	6.84	-6	-2.736	0.116	155.4	26.9	0.0257	-0.8371
7	ALG	ADM	6.13	0	-0.857	0.015	89.9	3.5	0.0001	-0.8572
8	ALG	ADM	6.13	0	0	0	0	0	0	0
9	ALG	ALG-L	0.15	0	0	0	0	0	0	0
10	ALG	ALG-L	0.15	-4.1	-2.522	0.084	148.4	19.54	0.0003	-0.0187
11	ADM	MAR	1.80	0	-0.019	0	90	0.08	0	-0.019
12	ADM	MAR	1.80	0	0	0	0	0	0	0
13	ADM	ANI	2.40	0	-0.125	0.002	89.9	0.51	0	-0.1253
				-15.44	**-9.943**				**0.0573**	**-2.9643**

Table 4.6c: Lines Power Flow Results at 09:00Hrs

S/N	SB	RB	LD (km)	P (MW)	Q (Mvar)	I (kA)	C/ANG (Deg.)	% LAG	P Loss (MW)	Q Loss (Mvar)
1	ALG	BAN-I	5.00	-3	-1.228	0.057	157.7	13.18	0.0044	-0.6276
2	ALG	BAN-I	5.00	0	-0.631	0.011	89.9	2.56	0	-0.6307
3	ALG	FOW	3.00	0	-0.377	0.007	89.9	1.54	0	-0.3767
4	ALG	FOW	3.00	-9.6	-5.573	0.195	149.8	45.24	0.033	-0.3469
5	ALG	ANI	6.84	-11.7	-6.28	0.235	151.6	54.49	0.1077	-0.7544
6	ALG	ANI	6.84	0	-0.847	0.015	89.8	3.48	0.0001	-0.8474
7	ALG	ADM	6.13	10.68	5.113	0.207	-25.6	48.06	0.0796	-0.6936
8	ALG	ADM	6.13	0	0	0	90	0	0.0001	-0.7625
9	ALG	ALG-L	0.15	-3.6	-2.212	0.074	148.4	17.15	0.0002	-0.0187
10	ALG	ALG-L	0.15	0	-0.019	0	90	0.08	0	-0.019
11	ADM	MAR	1.80	0	0	0	0	0	0	0
12	ADM	MAR	1.80	0	0	0	0	0	0	0
13	ADM	ANI	2.40	0	-0.124	0.002	89.8	0.51	0	-0.1239
				-17.22	**-12.178**				**0.2251**	**-5.2014**

Table 4.6d: Lines Power Flow Results at 12:00Hrs

S/N	SB	RB	LD (km)	P (MW)	Q (Mvar)	I (kA)	C/ANG (Deg.)	% LAG	P Loss (MW)	Q Loss (Mvar)
1	ALG	BAN-I	5.00	0	0	0	0	0	0	0
2	ALG	BAN-I	5.00	0	0	0	0	0	0	0
3	ALG	FOW	3.00	0	0	0	0	0	0	0
4	ALG	FOW	3.00	0	0	0	0	0	0	0
5	ALG	ANI	6.84	0	0	0	0	0	0	0
6	ALG	ANI	6.84	0	0	0	0	0	0	0
7	ALG	ADM	6.13	0	0	0	0	0	0	0
8	ALG	ADM	6.13	0	0	0	0	0	0	0
9	ALG	ALG-L	0.15	0	0	0	0	0	0	0
10	ALG	ALG-L	0.15	0	0	0	0	0	0	0
11	ADM	MAR	1.80	0	0	0	0	0	0	0
12	ADM	MAR	1.80	0	0	0	0	0	0	0
13	ADM	ANI	2.40	0	0	0	0	0	0	0
				0	**0**				**0**	**0**

Table 4.6e: Lines Power Flow Results at 21:00Hrs

S/N	SB	RB	LD (km)	P (MW)	Q (Mvar)	I (kA)	C/ANG (Deg.)	% LAG	P Loss (MW)	Q Loss (Mvar)
1	ALG	BAN-I	5.00	0	0	0	0	0	0	0
2	ALG	BAN-I	5.00	0	0	0	0	0	0	0
3	ALG	FOW	3.00	-12	-7.061	0.245	149.5	56.8	0.0522	-0.3283
4	ALG	FOW	3.00	0	0	0	90	0	0	-0.3759
5	ALG	ANI	6.84	0	-0.376	0.007	89.9	1.53	0	-0.3759
6	ALG	ANI	6.84	-14.5	-8.02	0.294	150.8	68.19	0.1695	-0.6933
7	ALG	ADM	6.13	0	-0.843	0.015	89.8	3.47	0.0001	-0.8426
8	ALG	ADM	6.13	0	0	0	0	0	0	0
9	ALG	ALG-L	0.15	0	0	0	0	0	0	0
10	ALG	ALG-L	0.15	-56	-34.705	1.154	148.2	26.76	0.0587	0.0368
11	ADM	MAR	1.80	-56	-34.705	1.154	148.2	26.76	0.0587	0.0368
12	ADM	MAR	1.80	0	0	0	0	0	0	0
13	ADM	ANI	2.40	0	0	0	90	0	0	-0.1232
				-138.5	**-85.71**				**0.3392**	**-2.6656**

Table 4.6f: Lines Power Flow Results at 23:00Hrs

S/N	SB	RB	LD (KM)	P (MW)	Q (Mvar)	I (kA)	C/ANG (Deg.)	% LAG	P Loss (MW)	Q Loss (Mvar)
1	ALG	BAN-I	5.00	0	0	0	0	0	0	0
2	ALG	BAN-I	5.00	0	0	0	0	0	0	0
3	ALG	FOW	3.00	-12	-7.061	0.245	149.5	56.8	0.0522	-0.3283
4	ALG	FOW	3.00	0	0	0	90	0	0	-0.3759
5	ALG	ANI	6.84	0	-0.376	0.007	89.9	1.53	0	-0.3759
6	ALG	ANI	6.84	-14.5	-8.02	0.294	150.8	68.19	0.1695	-0.6933
7	ALG	ADM	6.13	0	-0.843	0.015	89.8	3.47	0.0001	-0.8426
8	ALG	ADM	6.13	0	0	0	0	0	0	0
9	ALG	ALG-L	0.15	0	0	0	90	0	0.0048	-0.7164
10	ALG	ALG-L	0.15	0	-0.017	0	90	0.06	0	-0.017
11	ADM	MAR	1.80	0	0	0	0	0	0	0
12	ADM	MAR	1.80	0	0	0	0	0	0	0
13	ADM	ANI	2.40	0	0	0	90	0	0	-0.1232
					16.317				**0.2266**	**-3.4726**

4.2.2 Harmonic Simulation Results

4.2.2.1 Harmonic Results for the Scenarios of 17th January, 2014

Figures 4.1a to 4.4a are the harmonic analysis results for different cases and at different times of 17th January 2014, considering Tables 4.1a to 4.1f.

At 02:00Hrs

Case 1: Alagbon – Alagbon Local Distribution Line

AC Voltage Source Block Parameters

Amplitude of Source voltage = 33kV

Nominal Frequency = 50 Hz

Block Parameters of Shunt Reactor 110MVar

Nominal Voltage, V (Vrms) = 39.5kV

Nominal Frequency = 50Hz

Active Power, P (W) = 110MWInductive reactive Power, Q_L (+Var) = 110Mvar

Π Block Parameters

Line Distance = 0.15 km

The 2nd harmonic (100Hz) occurs at $10^{2.052}\Omega$ for a range of frequencies between 0 – 1500Hz.

Case 2: Alagbon – Fowler Distribution Line

AC Voltage Source Block Parameters

Amplitude of Source voltage = 33 kV

Nominal Frequency = 50 Hz

Block Parameters of Shunt Reactor 110MVar

Nominal Voltage, V (Vrms) = 91.13 kV

Nominal Frequency = 50 Hz

Active Power, P (W) = 110 MW

Inductive reactive Power, Q_L (+Var) = 110Mvar

Π Block Parameters

Line Distance = 3.00 km

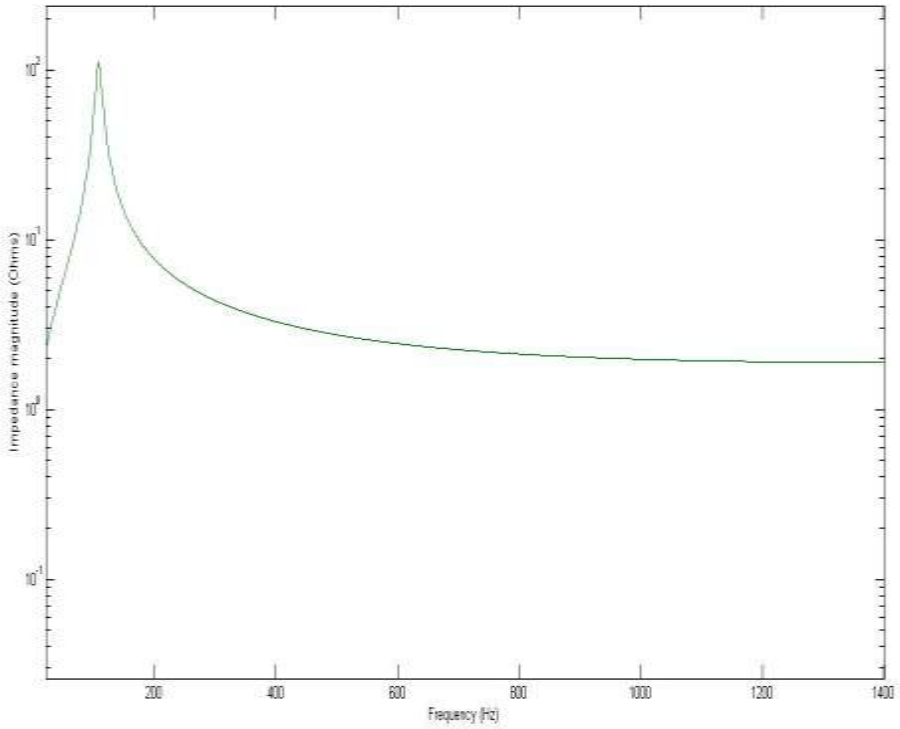

Figure 4.1a: Harmonic of the Alagbon – Alagbon Local Distribution Line at 02:00Hrs.

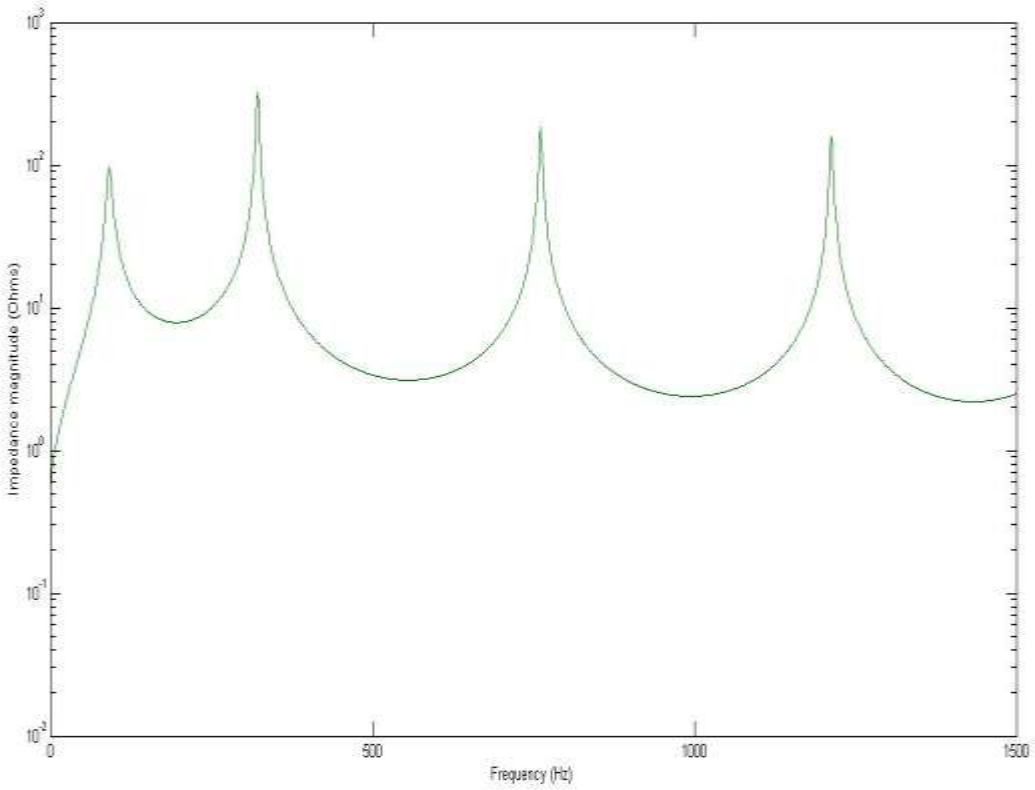

Figure 4.1b: Harmonics on Alagbon – Fowler Distribution Line at 02:00Hrs

Table 4.7a: Alagbon – Fowler Distribution Line Harmonics and Impedances at 02:00Hrs of 17th January, 2014

Nth Harmonic	Harmonic Frequency (Hz)	Harmonic Impedance (Ω)
2nd	100	$10^{1.985}$
6th	300	$10^{2.508}$
15th	750	$10^{2.268}$
24th	1200	$10^{2.198}$

Frequency range is between 0 – 1500Hz.

Table 4.7b: Distribution Lines Harmonics, Receiving end voltages and their Impedances for cases of 02:00Hrs of 17th January, 2014

S/N	Name of Line	LD (km)	Sending Voltage (kV)	Receiving Voltage (kV)	Observed Harmonics	Harmonic Impedance (Ω)
1	ALG-ADM	6.13	33	0	-	-
2	ALG-ALG-L	0.15	33	32.997	2^{nd}	$10^{2.052}$
3	ALG-ANI	6.84	33	0	-	-
4	ALG-FOW	3.00	33	32.881	2^{nd}, 6^{th}, 15^{th}, 24^{th}	$10^{1.985}$,$10^{2.51}$,$10^{2.27}$,$10^{2.2}$
5	ADM-MAR	1.80	0	0	-	-
6	ADM-ANI	2.40	0	0	-	-
7	ALG-BAN-I	5.00	33	0	-	-

At 09:00Hrs

Case 1: Alagbon – Ademola Distribution Line

AC Voltage Source Block Parameters

Amplitude of Source voltage = 33 kV

Nominal Frequency = 50 Hz

Block Parameters of Shunt Reactor 110MVar

Nominal Voltage, V (Vrms) = 117.5 kV

Nominal Frequency = 50 Hz

Active Power, P (W) = 110 MW

Inductive reactive Power, Q_L (+Var) = 110Mvar

Π Block Parameters

Line Distance = 6.13 km

Case 2: Alagbon – Alagbon Local Distribution Line

AC Voltage Source Block Parameters

Amplitude of Source voltage = 33 kV

Nominal Frequency = 50 Hz

Block Parameters of Shunt Reactor 110MVar

Nominal Voltage, V (Vrms) = 39.6 kV

Nominal Frequency = 50 Hz

Active Power, P (W) = 110 MW

Inductive reactive Power, Q_L (+Var) = 110Mvar

Π Block Parameters

Line Distance = 0.15 km

The 2^{nd} harmonic (100Hz) occurs at $10^{2.052}\Omega$ for a range of frequencies between 0 – 1500Hz.

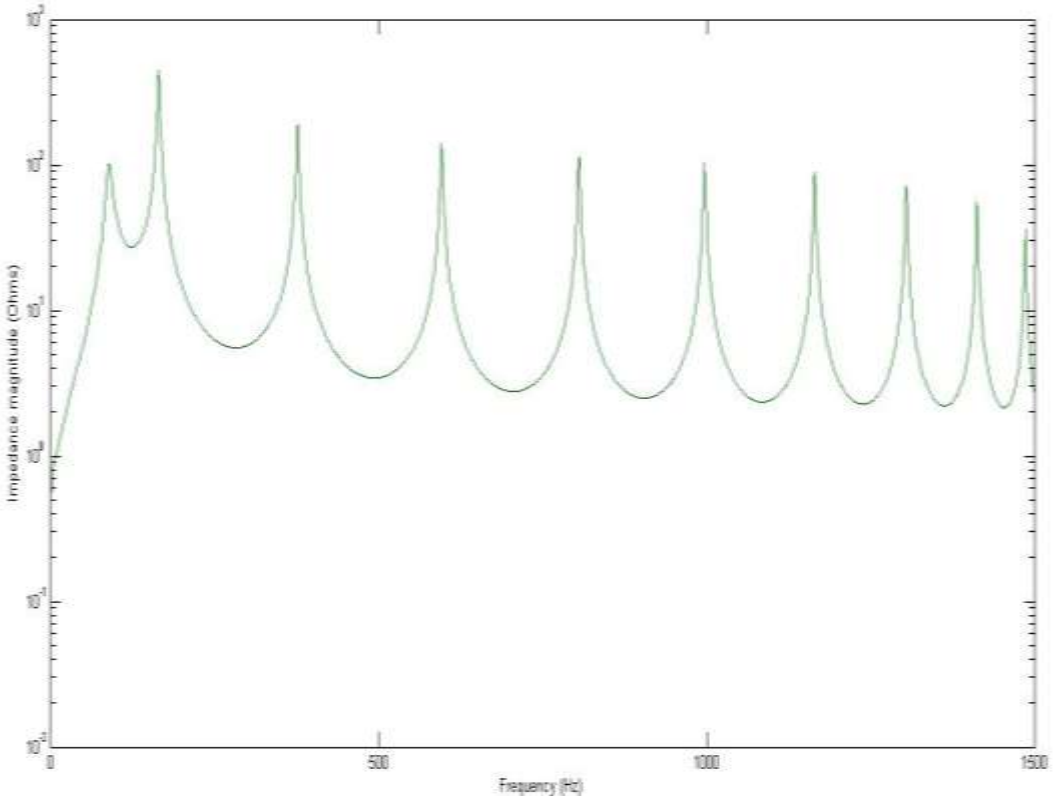

Figure 4.2a: Harmonics on Alagbon – Ademola Distribution Line at 09:00Hrs

Table 4.7c: Alagbon – Ademola Distribution Line Harmonics and Impedances at 09:00Hrs of 17th January, 2014

Nth Harmonic	Harmonic Frequency (Hz)	Harmonic Impedance (Ω)
2nd	100	$10^{2.007}$
3rd	150	$10^{2.648}$
8th	400	$10^{2.279}$
12th	600	$10^{2.148}$
16th	800	$10^{2.051}$
20th	1000	$10^{2.014}$
23rd	1150	$10^{1.945}$
26th	1300	$10^{1.859}$
28th	1400	$10^{1.741}$
29th	1450	$10^{1.556}$

Frequency range is between 0 – 1500Hz.

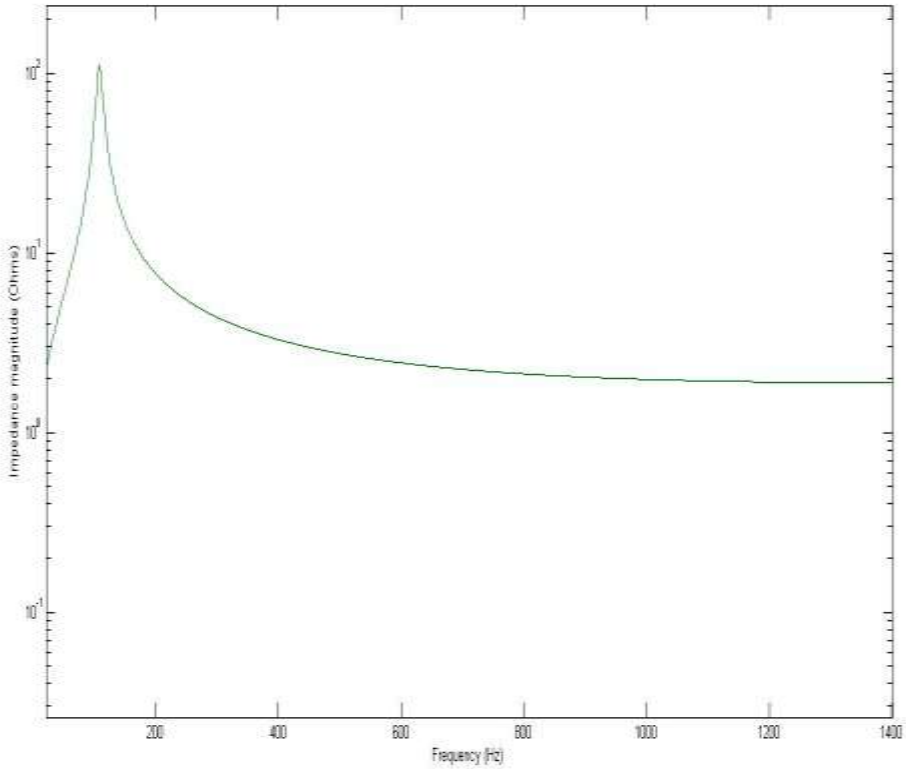

Figure 4.2b: Harmonic of the Alagbon – Alagbon Local Distribution Line at 09:00Hrs.

Case 3: Alagbon – Anifowoshe Distribution Line

AC Voltage Source Block Parameters

Amplitude of Source voltage = 33 kV

Nominal Frequency = 50 Hz

Block Parameters of Shunt Reactor 110MVar

Nominal Voltage, V (Vrms) = 116.5 kV

Nominal Frequency = 50 Hz

Active Power, P (W) = 110 MW

Inductive reactive Power, Q_L (+Var) = 110Mvar

Π Block Parameters

Line Distance = 6.84 km

Inductive Reactive Power, Q_L (+Var) = 110Mvar

Case 4: Alagbon – Fowler Distribution Line

AC Voltage Source Block Parameters

Amplitude of Source voltage = 33 kV

Nominal Frequency = 50 Hz

Block Parameters of Shunt Reactor 110MVar

Nominal Voltage, V (Vrms) = 91.1 kV

Nominal Frequency = 50 Hz

Active Power, P (W) = 110 MW

Inductive reactive Power, Q_L (+Var) = 110Mvar

Π Block Parameters

Line Distance = 3.00 km

Case 5: Alagbon – Banana Island Distribution Line

AC Voltage Source Block Parameters

Amplitude of Source voltage = 33 kV

Nominal Frequency = 50 Hz

Block Parameters of Shunt Reactor 110MVar

Nominal Voltage, V (Vrms) = 114.4 kV

Nominal Frequency = 50 Hz

Active Power, P (W) = 110 MW

Inductive reactive Power, Q_L (+Var) = 110Mvar

II Block Parameters

Line Distance = 5.00 km

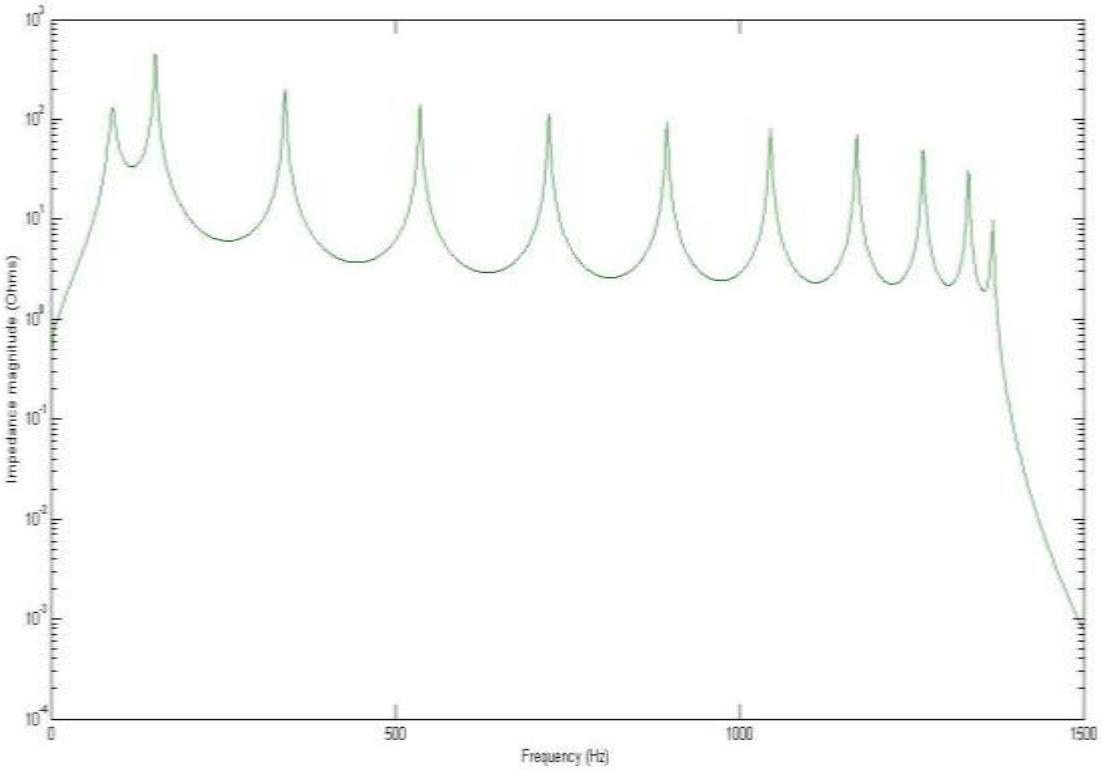

Figure 4.2c: Harmonics on Alagbon – Anifowoshe Distribution Line at 09:00Hrs

Table 4.7d: Alagbon – Anifowoshe Distribution Line Harmonics and Impedances at 09:00Hrs of 17th January, 2014

Nth Harmonic	Harmonic Frequency (Hz)	Harmonic Impedance (Ω)
2nd	100	$10^{2.116}$
3rd	150	$10^{2.650}$
7th	350	$10^{2.298}$
11th	550	$10^{2.143}$
14th	700	$10^{2.057}$
18th	900	$10^{1.973}$
21st	1050	$10^{1.914}$
23rd	1150	$10^{1.841}$
25th	1250	$10^{1.690}$
26th	1300	$10^{1.490}$
27th	1350	$10^{0.994}$

Frequency Range is between 0 – 1500Hz.

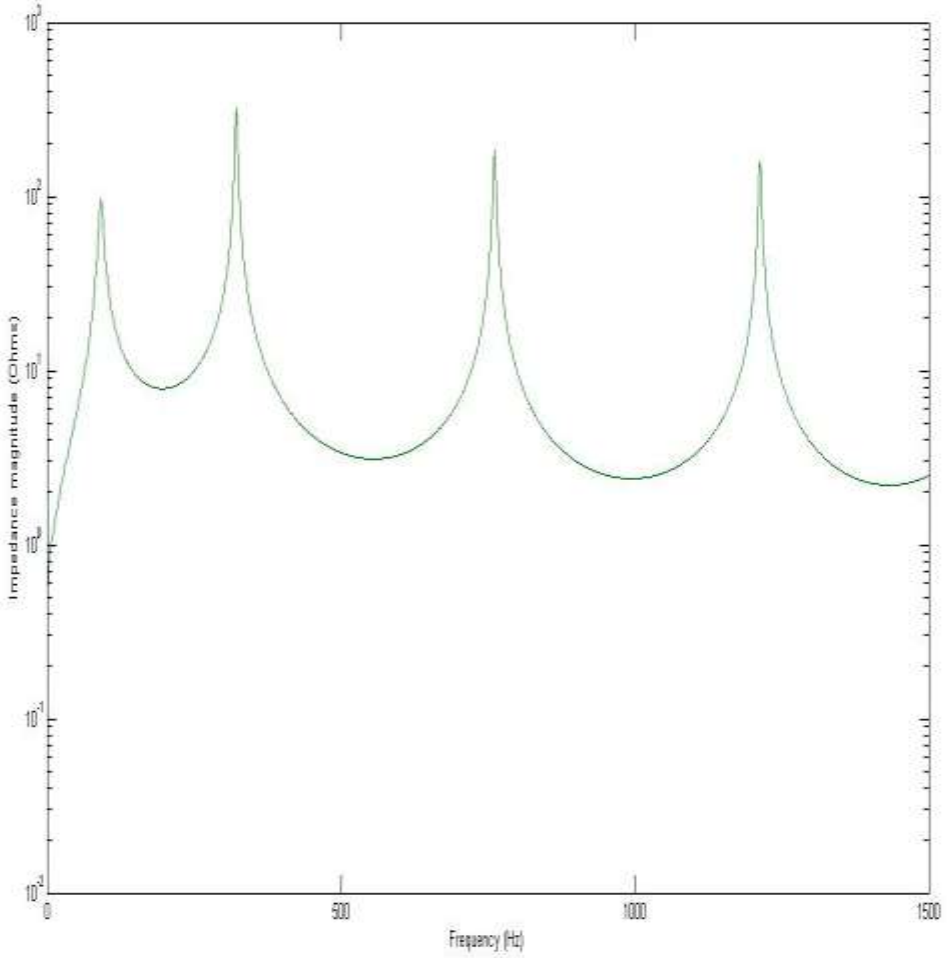

Figure 4.2d: Harmonics of the Alagbon – Fowler Distribution Line at 09:00Hrs

Table 4.7e: Alagbon – Fowler Distribution Line Harmonics and Impedances at 09:00Hrs of 17th January, 2014

Nth Harmonic	Harmonic Frequency (Hz)	Harmonic Impedance (Ω)
2nd	100	$10^{1.985}$
6th	300	$10^{2.508}$
15th	750	$10^{2.268}$
24th	1200	$10^{2.198}$

Frequency Range is between 0 – 1500Hz.

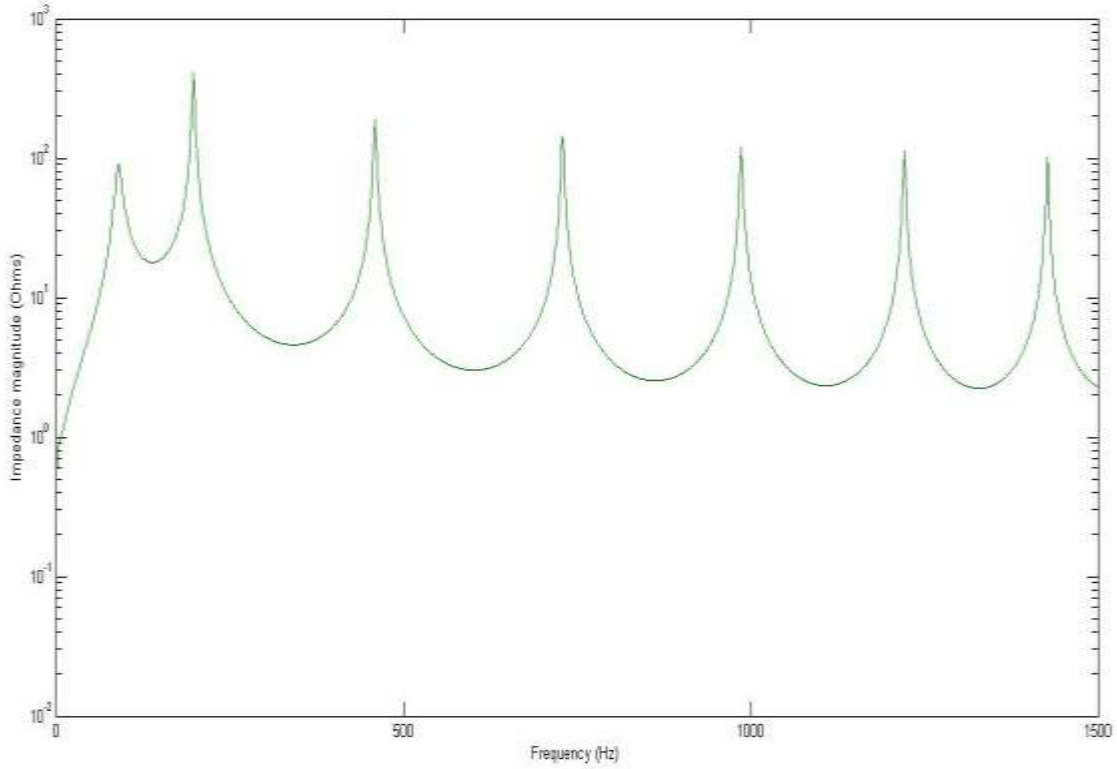

Figure 4.2e: Harmonics on Alagbon – Banana Island Distribution Line at 09:00Hrs

Table 4.7f: Alagbon – Banana Island Distribution Line Harmonics and Impedances at 09:00Hrs of 17th January, 2014

Nth Harmonic	Harmonic Frequency (Hz)	Harmonic Impedance (Ω)
2nd	100	$10^{1.962}$
3rd	200	$10^{2.610}$
9th	450	$10^{2.276}$
15th	750	$10^{2.152}$
20th	1000	$10^{2.083}$
24th	1200	$10^{2.048}$
29th	1450	$10^{2.007}$

Frequency range is between 0 – 1500Hz.

Table 4.7g: Distribution Lines Harmonics, Receiving end voltages and their Impedances for Cases of 09:00Hrs

S/N	Name of Line	Line Length (km)	Sending Voltage (kV)	Receiving Voltage (kV)	Observed Harmonics	Harmonic Impedance (Ω)
1	ALG-ADM	6.13	33	32.711	2^{nd}, 3^{rd}, 8^{th}, 12^{th}, 16^{th}, 20^{th}, 23^{rd}, 26^{th}, 28^{th}, 29^{th}	$10^{2.01}$, $10^{2.65}$, $10^{2.28}$, $10^{2.15}$, $10^{2.05}$, $10^{2.01}$, $10^{1.95}$, $10^{1.86}$, $10^{1.74}$, $10^{1.56}$
2	ALG-ALG-L	0.15	33	32.997	2^{nd}	$10^{2.05}$
3	ALG-ANI	6.84	33	32.645	2^{nd}, 3^{rd}, 7^{th}, 11^{th}, 14^{th}, 18^{th}, 21^{st},23^{rd}, 25^{th}, 26^{th}, 27^{th}	$10^{2.12}$, $10^{2.65}$, $10^{2.30}$, $10^{2.14}$, $10^{2.06}$, $10^{1.97}$, $10^{1.91,}$ $10^{1.84}$, $10^{1.69}$, $10^{1.49}$, $10^{0.99}$
4	ALG-FOW	3.00	33	32.860	2^{nd}, 6^{th}, 15^{th}, 24^{th}	$10^{1.99}$, $10^{2.51}$, $10^{2.27}$,$10^{2.20}$
5	ADM-MAR	1.80	32.711	0	-	-
6	ALG-BAN-I	5.00	33	32.942	2^{nd}, 3^{rd}, 9^{th}, 15^{th}, 20^{th}, 24^{th}, 29^{th}	$10^{1.96}$, $10^{2.61}$, $10^{2.28}$, $10^{2.15}$, $10^{2.08}$, $10^{2.05}$, $10^{2.01}$

At 21:00Hrs

Case 1: Alagbon – Ademola Distribution Line

AC Voltage Source Block Parameters

Amplitude of Source voltage = 33 kV

Nominal Frequency = 50 Hz

Block Parameters of Shunt Reactor 110MVar

Nominal Voltage, V (Vrms) = 117.7 kV

Nominal Frequency = 50 Hz

Active Power, P (W) = 110 MW

Inductive reactive Power, Q_L (+Var) = 110Mvar

Π Block Parameters

Line Distance = 6.13 km

Case 2: Alagbon – Anifowoshe Distribution Line

AC Voltage Source Block Parameters

Amplitude of Source voltage = 33 kV

Nominal Frequency = 50 Hz

Block Parameters of Shunt Reactor 110MVar

Nominal Voltage, V (Vrms) = 116.63 kV

Nominal Frequency = 50 Hz

Active Power, P (W) = 110 MW

Inductive reactive Power, Q_L (+Var) = 110Mvar

Π Block Parameters

Line Distance = 6.84 km

Case 3: Alagbon – Fowler Distribution Line

AC Voltage Source Block Parameters

Amplitude of Source voltage = 33 kV

Nominal Frequency = 50 Hz

Block Parameters of Shunt Reactor 110MVar

Nominal Voltage, V (Vrms) = 91.1 kV

Nominal Frequency = 50 Hz

Active Power, P (W) = 110 MW

Inductive reactive Power, Q_L (+Var) = 110Mvar

II Block Parameters

Line Distance = 3.00 km

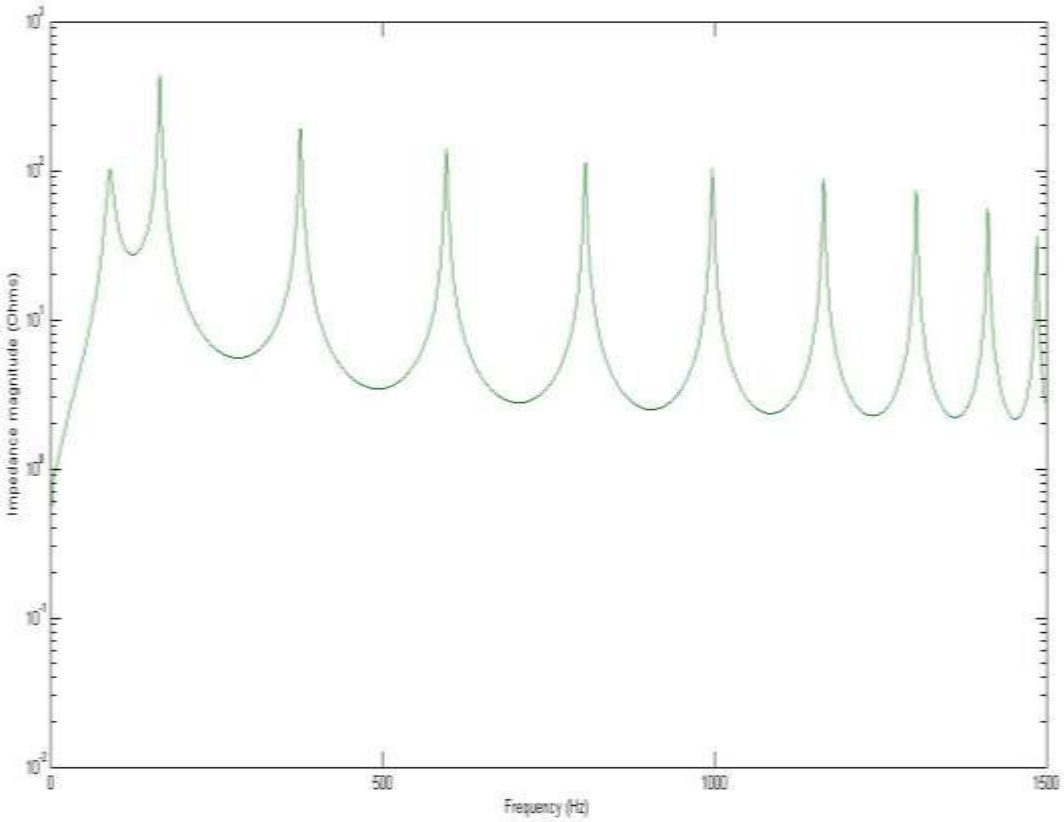

Figure 4.3a: Harmonics on Alagbon – Ademola Distribution Line at 21:00Hrs

Table 4.7h: Alagbon – Ademola Distribution Line Harmonics and Impedances at 21:00Hrs of 17th January, 2014

Nth Harmonic	Harmonic Frequency (Hz)	Harmonic Impedance (Ω)
2nd	100	$10^{2.008}$
3rd	150	$10^{2.644}$
8th	400	$10^{2.274}$
12th	600	$10^{2.149}$
16th	800	$10^{2.048}$
20th	1000	$10^{2.013}$
23rd	1150	$10^{1.943}$
26th	1300	$10^{1.861}$
28th	1400	$10^{1.743}$
29th	1450	$10^{1.556}$

Frequency range is between 0 – 1500Hz.

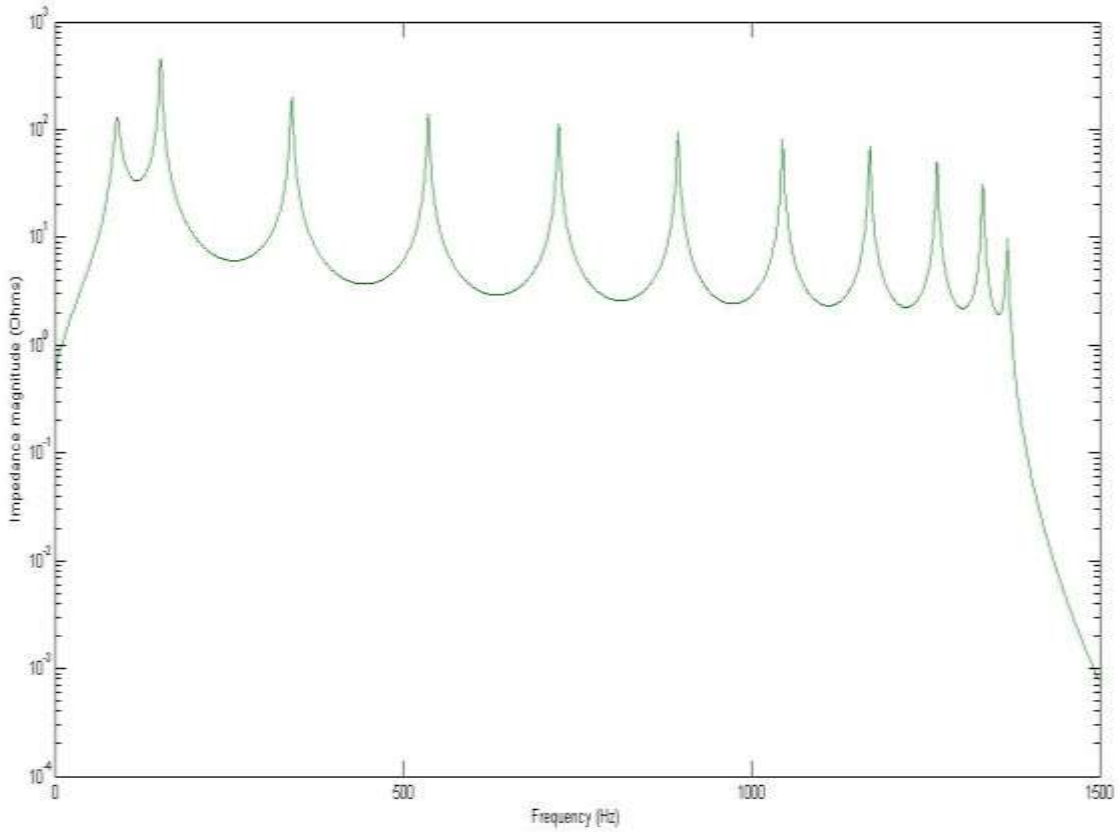

Figure 4.3b: Harmonics of the Alagbon – Anifowoshe Distribution Line at 21:00Hrs

Table 4.7i: Alagbon – Anifowoshe Distribution Line Harmonics and Impedances at 21:00Hrs of 17th January, 2014

Nth Harmonic	Harmonic Frequency (Hz)	Harmonic Impedance (Ω)
2nd	100	$10^{2.117}$
3rd	150	$10^{2.655}$
7th	350	$10^{2.297}$
11th	550	$10^{2.142}$
14th	700	$10^{2.057}$
18th	900	$10^{1.974}$
21st	1050	$10^{1.913}$
23rd	1150	$10^{1.840}$
25th	1250	$10^{1.692}$
26th	1300	$10^{1.491}$
27th	1350	$10^{0.991}$

Frequency range is between 0 – 1500Hz.

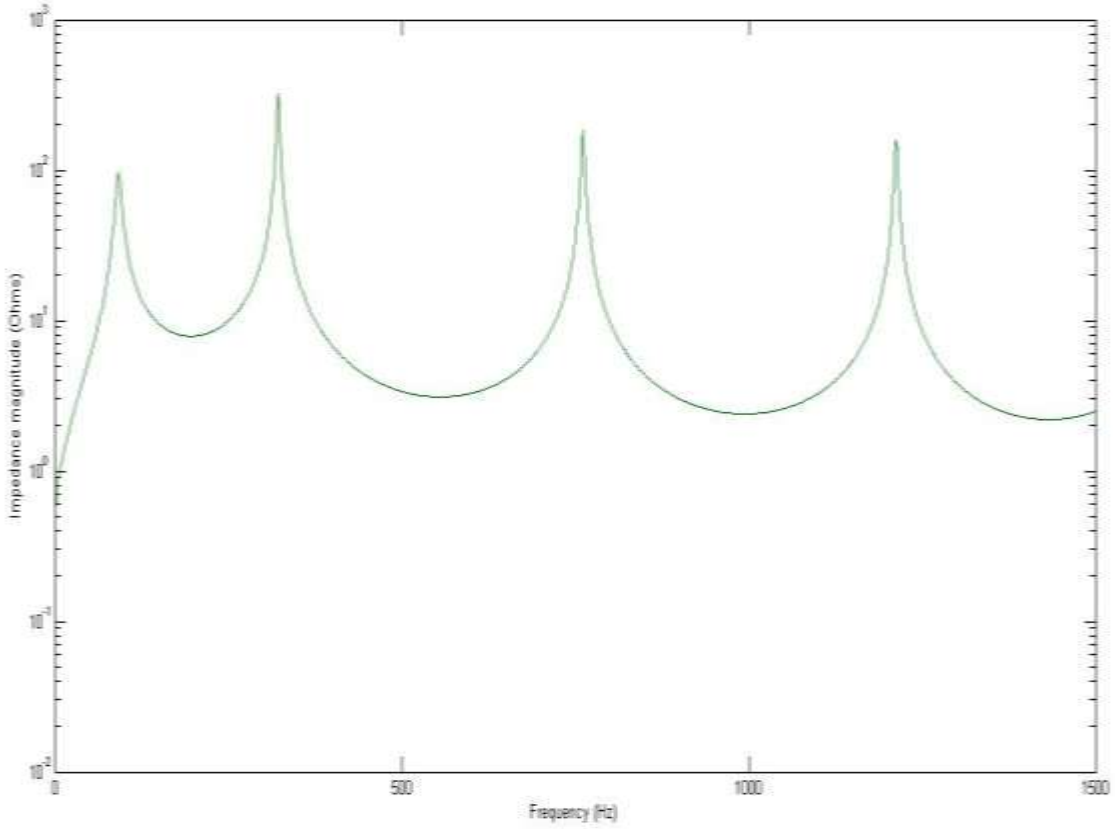

Figure 4.3c: Harmonics on Alagbon – Fowler Distribution Line at 21:00Hrs

Table 4.7j: Alagbon – Fowler Distribution Line Harmonics and Impedances at 21:00Hrs of 17th January, 2014

Nth Harmonic	Harmonic Frequency (Hz)	Harmonic Impedance (Ω)
2nd	100	$10^{1.985}\Omega$
6th	300	$10^{2.508}\Omega$
15th	750	$10^{2.268}\Omega$
24th	1200	$10^{2.198}\Omega$

Frequency range is between 0 – 1500Hz.

Table 4.7k: Distribution Lines Harmonics, Receiving end voltages and their Impedances for Cases of 21:00Hrs

S/N	Name of Line	Line Length (km)	Sending Voltage (kV)	Receiving Voltage (kV)	Observed Harmonics	Harmonic Impedance (Ω)
1	ALG-ADM	6.13	33	32.83	2^{nd}, 3^{rd}, 8^{th}, 12^{th}, 16^{th}, 20^{th}, 23^{rd}, 26^{th}, 28^{th}, 29^{th}	$10^{2.01}$,$10^{2.64}$, $10^{2.27}$, $10^{2.15}$, $10^{2.05}$, $10^{2.01}$, $10^{1.93}$, $10^{1.86}$, $10^{1.74}$, $10^{1.56}$
2	ALG-ALG-L	0.15	33	0	-	-
3	ALG-ANI	6.84	33	32.73	2^{nd}, 3^{rd}, 7^{th}, 11^{th}, 14^{th}, 18^{th}, 21^{st}, 23^{rd}, 25^{th}, 26^{th}, 27^{th}	$10^{2.12}$, $10^{2.66}$, $10^{2.30}$, $10^{2.14}$, $10^{2.06}$, $10^{1.97}$, $10^{1.91}$, $10^{1.84}$, $10^{1.69}$, $10^{1.49}$, $10^{0.99}$
4	ALG-FOW	3.00	33	32.87	2^{nd}, 6^{th}, 15^{th}, 24^{th}	$10^{1.99}$, $10^{2.51}$, $10^{2.27}$, $10^{2.20}$
5	ADM-MAR	1.80	32.83	0	-	-
6	ALG-BAN-I	5.00	33	0	-	-

At 23:00Hrs

Case 1: Alagbon – Anifowoshe Distribution Line

AC Voltage Source Block Parameters

Amplitude of Source voltage = 33 kV

Nominal Frequency = 50 Hz

Block Parameters of Shunt Reactor 110MVar

Nominal Voltage, V (Vrms) = 116.48 kV

Nominal Frequency = 50 Hz

Active Power, P (W) = 110 MW

Inductive reactive Power, Q_L (+Var) = 110Mvar

Π Block Parameters

Line Distance = 6.84 km

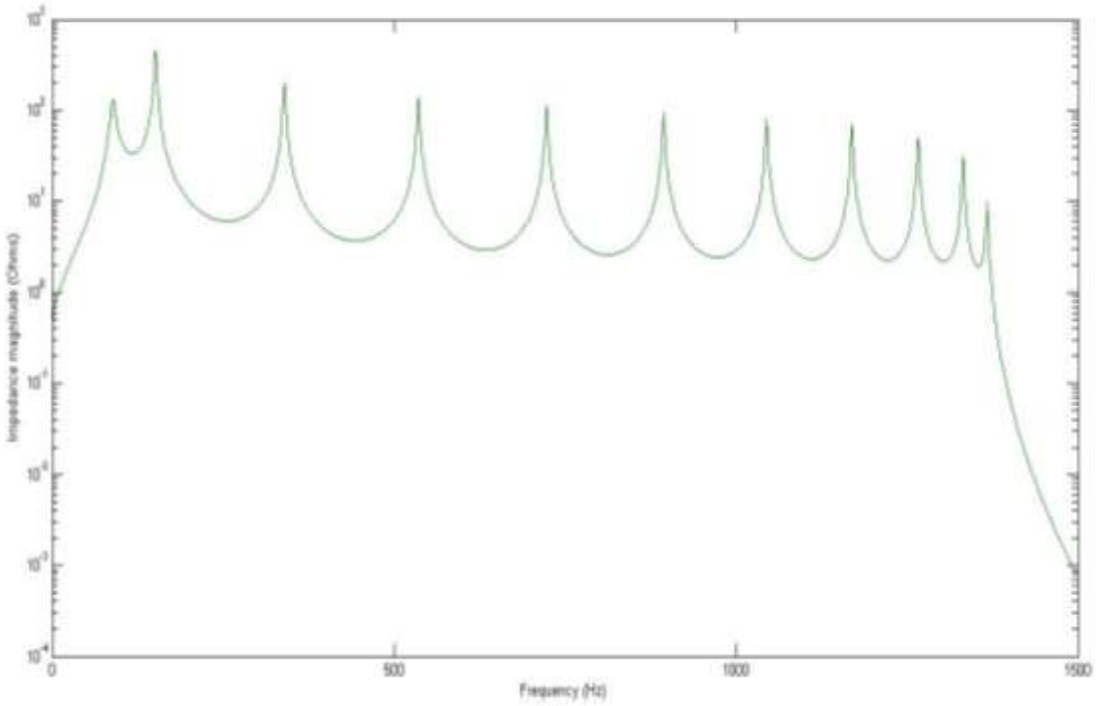

Figure 4.4a: Harmonics on Alagbon – Anifowoshe Distribution Line at 23:00Hrs

Table 4.7l: Alagbon – Anifowoshe Distribution Line Harmonics and Impedances at 23:00Hrs of 17th January, 2014

Nth Harmonic	Harmonic Frequency (Hz)	Harmonic Impedance (Ω)
2nd	100	$10^{2.116}$
3rd	150	$10^{2.649}$
7th	350	$10^{2.298}$
11th	550	$10^{2.143}$
14th	700	$10^{2.056}$
18th	900	$10^{1.973}$
21th	1050	$10^{1.914}$
23th	1150	$10^{1.841}$
25th	1250	$10^{1.690}$
26th	1300	$10^{1.490}$
27th	1350	$10^{0.994}$

Frequency Range is between 0 – 1500Hz.

Table 4.7m: Distribution Line Harmonics, Receiving end voltages and their Impedances for Cases of 23.00Hrs

S/N	Name of Line	Line Length (km)	Sending Voltage (kV)	Receiving Voltage (kV)	Observed Harmonics	Harmonic Impedance (Ω)
1	ALG-ADM	6.13	33	0	-	-
2	ALG-ALG-L	0.15	33	0	-	-
3	ALG-ANI	6.84	33	32.695	2^{nd}, 3^{rd}, 7^{th}, 11^{th}, 14^{th}, 18^{th}, 21^{st}, 23^{rd}, 25^{th}, 26^{th}, 27^{th}	$10^{2.12}$, $10^{2.65}$, $10^{2.30}$, $10^{2.14}$, $10^{2.06}$, $10^{1.97}$, $10^{1.91}$, $10^{1.84}$, $10^{1.69}$, $10^{1.49}$, $10^{0.99,}$
4	ALG-FOW	3.00	33	0	-	-
5	ADM-MAR	1.80	32.83	0	-	-
6	ADM-ANI	2.40	32.83	0	-	-
7	ALG-BAN-I	5.00	33	0	-	-

4.2.2.2 Harmonic Results for the Scenarios of 20th January 2014

Figures 4.5a to 4.8c are the harmonic analysis results for different cases and at different times of 20th January 2014, considering Tables 4.4a to 4.4f

At 02:00Hrs

Case 1: Alagbon – Alagbon Local Distribution Line

AC Voltage Source Block Parameters

Amplitude of Source voltage = 33 kV

Nominal Frequency = 50 Hz

Block Parameters of Shunt Reactor 110MVar

Nominal Voltage, V (Vrms) = 39.4999 kV

Nominal Frequency = 50 Hz

Active Power, P (W) = 110 MW

Inductive reactive Power, Q_L (+Var) = 110Mvar

Π Block Parameters

Line Distance = 0.15 km

2nd harmonic (100Hz) occurs at $10^{2.052}\Omega$ for a range of frequencies between 0 – 1500Hz.

Case 2: Alagbon – Ademola Distribution Line

AC Voltage Source Block Parameters

Amplitude of Source voltage = 33 kV

Nominal Frequency = 50 Hz

Block Parameters of Shunt Reactor 110MVar

Nominal Voltage, V (Vrms) = 117.41 kV

Nominal Frequency = 50 Hz

Active Power, P (W) = 110 MW

Inductive reactive Power, Q_L (+Var) = 110Mvar

Π Block Parameters

Line Distance = 6.13 km

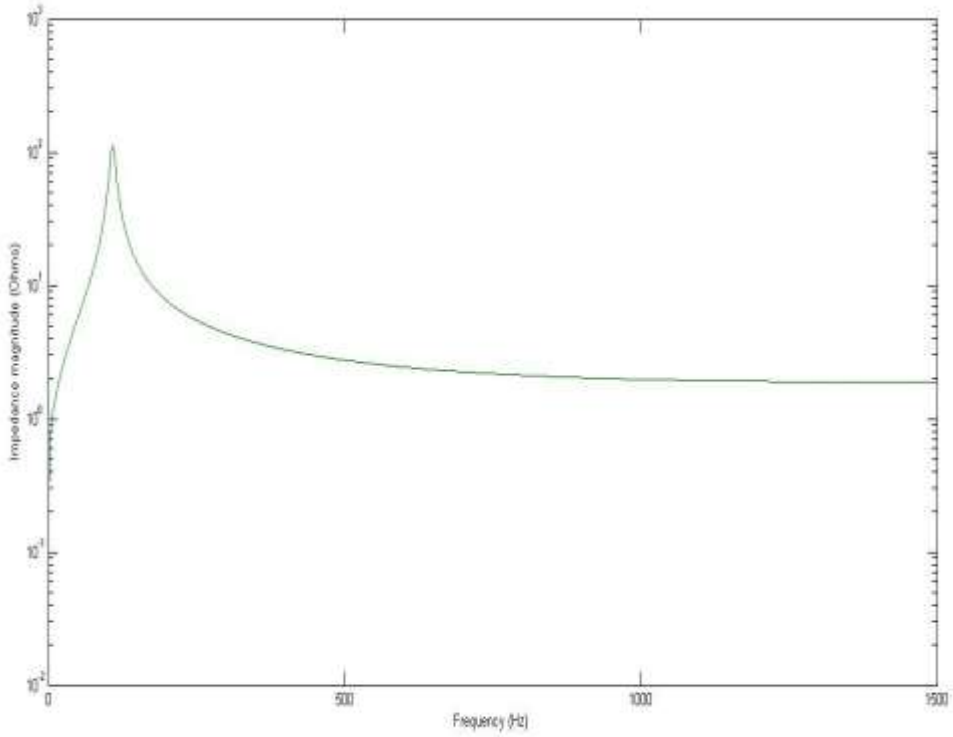

Figure 4.5a: Harmonic of the Alagbon – Alagbon Local Distribution Line at 02:00Hrs

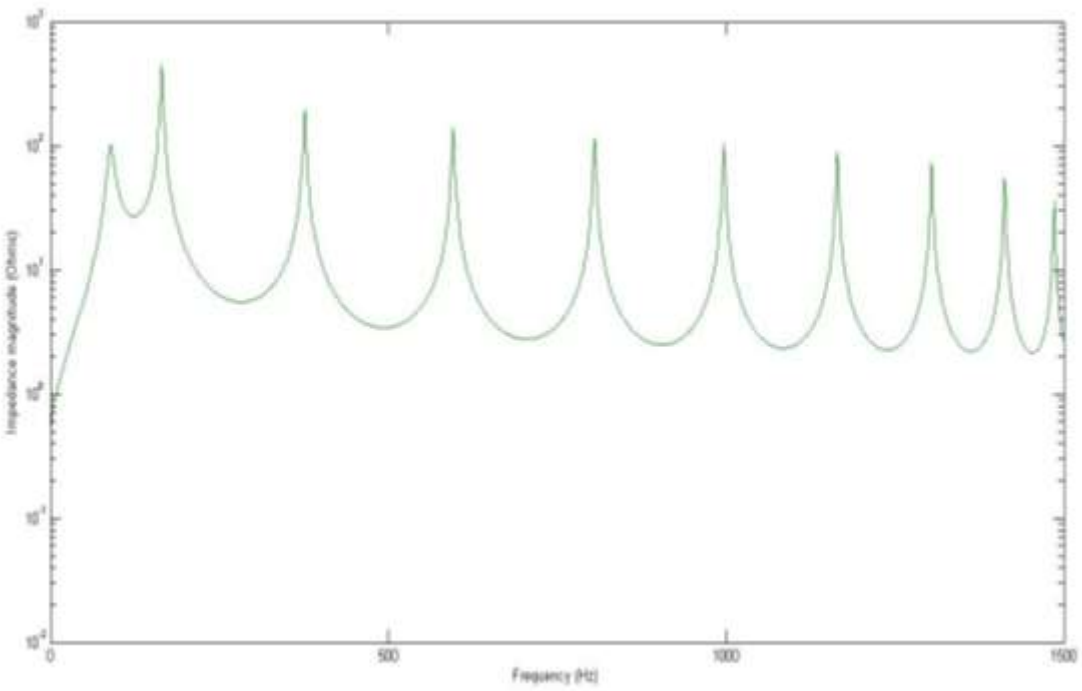

Figure 4.5b: Harmonics of the Alagbon – Ademola Distribution Line at 02:00Hrs

Table 4.8a: Alagbon – Ademola Distribution Line Harmonics and Impedances at 02:00Hrs of 20th January, 2014

Nth Harmonic	Harmonic Frequency (Hz)	Harmonic Impedance (Ω)
2nd	100	$10^{2.007}$
3rd	150	$10^{2.649}$
8th	400	$10^{2.281}$
12th	600	$10^{2.147}$
16th	800	$10^{2.052}$
20th	1000	$10^{2.014}$
23rd	1150	$10^{1.946}$
26th	1300	$10^{1.858}$
28th	1400	$10^{1.740}$
29th	1450	$10^{1.556}$

Frequency range is between 0 – 1500Hz.

Table 4.8b: Summary Table for 02:00hrs 20th January 2014

S/N	SB	V_b (kV)	RB	V_o (kV)	F (Hz)	Line Length (km)	No. of Harmonics	MATLAB Nominal Voltage Vrms (kV)
1	ALG	33	ALG-L	32.995	50	0.15	1	39.499
2	ALG	33	ADM	32.737	50	6.13	10	117.41

Table 4.8c: Distribution Line Harmonics, Receiving end voltages and their Impedancesfor Case of 02:00hrs

S/N	Name of Line	Line Length (km)	Sending Voltage (kV)	Receiving Voltage (kV)	Observed Harmonics	Harmonic Impedance (Ω)
1	ALG-ADM	6.13	33	32.737	2^{nd}, 3^{rd}, 8^{th}, 12^{th}, 16^{th}, 20^{th}, 23^{rd}, 26^{th}, 28^{th}, 29^{th}	$10^{2.007}$, $10^{2.649}$, $10^{2.281}$, $10^{2.147}$, $10^{2.052}$, $10^{2.014}$, $10^{1.946}$, $10^{1.858}$, $10^{1.740}$, $10^{1.556}$
2	ALG-ALG/L	0.15	33	32.995	2^{nd}	$10^{2.052}$
3	ALG-ANI	6.84	33	0	-	-
4	ALG-FOW	3.00	33	0	-	-
5	ADM-MAR	1.80	0	0	-	-
6	ADM-ANI	2.40	0	0	-	-
7	ALG-BAN-I	5.00	33	0	-	-

At 06:00Hrs

Case 1: Alagbon – Alagbon Local Distribution Line

AC Voltage Source Block Parameters

Amplitude of Source voltage = 33 kV

Nominal Frequency = 50 Hz

Block Parameters of Shunt Reactor 110MVar

Nominal Voltage, V (Vrms) = 39.52 kV

Nominal Frequency = 50 Hz

Active Power, P (W) = 110 MW

Inductive reactive Power, Q_L (+Var) = 110Mvar

Π Block Parameters

Line Distance = 0.15 km

2^{nd} harmonic (100Hz) occurs at $10^{2.052}\Omega$ for a range of frequencies between 0 – 1500Hz.

Case 2: Alagbon – Anifowoshe Distribution Line

AC Voltage Source Block Parameters

Amplitude of Source voltage = 33 kV

Nominal Frequency = 50 Hz

Block Parameters of Shunt Reactor 110MVar

Nominal Voltage, V (Vrms) = 116.86 kV

Nominal Frequency = 50 Hz

Active Power, P (W) = 110 MW

Inductive reactive Power, Q_L (+Var) = 110Mvar

Π Block Parameters

Line Distance = 6.84 km

Case 3: Alagbon – Fowler Distribution Line

AC Voltage Source Block Parameters

Amplitude of Source voltage = 33 kV

Nominal Frequency = 50 Hz

Block Parameters of Shunt Reactor 110MVar

Nominal Voltage, V (Vrms) = 91.13 kV

Nominal Frequency = 50 Hz

Active Power, P (W) = 110 MW

Inductive reactive Power, Q_L (+Var) = 110Mvar

Π Block Parameters

Line Distance = 3.00 km

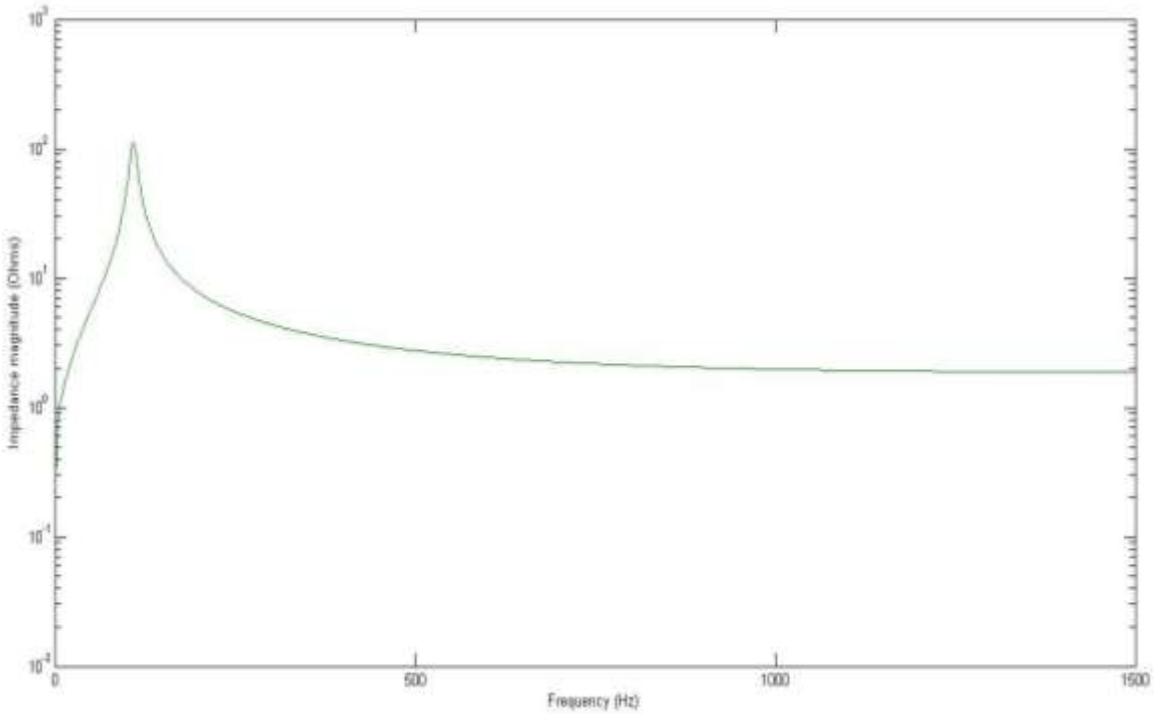

Figure 4.6a: Harmonic of the Alagbon – Alagbon Local Distribution Line at 06:00Hrs

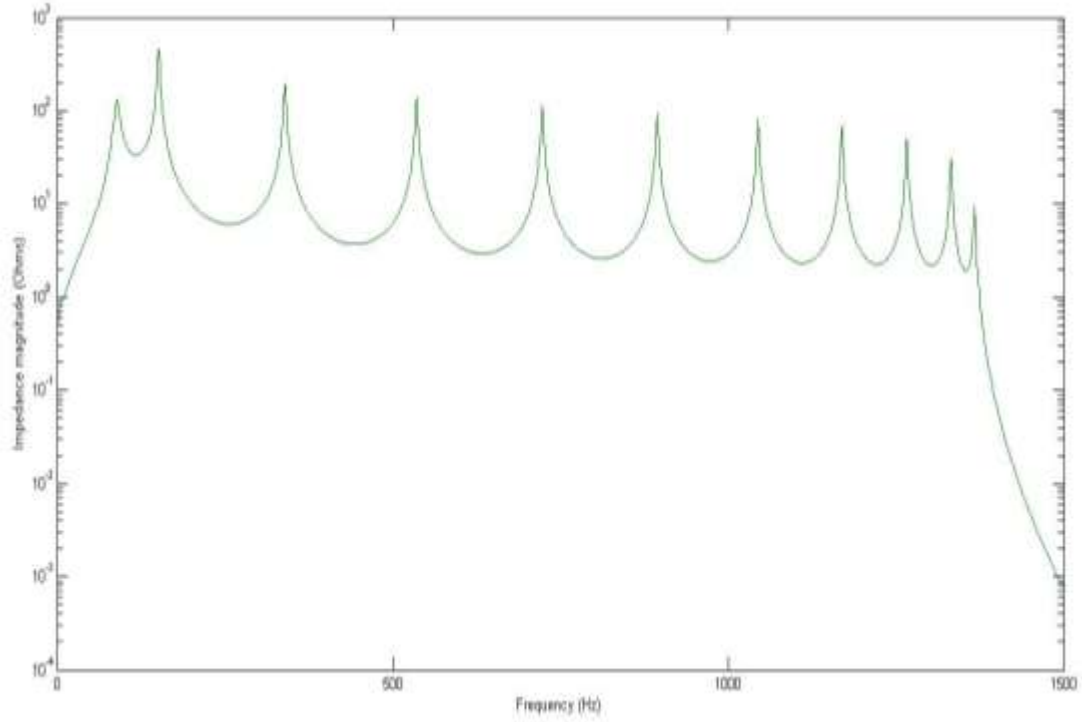

Figure 4.6b: Harmonics of the Alagbon – Anifowoshe Distribution Line at 06:00Hrs

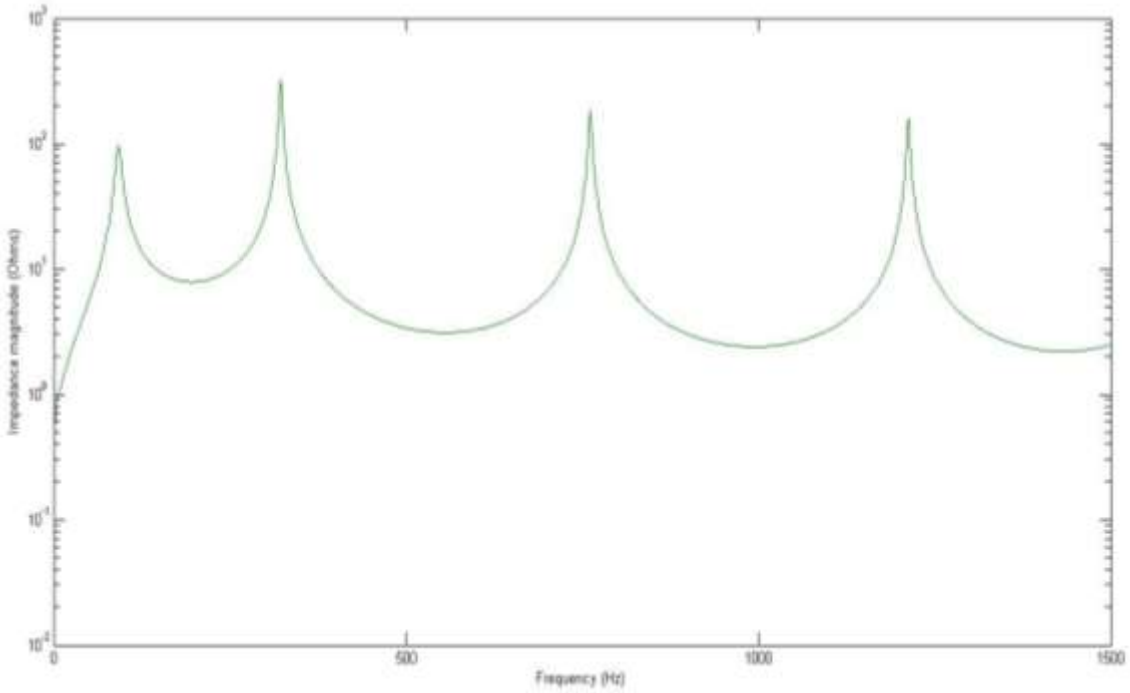

Figure 4.6c: Harmonics of the Alagbon–Fowler D/ Line at 06:00Hrs

Table 4.8d: Alagbon – Anifowoshe Distribution Line Harmonics and Impedances at 06:00Hrs of 20th January, 2014

Nth Harmonic	Harmonic Frequency (Hz)	Harmonic Impedance (Ω)
2nd	100	$10^{2.118}$
3rd	150	$10^{2.665}$
7th	350	$10^{2.292}$
11th	550	$10^{2.139}$
14th	700	$10^{2.058}$
18th	900	$10^{1.977}$
21st	1050	$10^{1.910}$
23rd	1150	$10^{1.838}$
25th	1250	$10^{1.695}$
26th	1300	$10^{1.494}$
27th	1350	$10^{0.985}$

Frequency range is between 0 – 1500Hz.

Table 4.8e: Alagbon – Fowler Distribution Line Harmonics and Impedances at 06:00Hrs of 20th January, 2014

Nth Harmonic	Harmonic Frequency (Hz)	Harmonic Impedance (Ω)
2nd	100	$10^{1.986}$
6th	300	$10^{2.505}$
15th	750	$10^{2.270}$
24th	1200	$10^{2.196}$

Frequency range is between 0 – 1500Hz.

Table 4.8f: Summary Table for 06:00Hrs

S/N	SB	V_b (kV)	RB	V_o (kV)	F (Hz)	Line Length (km)	No. of Harmonics	MATLAB Nominal Voltage Vrms (kV)
1	ALG	33	ALG-L	32.997	50	0.15	1	39.52
2	ALG	33	ANI	32.833	50	6.84	11	116.86
3	ALG	33	FOW	32.926	50	3.00	4	91.218

Table 4.8g: Distribution Lines Harmonics, Receiving end voltages and their Impedances for case 06:00Hrs, 20TH January 2014

S/N	Name of Line	Line Length (km)	Sending Voltage (kV)	Receiving Voltage (kV)	Observed Harmonics	Harmonic Impedance (Ω)
1	ALG-ADM	6.13	33	0	-	-
2	ALG-ALG-L	0.15	33	32.997	2^{nd}	$10^{2.052}$
3	ALG-ANI	6.84	33	32.833	2^{nd}, 3^{rd}, 7^{th}, 11^{th}, 14^{th}, 18^{th}, 21^{st}, 23^{rd}, 25^{th}, 26^{th}, 27^{th}	$10^{2.12}$, $10^{2.67}$, $10^{2.292}$, $10^{2.139}$, $10^{2.058}$, $10^{1.977}$, $10^{1.910}$, $10^{1.838}$, $10^{1.695}$, $10^{1.494}$, $10^{0.985}$
4	ALG-FOW	3.00	33	32.926	2^{nd}, 6^{th}, 15^{th}, 24^{th}	$10^{1.986}$, $10^{2.505}$, $10^{2.270}$, $10^{2.196}$
5	ADM-MAR	1.80	0	0	-	-
6	ADM-ANI	2.40	0	32.833	-	-
7	ALG-BAN-I	5.00	33	0	-	-

At 09:00Hrs

Case 1: Alagbon – Alagbon Local Distribution Line

AC Voltage Source Block Paameters

Amplitude of Source voltage = 33 kV

Nominal Frequency = 50 Hz

Block Parameters of Shunt Reactor 110MVar

Nominal Voltage, V (Vrms) = 39.515 kV

Nominal Frequency = 50 Hz

Active Power, P (W) = 110 MW

Inductive reactive Power, Q_L (+Var) = 110Mvar

Π Block Parameters

Line Distance = 0.15 km

2^{nd} harmonic (100Hz) occurs at $10^{2.052}\Omega$ for a range of frequencies between 0 – 1500Hz.

Case 2: Alagbon – Banana Island Distribution Line

AC Voltage Source Block Parameters

Amplitude of Source voltage = 33 kV

Nominal Frequency = 50 Hz

Block Parameters of Shunt Reactor 110MVar

Nominal Voltage, V (Vrms) = 108.47 kV

Nominal Frequency = 50 Hz

Active Power, P (W) = 110 MW

Inductive reactive Power, Q_L (+Var) = 110Mvar

Π Block Parameters

Line Distance = 5.00 km

Case 3: Alagbon – Fowler Distribution Line

AC Voltage Source Block Parameters

Amplitude of Source voltage = 33 kV

Nominal Frequency = 50 Hz

Block Parameters of Shunt Reactor 110MVar

Nominal Voltage, V (Vrms) = 91.13 kV

Nominal Frequency = 50 Hz

Active Power, P (W) = 110 MW

Inductive reactive Power, Q_L (+Var) = 110Mvar

Π Block Parameters

Line Distance = 3.00 km

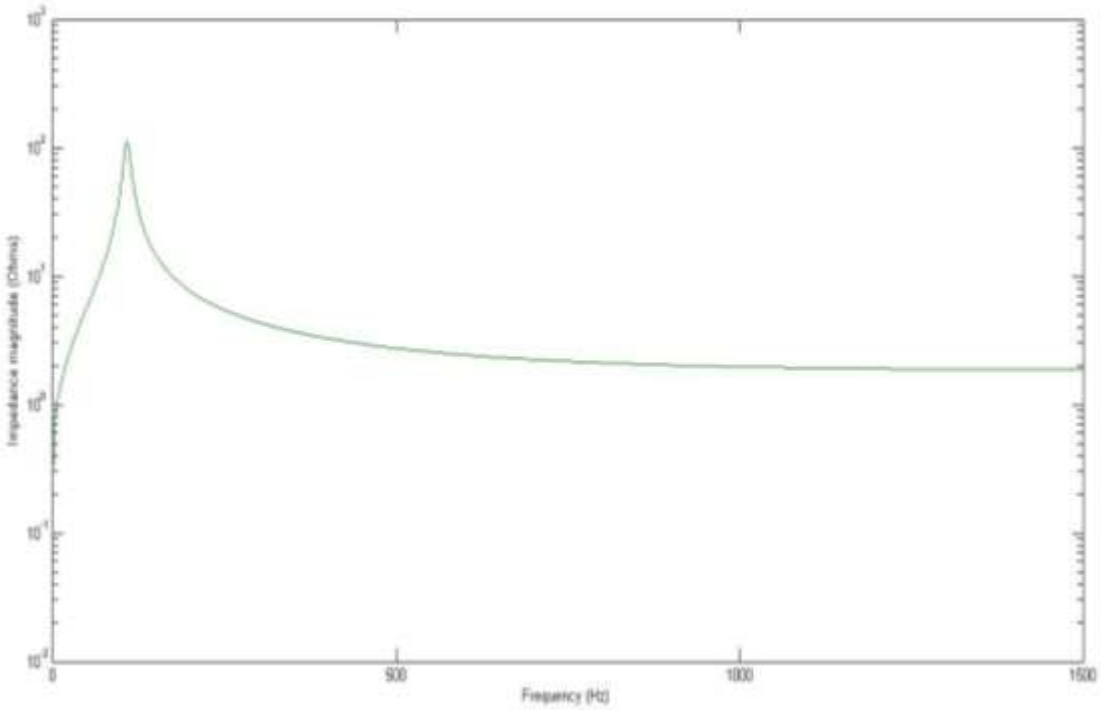

Figure 4.7a: Harmonics of the Alagbon – Alagbon Local Distribution Line at 09:00Hrs

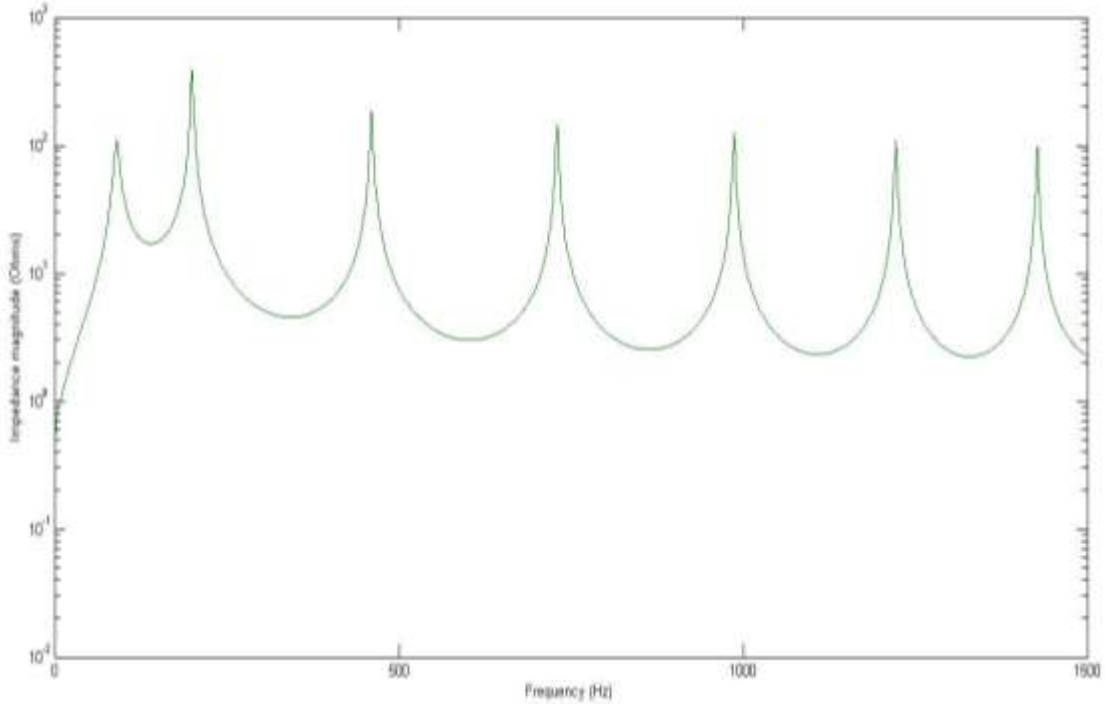

Figure 4.7b: Harmonics of the Alagbon – Banana Island bus Distribution Line at 09:00Hrs

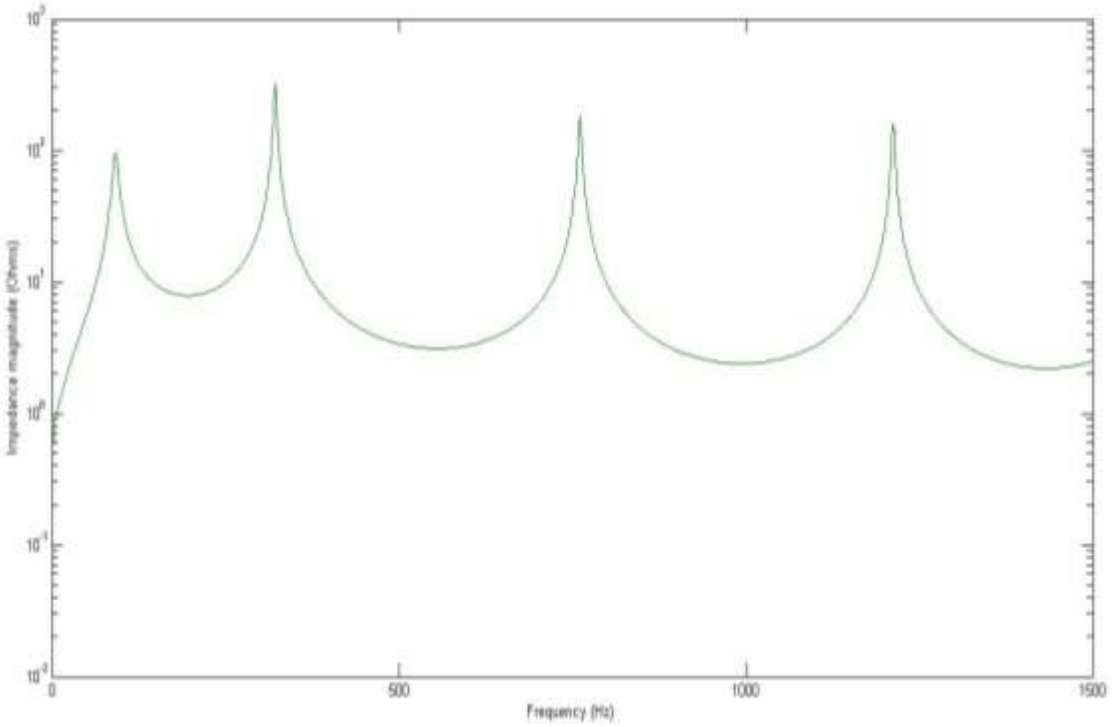

Figure 4.7c: Harmonics of the Alagbon – Fowler Distribution Line at 09:00Hrs

Table 4.8h: Alagbon – Banana Island Distribution Line Harmonics and Impedances at 09:00Hrs of 20th January, 2014

Nth Harmonic	Harmonic Frequency (Hz)	Harmonic Impedance (Ω)
2nd	100	$10^{2.039}$
4th	200	$10^{2.598}$
9th	450	$10^{2.267}$
15th	750	$10^{2.159}$
20th	1000	$10^{2.098}$
24th	1200	$10^{2.045}$
28th	1450	$10^{1.981}$

Frequency range is between 0 – 1500Hz.

Table 4.8i: Alagbon – Fowler Distribution Line Harmonics and Impedances at 09:00Hrs of 20th January, 2014

Nth Harmonic	Harmonic Frequency (Hz)	Harmonic Impedance (Ω)
2nd	100	$10^{1.985}$
6th	300	$10^{2.507}$
15th	750	$10^{2.269}$
24th	1200	$10^{2.198}$

Frequency range is between 0 – 1500Hz.

Table 4.8j: Summary Table for 09:00Hrs

S/N	SB	V_b (kV)	RB	V_o (kV)	F (Hz)	Line Length (km)	No. of Harmonics	MATLAB Nominal Voltage Vrms (kV)
1	ALG	33	ALG-L	32.996	50	0.15	1	39.515
2	ALG	33	BAN-I	32.942	50	5.00	7	108.47
3	ALG	33	FOW	32.904	50	3.00	4	91.15

Table 4.8k: Distribution Line Harmonics, Receiving end voltages and their Impedances for Cases of 09:00Hrs

S/N	Name of Line	Line Length (km)	Sending Voltage (kV)	Receiving Voltage (kV)	Observed Harmonics	Harmonic Impedance (Ω)
1	ALG-ADM	6.13	33	0	-	-
2	ALG-ALG/L	0.15	33	32.996	2^{nd}	$10^{2.052}$
3	ALG-ANI	6.84	33	0	-	-
4	ALG-FOW	3.00	33	32.904	2^{nd}, 6^{th}, 15^{th}, 24^{th}	$10^{1.985}$, $10^{2.507}$, $10^{2.269}$, $10^{2.198}$
5	ADM-MAR	1.80	0	0	-	-
6	ADM-ANI	2.40	0	0	-	-
7	ALG-BAN/I	5.00	33	32.942	2^{nd}, 4^{th}, 9^{th}, 15^{th}, 20^{th}, 24^{th}, 28^{th}	$10^{2.039}$, $10^{2.598}$, $10^{2.267}$, $10^{2.159}$, $10^{2.098}$, $10^{2.045}$, $10^{1.981}$

At 12:00Hrs

Case 1: Alagbon – Alagbon Local Distribution Line

AC Voltage Source Block Parameters

Amplitude of Source voltage = 33 kV

Nominal Frequency = 50 Hz

Block Parameters of Shunt Reactor 110MVar

Nominal Voltage, V (Vrms) = 39.493 kV

Nominal Frequency = 50 Hz

Active Power, P (W) = 110 MW

Inductive reactive Power, Q_L (+Var) = 110Mvar

Π Block Parameters

Line Distance = 0.15 km

2^{nd} harmonic (100Hz) occurs at $10^{2.052}\Omega$ for a range of frequencies between 0 – 1500Hz.

Case 2: Alagbon – Anifowoshe Distribution Line

AC Voltage Source Block Parameters

Amplitude of Source voltage = 33 kV

Nominal Frequency = 50 Hz

Block Parameters of Shunt Reactor 110MVar

Nominal Voltage, V (Vrms) = 116.11 kV

Nominal Frequency = 50 Hz

Active Power, P (W) = 110 MW

Inductive reactive Power, Q_L (+Var) = 110Mvar

Π Block Parameters

Line Distance = 6.84 km

Case 3: Alagbon – Fowler Distribution Line

AC Voltage Source Block Parameters

Amplitude of Source voltage = 33 kV

Nominal Frequency = 50 Hz

Block Parameters of Shunt Reactor 110MVar

Nominal Voltage, V (Vrms) = 90.99 kV

Nominal Frequency = 50 Hz

Active Power, P (W) = 110 MW

Inductive reactive Power, Q_L (+Var) = 110Mvar

II Block Parameters

Line Distance = 3.00 km

For each of the cases of the scenario hours of both days, the distribution line steady state parameters in magnitude and phase values displayed in the state-space model block are shown in Appendix B.

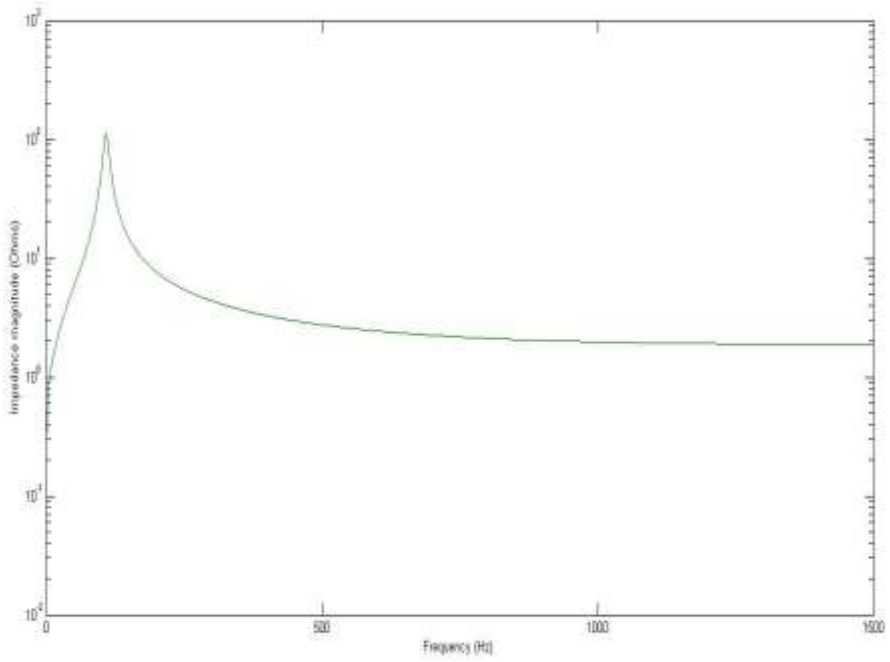

Figure 4.8a: Harmonics of the Alagbon – Alagbon Local Distribution Line at 12:00Hrs

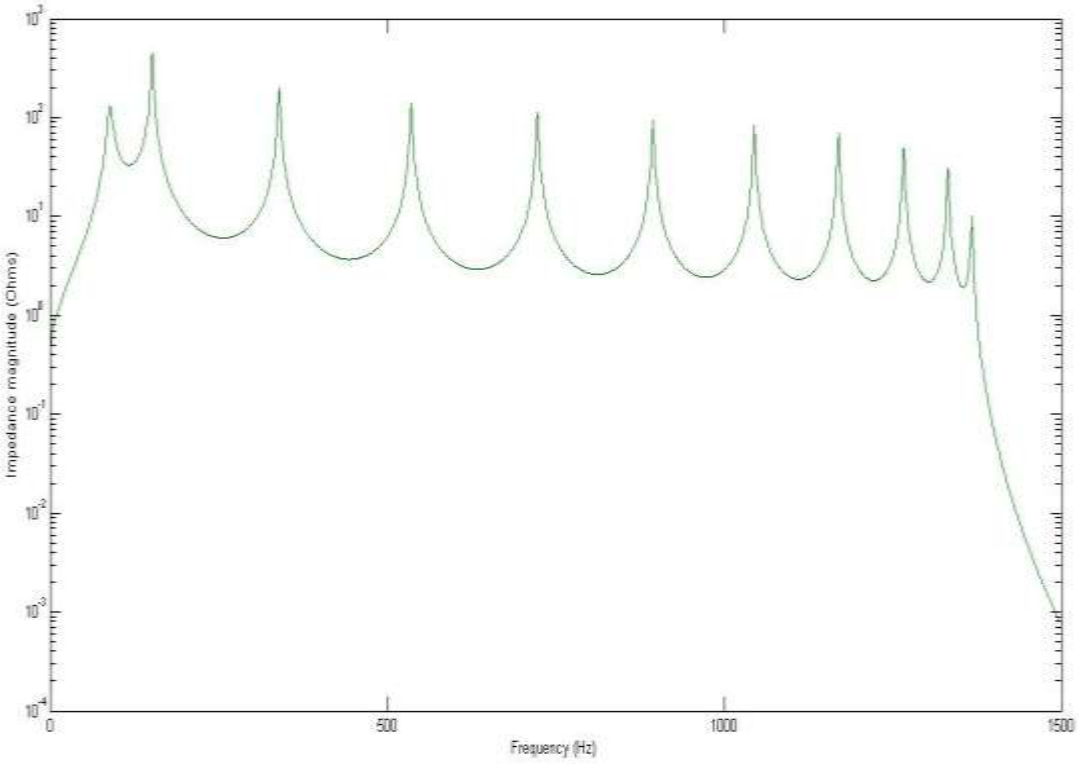

Figure 4.8b: Harmonics of the Alagbon – Anifowoshe Distribution Line at 12:00Hrs

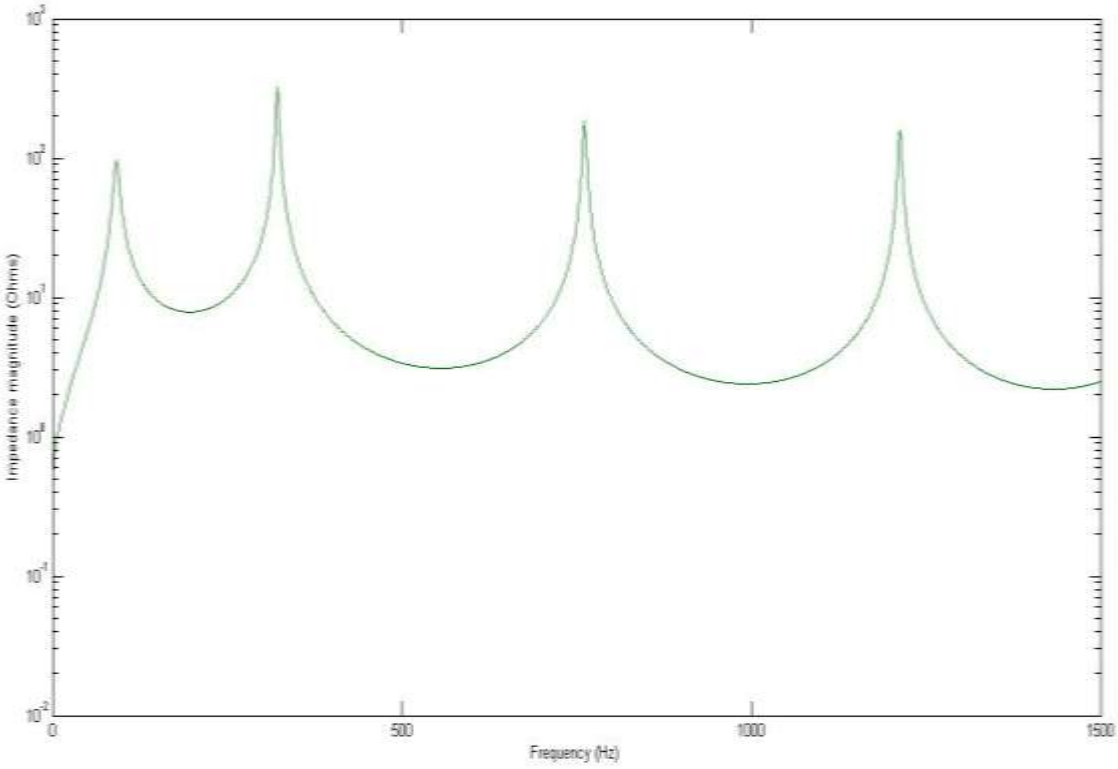

Figure 4.8c: Harmonics of the Alagbon – Fowler Distribution Line at 12:00Hrs

Table 4.8l: Alagbon – Fowler Distribution Line Harmonics and Impedances at 12:00Hrs of 20th January, 2014

Nth Harmonic	Harmonic Frequency (Hz)	Harmonic Impedance (Ω)
2nd	100	$10^{2.114}$
3rd	150	$10^{2.656}$
7th	350	$10^{2.302}$
11th	550	$10^{2.145}$
14th	700	$10^{2.054}$
18th	900	$10^{1.968}$
21st	1050	$10^{1.918}$
23rd	1150	$10^{1.843}$
25th	1250	$10^{1.689}$
26th	1300	$10^{1.485}$
27th	1350	$10^{1.002}$

Frequency range is between 0 – 1500Hz.

Table 4.8m: Alagbon – Fowler Distribution Line Harmonics and Impedances at 12:00Hrs of 20th January, 2014

Nth Harmonic	Harmonic Frequency (Hz)	Harmonic Impedance (Ω)
2nd	100	$10^{1.984}$
6th	300	$10^{2.508}$
15th	750	$10^{2.266}$
24th	1200	$10^{2.200}$

Frequency range is between 0 – 1500Hz.

Table 4.8n: Summary Table for 12:00hrs, 20th January 2014

S/N	SB	V_b (kV)	RB	V_o (kV)	F (Hz)	Line Length (km)	No. of Harmonics	MATLAB Nominal Voltage Vrms (kV)
1	ALG	33	ALG-L	32.96	50	0.15	1	39.493
2	ALG	33	ANI	32.553	50	5.00	11	116.11
3	ALG	33	FOW	32.834	50	3.00	4	90.99

Table 4.8o: Distribution Line Harmonics, Receiving end voltages and their Impedances for Cases of 12:00Hrs

S/N	Name of Line	Line Length (KM)	Sending Voltage (kV)	Receiving Voltage (kV)	Observed Harmonics	Harmonic Impedance
1	ALG-ADM	6.13	33	0	-	-
2	ALG-ALG/L	0.15	33	32.96	2^{nd}	$10^{2.052}$
3	ALG-ANI	6.84	33	32.55	-	-
4	ALG-FOW	3.00	33	32.834	2^{nd}, 6^{th}, 15^{th}, 24^{th}	$10^{2.114}$, $10^{2.656}$, $10^{2.302}$, $10^{2.145}$, $10^{2.054}$, $10^{1.968}$, $10^{1.918}$, $10^{1.843}$, $10^{1.689}$, $10^{1.485}$, $10^{1.002}$
5	ADM-MAR	1.80	0	0	-	$10^{1.984}$, $10^{2.508}$, $10^{2.266}$, $10^{2.200}$
6	ADM-ANI	2.40	0	32.555	-	-
7	ALG-BAN/I	5.00	33	0	-	-

4.2.3 Harmonic Mitigation Results

The values of electronic components; Resistance (R = 1Ω), Inductance (L = 1 mH), and Capacitance (C = 150μF) used in Figure 3.6 (shown in chapter three), were obtained using passive filter design equations illustrated in Equations 2.69 to 2.76. MATLAB simulations were carried out for a Band pass filter, Cascaded Band pass filter; LC filter and cascaded LC filter. The results obtained are shown in Figures 4.9 to 4.22, while the frequency spectrum of Figure 4.9 is shown in Figure 4.10. Figure 4.10 also shows a reduction in the number of harmonics from four (4) to three (3) harmonics, which is a direct result of the implementation of an RLC filter.

The range of operational frequency within which the harmonics occur, is from 0 – 1500Hz as shown in Figure 4.10.
Figure 4.11 shows the implementation of a second Band pass filter in cascade with the first, on Alagbon – Fowler Distribution Line. The resulting impedance magnitude/frequency result and the new harmonic peak impedance value are shown in Figures 4.12 and 4.13 respectively.

Figure 4.14 shows that the implementation of RLC Band pass filters in cascade results in a further drop in the output voltage on the Bus at Fowler to 73.80V.

In Figure 4.15, a single passive LC filter is also implemented on Alagbon - Fowler Distribution Line, by replacing the RLC filter that was previously used as shown. The simulation results are shown in Figures 4.16, 4.17 and 4.18.

Replacing the two (2) No. cascaded RLC filter with a single LC filter, the simulation results obtained are shown in Figures 4.16 and 4.17 for harmonic pattern and harmonic impedance characteristics.

Using 2 No. passive LC filters in cascade on Alagbon - Fowler Distribution Line as shown in figure 4.19, simulation results obtained are also shown in figures 4.20 and 4.21. Only one harmonic is eliminated. The output voltage result is also shown in figure 4.22.

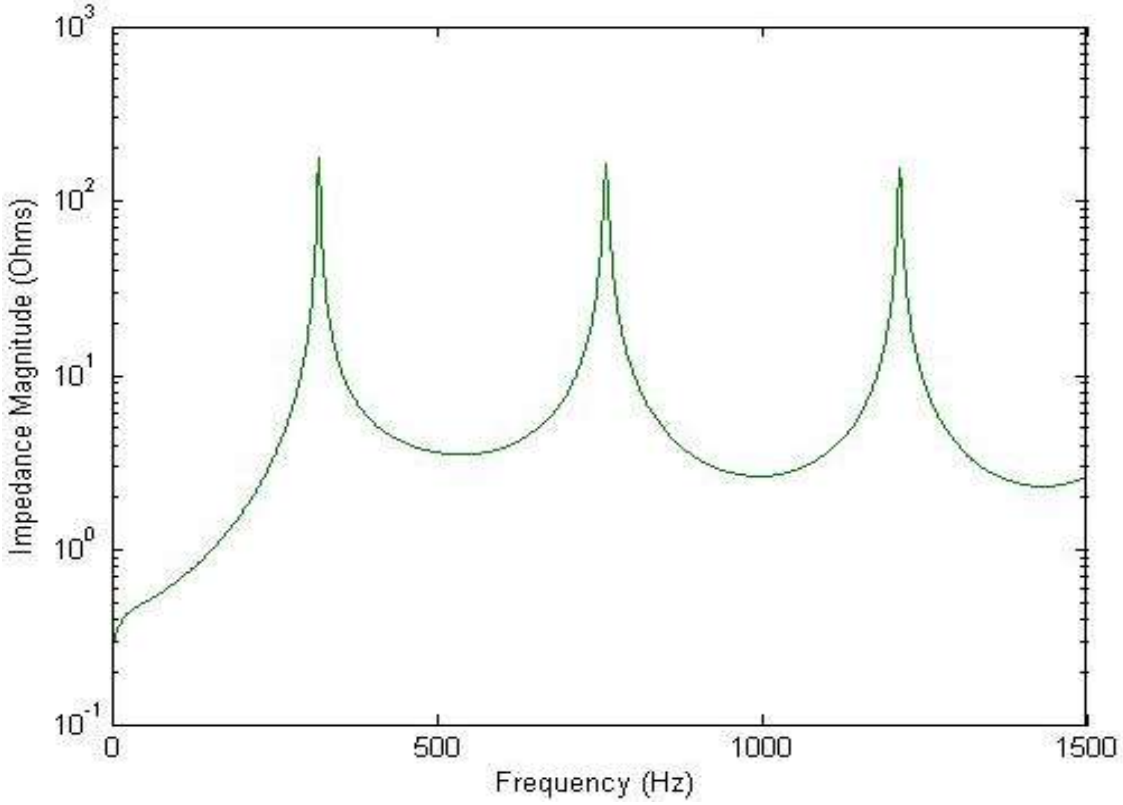

Figure 4.9: Mitigation Result on Application of an RLC Filter to Alagbon-Fowler D/L

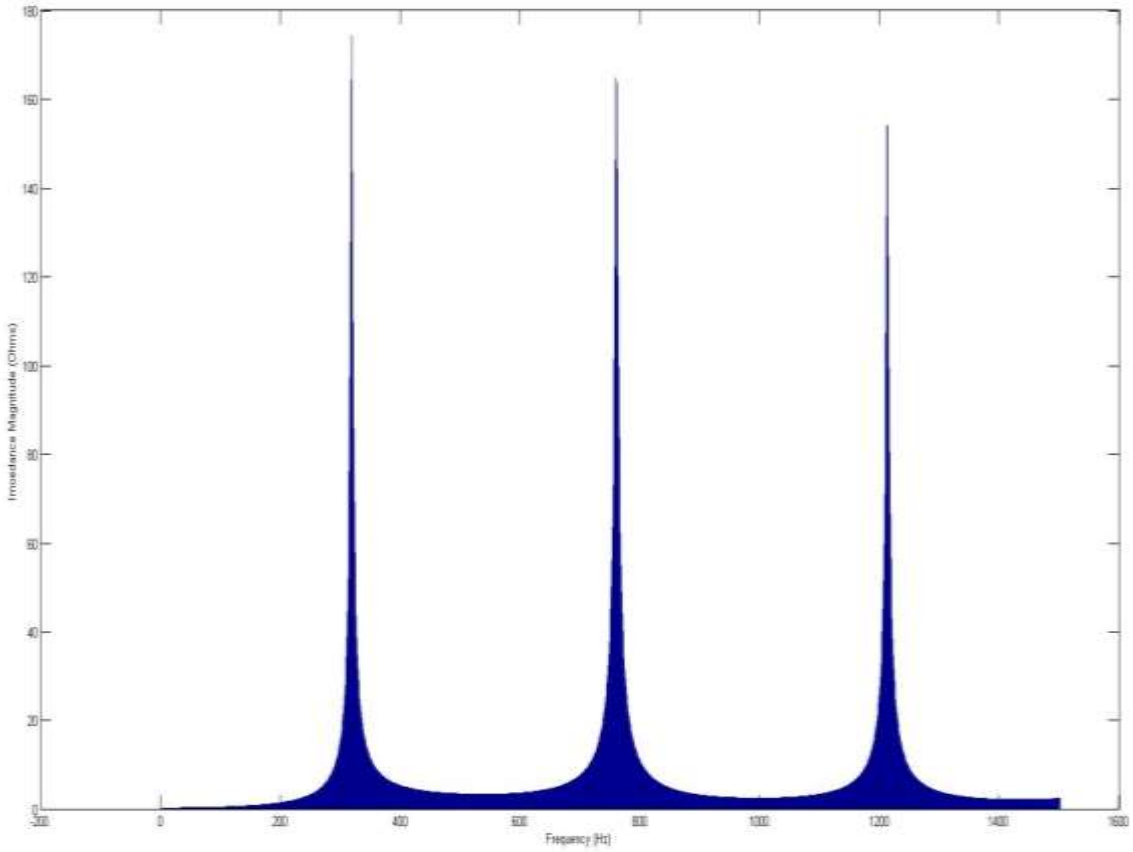

Figure 4.10: Frequency spectrum of the harmonics

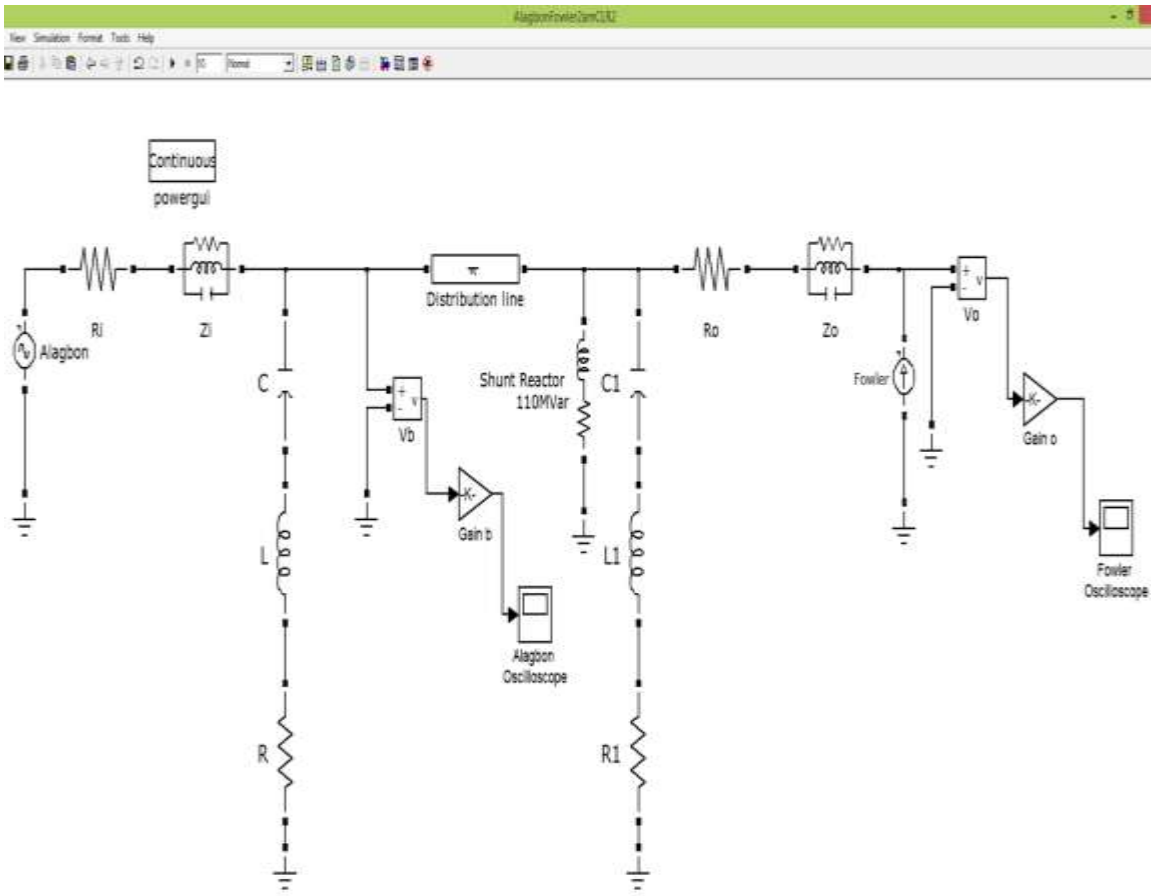

Figure 4.11: Model showing the Introduction of two RLC Band Pass Filters in Cascade into the Existing Alagbon - Fowler D/L

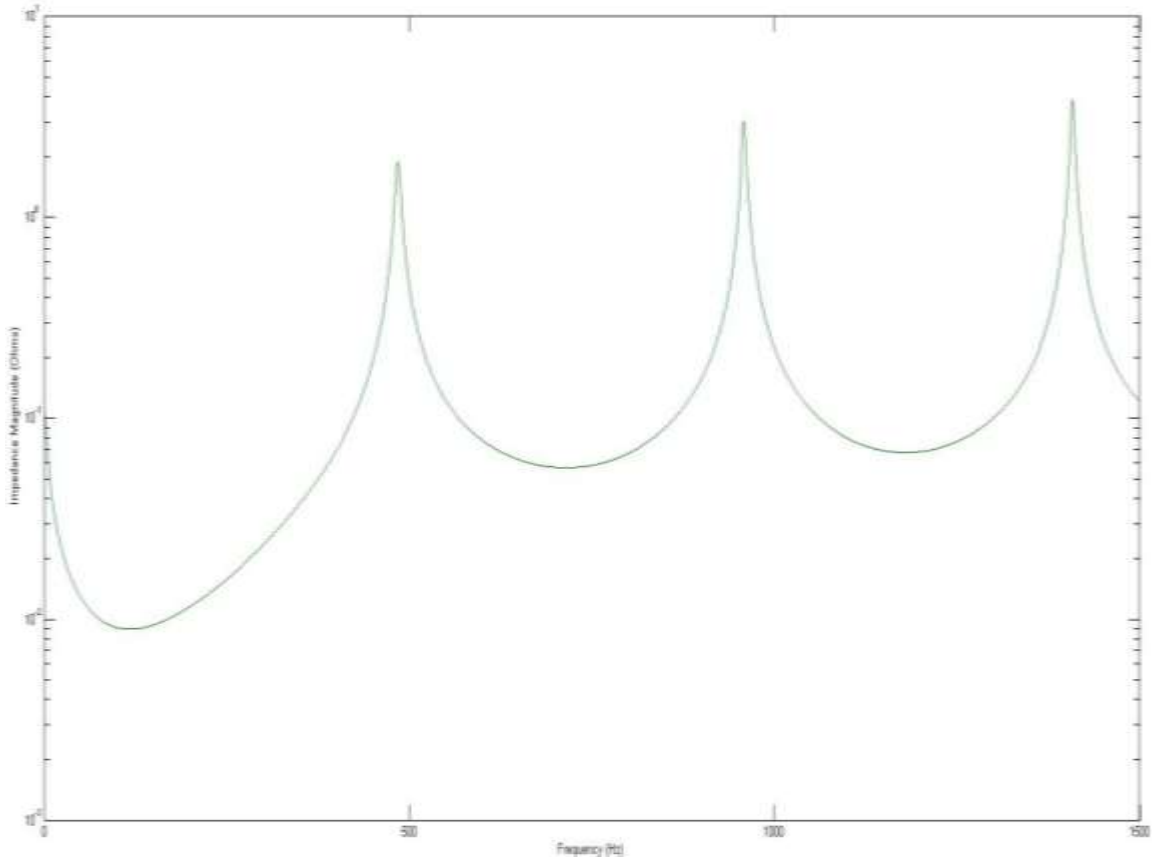

Figure 4.12: Mitigation Result on Application of two RLC Filters in Cascade to Alagbon-Fowler D/L

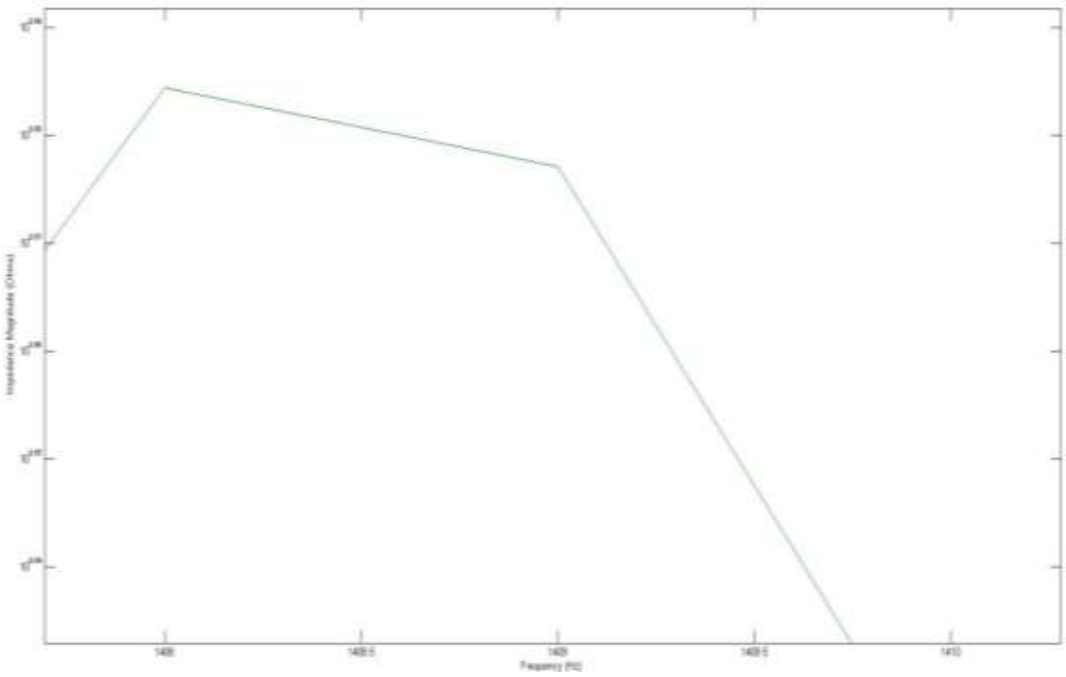

Figure 4.13: New Impedance Magnitude / Frequency Characteristic of Reduced Harmonic on Alagbon-Fowler D/L after Cascading two Band Pass Filters

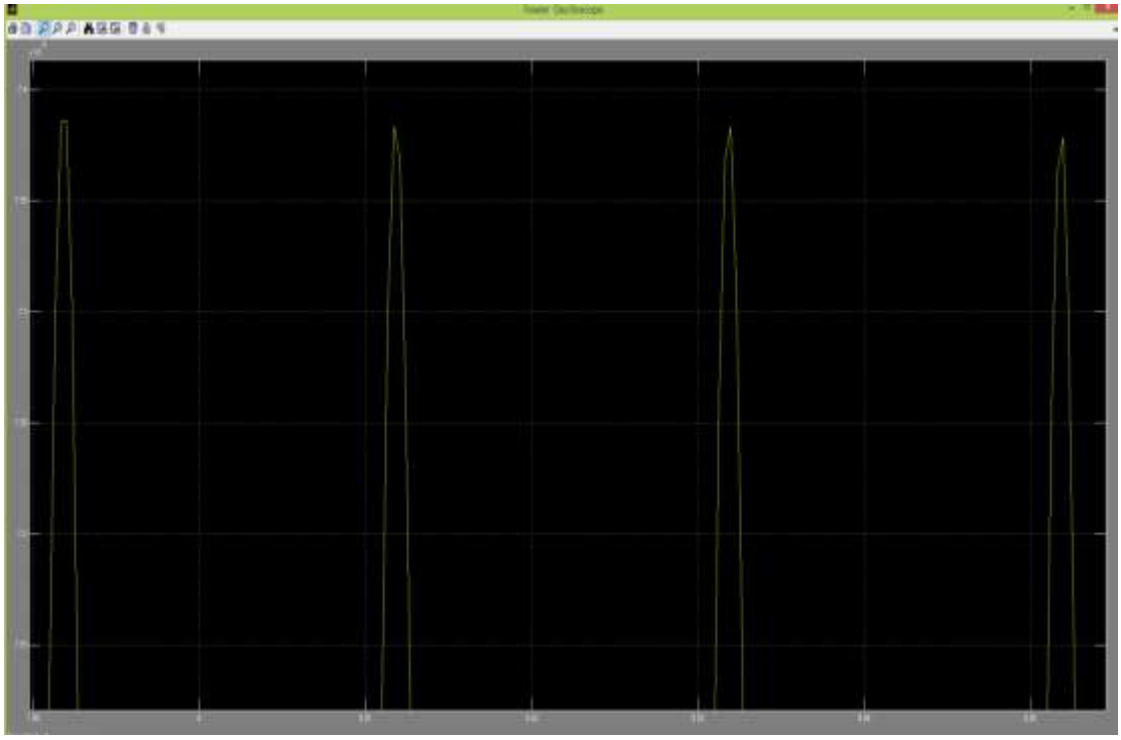

Figure 4.14: Result showing the Output Bus Voltage at Fowler to be 73.80V with the implementation of two RLC Band pass Filters in Cascade

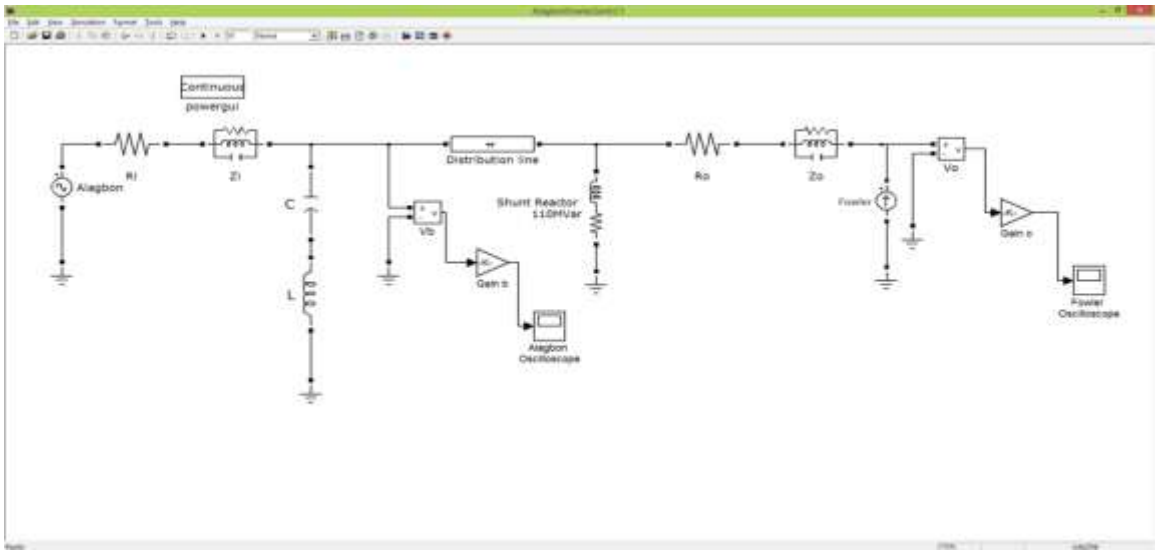

Figure 4.15: Model Showing the Introduction of a Passive LC Filter into the Existing Alagbon - Fowler D/L

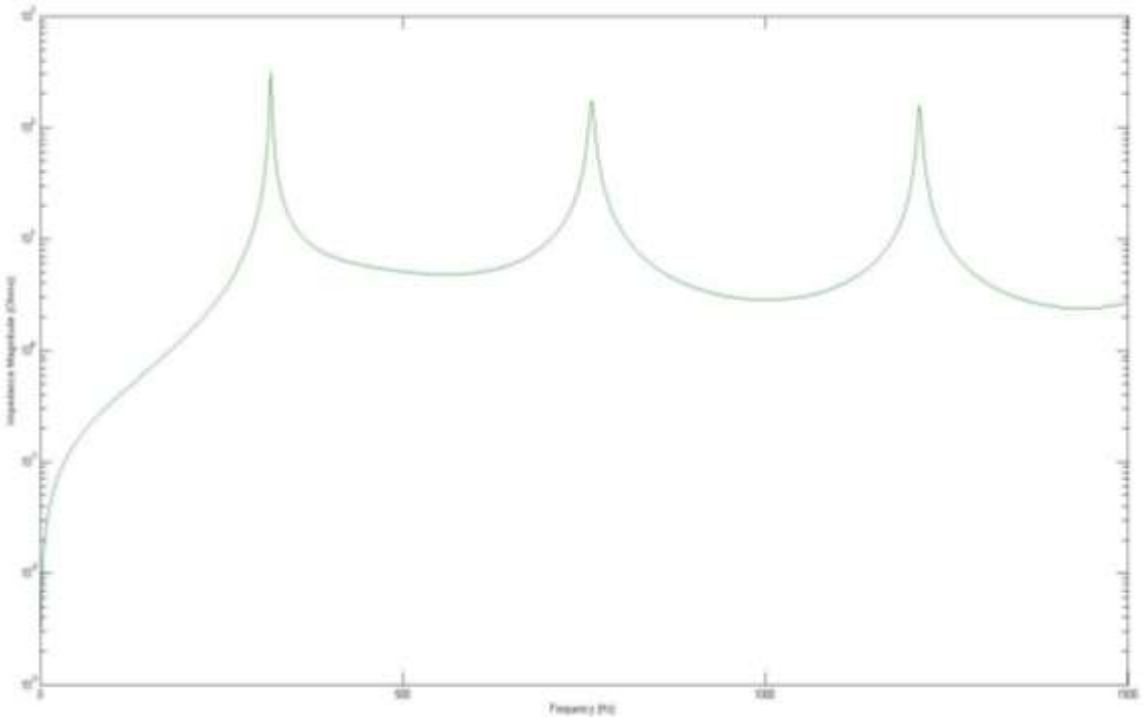

Figure 4.16: Mitigation Result after the Application of a Passive LC Filter on Alagbon – Fowler D/L

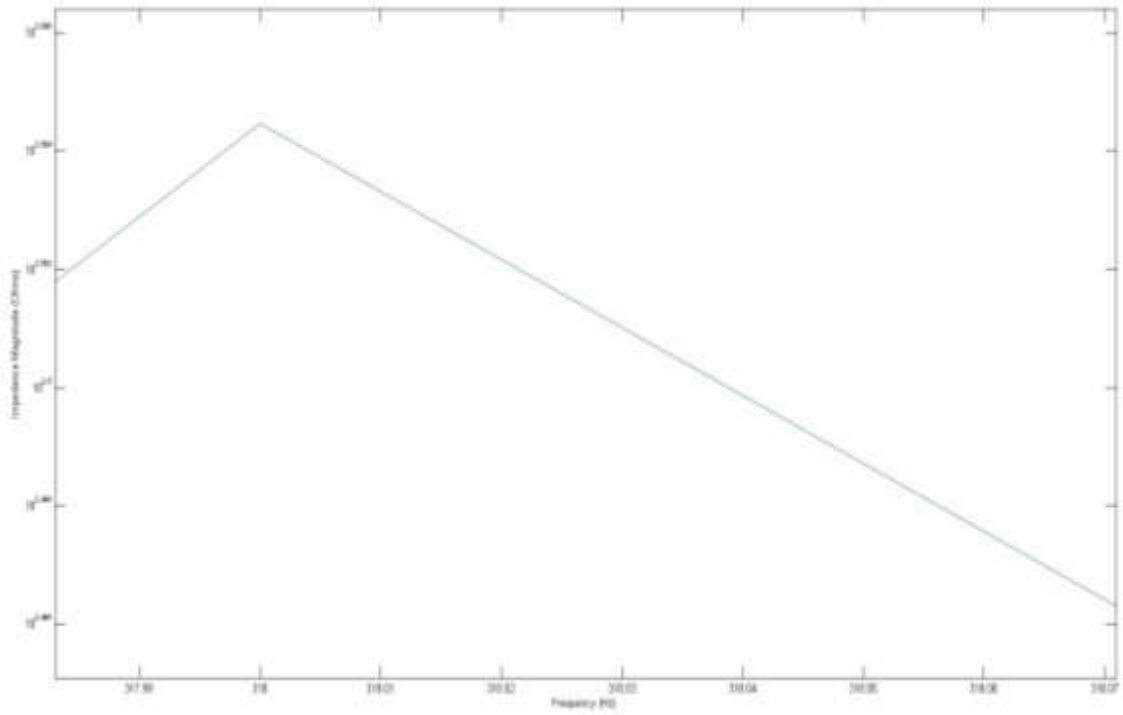

Figure 4.17: Impedance / Frequency Characteristic of Reduced Harmonics on Alagbon-Fowler D/L with Implementation of Single Passive LC Filter

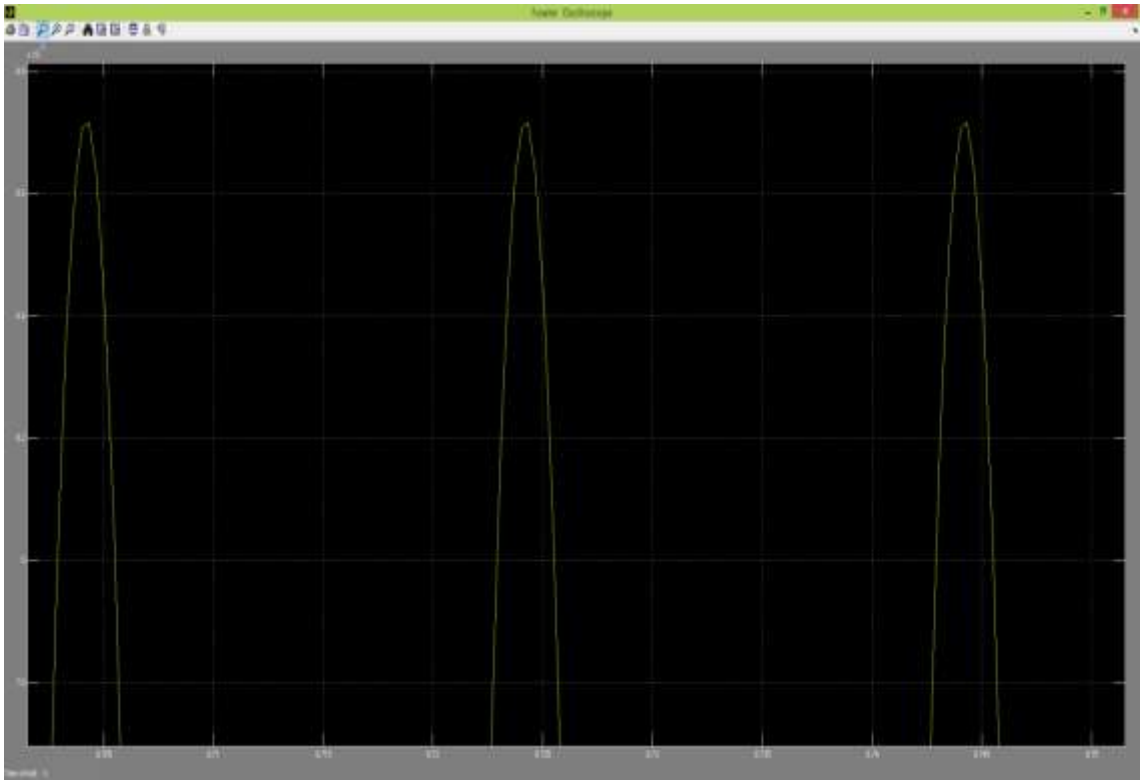

Figure 4.18: Result showing the Output Bus Voltage at Fowler to be 870V with the implementation of a Passive LC Filter

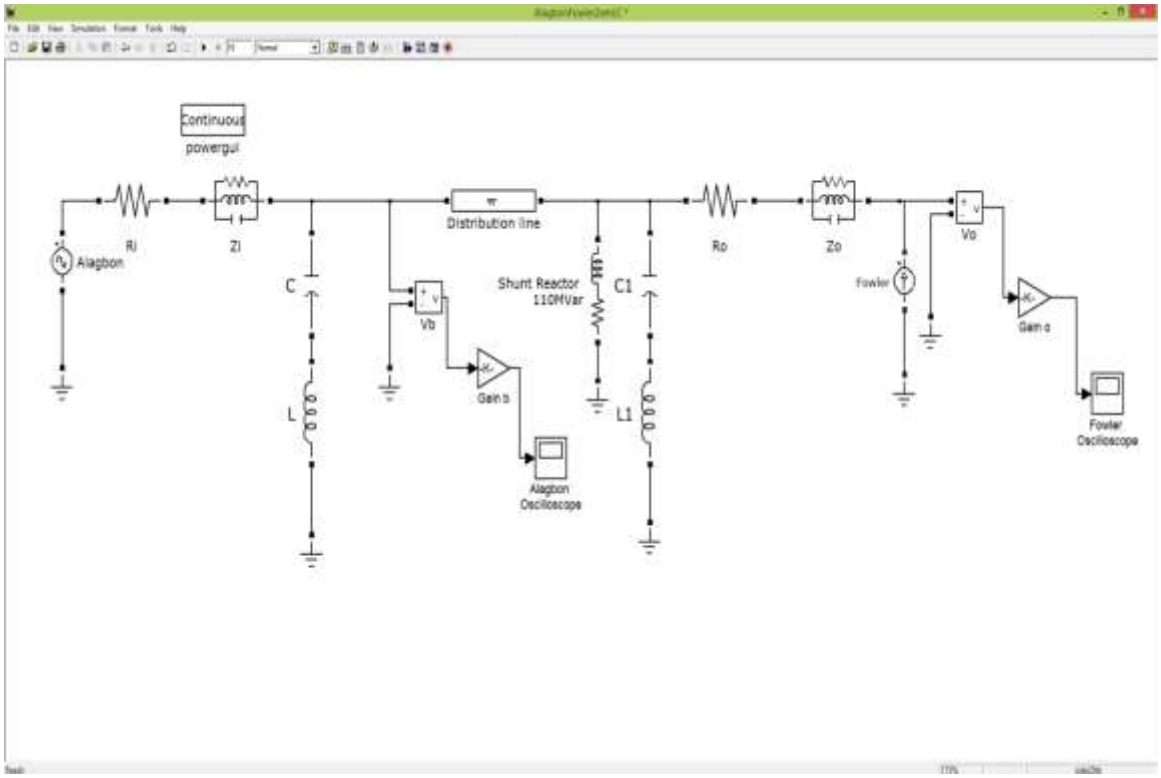

Figure 4.19: Model Showing the Implementation of two Passive LC Filters in Cascade on Alagbon-Fowler Distribution Line

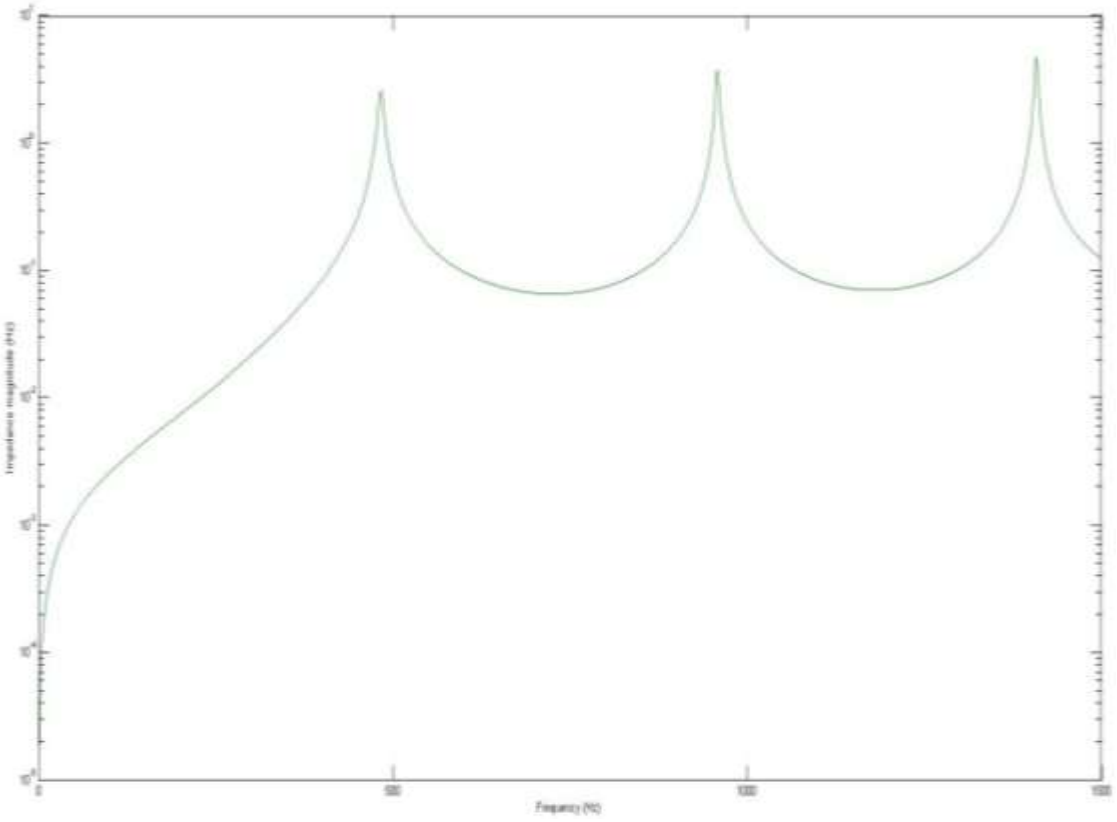

Figure 4.20: Impedance / Frequency Characteristic of Reduced Harmonics on Alagbon-Fowler D/L with the use of two Passive LC Filters in Cascade

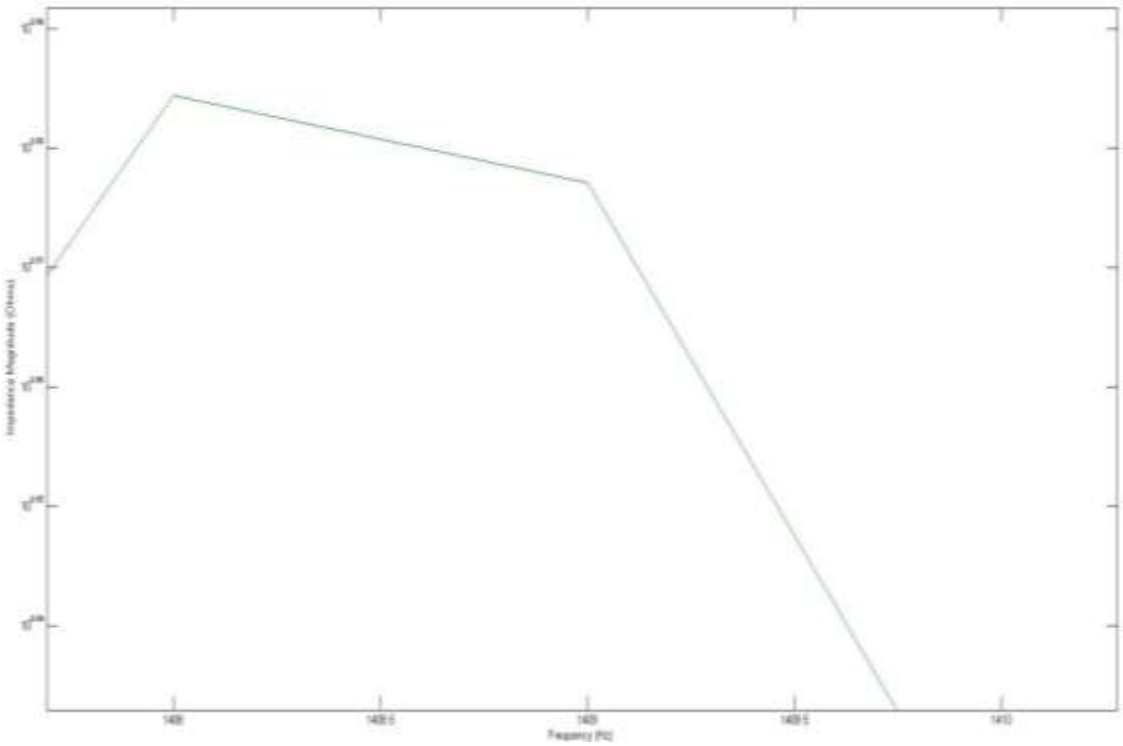

Figure 4.21: Impedance / Frequency Characteristic of Reduced Harmonics on Alagbon-Fowler D/L with Implementation of 2 No. Passive LC Filter in Cascade

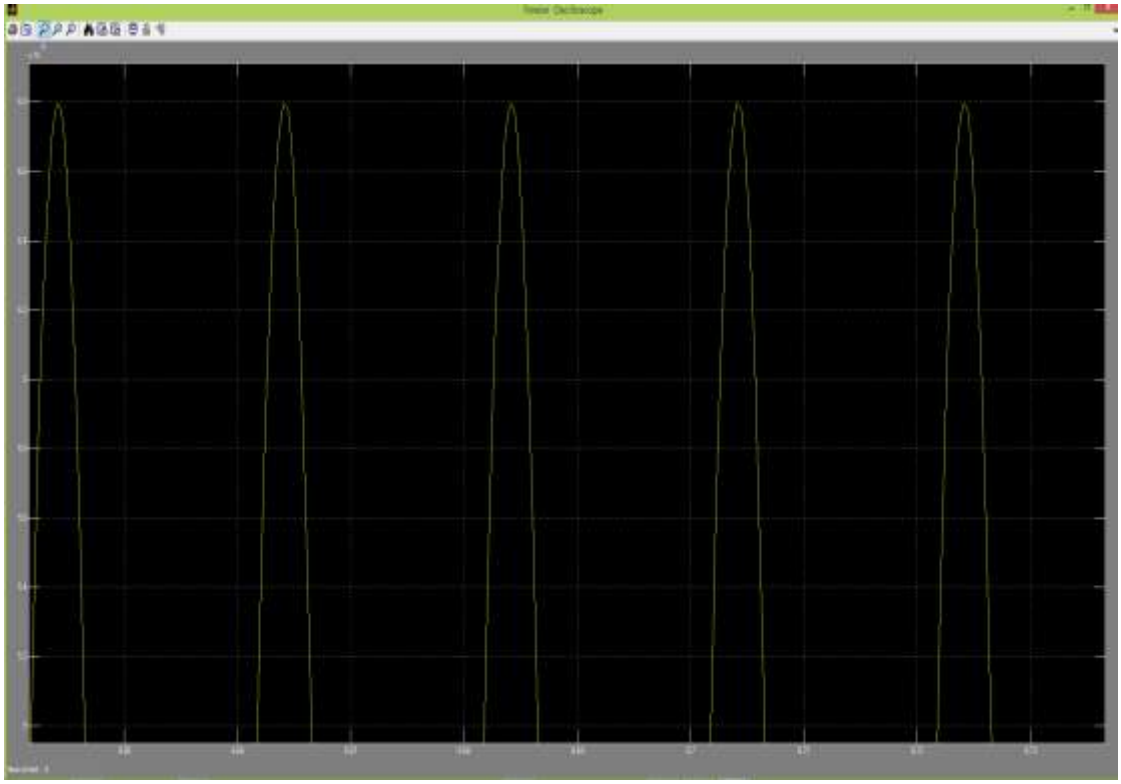

Figure 4.22: Result showing the Output Bus Voltage at Alagbon to be 6.80V with the implementation of two Passive LC Filters in Cascade

4.3 Discussion of Results

4.3.1 Discussion on Power Flow Results

The power flow analysis was carried out for Islands Business Unit's 33kV distribution network having seven (7) Bus bars and seven (7) distribution Lines. The minimum and maximum distribution line lengths are 0.15 km and 6.84 km respectively. Alagbon bus was used as the only source of supply and hence chosen as the slack bus for the power flow study. Table 3.2 shows that power flow studies were carried out for six (6) scenarios on 17/01/2014 and also 6 scenarios on 20/01/2014, making a total of twelve (12) scenarios. In all, the number of iteration convergence, k ranges from 3 – 5.

For 17/01/2014 scenario case, the Bus bar voltage evaluated ranges from 32.645kV to 32.997kV which are 98.92% and 99.99% of the nominal value, respectively. These voltage values are in order because they are within acceptable deviation limits from the ideal 33kV voltage. Also, in Tables 4.1 (a-f), summing the components of Input active power, P, and input reactive powers, Q, at each scenario and comparing with the corresponding output power, P_2, and output reactive power, Q_2, an algebraic sum of the active power ($\underline{P} = \underline{P}_1 + \underline{P}_2$) and reactive power ($\underline{Q} = \underline{Q}_1 + \underline{Q}_2$) obtained shows that it is only at 02:00Hrs that the net active power is a negative value, thus, necessitates the net reactive power Q to be a positive value. This clearly implies that the output power is higher than the input; hence the power system at that scenario time was not stable. The greater the value, the more unstable and prone to fault the system is The condition of power system at other scenario times such as 09:00Hrs, 21:00Hrs and 23:00Hrs are very stable, since their net active power, P and net reactive power, Q, are positive and negative values respectively. However, these values also account for losses at the various buses, which can be explained in terms of available power and customer demand at that time. Table 4.2 (a-f) presented results showing network loading at different scenario times. Importantly, current in magnitude and phase angle, drawn by utility customers based on the available power were presented. In Table 4.3 (a-f), Lines power flow results at different scenario time were presented. At 02:00Hrs of scenario, the output power P = 0 and Q = -0.377 on ALG – FOW distribution line shows that the line was energized (soaked) but either no load was drawn or a very negligible load was drawn

by point load power utility customers, since the percentage loading stood at 1.54% with zero percentage loss; while the power loss of 1.86% is within acceptable deviation standard of ±5%. At 09:00Hrs, ALG – BAN-I (Line 2), ALG – FOW (Line 1) and ALG – ANI (Line 2), ALG – ALG-L (Line 2) and ADM – ANI (Line 1), there are also zero output power, P, with output reactive power, Q, not zero. These lines equally have certain percentage of line loading with active power loss being zero. The implication is that the line are energized but not loaded at various 11kV outgoing feeders. The low percentage loading recorded may be due to point load customers connected along the lines. The current column shows that ALG – ANI (Line 1), ALG – ADM (Line 1) and ALG – FOW (Line 2) with 0.235kA, 0.207kA and 0.195kA loads respectively are considered heavily loaded lines compared to others. Also, the Active power loss for the two lines ALG – ANI (Line 1) and ALG – ADM (Line 1) are relatively higher (i.e 0.1077MW and 0.0796MW), compared to ALG – FOW (Line 2), whose active power loss is 0.0333MW. The lengths of these distribution lines play a major factor in this regard. ALG – ANI line is 6.84Km, ALG – ADM line is 6.13km and ALG – FOW line is 3.0km. The total active power loss in the network at this 09:00 Hrs scenario hour was 0.2251MW, which is higher than other network active power losses obtained in the remaining scenario times of the same day (for example, at 02:00Hrs, P_L loss = 0.0004MW, at 21:00Hrs, P_L loss = 0.1299MW, at 23:00Hrs, P_L loss = 0.0058MW) may not be unconnected with the fact that daily business activities start mostly at 8:30am. Therefore, 09:00Hrs to 15:00Hrs is considered the peak period of energy consumption on a commercial/industrial 33kV feeder. This further confirmed that the Island Business District's 33kV distribution network under study comprises of both commercially and industrially viable 33kV feeders.

For 20/01/2014 scenario case, the Bus bar voltage evaluated ranges from 32.553kV to 32.995 kV, which are 98.65% and 99.98% of the ideal 33kV voltage respectively. These range of voltage values are also within the permissible deviation range.

In Table 4.4 (a-f), obtaining an algebraic sum of input and output power for net active power ($\underline{P} = \underline{P}_1 + \underline{P}_2$) and that of the net reactive power ($\underline{Q} = \underline{Q}_1 + \underline{Q}_2$), it is seen

that at all scenario hours, the net active power is a positive value, while, the net reactive power is a negative value. As earlier depicted above, it depicts a stable power system.

In Table 4.5 (a-f) showing network loading at different hours, current in magnitude and phase drawn by power utility customers based on the power available (in MW) are presented. From the results, it can be observed that mostly ALG-L, FOW and MAR were heavily loaded Buses.

In Table 4.6 (a-f), line power flow results at different times of scenario were presented. As earlier discussed, for 17/01/2014 scenario, a situation where active power is zero and yet there exists a reactive power flow on the line, a low percentage loading and a very low percentage of active power loss on the line are observed generally on ALG – ADM (Line 2), ADM – MAR, ADM – ANI (Line 1), ALG – BAN-I (Line 2), ALG – FOW (Line 1), ALG – ALG-L (Line 2), ALG – ANI (Line 1), and ALG – ADM (Line 1). Across all the scenarios on this date, the losses per scenario are generally low because they are less than 1% of the total active power. However, there are cases of scenario where the active power is zero, yet, the line has a certain percentage loading; perhaps, due to the point loads connected along the line and the losses are also zero. Typical examples are ALG – BAN-I (Line 2) at 09:00Hrs, ALG – FOW (Line 1) at 09:00Hrs, ALG – ANI (Line 1) at 21:00Hrs and ALG – ANI (Line 1) at 23:00Hrs. Looking at the whole scenarios on this date, the highest losses of 0.3392MW was recorded at 21:00Hrs with a total active power of 138.5MW compared to 0.1134MW losses (16.761MW input power) at 02:00Hrs, 0.0573MW losses (15.44MW input power) at 06:00Hrs, 0.2251MW losses (17.22MW Input power) at 09:00Hrs and 0.2266MW losses (16.317MW Input power) at 23:00Hrs. At this point we can deduce that the higher the load, the more the losses.

Generally, to reduce the losses to a network acceptable value or standard has been a recurrent problem faced by Distribution Network Planners and Quality Assurance Engineers of Eko Electricity Distribution Plc.

4.3.2 Comparison of Harmonic Results of Scenario hours of 17th and 20th January 2014

At 02:00Hrs on 17th January, there are 2 Distribution Lines with harmonics namely ALG – ALG/L and ALG – FOW Distribution Lines, while on 20th January; there are also 2 Distribution Lines with harmonics namely, ALG – ALG/L and ALG – ADM Distribution Lines. The basis for comparison is the ALG – ALG/L Distribution Line that are common to the two days. Figure 4.1a and Figure 4.5a are harmonic patterns of the Alagbon – Alagbon Local D/L for both 17th and 20th January 2014 respectively at 02:00am. For ALG – ALG/L D/L, 2nd harmonic component is observed on the impedance magnitude versus frequency plotted (harmonic pattern) for both cases, at different nominal voltage V (Vrms) level of 39.5kV and 39.499kV respectively. However, the peak impedance magnitude remains $10^{2.052}\Omega$ for both cases. Alagbon 132/33kV Transmission station shared the same yard with Alagbon Local 33/11kV Injection Substation which necessitates the distribution line between Alagbon – Alagbon local to be a short distance of 0.15km.

At 06:00 of 17th January 2014, there was no energy in the system whereas on 20th January, 2014 of the same hour, there was energy in the system. So the basis for comparison does not arise.

At 09:00Hrs, a basis for comparison arises. On 17th January, there are harmonics on ALG-ADM D/L, ALG-ALG/L D/L, ALG – ANI D/L, ALG – FOW D/L and ADM – ANI D/L while on 20th January, there are harmonics on ALG – ALG/L D/L, ALG – BAN/I D/L and ALG – FOW D/L. The common distribution lines with harmonics at this hour of the 2 days are ALG – ALG/L D/L and ALG – FOW D/L. on 17th January, ALG-ALG/L D/L had only 2 harmonics with peak impedance amplitude of $10^{2.052}\Omega$ and an intercept of $10^{0.40}\Omega$ at nominal voltage of 39.6kV. Whereas, on 20th January, the same Distribution Line has only 2nd harmonics too with the same peak impedance amplitude and an intercept of $10^{-0.3}\Omega$ at a nominal voltage of 39.515kV.

Also, on 17th January, ALG – FOW D/L has 4 harmonics namely 2nd, 6th, 15th and 24th with peak impedance magnitude $10^{1.985}\Omega$, $10^{2.508}\Omega$, $10^{2.268}\Omega$ and $10^{2.198}\Omega$

respectively and at a nominal voltage of 91.1kV. On 20th January, the same parameters were observed. That is, the same Distribution line has the same list of harmonics and values of peak impedance amplitude with same the intercept and at a nominal voltage of 91.15kV.

At 21:00Hrs, a basis for comparison arises. On 17th January, there are harmonics on ALG – ADM D/L, ALG – ANI, ALG – FOW and ADM – ANI Distribution Lines. While, on 20th January there are harmonics on ALG – ALG/L, ALG – ANI and ALG – FOW Distribution Lines. The common distribution lines with harmonics at this hour of the two days are ALG – ANI and ALG – FOW Distribution Lines. Based on Figure 4.3b and Figure 4.8b, harmonics on ALG – ANI Distribution Line for 17th and 20th January respectively can be said to be similar in all ramification, including the nominal value. While, Figures 4.3c and 4.8c show ALG – FOW D/L with 4 Harmonics each, that is, 2nd, 6th, 15th and 24th. The two similar harmonics have an approximate magnitude. The former occurs at a nominal voltage of 83.9kV while the later occurs at a nominal voltage of 90.99kV.

4.3.3 Total Harmonic Distortion (THD) of the Distribution Lines for Selected Scenario Hours on 17th January 2014.

At 02:00Hrs

Case 1: Alagbon - Alagbon Local Distribution Line

2nd Harmonic = 100Hz

Harmonic Impedance = $10^{2.052}\Omega$

$V_{\text{Alagbon Local}}$ = 32.997kV

Number of cascaded distribution lines N_c = 10

$P_{\text{Alagbon Local}}$ = 4.5MW

Power Factor = 0.85

Cascaded Harmonic Voltage, $U_h = \sqrt{\frac{Power(p) \times Harmonic\ Impedance(Z)}{\sqrt{3}Cos\emptyset}} \times \frac{1}{10}$

$$= \sqrt{\frac{4.5 \times 10^{2.052}}{1.472}} \times \frac{1}{10}$$

$$= 1.856kV$$

$$THD = \frac{100}{U_1}\sqrt{\sum_{h=2}^{n} U_h^2}$$

$$= \frac{100\sqrt{(1.856)^2}}{32.99}$$

$$= 5.63\%$$

Case 2: Alagbon - Fowler Line Distribution Line

V_{Fowler} = 32.881kV

` P_{Fowler}= 8.7MW

Table 4.9a: Determination of Total Harmonics Distortion (THD) of Alagbon – Alagbon Local Distribution Line at 02:00Hrs.

S/N	Harmonic	Harmonic Frequency (Hz)	Harmonic Impedance (Ω)	Cascaded Harmonic Voltage (U_h) (V)	Square Cascaded Harmonic Voltage (U^2_h) (V)
1	2nd	100	$10^{1.985}$	23.89	570.73
2	6th	300	$10^{2.508}$	43.63	1903.58
3	15th	750	$10^{2.268}$	33.10	1095.61
4	24th	1200	$10^{2.198}$	30.54	932.42
					4502.34

$$\text{THD} = 20.41\%$$

At 09:00Hrs

Case 1: Alagbon - Ademola Distribution Line

$V_{Ademola}$ = 32.711kV

$P_{Ademola}$= 10.6MW

Case 2: Alagbon - Alagbon Local Distribution Line

2nd Harmonic = 100Hz

Harmonic Impedance = $10^{2.052}$ ohm

$V_{Alagbon\ Local}$ = 32.997kV

$P_{Alagbon\ Local}$ = 3.6MW

$$Cascaded\ Harmonic\ Voltage = \sqrt{\frac{3.6\times10^{2.052}}{1.472}} \times \frac{1}{10}$$

$$= 1.660kV$$

$$THD = \frac{100\sqrt{1.660^2}}{32.997} = 5.03\%$$

Case 3: Alagbon - Anifowoshe Distribution Line

$V_{Anifowoshe}$ = 32.645kV

$P_{Anifowoshe}$= 11.7MW

Case 4: Alagbon - Fowler Distribution Line

V_{Fowler} = 32.868kV

P_{Fowler}= 9.6MW

Case 5: Alagbon – Banana Island Distribution Line

$V_{Banana\ Island}$ = 32.942 kV

$P_{Banana\ Island}$ = 3.0 MW

Table 4.9b: Determination of Total Harmonics Distortion (THD) of Alagbon – Ademola Distribution Line at 09:00Hrs.

S/N	Nth Harmonic	Harmonic Frequency (Hz)	Harmonic Impedance (Ω)	Cascaded Harmonic Voltage (U_h) (V)	Square Cascaded Harmonic Voltage (U^2_h) (V)
1	2nd	100	$10^{2.007}$	27.05	731.70
2	3rd	150	$10^{2.648}$	56.58	3201.30
3	8th	400	$10^{2.279}$	37.00	1369.00
4	12th	600	$10^{2.148}$	31.82	1012.51
5	16th	800	$10^{2.051}$	28.46	809.97
6	20th	1000	$10^{2.014}$	27.27	743.70
7	23th	1150	$10^{1.945}$	25.19	634.45
8	26th	1300	$10^{1.859}$	22.81	520.47
9	28th	1400	$10^{1.741}$	19.92	396.64
10	29th	1450	$10^{1.556}$	16.09	259.06
					9678.80

$$THD = 30.0\%$$

Table 4.9c: Determination of Total Harmonics Distortion (THD) of Alagbon – Anifowoshe Distribution Line at 09:00Hrs.

S/N	Nth Harmonic	Harmonic Frequency (Hz)	Harmonic Impedance (Ω)	Cascaded Harmonic Voltage (U_h) (V)	Square Cascaded Harmonic Voltage (U^2_h) V
1	2nd	100	$10^{2.116}$	32.22	1038.19
2	3rd	150	$10^{2.650}$	59.59	3550.41
3	7th	350	$10^{2.298}$	39.73	1578.62
4	11th	550	$10^{2.143}$	33.24	1104.79
5	14th	700	$10^{2.057}$	30.11	906.31
6	18th	900	$10^{1.973}$	27.33	746.92
7	21th	1050	$10^{1.914}$	25.54	652.05
8	23th	1150	$10^{1.841}$	23.48	551.16
9	25th	1250	$10^{1.690}$	19.73	389.29
10	26th	1300	$10^{1.490}$	15.67	245.63
11	27th	1350	$10^{0.994}$	8.85	78.39
					10841.76

$$THD = 31.90\%$$

Table 4.9d: Determination of Total Harmonics Distortion (THD) of Alagbon – Fowler Distribution Line at 09:00Hrs.

S/N	Nth Harmonic	Harmonic Frequency (Hz)	Harmonic Impedance (Ω)	Cascaded Harmonic Voltage (U_h) (V)	Square Cascaded Harmonic Voltage (U^2_h) (V)
1	2nd	100	$10^{1.985}$	25.10	630.03
2	6th	300	$10^{2.508}$	45.83	2100.70
3	15th	750	$10^{2.268}$	34.77	1208.82
4	24th	1200	$10^{2.198}$	32.08	1028.88
					4968.43

$$THD = 21.4\%$$

Table 4.9e: Determination of Total Harmonics Distortion (THD) of Alagbon – Banana-Island Distribution Line at 09:00Hrs.

S/N	Nth Harmonic	Harmonic Frequency (Hz)	Harmonic Impedance (Ω)	Cascaded Harmonic Voltage (U_h) (V)	Square Cascaded Harmonic Voltage (U^2_h) (V)
1	2nd	100	$10^{1.962}$	13.66	186.73
3	9th	450	$10^{2.276}$	19.62	384.78
4	15th	750	$10^{2.152}$	17.00	289.21
5	20th	1000	$10^{2.083}$	15.71	246.73
6	24th	1200	$10^{2.048}$	15.09	227.62
7	29th	1450	$10^{2.007}$	14.39	207.12
					2372.45

$$THD = 14.8\%$$

At 21:00Hrs

Case 1: Alagbon - Ademola Distribution Line

$V_{Ademola}$ = 32.825kV

$P_{Ademola}$= 6.7MW

Case 2: Alagbon - Anifowoshe Distribution Line

$V_{Anifowoshe}$ = 32.725kV

$P_{Anifowoshe}$= 9.3MW

Case 3: Alagbon - Fowler Distribution Line

V_{Fowler} = 32.867kV

P_{Fowler}= 9.7MW

Table 4.9f: Determination of Total Harmonics Distortion (THD) of Alagbon – Ademola Distribution Line at 21:00Hrs.

S/N	Nth Harmonic	Harmonic Frequency (Hz)	Harmonic Impedance (Ω)	Cascaded Harmonic Voltage (U_h) (V)	Square Cascaded Harmonic Voltage (U^2_h) (V)
1	2nd	100	$10^{2.008}$	21.53	463.63
2	3rd	150	$10^{2.644}$	44.78	2005.24
3	8th	400	$10^{2.274}$	29.25	855.40
4	12th	600	$10^{2.149}$	25.33	641.46
5	16th	800	$10^{2.048}$	22.55	508.35
6	20th	1000	$10^{2.013}$	21.66	468.99
7	23th	1150	$10^{1.943}$	19.98	399.18
8	26th	1300	$10^{1.861}$	18.18	330.50
9	28th	1400	$10^{1.743}$	15.87	251.86
10	29th	1450	$10^{1.556}$	12.80	163.74
					6088.35

$$\text{THD} = 23.77.\%$$

Table 4.9g: Determination of Total Harmonics Distortion (THD) of Alagbon – Anifowoshe Distribution Line at 21:00Hrs.

S/N	Nth Harmonic	Harmonic Frequency (Hz)	Harmonic Impedance (Ω)	Cascaded Harmonic Voltage (U_h) (V)	Square Cascaded Harmonic Voltage (U^2_h) (V)
1	2nd	100	$10^{2.117}$	28.76	827.13
2	3rd	150	$10^{2.655}$	53.43	2854.79
3	7th	350	$10^{2.297}$	35.38	1251.92
4	11th	550	$10^{2.142}$	29.60	876.14
5	14th	700	$10^{2.057}$	26.84	720.40
6	18th	900	$10^{1.974}$	24.39	595.08
7	21th	1050	$10^{1.913}$	22.74	517.10
8	23th	1150	$10^{1.840}$	20.91	437.09
9	25th	1250	$10^{1.692}$	17.63	310.87
10	26th	1300	$10^{1.491}$	13.99	195.69
11	27th	1350	$10^{0.991}$	07.87	61.88
					8648.09

THD = 28.4%

Table 4.9h: Determination of Total Harmonics Distortion (THD) of Alagbon – Fowler Distribution Line at 21:00Hrs.

S/N	Nth Harmonic	Harmonic Frequency (Hz)	Harmonic Impedance (Ω)	Cascaded Harmonic Voltage (U_h) (V)	Square Cascaded Harmonic Voltage (U^2_h) (V)
1	2nd	100	$10^{1.982}$	24.62	606.14
2	8th	400	$10^{2.470}$	43.18	1864.55
3	19th	950	$10^{2.275}$	34.50	1190.08
					3660.77

THD= 18.5%

At 23.00Hrs

Case 1: Alagbon - Anifowoshe Distribution Line

$V_{Anifowoshe}$ = 32.695kV

$P_{Anifowoshe}$= 10.20MW

Table 4.9i: Determination of Total Harmonics Distortion (THD) of Alagbon – Anifowoshe Distribution Line at 23:00Hrs.

S/N	Nth Harmonic	Harmonic Frequency (Hz)	Harmonic Impedance (Ω)	Cascaded Harmonic Voltage (U_h) (V)	Square Cascaded Harmonic Voltage (U^2_h) (V)
1	2nd	100	$10^{2.116}$	30.22	913.25
2	3rd	150	$10^{2.649}$	55.64	3095.81
3	7th	350	$10^{2.298}$	37.18	1382.35
4	11th	550	$10^{2.143}$	30.93	956.66
5	14th	700	$10^{2.056}$	23.21	795.80
6	18th	900	$10^{1.973}$	25.42	646.18
7	21th	1050	$10^{1.914}$	23.73	563.11
8	23th	1150	$10^{1.841}$	21.89	479.17
9	25th	1250	$10^{1.690}$	18.42	339.30
10	26th	1300	$10^{1.490}$	14.63	214.04
11	27th	1350	$10^{0.994}$	08.23	67.73
					9453.41

THD = 18.5%

4.3.4 Total Harmonic Distortion (THD) of the Distribution Lines for Selected Scenario Hours on 20th January, 2014.

At 02:00Hrs

Case 1: Alagbon - Alagbon Local Distribution Line

2^{nd} Harmonic = 100Hz

Harmonic Impedance = $10^{2.052}\Omega$

$V_{Alagbon\ Local}$ = 32.995kV

Number cascaded distribution lines N_c = 10

$P_{Alagbon\ Local}$ = 6.5MW

Power Factor = 0.85

$$CascadedHarmonicVoltage = \sqrt{\frac{Power(P) \times HarmonicImpedance(z)}{\sqrt{3}Cos\emptyset 0}} \times \frac{1}{10}$$

$$= \sqrt{\frac{6.5 \times 10^{2.052}}{1.472}} \times \frac{1}{10}$$

$$= 2.231kV$$

$$THD = \frac{100}{U_1}\sqrt{\sum_{h=2}^{n} U_h^2}$$

$$= \frac{100\sqrt{(2.231)^2}}{32.995}$$

$$= 6.76\%$$

Case 2: Alagbon - Ademola Distribution Line

V_{Fowler} = 32.737 kV

`

P_{Fowler}= 9.7 MW

Table 4.10a: Determination of Total Harmonics Distortion (THD) of Alagbon – Ademola Distribution Line at 02:00Hrs.

S/N	Nth Harmonic	Harmonic Frequency (Hz)	Harmonic Impedance (Ω)	Cascaded Harmonic Voltage (U_h) (V)	Square Cascaded Harmonic Voltage (U^2_h) (V)
1	2nd	100	$10^{2.007}$	25.88	669.67
2	3rd	150	$10^{2.649}$	54.19	2936.73
3	8th	400	$10^{2.281}$	35.48	1258.53
4	12th	600	$10^{2.147}$	30.40	924.41
5	16th	800	$10^{2.052}$	27.25	742.79
6	20th	1000	$10^{2.014}$	26.09	680.55
7	23rd	1150	$10^{1.946}$	24.12	581.92
8	26th	1300	$10^{1.858}$	21.80	475.19
9	28th	1400	$10^{1.740}$	19.03	362.13
10	29th	1450	$10^{1.556}$	15.40	237.06
					8868.98

THD = 28.77%

At 06:00Hrs

Case 1: Alagbon - Alagbon Local Distribution Line

2^{nd} Harmonic = 100Hz

Harmonic Impedance = $10^{2.052}\Omega$

$V_{Alagbon\ Local}$ = 32.997kV

Number cascaded distribution lines N_c = 10

$P_{Alagbon\ Local}$ = 4.1MW

Power Factor = 0.85

$$CascadedHarmonicVoltage = \sqrt{\frac{Power(P) \times HarmonicImpedance(z)}{\sqrt{3}Cos\emptyset 0}} \times \frac{1}{10}$$

$$= \sqrt{\frac{4.1 \times 10^{2.052}}{1.472}} \times \frac{1}{10}$$

$$= 35.88kV$$

$$THD = \frac{100}{U_1}\sqrt{\sum_{h=2}^{n} U_h^2}$$

$$= \frac{(22.3102)}{32.997} \times \frac{1}{10} \quad = 10.87\%$$

Case 2: Alagbon - Anifowoshe Distribution Line

$V_{Anifowoshe}$ = 32.833kV

$P_{Anifowoshe}$= 6 MW

Case 3: Alagbon - Fowler Distribution Line

V_{Fowler} = 32.926kV

P_{Fowler}= 10.7MW

Table 4.10b: Determination of Total Harmonics Distortion (THD) of Alagbon – Anifowoshe Distribution Line at 06:00Hrs.

S/N	Nth Harmonic	Harmonic Frequency (Hz)	Harmonic Impedance (Ω)	Cascaded Harmonic Voltage (U_h) (V)	Square Cascaded Harmonic Voltage (U^2_h) (V)
1	2nd	100	$10^{2.118}$	56.65	3209.18
2	3rd	150	$10^{2.665}$	43.41	1884.71
3	7th	350	$10^{2.292}$	28.26	798.44
4	11th	550	$10^{2.139}$	23.69	561.36
5	14th	700	$10^{2.058}$	21.58	465.85
6	18th	900	$10^{1.977}$	19.66	386.58
7	21^{st}	1050	$10^{1.910}$	18.20	331.32
8	23th	1150	$10^{1.838}$	16.75	280.70
9	25th	1250	$10^{1.695}$	14.21	201.95
10	26th	1300	$10^{1.494}$	11.28	127.13
11	27th	1350	$10^{0.985}$	6.28	39.38
					8286.6

THD = 27.7%

Table 4.10c: Determination of Total Harmonics Distortion (THD) of Alagbon – Fowler Distribution Line at 06:00Hrs.

S/N	Nth Harmonic	Harmonic Frequency (Hz)	Harmonic Impedance (Ω)	Cascaded Harmonic Voltage (U_h) (V)	Square Cascaded Harmonic Voltage (U^2_h) (V)
1	2nd	100	$10^{1.986}$	26.53	703.84
2	6th	300	$10^{2.505}$	48.22	2325.28
3	15th	750	$10^{2.270}$	36.79	1353.55
4	24th	1200	$10^{2.196}$	33.79	1141.50
					5524.17

$$THD = 27.7\%$$

At 09:00Hrs

Case 1: Alagbon - Alagbon Local Distribution Line

2^{nd} Harmonic = 100Hz

Harmonic Impedance = $10^{2.052}$ ohm

$V_{Alagbon\ Local}$ = 32.996kV

$P_{Alagbon\ Local}$ = 10.2MW

$$Cascaded\ Harmonic\ Voltage = \sqrt{\frac{10.2\times10^{2.052}}{1.472}} \times \frac{1}{10} \quad = 2.795kV.$$

$$\text{THD} = 8.47\%$$

Case 2: Alagbon - Banana Island Distribution Line

$V_{Banana\ Island}$ = 32.942kV

$P_{Banana\ Island}$= 3.0MW

Case 3: Alagbon – Fowler Distribution Line

V_{Fowler} = 32.904kV

P_{Fowler}= 13.8MW

Table 4.10d: Determination of Total Harmonics Distortion (THD) of Alagbon – Banana Island Distribution Line at 09:00Hrs.

S/N	Nth Harmonic	Harmonic Frequency (Hz)	Harmonic Impedance (Ω)	Cascaded Harmonic Voltage (U_h) (V)	Square Cascaded Harmonic Voltage (U^2_h) (V)
1	2nd	100	$10^{2.039}$	14.93	222.95
2	4th	200	$10^{2.598}$	28.42	807.63
3	9th	450	$10^{2.267}$	19.41	376.89
4	15th	750	$10^{2.159}$	17.14	293.91
5	20th	1000	$10^{2.098}$	15.98	255.40
6	24th	1200	$10^{2.045}$	15.04	226.06
7	28th	1450	$10^{1.981}$	13.97	195.08
					2377.92

$THD = 14.8\%$

Table 4.10e: Determination of Total Harmonics Distortion (THD) of Alagbon – Fowler Distribution Line at 09:00Hrs.

S/N	Nth Harmonic	Harmonic Frequency (Hz)	Harmonic Impedance (Ω)	Cascaded Harmonic Voltage (U_h) (V)	Square Cascaded Harmonic Voltage (U^2_h) (V)
1	2nd	100	$10^{1.985}$	30.09	905.67
2	6th	300	$10^{2.507}$	54.89	3012.81
3	15th	750	$10^{2.269}$	41.73	1741.69
4	24th	1200	$10^{2.198}$	38.46	1479.01
					7139.18

$$THD = 25.7\%$$

At 12.00Hrs

Case 1: Alagbon - Alagbon Local Distribution Line

2^{nd} Harmonic = 100Hz

Harmonic Impedance = $10^{2.052}$ ohm

$V_{Alagbon\ Local}$ = 32.96kV

$P_{Alagbon\ Local}$= 11.2MW

$$Cascaded\ Harmonic\ Voltage = \sqrt{\frac{11.2 \times 10^{2.052}}{1.472}} \times \frac{1}{10}$$

$$= 29.286kV$$

$$THD = 8.89\%$$

Case 2: Alagbon - Anifowoshe Distribution Line

$V_{Anifowoshe}$ = 32.553kV

$P_{Anifowoshe}$= 4.5MW

Case 3: Alagbon - Fowler Distribution Line

V_{Fowler} = 32.834kV

P_{Fowler}= 12 MW

Table 4.10f: Determination of Total Harmonics Distortion (THD) of Alagbon – Anifowoshe Distribution Line at 12:00Hrs.

S/N	Nth Harmonic	Harmonic Frequency (Hz)	Harmonic Impedance (Ω)	Cascaded Harmonic Voltage (U_h) (V)	Square Cascaded Harmonic Voltage (U^2_h) (V)
1	2nd	100	$10^{2.114}$	19.94	397.47
2	3rd	150	$10^{2.656}$	37.21	1384.54
3	7th	350	$10^{2.302}$	24.75	612.78
4	11th	550	$10^{2.145}$	20.66	426.88
5	14th	700	$10^{2.054}$	18.61	346.18
6	18th	900	$10^{1.968}$	16.85	283.99
7	21th	1050	$10^{1.918}$	15.91	253.11
8	23th	1150	$10^{1.843}$	14.59	212.96
9	25th	1250	$10^{1.689}$	12.22	149.38
10	26th	1300	$10^{1.485}$	9.66	93.39
11	27th	1350	$10^{1.002}$	5.54	30.71
					4191.39

THD = 19.89%

Table 4.10g: Determination of Total Harmonics Distortion (THD) of Alagbon – Fowler Distribution Line at 12:00Hrs.

S/N	Nth Harmonic	Harmonic Frequency (Hz)	Harmonic Impedance (Ω)	Cascaded Harmonic Voltage (U_h) (V)	Square Cascaded Harmonic Voltage (U^2_h) (V)
1	2nd	100	$10^{1.984}$	28.03	785.73
2	6th	300	$10^{2.508}$	51.24	2625.87
3	15th	750	$10^{2.266}$	38.78	1504.09
4	24th	1200	$10^{2.200}$	35.94	1292.03
					6207.72

$$THD = 23.99\%$$

4.3.5 Discussions on Passive Harmonic Mitigation Results

Considering Figures 4.9, the peak impedance magnitudes which are $10^{2.508}\,\Omega$ and $10^{2.24}\Omega$ respectively shows a percentage reduction in harmonics as shown below to be:

$$\frac{10^{2.508}\Omega - 10^{2.24}\Omega}{10^{2.508}\Omega} \times 100 = 46.05\%$$

Consequently, an additional Band pass filter was introduced to the distribution line for a further elimination of the harmonics as already shown in Figure 4.11. This is aimed at attaining a desired impedance level of $10^{0}\Omega$, as an RLC filter has significantly eliminated one out of the four harmonics from the distribution line. The voltage at Fowler Bus bar dropped to 2.85kV.

With the cascading of two RLC filters on Alagbon-Fowler Distribution Line, the simulation result shows that the number of harmonics remain the same three (3) but with a suppression of harmonic intensity as shown in Figure 4.12 and 4.13. This is because the impedance magnitude reduced to $10^{0.585}\Omega$, which eventually makes the percentage of harmonic strength reduced by 98.81%. However, the voltage measured at Fowler Bus dropped drastically to 73.80V.It can therefore be inferred that an increase in the number of RLC filters implemented in the distribution line, would result in a further reduction of the impedance magnitude of the harmonics in the distribution line, thereby mitigating the harmonics.

With a single LC filter, simulations shows that the number of harmonics without applying a filter and after the introduction of a single passive LC filter dropped from four (4) to three (3) as shown in Figure 4.16. The peak impedance magnitude in this case is about $10^{2.504}\Omega$, which is relatively higher than the case for which two RLC filters were introduced on the Distribution Line. This is illustrated in Figure 4.17.The voltage at Fowler Bus bar, however, increased marginally to about 870V from 73.80V (which was the voltage before the single Passive LC filter was implemented). This is also illustrated in figure 4.18.Simulation results also shows that the overall harmonic mitigation level still remains the same, as the number of harmonics was reduced from four (4) to three (3),

while the output voltage at Fowler dropped further to 680V as shown in Figure 4.22. However, impedance magnitude reduced to $10^{0.585}\Omega$ as shown in Figure 4.21.

It can therefore be inferred from the simulation results that the RLC Filter is preferable to the passive LC filter in terms of the output voltages obtained on Fowler Bus bar, as RLC filters (both single and cascaded configurations) give higher output voltage values in comparison to corresponding configurations of passive LC filters.

Finally, comparing the harmonic suppression patterns in Figure 4.12 and 4.20 for cascaded RLC filter and cascaded LC filter respectively, it can be observed that the impedance magnitude at 0Hz are different. For the cascaded RLC filter, the impedance magnitude is $10^{-1}\Omega$, which is higher than that of the cascaded LC filter whose value is $10^{-5}\Omega$. However, the harmonic mitigated in both cases was one out of four and their peak impedance magnitude of about $10^{0.585}\Omega$ remains the same.

CHAPTER FIVE

CONCLUSION AND RECOMMENDATIONS

5.1 Conclusion

The aim of this study has been to investigate harmonics and its effective control in a power system network to enhance quality of power supply. It involved power flow analysis, harmonic evaluation and development of a solution method for harmonic mitigation.

The fundamentals of harmonic studies and the related issues were reviewed in chapters one and two. A detailed literature survey is presented to summarize the state of the art techniques that are pertinent to the methods proposed in this research.

Furthermore, a description of the modelling and simulation of a typical 33kV Distribution network for power flow was given and this was achieved using NEPLAN software. The results of this power flow study were also presented. Subsequently, these results were applied to a developed algorithm to evaluate harmonics in each of the Distribution lines of the network considered. This was done using the MATLAB/Simulink platform to carry out the simulation. The various harmonics in the distribution network taken as a case study (Figure 3.1) were obtained and results are presented. A sample of the harmonic patterns from the distribution network results was used as a case study for the purpose of mitigation. To achieve this, RLC, Cascaded RLC, LC and Cascaded LC passive filters were differently connected to the modelled Distribution line. Similarly, MATLAB/Simulink was used to carry out the simulations. The harmonic mitigation results from the four categories of passive filter obtained from the simulation are presented.

Finally, a detailed discussion and analysis of the results obtained in this research was presented in chapter four. It includes a discussion on power flow and losses on the line. A comparison of harmonic results obtained for the 2 day scenarios considered were recorded as well. The total harmonic distortion (THD) analysis of the network carried out

based on each Distribution line consideration were also presented for the 2 day scenarios and a discussion on harmonic mitigation results was highlighted.

5.2 Recommendations for Future work

The following recommendations would be very useful in improving the reliability performance of the Island Business District's 33kV Distribution Network and enhance future works related to this research topic:

- During MATLAB simulation, ten cascaded π-distribution lines were used so that all harmonics on the line could be observed. In future works, twenty cascadedπ-distribution lines are recommended to be used.
- Derive a scientific means of obtaining an approximate value of source impedance $L_{s,}$ i.e. inductance present in the network before connection of filter.
- Since Single tuned (passive) filter was used for mitigation, it was observed that the higher the order of harmonic, the more efficient the filter is. Therefore, a second or third order damped filter is recommended for more efficient performance.
- Because the power flow results obtained shows that high reactive power flows within the distribution network, reactors are hereby recommended to be installed in strategic locations within the network.
- Based on the power flow study results, there is a need to site two new 33/11kV, 15MVA Injection Substations in two locations within the distribution network, particularly between Alagbon/Anifowoshe Bus bars and Alagbon/Ademola Busbars, where relatively high power losses are observed as a result of the long distances of 6.84km and 6.13km between the Bus bars.
- In power flow analysis, overloaded lines within the distribution network could be compensated by the addition of new parallel distribution lines. However, considering the overall economic cost of operating the system and maximum load point reliability level, four is the maximum number of lines recommended for any load bus.

- For all simulations carried out on harmonic mitigation techniques, it was discovered that the output voltages at the receiving Bus bars were generally lower than the conventional 33kV. Thus, a Voltage Boost Converter can be introduced at the receiving Bus bar to step up voltage back to 33kV.

REFERENCES

Adejumobi, I., Adepoju, G., & Hamzat, K. (2013). Iterative Techniques for Load Flow Study: A Comparative Study for Nigerian 330kV Grid System as a Case Study. *International Journal of Engineering and Advanced Technology (IJEAT), 3* (1), 153-158.

Akagi, H. (2006). Modern Active Filters and Traditional Passive Filters. *Bulletin of the Polish Academy of Sciences Technical Sciences, 54* (3), pp. 255-269.

Allah, R. (2014). Automatic Power Factor Correction Based on Alienation Technique. *International Journal of Engineering and Advanced Technology (IJEAT), 3* (4), 194-202.

Allen, J. W., & Bruce, F. W. (2012). *Power Generation and Operation Control* (Vol. Second Edition). John wiley & Sons, Inc.

Al-Naseem, O. A., & Adi, A. K. (2003). Impact of Power Factor Correction on the Electrical Distribution Network of Kuwait – A Case Study. *The Online Journal on Power and Energy Engineering (OJPEE), 2* (1), 173-76.

Alqadi, R., & Khammash, M. (2007). An Efficient Parallel Gauss-Seidel Algorithm for the Solution of Load Flow Problems. *The International Arab Journal of Information Technology, 4* (2), 148-152.

Al-Zamil, A., & Torrey, D. (2001). A Passive Series, Active Shunt Filters for High Power Applications. *Power Electronics, IEEE Transactions on,, 16* (1), 101-109.

Arrillaga, J., Bollen, M., & Watson, N. (2000). Power Quality Following Deregulation. *Proceedings of the IEEE, 88* (2), 246-261.

Artega, J., Payan, B., & Mitchell, C. (2000). Power Factor Correction and Harmonic Mitigation. *IEEE Industry Applications Conference, 5*, 3127-3134.

Babu, S. G., Choudhury, U., & Ramdas, G. T. (2010). A Novel Approach in the Design of Optimal Tuning Frquency of a Single Tuned Harmonic Filter for an Alternatator with Rectifier. *Journal of Theoretical and Applied Information Technology, 11* (1), 65-72.

Bachry, A. (2004). *Power Quality Studies in Distribution Systems involving Spectral Decomposition* . PhD Thesis, Otto-von-Guericke-University, Faculty of Electrical Engineering and Information Technology, Magdeburg, Germany.

Balci, M. E., & Sakar, S. (2014). Optimal Design of Single-Tuned Passive Filters to MInimize Harmonic Loss Factor. *Middle-East Journal of Scientific Research, 21* (11), 2149-2155.

Bandgar, C. S., & Patil, S. B. (2013). Mitigation of Harmonics Using Shunt Active Filter. *Journal of Electronics and Communication Engineering* , 44-54.

Bangia, S., Sharma, P., & Garg, M. (2013). Simulation of Fuzzy Logic Based Shunt Hybrid Active Filter for Power Quality Improvement. *International Journal of Intelligent Systems and Application, 5* (2), 96-104.

Belgin, T., & Kaypmaz, T. C. (1999). Harmonic Measurements and Power Factor Correction in a Cement Factory. *ELECO'99 International Conference on Electrical and Electronics Engineering*, (pp. 199-202). Istanbul.

Benoudjafer, C., Benachaiba, C., & Saidi, A. (2014). Hybrid shunt active filter: Impact of the network's impedance on the filtering characteristic. *WSEAS TRANSACTIONS on POWER SYSTEMS, 9*, 171-177.

Bică, D., Moldovan, C., & Muji, M. (2008). Power Engineering Education using NEPLAN software. *43rd International Universities Power Engineering Conference, 2008* (pp. 1-3). Padova: IEEE.

Bollen, M. (2000). *Understanding Power Quality Problems.* New York, New York, USA: IEEE Press.

Brown, R. (2001). *Lecture notes: Harmonic analysis.* University of Kentucky, Lexington, Department of Mathematics.

Bukka, S., Hakim, M. M., Ankaliki, S., & Sanjeev, T. (2014). Performance Analysis of Three Phase Shunt Hybrid Active Power Filter. *International Journal of Research in Engineering and Technology, 03* (03), 256-263.

Chou, C., Liu, J., & Lee, K. (2000). Optimal Planning of Large Passive-harmonic filters set at High Voltage Level. *Power Electronics, IEEE Transactions on,, 15* (1), 433-441.

Costa-Castello, R., & Cardoner, E. F. (2007). *High Performance Control of a Single-Phase Shunt Active Filter*. Barcelona.

Dalila, M. S., Nasarudin, A., & Zin, A. A. (2003). Power Supply Quality Improvement: Harmonic Measurement and Simulation. *National Power and Energy Conference (PECon)*, (pp. 352-358). Bangi.

Dan, A., & Czira, Z. (1998). Identification of Harmonic Sources. *8th International Conference on Harmonics and Quality of Power.2*, pp. 831-836. Budapest, Hungary: ICHQP-98-311.

Das, J. (2004). Passive Filter Potentialities and Limitations. *IEEE Transactions on Industry Applications, 40* (1).

Das, J. (2003). Passive Filters-Potentials and Limitations. *Pulp and Paper Industrial Technical Conference, 2003* (pp. 187-197). IEEE.

Deckmann, S., Pomilio, J., Mertens, E., Dias, L., Aoki, A., Teixeira, M., et al. (2005). Capacitive Compensation in Distribution Grid with Non-Linear Voltage Type Loads. *8th Brazilian Power Electronics Conference - COPEB*, (pp. 399-403).

Diwan, S., Inamdar, H., & Vaidya, A. (2011). Simulation Studies of Shunt Passive Harmonic Filters: Six Pulse Rectifier Load Power Factor Improvement and Harmonic Control. *International Journal on Electrical and Power Engineering, 02* (01), 1-6.

Diwan, S., Indamar, H., & Vaidaya, A. (2010). Simulation Studies of Shunt Passive Harmonic Filters: Six Pulse Rectifier Load – Power Factor Improvement and Harmonic Control. *Procedings of International Conference on Advances in Electrical & Electronics* , 205-211.

Dugan, E., McGranagham, M., Santoso, S., & Beaty, H. (2002). *Electrical Power Systems Quality.* McGraw-Hill.

Dwane, R. (2003). *Harmonic Management in MV Distribution Systems.* PhD Thesis, University of Wollongong, School of Electrical and Computer Teleommunication Engineering, Wollongong.

Eid, A., Abdel-Salam, M., El-Kishky, H., & El-Mohandes, T. (2009). Active Power Filters for Harmonic Cancellation in Conventional and Advanced Aircraft Electric Power Systems. *Electric Power System Research, 79* (1), 80-88.

Ekrem, G. (2007). *Independent Component Analysis for Harmonic Source Identification in Electric Power Systems.* PhD Thesis, Drexel University, Electrical Engineering Department, Philadelphia.

Fauri, M., & Ribeiro, P. (1996). A novel approach to nonlinear load modeling. *Proceedings of the 6th International Conference on Harmonics in Power Systems.* Bologna, Italy.

Ferrero, A., Peretto, L., & Sasdelli, R. (1998). Revenue Metering in the Presence of Distortion and Unbalance: Myths and Reality. *Proceedings of the International Conference on Harmonics and Quality of Power (ICHQP98), 1*, 42-47.

Ganguli, A., Sharma, A. K., & Raajdeep, G. (2014). Harmonic Analysis in the Power System to Reduce Transmission Losses and Save Energy. *International Journal of Engineering Research and Applications, 4* (3), 167-171.

George, S., & Agarwal, V. (2003). A Novel Technique for Optimizing Harmonics and Reactive Power with Load Balancing Under Non-sinusoidal Supply and

UNbalanced Load Conditions. *IEEE Power Electronics Specialist Conference (PESC03), 4*, pp. 1537-1541. Acapulco.

Ghallab, M. (2011). Damping Techniques of Harmonic Resonances in Power Distribution Systems. *21st International Conference on Electricity Distribution* (pp. 6-9). Frankfurth: CIRED.

Golkar, M. (2004). Electric Power Quality:Types and Measurement. *IEEE International Conference on Electric Utility Deregulation, Restructuring & Power Technologies* .

Gonzalo, S., & John, H. (2005). *A Review of Harmonic Mitigation Techniques.*

Gougler, C., & Johnson, J. (1999). Parallel Active Harmonic Filters: Economical Viable Technology. *In Power Engineering Society 1999 Winter Meeting, 2*, 1142-1146.

Gour, D., Dohare, D., & Saxena, A. (2015). A Study of Various Filters for Power Quality Improvement. *International Journal of Advanced Research in Electrical, Electronics and Instrumentation Engineering, 4* (1), 138-143.

Grady, W., Mansoor, A., Fuchs, E., Verde, P., & Doyle, M. (2002). Estimating the Net Harmonic Currents Produced by Selected Distributed Single-Phase Loads: Computers, Televisions ans Incandescent Lamp Dimmers. *Proceedings of IEEE Power Engineering Society Winter Meeting.2*, pp. 1090-1094. IEEE.

Gursey, E. (2007). *Independent Component Analysis for Harmonic Source Identification in Electric Power Systems.* Drexel University, Faculty of Engineering, Philadelphia.

Gyugyi, L., & Strycula, E. (1976). Active Power Filters. *Proceedings of the IEEE Industry Application Society Annual Meeting* , 529-535.

Halpin, S. (2003). Overview of Revisions to IEEE Standard 519-1992. *Proceedings of the IEEE International Symposium on Quality and Security of Electric Power Delivery Systems CIGRE/PES* , 65-68.

Hasan, K., & Romlie, M. (2007). Comparative Study on Combined Series Active Shunt Passive Power Filter using Two Different Control Methods. *International Conference on Intelligence and Advance Systems ICAS,* (pp. 928-933).

Hernandez, J., Castro, M., Carpio, J., & Colmenar, A. (2009). Harmonics in Power Systems. *International Conference on Renewable Energy and Power Quality.* Valencia, Spain: EA4EPQ.

Hoevenarrs, T., & LeDoux, K. a. (2003, September 15-17). Interpreting IEEE STD 519 and Meeting its Harmonic Limits in VFD applications. *Proceedings of the IEEE Industry Applications Society 50th Annual Petroleum and Chemical Industry Conference* , 145-150.

Hota, B., & Mallick, A. (2011). *Load Flow studies in Power Systems.* BSc Thesis, National Institute of Technology, Department of Electrical Engineering, Rourkela, India.

Hsiao, Y.-T. (2001). Design of Filters for Reducing Harmonic Distortion and Correcting Power Factor in Industrial Distribution Systems. *Tamkang Journal of Science and Engineering, 4* (3), 193-199.

IEEE Standard 1159-1995. (1995). IEEE Recommended Practice for Monitoring Electric Power Quality.

IEEE Standard 519-1992. (1993). IEEE Recommended Practices and Requirements for Harmonic Control in Electric power Systems.

Isa, M. S. (2007). *Power Flow Analysis Software Using MATLAB.* PhD Thesis, University Malaysia Pahang, Department of Electrical Engineering.

J - VTU e-Learning Centre. (n.d.). Retrieved March 24, 2014, from elearning.vtu.ac.in/p9/notes/EE%2072/Unit3-MSR.pdf

Jansen, M. (2011). Harmonic Filter Design for IEC 61000 Compliance. *DigSILENT User Conference*, (pp. 1-8). Melbourne, Australia.

Jayakrishna, G., & Vamsipriya, B. (2013). Seven Level Inverter Based Shunt Hybrid Active Power Filter Topology for Harmonic Reduction. *Internationsl Journal of Advanced Research in Eletrica, Electronics and Instrumentation Engineering, 2* (10), 4939-4947.

Jonas, F. (1996). Telecommunication Disturbances from the Baltic Cable. *IEEE Transaction on industry Applications, 26* (6), 1034-1042.

Jong-Gyeum, K., Young-Jeen, P., & Dong-ju, L. (2011). Harmonic Analysis of Reactor and Capacitor in Single-tuned Harmonic Filter Application. *Journal of Electrical Engineering & Technology, 6* (2), 239-244.

Kampen, D., Paspour, N., Probst, U., & Thiel, U. (2008). Comparative Analysis of Passive Harmonic Mitigation Techniques for Six Pulse Rectifiers. *11th International Conference on Optimization of Electrical and Electronic Equipment* (pp. 219-225). IEEE.

Key, T., & Lai, J.-S. (1996). Effect of supply voltage harmonics on the input current of single-phase. *IEEE Transactions on Power Delivery, 10* (3), 1017-1025.

Khan, S. M., Raheel, M. I., Ali, B. M., Asad, U., Ahmed, U., Farid, M., et al. (2011). Implementation of a Passive Tune Filter to Reduce Harmonics in Single Phase Induction Motor with Varying Load. *Interntional Journal of Engineering and Technology, 11* (03), 204-208.

Khanchi, S., & Garg, V. (2013). Power Factor Improvement of Induction Motor by Using Capacitors. *International Journal of Engineering Trends and Technology (IJETT), 4* (7), 2967-2971.

Kim, H., Samann, N., Shin, D., Ko, B., Jang, G., & Cha, J. (2007). A New Concept of Power Flow Analysis. *Journal of Electrical Engineering & Technology, 2* (3), 312-319.

Kiran, N. C., Dash, S. S., & Latha, P. S. (2011). A few Aspects of Power Quality Improvement Using Active Power Filter. *International Journal of Scientific & Engineering Research , 2* (5), 1-11.

Kumar, A., & Singh, J. (2013). Harmonic Mitigation and Power Quality Improvement Using Shunt Active Power Filter. *International Journal of Electrical, Electronics and Mechanical , 2* (2).

Kumar, B. (2011). *Design of Harmonic Filters for Renewable Energy Applications.* MSc Thesis, Gotland University, Department of Wind Energy, Visby, Sweden.

Kumar, G., Lokya, M., & Muni, V. (2012). Estimation and Minimization of Harmonics in IEEE 13 Bus Distribution System. *International Journal of Engineering Research & Technology (IJERT), 1* (7), 1-6.

Kumkratug, P. (2010). Fast Decoupled Power Flow for Power System with High Voltage Direct Current Transmission Line System. *American Journal of Applied Science, 7* (7), 1115-1117.

Li, C., & Xu, W. (2002). On Defining Harmonic Contributions at the Point of Common Coupling. *IEEE Power Engineering Review, ,* 44-45.

Ludbrook, A. (2001). IEEE 519-Harmonic Current Goals and Diversity - A Proposal. *Proceedings of the International Conference on Harmonics and Quality of Power (ICHQP98) ,* 797-800.

Mahmoud, F. A. (2011). *An 'Active' Passive-Filter Topology for Low Power DC/AC Inverters.* PhD Thesis, Brunel University, School of Engineering Design, London.

Mansoor, A., Grady, W., Staats, P., Thallam, R., Doyle, M., & Samotyi, M. (1995). Predicting the net Harmonic currents produced by Large Numbers of Distributed single-phase computer loads. *IEEE Transactions on Power Delivery, 10* (4), pp. 2001-2006.

Mansoor, A., Grady, W., Thallam, R., Doyle, M., Krein, S., & M.J. (1995). Effect of supply voltage harmonics on the input current of single-phase. *IEEE Transactions on Power Delivery, Vol. 10* (3), 1416 - 1422.

Maswood, A. I., & Haque, M. (2002). Harmonics, Sources, Effects and Mitigation Techniques. *Second International Conference on Electrical and Computer Engineering ICECE* , 26-28.

Mazumdar, J. (2006). *System and Method for Determining Harmonic Contributions from Non-linear Loads in Power Systems.* PhD Thesis, Georgia Institute of Technology, Electrical and Computer Engineering, Atlanta.

Mc Granaghan, M. (2002). Economical Evaluation of Power Quality. *IEEE Power Engineering Review, 22* (2), 8-12.

McEachern, A., Grady, W., Moncrief, G., & McGranaghan, M. (1995). Revenue and Harmonics: An Evaluation of some Proposed Rate Structures. *IEEE Transactions on Power Delivery, 101* (1), 474-482.

Mishra, K. K., & Gupta, R. (2011). Load Compensation for Single Phase System Using Series Active Filter. *International Journal of Engineering Science an Technology, 3* (3), 83-93.

Mohammad, M., & Samimi, A. (2014). The Performance of GA-Based Optimized Passive Harmonic Filter for Harmonic Compensation Under CPF and DPF Modes. *Indian Journal of Fundamental and Life Sciences, 4* (4), 1710-1724.

Mohan, N., & Peterson, H. L. (1977). Active Filter for AC Harmonic Suppression. *IEEE PES Winter Power Meeting* .

Murthy, P. (2007). *Power System Analysis.* Hyderabad, India: B.S. Publications.

Olivio C.N. Souto, Jose carlos Oliveira, Aloisio de Oliveira and Paulo F.Ribeiro, (1996) "A Reflection on the subject of converters Internal Harmonic impedance", in proceedings of the7th international conference on harmonic and quality of power,1996,pp.770 -774, ICHQP -96 -U5

Owen, E. (1998). A history of harmonics in power systems. *IEEE Industry Applications Magazines, 4* (1), pp. 6-12.

Pacis, M. C., Martinez Jr., J. M., & Tecson, J. V. (2010). Modelling and Simulation of Active Power Filters for Harmonic Compensation, VOltage Sags and Swells Mitigation Power Factor Correction. *Proceedings of the World Congress on Engineering and Computer Science.II.* San Francisco, USA: WCECS.

Parthasarathy, S., & Jeyasri, E. (2014). Harmonic Distortion Evaluation and Reduction in radial Distribution System. *International Journal of Innovative Research inScience, Engineering and Technology, 3* (3), 113-117.

Pradhan, A., & Thatoi, P. (2012). *Study on the performance of Newton-Rapson Load Flow in Distribution Systems* . Project Thesis, National Institute of Technology, Rourkela, Department of Electrical Engineering, India.

Prechanon, K. (2010). Fast Decoupled Power Flow for Power System with High Voltage Direct Current Transmission Line. *American Journal of Applied Sciences, 7* (8), 1115-1117.

Rafiei, S., & Ghazi, R. a. (2002). IEEE-519-Based Real-time and Optimal Control of Active Filters Under Nonsinusoidal Line Voltages Using Neutral Networks. *IEEE Transactions on Power Delivery, 17* (3), 815-821.

Raneru, N. R. (2013). Harmonic Analysis of small Industrial Loads and Harmonic Mitigation Techniques in Industrial Distribution Systems. *International Journal of Engineering Research and Applications, 3* (4), 1511-1540.

Rashid, M. (2001). *Power Electronics Handbook.* Academic Press.

Reena, M. (2014). Design and development of shunt hybrid power filter for harmonic mitigation. *International Journal of Engineering and Computer Science, 3* (10), 8597-8601.

Rice, D. (1994). A detailed analysis of six-pulse converter harmonic currents. *IEEE Transactions on Industry Applications, 30*, 294-304.

Rivas, D., Moran, L., Juan, D., & Espinoza, J. (2003). Improving Passive Filter Compensation Performance with Active Techniques. *Industrial Electronics, IEEE Transactions on , 50* (1), 161-170.

Roger, C. D., McGranaghan, F., & Wayne, B. H. (1996). *Electric Power Systems Quality.* Reference Book on Power Quality, McGraw-Hill.

Sadeghi, S., Kouhsari, S., & Minassians, A. D. (2000). The Effects of Transformers Phase-shifts on Harmonic Penetration Calculation in a Steel Mill Plant. *9th International Conference , 3*, pp. 868-873.

Sakshi, B., P.R., S., & Garg, M. (2013). Comparison Analysis of Shunt Active Filter and transformerless Parallel Hybrid Active Filter. *CS & IT-CSCP* (pp. 373-382). Computer Science & Information Technology.

Sandesh, J., Singh, S., & Phulambrikar, S. (2012). Improve Power Factor and Reduce the Harmonics Distortion of the System. *Research Journal of Engineering Sciences, 1* (5), 31-36.

Sandoval, G., & Houdek, J. (2005). *A Review of Harmonic Mitigation Techniques.*

Sanjay, A. D., & Laxman, M. W. (2011). Analysis of Distribution Transformer Performance Under Non-linear Balanced Load Conditions and Its Remedial Measures. *International Journal of Emerging Technology and Advanced Engineering, 1* (2), 2250-2459.

Sanjeev, K. O., Nadir, A. K., Chauhan, M., & Kumar, A. (2014). Identification and Minimization of Harmonics in Power System Networks. *International Journal of Emerging Technology and Advanced Engineering, 4* (1), 58-68.

Sankowa, C. (2001). *Power Quality* (Ist Edition ed.). Florida, USA: CRC Press.

Sasaki, H., & Machida, T. (1971). A New Method to Eliminate AC Harmonic Currents by Magnetic Flux Compensation - Consideration on Basic Design. *IEEE Transactions on Power Apparatus and Systems* , 380-385.

Sergio, F. (2003). *Design with Operational Amplifiers and Analog Integrated Circuits* (3rd ed.). McGraw Hill.

Shah, N. (2014, 5 20). *Control Engineering.* Retrieved 3 30, 2015, from Reducing harmonics with IEEE 519 practices, procedures: http://www.controleng.com/single-article/reducing-harmonics-with-ieee-519-practices-procedures

Sharma, V., & Thomson, A. (1993, May). Power System Harmomnic Guidelines and How to Evaluate the Impact of Customer Generated Harmonics. *Proceedings of the IEEE Communications, Computers and Power in Modern Environment (WESCANEX)* , 797-800.

Sher, A. H., Addoweesh, E. K., & Khan, Y. (2013). *Harmonics Generation, Propagation and Purging Techniques in Non-Linear Loads.* King Saud University, Electrical Engineering. Riyadh: INTECH.

Shukla, V., & Bhadoria, A. (2013). Understanding Load FLow Studies by Using PSAT. *International Journal for enhanced Research in Science Technology & Engineering, 2* (6), 50-57.

Siemens. (2013). *Harmonics in Power Systems - Causes, Effects and Control.* Georgia, Norcross, United States of America: Siemens Industry, Inc.

Singh, B., Al-Haddad, K., & Chandra, A. (1999). A Review of Active Filters for Power Quality Improvement. *IEEE Transactions on Industrial Electronics, 46* (6), 960-971.

Singla, D., Sharma, P. R., & Hooda, N. (2011). Power Quality Improvement Using Multilevel Inverters – A Review. *INTERNATIONAL JOURNAL OF ENGINEERING SCIENCES & MANAGEMENT, 1* (1), 64-76.

Siriadi, S. (2006). *Analysis of Harmonics Current Minimization on Power Distribution System Using Voltage Phase Shifting Concept.* PhD Thesis, Universiti Sains Malaysia, Department of Electrical and Electronic Engineering.

Srinivasan, K. (1996). On Separating Customer and Supply Side Harmonics. *IEEE Transactions on Power Delivery, 11* (2), 1003-1012.

Sriranjani, R., & Jayalalitha, S. (2012). Comparison of Passive and Active Hybrid filter in Front-end System. *International Journal of Communication Engineering Applications, 03* (03), 503-506.

Sriranjani, R., & Jayalalitha, S. (2012). Investigation of the Performance of the Various Types of Harmonic Filters. *World Applied Sciences Journal, 17* (5), 643-650.

Sriranjani, R., Geetha, M., & Jayalalitha, S. (2013). Harmonics and Power Compensation using sunt hybrid filter. *Research Journal of Applied Sciences, Engineering and Technology, 5* (1), 123-128.

Srivastava, K. K., Shakil, S., & Pandey, A. V. (2013). Harmonics and Its Mitigation Technique by Passive Shunt Filter. *International Journal of Soft Computing and Engineering, 2* (2), 325-331.

Subhash, M., & Patil, S. (2012). Improvement of Power Quality by using Active Filter based on Vectorial Power Theory Control Strategy on the MATLAB-Simulink Platform. *Journal of Electronics and Communication Engineering, 4* (48), 37-40.

Syai'in, M., & Soeprijanto, A. (2012). Improved Algorithm of Newton-Raphson Power Flow using GCC limit based on Neural Network. *Interbnational Journal of Electrical & Computer Sciences IJECS-IJENS, 12* (01), 7-12.

Thakker, H. K., Soori, P. K., & Chacko, S. (2014). Harmonics in Industrial Power Networks of Aluminium Smelters - A Comprehensive Mitigation Approach. *International Journal of Smart Grid and Clean Energy, 4* (1), 77-84.

Thunberg, E., & Soder, L. (1998). A Norton Model of Real Distribution Network. *8th INternational Conference on Harmonics and Quality of Power.1*, pp. 279-284. ICHQP-98-183.

Uzunoglu, M. (2005). Harmonics and Voltage Stability Analysis in Power Systems Including Thyristor Controlled Reactor. *Sadhana Academy Proceedings in Engineering Sciences, 30* (1), 57-67.

Winter, T. (2011). *Reliability and economic analysis of offshore wind power systems - A comparison of internal grid topologies.* MSc Thesis, CHALMERS UNIVERSITY OF TECHNOLOGY, Department of Energy and Environment, Gothenburg, Sweden.

Xu, W. (2004). Status and Future Directions of Power System Harmonic Analysis. *Proceedings of the IEEE PES General Meeting, 1*, 756-761.

Xu, W., & Liu, Y. (2000). A Method for Determining Customer and Utility Harmonic Contributions at the PCC. *IEEE Transactions on Power Delivery, 15* (2), 804-811.

APPENDIX A

IEEE 519 HARMONIC STANDARDS

The requirements of current distortion and voltage distortion of IEEE 519 harmonic standard are given in Table A.1 for reference.

Table A.1: Recommended Practice for Individual Customers for Voltages < 69kV

Utility Voltage Limits < 69kV						
Individual Harmonic 3%					Voltage THD 5%	
Customer Current Limits						
Isc/I_L	h <11	11≤h<17	17≤h<23	23≤h<35	35≤h	TDD
<20	4.0%	2.0%	1.5%	0.6%	0.3%	5.0%
20 - 50	7.0%	3.5%	2.5%	1.0%	0.5%	8.0%
50 - 100	10.0%	4.5%	4.0%	1.5%	0.7%	12%
100 - 1000	12.0%	5.5%	5.5%	2.0%	1.0%	15%
>1000	15.0%	7.0%	6.0%	2.5%	1.4%	20%

Table A.2: Recommended Practice for Individual Customers for Voltages 69-161kV

Utility Voltage Limits 69-161kV						
Individual Harmonic 1.5%				Voltage THD 2.5%		
Customer Current Limits						
Isc/I_L	h <11	11≤h<17	17≤h<23	23≤h<35	35≤h	TDD
<20	2.0%	1.0%	0.75%	0.3%		2.5%
20 - 50	3.5%	1.75%	1.25%	0.5%	0.25%	4.0%
50 - 100	5.0%	2.25%	2.0%	0.75%	0.35%	6.0%
100 - 1000	6.0%	2.75%	2.5%	1.0%	0.5%	7.5%
>1000	7.5%	3.5%	3.0%	1.25%	0.7%	10.0%

Table A.3: Recommended Practice for Individual Customers for Voltages >161kV

Utility Voltage Limits >161kV						
Individual Harmonic					Voltage THD	
					5%	
Customer Current Limits						
Isc/I_L	h <11	11≤h<17	17≤h<23	23≤h<35	35≤h	TDD
<50	2.0%	1.0%	1.0%	0.3%	0.15%	2.5%
≥50	3.0%	3.0%	1.5%	0.45%	0.22%	3.75%

APPENDIX B

The distribution line steady state parameters, in magnitude and phase values, are displayed in the state-space model block.

Steady State Values for cases of 02:00Hrs of 17th January 2014

Steady State Parameters of ALG – ALG/L D/L:

1564.51 A	-88.14^o	----→	I_1 _ Z_i
13037.14 V	1.86^o	----→	V_c_ Z_i
0.00 A	0.00^o	----→	I_1 _ Z_o
0.00 V	0.00^o	----→	V_c _ Z_o
1085.40 A	95.69^o	----→	I_1_ Shunt Reactor 110MVar
19830.93 V	5.02^o	----→	V_c _ input: Distribution line
1084.35 A	-84.31^o	----→	I_1 _ section_1: Distribution line
19387.52 V	5.06^o	----→	V_c_section_2: Distribution line
1084.47 A	-84.31^o	----→	I_1 _section_2: Distribution line
18944.08 V	5.10^o	----→	V_c_section_3: Distribution line
1084.59 A	-84.31^o	----→	I_1 _ section_3: Distribution line
18500.60 V	5.14^o	----→	V_c_section_4: Distribution line
1084.70 A	-84.31^o	----→	I_1 _ section_4: Distribution line
18057.52 V	5.18^o	----→	V_c_section_5: Distribution line
1084.82 A	-84.31^o	----→	I_1 _ section_5: Distribution line
17613.52 V	5.23^o	----→	V_c_section_6: Distribution line
1084.93 A	-84.31^o	----→	I_1 _ section_6: Distribution line
17169.93 V	5.28^o	----→	V_c_section_7: Distribution line
1085.04 A	-84.31^o	----→	I_1 _ section_7: Distribution line
16726.31 V	5.33^o	----→	V_c_section_8: Distribution line
1085.14 A	-84.31^o	----→	I_1 _ section_8: Distribution line
16282.65 V	5.38^o	----→	V_c_section_9: Distribution line
1085.25 A	-84.31^o	----→	I_1 _ section_9: Distribution line

15838.97 V	5.43^o	- - - →	V_c_section_10: Distribution line
1085.35 A	-84.31^o	- - - →	I_1 _ section_10: Distribution line
15395.27 V	5.49^o	- - - →	V_c_output: Distribution line

SOURCES:

33000.00 V	0.00^o	- - - →	Alagbon
0.00 A	0.00^o	- - - →	Alagbon Local

Steady State Parameters of ALG – FOW D/L:

250.77 A	-91.68^o	- - - →	I_1 _ Z_i
2089.70 V	-1.68^o	- - - →	V_c_ Z_i
0.00 A	0.00^o	- - - →	I_1 _ Z_o
0.00 V	0.00^o	- - - →	V_c _ Z_o
203.27 A	91.99^o	- - - →	I_1_ Shunt Reactor 110MVar
30900.89 V	0.76^o	- - - →	V_c _ input: Distribution line
175.75 A	-87.87^o	- - - →	I_1 _ section_1: Distribution line
29463.40 V	0.80^o	- - - →	V_c_section_2: Distribution line
179.47 A	-87.94^o	- - - →	I_1 _section_2: Distribution line
27995.50 V	0.86^o	- - - →	V_c_section_3: Distribution line
183.01 A	-87.92^o	- - - →	I_1 _ section_3: Distribution line
26498.70 V	0.92^o	- - - →	V_c_section_4: Distribution line
186.36 A	-87.94^o	- - - →	I_1 _ section_4: Distribution line
24974.55 V	0.99^o	- - - →	V_c_section_5: Distribution line
189.52 A	-87.96^o	- - - →	I_1 _ section_5: Distribution line
23424.66 V	1.07^o	- - - →	V_c_section_6: Distribution line
192.48 A	-87.98^o	- - - →	I_1 _ section_6: Distribution line
21850.62 V	1.17^o	- - - →	V_c_section_7: Distribution line
195.24 A	-87.99^o	- - - →	I_1 _ section_7: Distribution line
20254.08 V	1.29^o	- - - →	V_c_section_8: Distribution line
197.80 A	-88.00^o	- - - →	I_1 _ section_8: Distribution line
18636.71 V	1.43^o	- - - →	V_c_section_9: Distribution line

200.15 A	-88.00^o	- - - →	I_1 _ section_9: Distribution line
17000.23 V	1.43^o	- - - →	V_c_section_10: Distribution line
202.30 A	-88.01^o	- - - →	I_1 _ section_10: Distribution line
15346.36 V	1.80^o	- - - →	V_c_output: Distribution line

SOURCES:

33000.00 V	0.00^o	- - - →	Alagbon
0.00 A	0.00^o	- - - →	Fowler

Steady State Values for cases of 09:00Hrs of 17th January 2014

Steady State Parameters of ALG – ADM D/L:

94.37 A	-92.43	- - - →	I_1 _ Z_i
786.42 V	-2.43^o	- - - →	V_c_ Z_i
10.11 A	-93.24^o	- - - →	I_1 _ Z_o
84.23 V	-3.24^o	- - - →	V_c _ Z_o
122.16 A	91.53^o	- - - →	I_1_ Shunt Reactor 110MVar
32209.41V	0.29^o	- - - →	V_c _ input: Distribution line
69.64 A	-87.80^o	- - - →	I_1 _ section_1: Distribution line
31045.99 V	0.31^o	- - - →	V_c_section_2: Distribution line
77.66 A	-88.00^o	- - - →	I_1 _section_2: Distribution line
29748.69 V	0.33^o	- - - →	V_c_section_3: Distribution line
85.34 A	-88.15^o	- - - →	I_1 _ section_3: Distribution line
28323.12 V	0.37^o	- - - →	V_c_section_4: Distribution line
92.66 A	-88.26^o	- - - →	I_1 _ section_4: Distribution line
26775.43 V	0.43^o	- - - →	V_c_section_5: Distribution line
99.57 A	-88.35^o	- - - →	I_1 _ section_5: Distribution line
25112.31 V	0.59^o	- - - →	V_c_section_6: Distribution line
106.06 A	-88.42^o	- - - →	I_1 _ section_6: Distribution line
23340.94 V	0.72^o	- - - →	V_c_section_7: Distribution line
112.09 A	-88.48^o	- - - →	I_1 _ section_7: Distribution line

21469.01 V	0.72^o	- - - →	V_c_section_8: Distribution line
117.63 A	-88.52^o	- - - →	I_1 _ section_8: Distribution line
19504.61 V	0.87^o	- - - →	V_c_section_9: Distribution line
122.67 A	-88.54^o	- - - →	I_1 _ section_9: Distribution line
17456.30 V	1.07^o	- - - →	V_c_section_10: Distribution line
127.18 A	-88.55^o	- - - →	I_1 _ section_10: Distribution line
15332.99 V	1.34^o	- - - →	V_c_output: Distribution line

SOURCES:

33000.00 V	0.00^o	- - - →	Alagbon
7.00 A	89.90^o	- - - →	Fowler

Steady State Parameters of ALG – ALG/L D/L:

1564.51 A	-88.14^o	- - - →	I_1 _ Z_i
1307.14 V	1.86^o	- - - →	V_c_ Z_i
0.00 A	0.00^o	- - - →	I_1 _ Z_o
0.00 V	0.00^o	- - - →	V_c _ Z_o
1085.4 A	95.69^o	- - - →	I_1_ Shunt Reactor 110MVar
19830.93 V	5.02^o	- - - →	V_c _ input: Distribution line
1084.35 A	-84.31^o	- - - →	I_1 _ section_1: Distribution line
19387.52 V	5.06^o	- - - →	V_c_section_2: Distribution line
1084.47 A	-84.31^o	- - - →	I_1 _section_2: Distribution line
18944.08 V	5.10^o	- - - →	V_c_section_3: Distribution line
1084.59 A	-84.31^o	- - - →	I_1 _ section_3: Distribution line
18500.60 V	5.14^o	- - - →	V_c_section_4: Distribution line
1084.70 A	-84.31^o	- - - →	I_1 _ section_4: Distribution line
18057.08 V	5.18^o	- - - →	V_c_section_5: Distribution line
1084.82 A	-84.31^o	- - - →	I_1 _ section_5: Distribution line
17169.93 V	5.28^o	- - - →	V_c_section_6: Distribution line
1085.04 A	-84.31^o	- - - →	I_1 _ section_6: Distribution line

16726.31 V	5.33^{o}	- - - →	V_c_section_7: Distribution line
1085.14 A	-84.31^{o}	- - - →	I_1 _ section_7: Distribution line
16726.31 V	5.33^{o}	- - - →	V_c_section_8: Distribution line
1085.14 A	-84.31^{o}	- - - →	I_1 _ section_8: Distribution line
16282.65 V	5.38^{o}	- - - →	V_c_section_9: Distribution line
1085.25 A	-84.31^{o}	- - - →	I_1 _ section_9: Distribution line
15838.97 V	5.43^{o}	- - - →	V_c_section_10: Distribution line
1085.35 A	-88.31^{o}	- - - →	I_1 _ section_10: Distribution line
15395.27 V	5.49^{o}	- - - →	V_c_output: Distribution line

SOURCES:

33000.00 V	0.00^{o}	- - - →	Alagbon
0.00 A	0.00^{o}	- - - →	Alagbon Local

Steady State Parameters of ALG – ANI D/L:

74.68 A	-91.13^{o}	- - - →	I_1 _ Z_i
622.34 V	-1.13^{o}	- - - →	V_c_ Z_i
0.00 A	0.00^{o}	- - - →	I_1 _ Z_o
0.00 V	0.00^{o}	- - - →	V_c _ Z_o
123.59 A	91.37^{o}	- - - →	I_1_ Shunt Reactor 110MVar
32373.11 V	0.20^{o}	- - - →	V_c _ input: Distribution line
56.42 A	-87.50^{o}	- - - →	I_1 _ section_1: Distribution line
31321.54 V	0.21^{o}	- - - →	V_c_section_2: Distribution line
65.45 A	-87.82^{o}	- - - →	I_1 _section_2: Distribution line
30101.83 V	0.22^{o}	- - - →	V_c_section_3: Distribution line
74.12 A	-88.05^{o}	- - - →	I_1 _ section_3: Distribution line
28720.51 V	0.25^{o}	- - - →	V_c_section_4: Distribution line
82.40 A	-88.22^{o}	- - - →	I_1 _ section_4: Distribution line
27185.01 V	0.29^{o}	- - - →	V_c_section_5: Distribution line
90.23 A	-88.35^{o}	- - - →	I_1 _ section_5: Distribution line
25503.58 V	0.35^{o}	- - - →	V_c_section_6: Distribution line

97.58 A	-88.45^o	----→	I_1 _ section_6: Distribution line
23685.28 V	0.44^o	----→	V_c_section_7: Distribution line
104.41 A	-88.52^o	----→	I_1 _ section_7: Distribution line
21739.90 V	0.55^o	----→	V_c_section_8: Distribution line
110.67 A	-88.57^o	----→	I_1 _ section_8: Distribution line
19677.91 V	0.70^o	----→	V_c_section_9: Distribution line
116.35 A	-88.61^o	----→	I_1 _ section_9: Distribution line
17510.46 V	0.90^o	----→	V_c_section_10: Distribution line
121.39 A	-88.63^o	----→	I_1 _ section_10: Distribution line
15249.29 V	1.18^o	----→	V_c_output: Distribution line

SOURCES:

33000.00 V	0.00^o	----→	Alagbon
0.00 A	0.00^o	----→	Anifowoshe

Steady State Parameters of ALG – FOW D/L:

250.86 A	-91.68^o	----→	I_1 _ Z_i
2090.45 V	-1.68^o	----→	V_c_ Z_i
0.00 A	0.00^o	----→	I_1 _ Z_o
0.00 V	0.00^o	----→	V_c _ Z_o
203.33 A	91.99^o	----→	I_1_ Shunt Reactor 110MVar
30900.14 V	0.76^o	----→	V_c _ input: Distribution line
175.81 A	-87.87^o	----→	I_1 _ section_1: Distribution line
29496.42 V	0.80^o	----→	V_c_section_2: Distribution line
179.54 A	-87.90^o	----→	I_1 _section_2: Distribution line
27993.73 V	0.86^o	----→	V_c_section_3: Distribution line
183.07 A	-87.92^o	----→	I_1 _ section_3: Distribution line
26496.42 V	0.92^o	----→	V_c_section_4: Distribution line
186.42 A	-87.94^o	----→	I_1 _ section_4: Distribution line
24971.78 V	0.99^o	----→	V_c_section_5: Distribution line

189.58 A	-87.96^o	----→	I_1 _ section_5: Distribution line
23421.38 V	1.07^o	----→	V_c_section_6: Distribution line
192.54 A	-87.98^o	----→	I_1 _ section_6: Distribution line
21846.84 V	1.17^o	----→	V_c_section_7: Distribution line
195.30 A	-87.99^o	----→	I_1 _ section_7: Distribution line
20249.81 V	1.29^o	----→	V_c_section_8: Distribution line
197.86 A	-88.00^o	----→	I_1 _ section_8: Distribution line
18631.95 V	1.43^o	----→	V_c_section_9: Distribution line
200.21 A	-88.00^o	----→	I_1 _ section_9: Distribution line
18631.95 V	1.43^o	----→	V_c_section_10: Distribution line
200.21 A	-88.01^o	----→	I_1 _ section_10: Distribution line
15340.64 V	1.80^o	----→	V_c_output: Distribution line

SOURCES:

33000.00 V	0.00^o	----→	Alagbon
0.00 A	0.00^o	----→	Fowler

Steady State Parameters of ADM – ANI D/L:

309.61 A	-91.56^o	----→	I_1 _ Z_i
2579.99 V	-1.56^o	----→	V_c_ Z_i
0.00 A	0.00^o	----→	I_1 _ Z_o
0.00 V	0.00^o	----→	V_c _ Z_o
237.63 A	92.17^o	----→	I_1_ Shunt Reactor 110MVar
30119.13 V	0.95^o	----→	V_c _ input: Distribution line
216.10 A	-87.74^o	----→	I_1 _ section_1: Distribution line
28705.08 V	1.00^o	----→	V_c_section_2: Distribution line
219.00 A	-87.76^o	----→	I_1 _section_2: Distribution line
27272.07 V	1.05^o	----→	V_c_section_3: Distribution line
221.76 A	-87.77^o	----→	I_1 _ section_3: Distribution line
25821.06 V	1.12^o	----→	V_c_section_4: Distribution line

224.37 A	-87.79^o	----→	I_1 _ section_4: Distribution line
24353.02 V	1.19^o	----→	V_c_section_5: Distribution line
226.83 A	-87.80^o	----→	I_1 _ section_5: Distribution line
22868.92 V	1.28^o	----→	V_c_section_6: Distribution line
229.14 A	-87.81^o	----→	I_1 _ section_6: Distribution line
21369.75 V	1.37^o	----→	V_c_section_7: Distribution line
231.30 A	-87.81^o	----→	I_1 _ section_7: Distribution line
19856.53 V	1.49^o	----→	V_c_section_8: Distribution line
233.31 A	-87.82^o	----→	I_1 _ section_8: Distribution line
18330.27 V	1.62^o	----→	V_c_section_9: Distribution line
235.16 A	-87.82^o	----→	I_1 _ section_9: Distribution line
16792.01 V	1.79^o	----→	V_c_section_10: Distribution line
236.86 A	-87.83^o	----→	I_1 _ section_10: Distribution line
15242.81 V	1.98^o	----→	V_c_output: Distribution line

SOURCES:

32711.00 V	0.00^o	----→	Alagbon
0.00 A	0.00^o	----→	Anifowoshe

Steady State Parameters of ALG – BAN/I D/L:

133.31 A	-92.66^o	----→	I_1 _ Z_i
1110.84 V	-2.66^o	----→	V_c_ Z_i
10.11 A	-93.24^o	----→	I_1 _ Z_o
84.23 V	-3.24^o	----→	V_c _ Z_o
136.52 A	91.69^o	----→	I_1_ Shunt Reactor 110MVar
31884.49 V	0.42^o	----→	V_c _ input: Distribution line
95.86 A	-87.97^o	----→	I_1 _ section_1: Distribution line
30578.10 V	0.46^o	----→	V_c_section_2: Distribution line
102.30 A	-88.07^o	----→	I_1 _section_2: Distribution line
29183.98 V	0.49^o	----→	V_c_section_3: Distribution line
108.44 A	-88.15^o	----→	I_1 _ section_3: Distribution line

27706.14 V	0.55^o	- - - →	V_c_section_4: Distribution line
114.28 A	-88.22^o	- - - →	I_1 _ section_4: Distribution line
26148.83 V	0.61^o	- - - →	V_c_section_5: Distribution line
119.79 A	-88.27^o	- - - →	I_1 _ section_5: Distribution line
24516.53 V	0.69^o	- - - →	V_c_section_6: Distribution line
124.95 A	-88.31^o	- - - →	I_1 _ section_6: Distribution line
22813.94 V	0.79^o	- - - →	V_c_section_7: Distribution line
129.76 A	-88.35^o	- - - →	I_1 _ section_7: Distribution line
21045.97 V	0.91^o	- - - →	V_c_section_8: Distribution line
134.19 A	-88.37^o	- - - →	I_1 _ section_8: Distribution line
19217.73 V	1.06^o	- - - →	V_c_section_9: Distribution line
138.24 A	-88.39^o	- - - →	I_1 _ section_9: Distribution line
17334.52 V	1.25^o	- - - →	V_c_section_10: Distribution line
141.89 A	-88.40^o	- - - →	I_1 _ section_10: Distribution line
15401.82V	1.50^o	- - - →	V_c_output: Distribution line

SOURCES:

33000.00 V	0.00^o	- - - →	Alagbon
7.00 A	89.90^o	- - - →	Banana Island

Steady State Values for cases of 21:00Hrs of 17th January 2014

Steady State Parameters of ALG – ADM D/L:

94.09 A	-92.43^o	- - - →	I_1 _ Z_i
784.02 V	-2.43^o	- - - →	V_c_ Z_i
10.11 A	-93.24^o	- - - →	I_1 _ Z_o
84.23 V	-3.24^o	- - - →	V_c _ Z_o
122.01 A	91.53^o	- - - →	I_1_ Shunt Reactor 110MVar
32211.82 V	0.29^o	- - - →	V_c _ input: Distribution line
69.44 A	-87.80^o	- - - →	I_1 _ section_1: Distribution line
31051.74 V	0.31^o	- - - →	V_c_section_2: Distribution line

77.46 A	-88.00^o	- - - →	I_1 _section_2: Distribution line
29757.76 V	0.33^o	- - - →	V_c_section_3: Distribution line
85.15 A	-88.15^o	- - - →	I_1 _ section_3: Distribution line
28335.47 V	0.37^o	- - - →	V_c_section_4: Distribution line
92.46 A	-88.27^o	- - - →	I_1 _ section_4: Distribution line
26791.00 V	0.43^o	- - - →	V_c_section_5: Distribution line
99.38 A	-88.36^o	- - - →	I_1 _ section_5: Distribution line
25131.03 V	0.50^o	- - - →	V_c_section_6: Distribution line
105.87 A	-88.43^o	- - - →	I_1 _ section_6: Distribution line
23362.74 V	0.59^o	- - - →	V_c_section_7: Distribution line
111.91 A	-88.48^o	- - - →	I_1 _ section_7: Distribution line
21493.78 V	0.71^o	- - - →	V_c_section_8: Distribution line
117.46 A	-88.52^o	- - - →	I_1 _ section_8: Distribution line
19532.26 V	0.87^o	- - - →	V_c_section_9: Distribution line
122.51 A	-88.54^o	- - - →	I_1 _ section_9: Distribution line
17486.69 V	1.07^o	- - - →	V_c_section_10: Distribution line
127.02 A	-88.56^o	- - - →	I_1 _ section_10: Distribution line
15366.01V	1.34^o	- - - →	V_c_output: Distribution line

SOURCES:

33000.00 V	0.00^o	- - - →	Alagbon
7.00 A	89.90^o	- - - →	Ademola

Steady State Parameters of ALG – ANI D/L:

74.54 A	-91.13^o	- - - →	I_1 _ Z_i
621.16 V	-1.13^o	- - - →	V_c_ Z_i
0.00 A	0.00^o	- - - →	I_1 _ Z_o
0.00 V	0.00^o	- - - →	V_c _ Z_o
123.52 A	91.37^o	- - - →	I_1_ Shunt Reactor 110MVar
32374.29 V	0.20^o	- - - →	V_c _ input: Distribution line
56.32 A	-87.50^o	- - - →	I_1 _ section_1: Distribution line

31324.55 V	0.20^o	----→	V_c_section_2: Distribution line
65.35 A	-87.82^o	----→	I_1 _section_2: Distribution line
30106.64 V	0.22^o	----→	V_c_section_3: Distribution line
74.02 A	-88.05^o	----→	I_1 _ section_3: Distribution line
28727.11 V	0.25^o	----→	V_c_section_4: Distribution line
82.30 A	-88.22^o	----→	I_1 _ section_4: Distribution line
27193.35 V	0.29^o	----→	V_c_section_5: Distribution line
90.14 A	-88.35^o	----→	I_1 _ section_5: Distribution line
25513.63 V	0.35^o	----→	V_c_section_6: Distribution line
97.49 A	-88.45^o	----→	I_1 _ section_6: Distribution line
23696.98 V	0.44^o	----→	V_c_section_7: Distribution line
104.32 A	-88.52^o	----→	I_1 _ section_7: Distribution line
21753.18 V	0.55^o	----→	V_c_section_8: Distribution line
110.59 A	-88.57^o	----→	I_1 _ section_8: Distribution line
19692.70 V	0.70^o	----→	V_c_section_9: Distribution line
116.27 A	-88.61^o	----→	I_1 _ section_9: Distribution line
17526.69 V	0.90^o	----→	V_c_section_10: Distribution line
121.32 A	-88.63^o	----→	I_1 _ section_10: Distribution line
15266.87V	1.18^o	----→	V_c_output: Distribution line

SOURCES:

33000.00 V	0.00^o	----→	Alagbon
0.00 A	0.00^o	----→	Anifowoshe

Steady State Parameters of ALG – FOW D/L:

250.86 A	-91.68^o	----→	I_1 _ Z_i
2090.45 V	-1.68^o	----→	V_c_ Z_i
0.00 A	0.00^o	----→	I_1 _ Z_o
0.00 V	0.00^o	----→	V_c _ Z_o
203.33 A	91.99^o	----→	I_1_ Shunt Reactor 110MVar

30900.14 V	0.76^{o}	----→	V_c _ input: Distribution line
175.81 A	-87.87^{o}	----→	I_1 _ section_1: Distribution line
29462.14 V	0.80^{o}	----→	V_c_section_2: Distribution line
179.54 A	-87.90^{o}	----→	I_1 _section_2: Distribution line
27993.73 V	0.86^{o}	----→	V_c_section_3: Distribution line
183.07 A	-87.92^{o}	----→	I_1 _ section_3: Distribution line
26496.42 V	0.92^{o}	----→	V_c_section_4: Distribution line
186.42 A	-87.94^{o}	----→	I_1 _ section_4: Distribution line
24971.78 V	0.99^{o}	----→	V_c_section_5: Distribution line
189.58 A	-87.96^{o}	----→	I_1 _ section_5: Distribution line
23421.38 V	1.07^{o}	----→	V_c_section_6: Distribution line
192.54 A	-87.98^{o}	----→	I_1 _ section_6: Distribution line
21846.84 V	1.17^{o}	----→	V_c_section_7: Distribution line
195.30 A	-87.99^{o}	----→	I_1 _ section_7: Distribution line
20249.81 V	1.29^{o}	----→	V_c_section_8: Distribution line
197.86 A	-88.00^{o}	----→	I_1 _ section_8: Distribution line
18631.95 V	1.43^{o}	----→	V_c_section_9: Distribution line
200.21 A	-88.00^{o}	----→	I_1 _ section_9: Distribution line
16994.98 V	1.59^{o}	----→	V_c_section_10: Distribution line
202.36 A	-88.01^{o}	----→	I_1 _ section_10: Distribution line
15340.64V	1.80^{o}	----→	V_c_output: Distribution line

SOURCES:

33000.00 V	0.00^{o}	----→	Alagbon
0.00 A	0.00^{o}	----→	Anifowoshe

Steady State Parameters of ALG – FOW D/L:

250.86 A	-91.68^{o}	----→	I_1 _ Z_i
2090.45 V	-1.68^{o}	----→	V_c_ Z_i
0.00 A	0.00^{o}	----→	I_1 _ Z_o
0.00 V	0.00^{o}	----→	V_c _ Z_o
203.33 A	91.99^{o}	----→	I_1_ Shunt Reactor 110MVar

30900.14 V	0.76^{o}	----→	V_c _ input: Distribution line
175.81 A	-87.87^{o}	----→	I_1 _ section_1: Distribution line
29462.14 V	0.80^{o}	----→	V_c_section_2: Distribution line
179.54 A	-87.90^{o}	----→	I_1 _section_2: Distribution line
27993.73 V	0.86^{o}	----→	V_c_section_3: Distribution line
183.07 A	-87.92^{o}	----→	I_1 _ section_3: Distribution line
26496.42 V	0.92^{o}	----→	V_c_section_4: Distribution line
186.42 A	-87.94^{o}	----→	I_1 _ section_4: Distribution line
24971.78 V	0.99^{o}	----→	V_c_section_5: Distribution line
189.58 A	-87.96^{o}	----→	I_1 _ section_5: Distribution line
23421.38 V	1.07^{o}	----→	V_c_section_6: Distribution line
192.54 A	-87.98^{o}	----→	I_1 _ section_6: Distribution line
21846.84 V	1.17^{o}	----→	V_c_section_7: Distribution line
195.30 A	-87.99^{o}	----→	I_1 _ section_7: Distribution line
20249.81 V	1.29^{o}	----→	V_c_section_8: Distribution line
197.86 A	-88.00^{o}	----→	I_1 _ section_8: Distribution line
18631.95 V	1.43^{o}	----→	V_c_section_9: Distribution line
200.21 A	-88.00^{o}	----→	I_1 _ section_9: Distribution line
16994.98 V	1.59^{o}	----→	V_c_section_10: Distribution line
202.36 A	-88.01^{o}	----→	I_1 _ section_10: Distribution line
15340.64 V	1.80^{o}	----→	V_c_output: Distribution line

SOURCES:

33000.00 V	0.00^{o}	----→	Alagbon
0.00 A	0.00^{o}	----→	Fowler

Steady State Parameters of ADM – ANI D/L:

311.07 A	-91.56^{o}	----→	I_1 _ Z_i
2592.16 V	-1.56^{o}	----→	V_c_ Z_i
0.00 A	0.00^{o}	----→	I_1 _ Z_o
0.00 V	0.00^{o}	----→	V_c _ Z_o

238.71 A	92.17^{o}	---→	I_1_ Shunt Reactor 110MVar
30220.88 V	0.95^{o}	---→	V_c _ input: Distribution line
217.11 A	-87.74^{o}	---→	I_1 _ section_1: Distribution line
28800.17 V	1.00^{o}	---→	V_c_section_2: Distribution line
220.03 A	-87.76^{o}	---→	I_1 _section_2: Distribution line
27360.45 V	1.06^{o}	---→	V_c_section_3: Distribution line
222.79 A	-87.77^{o}	---→	I_1 _ section_3: Distribution line
25902.66 V	1.12^{o}	---→	V_c_section_4: Distribution line
225.41 A	-87.78^{o}	---→	I_1 _ section_4: Distribution line
24427.78 V	1.19^{o}	---→	V_c_section_5: Distribution line
227.88 A	-87.79^{o}	---→	I_1 _ section_5: Distribution line
22936.79 V	1.28^{o}	---→	V_c_section_6: Distribution line
230.20 A	-87.80^{o}	---→	I_1 _ section_6: Distribution line
21430.70 V	1.38^{o}	---→	V_c_section_7: Distribution line
232.37 A	-87.81^{o}	---→	I_1 _ section_7: Distribution line
19910.51 V	1.49^{o}	---→	V_c_section_8: Distribution line
234.38 A	-87.82^{o}	---→	I_1 _ section_8: Distribution line
18377.25 V	1.63^{o}	---→	V_c_section_9: Distribution line
236.24 A	-87.82^{o}	---→	I_1 _ section_9: Distribution line
16831.96 V	1.79^{o}	---→	V_c_section_10: Distribution line
237.94 A	-87.83^{o}	---→	I_1 _ section_10: Distribution line
15275.70 V	1.98^{o}	---→	V_c_output: Distribution line

SOURCES:

32825.00 V	0.00^{o}	---→	Ademola
0.00 A	0.00^{o}	---→	Anifowoshe

Steady State Values for case of 23:00Hrs of 17th January 2014

Steady State Parameters of ALG – ANI D/L:

74.71 A	-91.13^{o}	---→	I_1 _ Z_i

622.58 V	1.13^o	----→	V_c_ Z_i
0.00 A	0.00^o	----→	I_1 _ Z_o
0.00 V	0.00^o	----→	V_c _ Z_o
123.61 A	91.37^o	----→	I_1_ Shunt Reactor 110MVar
32372.87 V	0.20^o	----→	V_c _ input: Distribution line
56.44 A	-87.50^o	----→	I_1 _ section_1: Distribution line
31320.94 V	0.21^o	----→	V_c_section_2: Distribution line
65.46 A	-87.82^o	----→	I_1 _section_2: Distribution line
30100.86 V	0.22^o	----→	V_c_section_3: Distribution line
74.14 A	-88.05^o	----→	I_1 _ section_3: Distribution line
28719.19 V	0.25^o	----→	V_c_section_4: Distribution line
82.41 A	-88.22^o	----→	I_1 _ section_4: Distribution line
27183.34 V	0.29^o	----→	V_c_section_5: Distribution line
90.25 A	-88.35^o	----→	I_1 _ section_5: Distribution line
25501.57 V	0.35^o	----→	V_c_section_6: Distribution line
97.60 A	-88.45^o	----→	I_1 _ section_6: Distribution line
23682.94 V	0.44^o	----→	V_c_section_7: Distribution line
104.42 A	-88.52^o	----→	I_1 _ section_7: Distribution line
21737.24 V	0.55^o	----→	V_c_section_8: Distribution line
110.69 A	-88.57^o	----→	I_1 _ section_8: Distribution line
19674.95 V	0.70^o	----→	V_c_section_9: Distribution line
116.36 A	-88.61^o	----→	I_1 _ section_9: Distribution line
17507.21 V	0.90^o	----→	V_c_section_10: Distribution line
121.41 A	-88.63^o	----→	I_1 _ section_10: Distribution line
15245.78 V	1.18^o	----→	V_c_output: Distribution line

SOURCES:

33000.00 V	0.00^o	----→	Alagbon
0.00 A	0.00^o	----→	Anifowoshe

Steady State Values for cases of 02:00Hrs of 20th January 2014

Steady State Parameters of ALG – ALG/L D/L:

1564.51 A	-88.14^o	----→	I_1 _ Z_i
13037.14 V	1.86^o	----→	V_c_ Z_i
0.00 A	0.00^o	----→	I_1 _ Z_o
0.00 V	0.00^o	----→	V_c _ Z_o
1085.40 A	95.69^o	----→	I_1_ Shunt Reactor 110MVar
19830.90 V	5.02^o	----→	V_c _ input: Distribution line
1084.35 A	-84.31^o	----→	I_1 _ section_1: Distribution line
19387.49 V	5.06^o	----→	V_c_section_2: Distribution line
1084.47 A	-84.31^o	----→	I_1 _section_2: Distribution line
18944.05 V	5.10^o	----→	V_c_section_3: Distribution line
1084.59 A	-84.31^o	----→	I_1 _ section_3: Distribution line
18500.56 V	5.14^o	----→	V_c_section_4: Distribution line
1084.71 A	-84.31^o	----→	I_1 _ section_4: Distribution line
18057.04 V	5.18^o	----→	V_c_section_5: Distribution line
1084.82 A	-84.31^o	----→	I_1 _ section_5: Distribution line
17613.48 V	5.23^o	----→	V_c_section_6: Distribution line
1084.93 A	-84.31^o	----→	I_1 _ section_6: Distribution line
17169.89 V	5.28^o	----→	V_c_section_7: Distribution line
1085.04 A	-84.31^o	----→	I_1 _ section_7: Distribution line
16726.27 V	5.33^o	----→	V_c_section_8: Distribution line
1085.15 A	-84.31^o	----→	I_1 _ section_8: Distribution line
16282.61 V	5.38^o	----→	V_c_section_9: Distribution line
1085.25 A	-84.31^o	----→	I_1 _ section_9: Distribution line
15838.93 V	5.43^o	----→	V_c_section_10: Distribution line
1085.35 A	-84.31^o	----→	I_1 _ section_10: Distribution line
15395.23 V	5.49^o	----→	V_c_output: Distribution line

SOURCES:

33000.00 V	0.00^o	----→	Alagbon

0.00 A	0.00^{o}	----→	Alagbon Local

Steady State Parameters of ALG – ADM D/L:

94.50 A	-92.43^{o}	----→	I_1 _ Z_i
787.50 V	-2.43^{o}	----→	V_c_ Z_i
10.11 A	-93.24^{o}	----→	I_1 _ Z_o
84.23 V	-3.24^{o}	----→	V_c _ Z_o
122.23 A	91.53^{o}	----→	I_1_ Shunt Reactor 110MVar
32208.32 V	0.29^{o}	----→	V_c _ input: Distribution line
69.73 A	-87.80^{o}	----→	I_1 _ section_1: Distribution line
31043.39 V	0.31^{o}	----→	V_c_section_2: Distribution line
77.75 A	-88.00^{o}	----→	I_1 _section_ 2: Distribution line
29743.39 V	0.33^{o}	----→	V_c_section_3: Distribution line
85.43 A	-88.15^{o}	----→	I_1 _ section_3: Distribution line
28317.56 V	0.37^{o}	----→	V_c_section_4: Distribution line
92.74 A	-88.26^{o}	----→	I_1 _ section_4: Distribution line
26768.42 V	0.43^{o}	----→	V_c_section_5: Distribution line
99.66 A	-88.35^{o}	----→	I_1 _ section_5: Distribution line
25103.88 V	0.50^{o}	----→	V_c_section_6: Distribution line
106.14 A	-88.42^{o}	----→	I_1 _ section_6: Distribution line
23331.13 V	0.60^{o}	----→	V_c_section_7: Distribution line
112.17 A	-88.48^{o}	----→	I_1 _ section_7: Distribution line
21457.85 V	0.72^{o}	----→	V_c_section_8: Distribution line
117.71 A	-88.51^{o}	----→	I_1 _ section_8: Distribution line
19492.17 V	0.87^{o}	----→	V_c_section_9: Distribution line
122.75 A	-88.54^{o}	----→	I_1 _ section_9: Distribution line
17442.61 V	1.07^{o}	----→	V_c_section_10: Distribution line
127.25 A	-88.55^{o}	----→	I_1 _ section_10: Distribution line
15318.12V	1.34^{o}	----→	V_c_output: Distribution line

SOURCES:

33000.00 V	0.00^{o}	- - - →	Alagbon
7.00 A	89.90^{o}	- - - →	Ademola

Steady State Values for cases of 06:00Hrs of 20th January 2014

Steady State Parameters of ALG – ALG/L D/L:

1563.77 A	-88.14^{o}	- - - →	I_1 _ Z_i
13031.01 V	1.86^{o}	- - - →	V_c_ Z_i
0.00 A	0.00^{o}	- - - →	I_1 _ Z_{o+}
0.00 V	0.00^{o}	- - - →	V_c _ Z_o
1084.89 A	95.68^{o}	- - - →	I_1_ Shunt Reactor 110MVar
19837.20 V	5.02^{o}	- - - →	V_c _ input: Distribution line
1083.84 A	-84.32^{o}	- - - →	I_1 _ section_1: Distribution line
18950.77 V	5.02^{o}	- - - →	V_c_section_2: Distribution line
1084.08 A	-84.32^{o}	- - - →	I_1 _section_2: Distribution line
18507.49 V	5.06^{o}	- - - →	V_c_section_3: Distribution line
1084.19 A	-84.32^{o}	- - - →	I_1 _ section_3: Distribution line
18064.18 V	5.09^{o}	- - - →	V_c_section_4: Distribution line
1084.31 A	-84.32^{o}	- - - →	I_1 _ section_4: Distribution line
17620.83 V	5.18^{o}	- - - →	V_c_section_5: Distribution line
1084.42 A	-84.32^{o}	- - - →	I_1 _ section_5: Distribution line
17177.45 V	5.22^{o}	- - - →	V_c_section_6: Distribution line
1084.53 A	-84.32^{o}	- - - →	I_1 _ section_6: Distribution line
16734.03 V	5.27^{o}	- - - →	V_c_section_7: Distribution line
1084.63 A	-84.32^{o}	- - - →	I_1 _ section_7: Distribution line
16290.59 V	5.32^{o}	- - - →	V_c_section_8: Distribution line
1084.63 A	-84.32^{o}	- - - →	I_1 _ section_8: Distribution line
16290.59 V	5.38^{o}	- - - →	V_c_section_9: Distribution line
1084.74 A	-84.32^{o}	- - - →	I_1 _ section_9: Distribution line
15847.12 V	5.43^{o}	- - - →	V_c_section_10: Distribution line
1084.84 A	-88.32^{o}	- - - →	I_1 _ section_10: Distribution line

15403.62 V	5.49^{o}	----→	V_c_output: Distribution line

SOURCES:

33000.00 V	0.00^{o}	----→	Alagbon
0.00 A	0.00^{o}	----→	Alagbon Local

Steady State Parameters of ALG – ANI D/L:

74.17 A	-91.13^{o}	----→	I_1 _ Z_i
618.10 V	-1.13^{o}	----→	V_c_ Z_i
0.00 A	0.00^{o}	----→	I_1 _ Z_o
0.00 V	0.00^{o}	----→	V_c _ Z_o
123.34 A	91.36^{o}	----→	I_1_ Shunt Reactor 110MVar
32377.38 V	0.20^{o}	----→	V_c _ input: Distribution line
65.10 A	-87.51^{o}	----→	I_1 _ section_1: Distribution line
31332.38 V	0.20^{o}	----→	V_c_section_2: Distribution line
65.10 A	-87.82^{o}	----→	I_1 _section_2: Distribution line
30119.16 V	0.22^{o}	----→	V_c_section_3: Distribution line
73.77 A	-88.05^{o}	----→	I_1 _ section_3: Distribution line
28744.26 V	0.25^{o}	----→	V_c_section_4: Distribution line
82.06 A	-88.23^{o}	----→	I_1 _ section_4: Distribution line
27215.04 V	0.29^{o}	----→	V_c_section_5: Distribution line
89.90 A	-88.36^{o}	----→	I_1 _ section_5: Distribution line
25539.74 V	0.35^{o}	----→	V_c_section_6: Distribution line
97.26 A	-88.45^{o}	----→	I_1 _ section_6: Distribution line
23727.37 V	0.44^{o}	----→	V_c_section_7: Distribution line
104.10 A	-88.53^{o}	----→	I_1 _ section_7: Distribution line
21787.69 V	0.55^{o}	----→	V_c_section_8: Distribution line
110.38 A	-88.58^{o}	----→	I_1 _ section_8: Distribution line
19731.15 V	0.70^{o}	----→	V_c_section_9: Distribution line
116.07 A	-88.61^{o}	----→	I_1 _ section_9: Distribution line

17568.86 V	0.90^o	----→	V_c_section_10: Distribution line
121.13 A	-88.63^o	----→	I_1 _ section_10: Distribution line
15312.54 V	1.17^o	----→	V_c_output: Distribution line

SOURCES:

33000.00 V	0.00^o	----→	Alagbon
0.00 A	0.00^o	----→	Anifowoshe

Steady State Parameters of ALG – FOW D/L:

250.51 A	-91.68^o	----→	I_1 _ Z_i
2087.50 V	-1.68^o	----→	V_c_ Z_i
0.00 A	0.00^o	----→	I_1 _ Z_o
0.00 V	0.00^o	----→	V_c _ Z_o
203.10 A	91.99^o	----→	I_1_ Shunt Reactor 110MVar
30903.12 V	0.76^o	----→	V_c _ input: Distribution line
175.57 A	-87.87^o	----→	I_1 _ section_1: Distribution line
29467.13 V	0.80^o	----→	V_c_section_2: Distribution line
179.29 A	-87.90^o	----→	I_1 _section_2: Distribution line
28000.72 V	0.86^o	----→	V_c_section_3: Distribution line
182.83 A	-87.92^o	----→	I_1 _ section_3: Distribution line
26505.40 V	0.92^o	----→	V_c_section_4: Distribution line
186.18 A	-87.94^o	----→	I_1 _ section_4: Distribution line
24982.74 V	0.99^o	----→	V_c_section_5: Distribution line
189.34 A	-87.96^o	----→	I_1 _ section_5: Distribution line
23434.32 V	1.07^o	----→	V_c_section_6: Distribution line
192.30 A	-87.98^o	----→	I_1 _ section_6: Distribution line
21861.74 V	1.17^o	----→	V_c_section_7: Distribution line
195.06 A	-87.99^o	----→	I_1 _ section_7: Distribution line
20266.66 V	1.29^o	----→	V_c_section_8: Distribution line
197.62 A	-88.00^o	----→	I_1 _ section_8: Distribution line

18650.73 V	1.42^{o}	- - - →	V_c_section_9: Distribution line
199.98 A	-88.01^{o}	- - - →	I_1 _ section_9: Distribution line
17015.67 V	1.59^{o}	- - - →	V_c_section_10: Distribution line
202.13 A	-88.01^{o}	- - - →	I_1 _ section_10: Distribution line
15363.21 V	1.80^{o}	- - - →	V_c_output: Distribution line

SOURCES:

33000.00 V	0.00^{o}	- - - →	Alagbon
0.00 A	0.00^{o}	- - - →	Fowler

Steady State Values for cases of 09:00Hrs of 20th January 2014

Steady State Parameters of ALG – ALG/L D/L:

1563.95 A	-88.14^{o}	- - - →	I_1 _ Z_i
13032.54 V	1.86^{o}	- - - →	V_c_ Z_i
0.00 A	0.00^{o}	- - - →	I_1 _ Z_{o+}
0.00 V	0.00^{o}	- - - →	V_c _ Z_o
1085.01 A	95.68^{o}	- - - →	I_1_ Shunt Reactor 110MVar
19835.63 V	5.02^{o}	- - - →	V_c _ input: Distribution line
1083.96 A	-84.32^{o}	- - - →	I_1 _ section_1: Distribution line
19392.38 V	5.06^{o}	- - - →	V_c_section_2: Distribution line
1084.09 A	-84.32^{o}	- - - →	I_1 _section_2: Distribution line
18949.10 V	5.10^{o}	- - - →	V_c_section_3: Distribution line
1084.21 A	-84.32^{o}	- - - →	I_1 _ section_3: Distribution line
18505.77 V	5.14^{o}	- - - →	V_c_section_4: Distribution line
1084.32 A	-84.32^{o}	- - - →	I_1 _ section_4: Distribution line
18062.40 V	5.18^{o}	- - - →	V_c_section_5: Distribution line
1084.44 A	-84.32^{o}	- - - →	I_1 _ section_5: Distribution line
17619.00 V	5.23^{o}	- - - →	V_c_section_6: Distribution line
1084.55 A	-84.32^{o}	- - - →	I_1 _ section_6: Distribution line
17175.57 V	5.27^{o}	- - - →	V_c_section_7: Distribution line
1084.66 A	-84.32^{o}	- - - →	I_1 _ section_7: Distribution line

16732.10 V	5.32^{o}	- - - →	V_c_section_8: Distribution line
1084.76 A	-84.32^{o}	- - - →	I_1 _ section_8: Distribution line
16288.61 V	5.38^{o}	- - - →	V_c_section_9: Distribution line
1084.86 A	-84.32^{o}	- - - →	I_1 _ section_9: Distribution line
15845.08 V	5.43^{o}	- - - →	V_c_section_10: Distribution line
1084.96 A	-88.32^{o}	- - - →	I_1 _ section_10: Distribution line
15401.54 V	5.49^{o}	- - - →	V_c_output: Distribution line

SOURCES:

33000.00 V	0.00^{o}	- - - →	Alagbon
0.00 A	0.00^{o}	- - - →	Alagbon Local

Steady State Parameters of ALG – BAN/I D/L:

133.78 A	-92.66^{o}	- - - →	I_1 _ Z_i
1114.78 V	-2.66^{o}	- - - →	V_c_ Z_i
0.00 A	-91.71^{o}	- - - →	I_1 _ Z_o
0.00 V	-1.71^{o}	- - - →	V_c _ Z_o
143.69 A	91.61^{o}	- - - →	I_1_ Shunt Reactor 110MVar
31879.60 V	0.39^{o}	- - - →	V_c _ input: Distribution line
96.07 A	-87.94^{o}	- - - →	I_1 _ section_1: Distribution line
30570.26 V	0.42^{o}	- - - →	V_c_section_2: Distribution line
102.51 A	-88.04^{o}	- - - →	I_1 _section_2: Distribution line
29173.22 V	0.46^{o}	- - - →	V_c_section_3: Distribution line
108.65 A	-88.13^{o}	- - - →	I_1 _ section_3: Distribution line
27692.48 V	0.50^{o}	- - - →	V_c_section_4: Distribution line
114.49 A	-88.20^{o}	- - - →	I_1 _ section_4: Distribution line
26132.31 V	0.57^{o}	- - - →	V_c_section_5: Distribution line
119.99 A	-88.25^{o}	- - - →	I_1 _ section_5: Distribution line
24497.20 V	0.64^{o}	- - - →	V_c_section_6: Distribution line
125.15 A	-88.30^{o}	- - - →	I_1 _ section_6: Distribution line

22791.84 V	0.73^{o}	- - - →	V_c_section_7: Distribution line
129.95 A	-88.33^{o}	- - - →	I_1 _ section_7: Distribution line
21021.17 V	0.85^{o}	- - - →	V_c_section_8: Distribution line
134.38 A	-88.36^{o}	- - - →	I_1 _ section_8: Distribution line
19190.28 V	1.00^{o}	- - - →	V_c_section_9: Distribution line
138.43 A	-88.38^{o}	- - - →	I_1 _ section_9: Distribution line
17304.49 V	1.18^{o}	- - - →	V_c_section_10: Distribution line
142.07 A	-88.39^{o}	- - - →	I_1 _ section_10: Distribution line
15369.27 V	1.42^{o}	- - - →	V_c_output: Distribution line

SOURCES:

33000.00 V	0.00^{o}	- - - →	Alagbon
0.00 A	0.00^{o}	- - - →	Banana Island

Steady State Parameters of ALG – FOW D/L:

250.71 A	-91.68^{o}	- - - →	I_1 _ Z_i
2089.21 V	-1.68^{o}	- - - →	V_c_ Z_i
0.00 A	0.00^{o}	- - - →	I_1 _ Z_o
0.00 V	0.00^{o}	- - - →	V_c _ Z_o
203.23 A	91.99^{o}	- - - →	I_1_ Shunt Reactor 110MVar
30901.40 V	0.76^{o}	- - - →	V_c _ input: Distribution line
175.71 A	-87.87^{o}	- - - →	I_1 _ section_1: Distribution line
29464.25 V	0.80^{o}	- - - →	V_c_section_2: Distribution line
179.43 A	-87.90^{o}	- - - →	I_1 _section_2: Distribution line
27996.68 V	0.86^{o}	- - - →	V_c_section_3: Distribution line
182.97 A	-87.92^{o}	- - - →	I_1 _ section_3: Distribution line
26500.21 V	0.92^{o}	- - - →	V_c_section_4: Distribution line
186.32 A	-87.94^{o}	- - - →	I_1 _ section_4: Distribution line
24976.41 V	0.99^{o}	- - - →	V_c_section_5: Distribution line
189.48 A	-87.96^{o}	- - - →	I_1 _ section_5: Distribution line

23426.84 V	1.07^{o}	----→	V_c_section_6: Distribution line
192.44 A	-87.98^{o}	----→	I_1 _ section_6: Distribution line
21853.13 V	1.17^{o}	----→	V_c_section_7: Distribution line
195.20 A	-87.99^{o}	----→	I_1 _ section_7: Distribution line
20256.92 V	1.29^{o}	----→	V_c_section_8: Distribution line
197.76 A	-88.00^{o}	----→	I_1 _ section_8: Distribution line
18639.88 V	1.43^{o}	----→	V_c_section_9: Distribution line
200.11 A	-88.00^{o}	----→	I_1 _ section_9: Distribution line
17003.72 V	1.59^{o}	----→	V_c_section_10: Distribution line
202.26 A	-88.01^{o}	----→	I_1 _ section_10: Distribution line
15350.17 V	1.80^{o}	----→	V_c_output: Distribution line

SOURCES:

33000.00 V	0.00^{o}	----→	Alagbon
0.00 A	0.00^{o}	----→	Fowler

Steady State Values for cases of 21:00Hrs of 20th January 2014

Steady State Parameters of ALG – ALG/L D/L:

1564.76 A	-88.14^{o}	----→	I_1 _ Z_i
13039.29 V	1.86^{o}	----→	V_c_ Z_i
0.00 A	0.00^{o}	----→	I_1 _ Z_{o+}
0.00 V	0.00^{o}	----→	V_c _ Z_o
1085.57 A	95.69^{o}	----→	I_1_ Shunt Reactor 110MVar
19828.73 V	5.02^{o}	----→	V_c _ input: Distribution line
1084.52 A	-84.31^{o}	----→	I_1 _ section_1: Distribution line
19385.26 V	5.06^{o}	----→	V_c_section_2: Distribution line
1084.65 A	-84.31^{o}	----→	I_1 _section_2: Distribution line
18941.74 V	5.10^{o}	----→	V_c_section_3: Distribution line
1084.77 A	-84.31^{o}	----→	I_1 _ section_3: Distribution line

18498.18 V	5.14^{o}	----→	V_c_section_4: Distribution line
1084.88 A	-84.31^{o}	----→	I_1 _ section_4: Distribution line
18054.59 V	5.18^{o}	----→	V_c_section_5: Distribution line
1085.00 A	-84.31^{o}	----→	I_1 _ section_5: Distribution line
17610.96 V	5.23^{o}	----→	V_c_section_6: Distribution line
1085.11 A	-84.31^{o}	----→	I_1 _ section_6: Distribution line
17167.29 V	5.28^{o}	----→	V_c_section_7: Distribution line
1085.22 A	-84.31^{o}	----→	I_1 _ section_7: Distribution line
16723.60 V	5.33^{o}	----→	V_c_section_8: Distribution line
1085.32 A	-84.31^{o}	----→	I_1 _ section_8: Distribution line
16279.87 V	5.38^{o}	----→	V_c_section_9: Distribution line
1085.43 A	-84.31^{o}	----→	I_1 _ section_9: Distribution line
15836.12 V	5.44^{o}	----→	V_c_section_10: Distribution line
1085.53 A	-84.31^{o}	----→	I_1 _ section_10: Distribution line
15392.34 V	5.50^{o}	----→	V_c_output: Distribution line

SOURCES:

33000.00 V	0.00^{o}	----→	Alagbon
0.00 A	0.00^{o}	----→	Alagbon Local

Steady State Parameters of ALG – ANI D/L:

75.24 A	-91.13^{o}	----→	I_1 _ Z_i
626.94 V	-1.13^{o}	----→	V_c_ Z_i
0.00 A	0.00^{o}	----→	I_1 _ Z_o
0.00 V	0.00^{o}	----→	V_c _ Z_o
123.86 A	91.37^{o}	----→	I_1_ Shunt Reactor 110MVar
32368.48 V	0.21^{o}	----→	V_c _ input: Distribution line
56.80 A	-87.51^{o}	----→	I_1 _ section_1: Distribution line
31309.80 V	0.21^{o}	----→	V_c_section_2: Distribution line
65.82 A	-87.82^{o}	----→	I_1 _section_2: Distribution line

30083.02 V	0.22^o	----→	V_c_section_3: Distribution line
74.49 A	-88.05^o	----→	I_1 _ section_3: Distribution line
28694.75 V	0.25^o	----→	V_c_section_4: Distribution line
82.76 A	-88.22^o	----→	I_1 _ section_4: Distribution line
27152.43 V	0.29^o	----→	V_c_section_5: Distribution line
90.59 A	-88.35^o	----→	I_1 _ section_5: Distribution line
25464.37 V	0.36^o	----→	V_c_section_6: Distribution line
97.93 A	-88.44^o	----→	I_1 _ section_6: Distribution line
23639.64 V	0.44^o	----→	V_c_section_7: Distribution line
104.74 A	-88.52^o	----→	I_1 _ section_7: Distribution line
21688.07 V	0.55^o	----→	V_c_section_8: Distribution line
110.99 A	-88.57^o	----→	I_1 _ section_8: Distribution line
19620.17 V	0.71^o	----→	V_c_section_9: Distribution line
116.65 A	-88.60^o	----→	I_1 _ section_9: Distribution line
17447.13 V	0.91^o	----→	V_c_section_10: Distribution line
121.68 A	-88.62^o	----→	I_1 _ section_10: Distribution line
15180.71 V	1.18^o	----→	V_c_output: Distribution line

SOURCES:

33000.00 V	0.00^o	----→	Alagbon
0.00 A	0.00^o	----→	Anifowoshe

Steady State Parameters of ALG – FOW D/L:

251.19 A	-91.68^o	----→	I_1 _ Z_i
2093.20 V	-1.68^o	----→	V_c_ Z_i
0.00 A	0.00^o	----→	I_1 _ Z_o
0.00 V	0.00^o	----→	V_c _ Z_o
203.54 A	91.99^o	----→	I_1_ Shunt Reactor 110MVar
30897.37 V	0.76^o	----→	V_c _ input: Distribution line
176.04 A	-87.87^o	----→	I_1 _ section_1: Distribution line
29457.50 V	0.80^o	----→	V_c_section_2: Distribution line

179.76 A	-87.90^{o}	---→	I_1 _section_2: Distribution line
27987.23 V	0.86^{o}	---→	V_c_section_3: Distribution line
183.30 A	-87.92^{o}	---→	I_1 _ section_3: Distribution line
26488.07 V	0.92^{o}	---→	V_c_section_4: Distribution line
186.65 A	-87.94^{o}	---→	I_1 _ section_4: Distribution line
24961.58 V	0.99^{o}	---→	V_c_section_5: Distribution line
189.80 A	-87.96^{o}	---→	I_1 _ section_5: Distribution line
23409.34 V	1.07^{o}	---→	V_c_section_6: Distribution line
192.76 A	-87.97^{o}	---→	I_1 _ section_6: Distribution line
21832.98 V	1.17^{o}	---→	V_c_section_7: Distribution line
195.52 A	-87.98^{o}	---→	I_1 _ section_7: Distribution line
20234.14 V	1.29^{o}	---→	V_c_section_8: Distribution line
198.08 A	-87.99^{o}	---→	I_1 _ section_8: Distribution line
18614.50 V	1.43^{o}	---→	V_c_section_9: Distribution line
200.43 A	-88.00^{o}	---→	I_1 _ section_9: Distribution line
16975.75 V	1.60^{o}	---→	V_c_section_10: Distribution line
202.58 A	-88.01^{o}	---→	I_1 _ section_10: Distribution line
15319.65 V	1.80^{o}	---→	V_c_output: Distribution line

SOURCES:

33000.00 V	0.00^{o}	---→	Alagbon
0.00 A	0.00^{o}	---→	Fowler